Phenotypes and genetic mechanisms of C. elegans enhanced RNAi

Phenotypes and genetic mechanisms of *C. elegans* enhanced RNAi

A dissertation presented

by

Jimmy Jiajia Zhuang

to

The Department of Molecular and Cellular Biology

in partial fulfillment of the requirements

for the degree of

Doctor of Philosophy

in the subject of

Biochemistry

Harvard University

Cambridge, Massachusetts

March 2013

Dissertation Advisor: Professor Craig Hunter By: Jimmy Jiajia Zhuang

Phenotypes and genetic mechanisms of *C. elegans* enhanced RNAi

Abstract

RNA interference (RNAi) potently and specifically induces gene knockdown, and its potential for reverse genetics in *Caenorhabditis elegans* is enormous. However, even in these nematodes, RNAi can be induced more effectively via enhanced RNAi (Eri) mutant backgrounds. With advances in small RNA sequencing, evidence has suggested that the *eri* pathway plays an endogenous gene regulatory role, which competes with experimentally introduced RNAi triggers for limiting resources. However, the nature, cellular location, and physiological consequences of this small RNA pathways competition remain unclear. To answer these questions, I first fully characterized the genetic phenotypes of all known Eri mutants. I discovered that different components of the *eri* pathway have subtle differences upon mutation, which affects more than exogenous RNAi. I then attempted to screen for novel enhanced RNAi mutants, guided by hypothetical mechanisms or tissues of expression not associated with known mutants. After these attempts, I fully characterized the genetic mechanisms that account for enhanced RNAi. Surprisingly, I discovered that the nuclear Argonaute *nrde-3* and the peri-nuclear P-granule component *pgl-1* are necessary and sufficient for an Eri response. Finally, I examined the impact of the competition among microRNA, endogenous siRNA, and exogenous RNAi pathways. I discovered that *C. elegans* develops slower upon perturbations to its normal flux of small RNA pathways. Insights from these phenotypes and genetic mechanisms shed light on the importance of small RNA biology and offer a novel suite of tools for sensitizing RNAi in broader contexts, especially given the deep evolutionary conservation of most *eri*-associated genes.

Table of Contents

Thesis Outline

In **Chapter One**, I present my published review of RNAi (ZHUANG, J. J., and C. P. HUNTER, 2012. RNA interference in *Caenorhabditis elegans*: uptake, mechanism, and regulation. *Parasitology* **139**: 560-573). In it, I discuss the mechanisms and regulation of RNAi in the context of *C. elegans*. I also highlight enhanced RNAi via both systemic and cell-autonomous mechanisms. Using this survey of literature, I frame my thesis aims and questions that guided my research findings for the subsequent chapters.

In **Chapter Two**, I present my published report on phenotypic analyses of enhanced RNAi mutants (ZHUANG, J. J., and C. P. HUNTER, 2011. Tissue Specificity of *Caenorhabditis elegans* enhanced RNA interference mutants. *Genetics* **188**: 235-237). In it, I report that RNAi responses follow a sigmoidal curve, that there are optimal tissue-specific enhanced RNAi differences amongst Eri mutants, and that the Eri phenotype is maternally rescued.

In **Chapter Three**, I present my analyses of three screens designed to discover novel RNAi mutants. I analyzed a screen for enhanced systemic RNAi with 13 candidate mutants. I also probed for possible enhanced systemic RNAi amongst the nine known Eri mutants. Finally, I screened for somatic RNAi defective mutants and found one promising candidate.

In **Chapter Four**, I present my in-press report on the role of *nrde-3* in enhanced RNAi (ZHUANG, J. J., S.A. BANSE and C. P. HUNTER, 2013. The Nuclear Argonaute NRDE-3 Contributes to Transitive RNAi in *Caenorhabditis elegans*. *Genetics* **doi: 10.1534/genetics. 113.149765**). In it, I report that nuclear RNAi defective mutants are generally RNAi defective,

including for transgene silencing and trans-generational RNAi. I also report that *nrde-3* is uniquely necessary and sufficient for enhanced RNAi, and that a possible mechanism for this may be the phenomenon of transitive RNAi. Finally, I report that *eri*-regulated gene targets also depend on *nrde-3*, suggesting a functional endogenous gene regulatory role for nuclear RNAi.

In **Chapter Five**, I present my analysis of *pgl-1*'s contribution to enhanced RNAi. Within the in-press report from Chapter Four, I provide evidence that *nrde-3* and *pgl-1* contribute complementarily to enhanced RNAi; in the absence of both factors, the enhanced RNAi response is entirely absent. I also report that *pgl-1* mutants do not exhibit common RNAi pathway defects, suggesting a uniquely parallel contribution to RNAi, which is confirmed by a drastically different expression profile of *eri*-regulated gene targets. Finally, I present techniques developed to pool small RNAs from *pgl-1* mutants to better examine in the future endogenous small RNA expression via deep sequencing.

In **Chapter Six**, I present my published report on small RNA competition's impact on development (ZHUANG, J. J., and C. P. HUNTER, 2012. The influence of competition among *C. elegans* small RNA pathways on development. *Genes* **3**: 671-685). In it, I report that the microRNAi, endogenous RNAi, and exogenous RNAi pathways interact with each other to perturb each others' gene silencing efficacy. Furthermore, I report that this competition induces developmental delays when any of the pathways are perturbed from the wild type flux.

In **Chapter Seven**, I present a historical discussion of the small RNA field and its likely future directions. I also contextualize some of my findings within these field trends.

Finally, in the **Addendum**, I present my analysis of the homologs of *sid-1*, a gene largely responsible for systemic RNA in *C. elegans*. In it, I show that RNAi knockdowns of these genes sometimes induce decreased RNAi sensitivity.

Acknowledgements

I'd like to first and foremost thank my adviser Professor Craig Hunter for his support over the last five years. His enthusiasm for science and his optimistic outlook for mentoring created so many positive outcomes that wouldn't have been. I'd also like to thank many members of the Hunter lab over the years for creating enjoyable lab moments, especially Drs. Stephen Banse, Andrea Hinas, Antony Jose, and Kenneth Pang.

I'd like to thank many members of the *C. el*egans community, both near and far, for assisting through materials, strains, advice, or equipment, most of which were instrumental to my research. Dr. Susan Mango and her lab were especially helpful. Dr. Scott Kennedy, Dr. Weifeng Gu, and the *Caenorhabditis* Genetics Center also helped tremendously in many ways.

I'd like to thank my dissertation advisory committee, Drs. Alex Schier, Briana Burton, and Gary Ruvkun for their guidance and support over the years.

I'd like to thank the National Science Foundation for my Graduate Research Fellowship. I'd also like to thank the Department of Molecular and Cellular Biology at Harvard University for providing a supportive environment to undertake research and graduate-level training, as well as allowing me meet some amazing friends through the MCO program.

I'd like to thank the undergraduates I've mentored in lab and taught in courses. Elizabeth Wang was instrumental for the discoveries reported in the Addendum and the students of MCB153 were instrumental for the discoveries of somatic RNAi defective mutants reported in Chapter 3. Furthermore, my students from LS1A inspired me to better my scientific communication, an endeavor that will surely reap many rewards in the next stage of my career.

Last but not least, I'd like to thank my family and friends, old and new, for unending support and understanding.

Chapter One

RNA interference in *C. elegans*: uptake, mechanism, and regulation

The majority of the contents were previously published in ZHUANG, J. J., and C. P. HUNTER, 2012. RNA interference in *Caenorhabditis elegans*: uptake, mechanism, and regulation. *Parasitology* **139**: 560-573. Permission to reuse was granted by Cambridge University Press License Number 3060851284559.

ABSTRACT

RNA interference (RNAi) is a powerful research tool that has enabled molecular insights into gene activity, pathway analysis, partial loss-of-function phenotypes, and large-scale genomic discovery of gene function. While RNAi works extremely well in the non-parasitic nematode *C. elegans,* it is also especially useful in organisms that lack facile genetic analysis. Extensive genetic analysis of the mechanisms, delivery, and regulation of RNAi in *C. elegans* has provided mechanistic and phenomenological insight into why RNAi is so effective in this species. These insights are useful for the testing and development of RNAi in other nematodes, including parasitic nematodes where more effective RNAi would be extremely useful. Here, we review the current advances in *C. elegans* for RNA delivery methods, regulation of cell autonomous and systemic RNAi phenomena, and implications of enhanced RNAi mutants. These discussions, with a focus on mechanism and cross-species application, provide new perspectives for optimizing RNAi in other species.

INTRODUCTION

RNA interference (RNAi) is triggered by double-stranded RNA (dsRNA). This dsRNA is processed into single-stranded small interfering RNAs (siRNAs) that act as guide sequences to target homologous mRNAs and nascent transcripts for post-transcriptional gene silencing (PTGS) (CHEKULAEVA and FILIPOWICZ 2009) and transcriptional gene silencing (TGS) (MOAZED 2009), respectively. A broad array of endogenous RNAi-related mechanisms is used to control gene expression (MOCHIZUKI 2010; TEIXEIRA and COLOT 2010; WHITE and ALLSHIRE 2008). Likely because it accesses these endogenous gene activities, experimentally induced RNAi is potent and specific (SHARP 1999), leading to its popular and wide use as a genetic tool

(SIOUD 2011). However, many challenges remain. For many organisms, intracellular delivery of dsRNA presents a significant experimental obstacle; coupled to this is variable or low potency. In contrast, RNAi works very well in *C. elegans* because of ease of delivery coupled to efficient RNA-directed RNA polymerase (RdRP) amplification of effector siRNAs. Here we review what is known about RNA delivery and genetic control of RNAi efficacy in *C. elegans* with the goal of using this knowledge to enable RNAi in other organisms.

Reverse genetics via RNAi has become extremely popular over the past decade (SILVA *et al.* 2004). This is particularly true in organisms like *C. elegans, Planaria,* and *Apidae* that readily take up and apparently spread the triggering dsRNA and/or derived silencing signals. However, biological and methodlogical diversity in dsRNA delivery can lead to variability in RNAi efficacy. Therefore, to maximize RNAi silencing, it is important to understand the organism-specific limitations as well as advantages of dsRNA uptake (GELDHOF *et al.* 2007; KNOX *et al.* 2007). The ease of both classic genetics and RNAi has made *C. elegan*s the exemplary model organism for this analysis.

The discovery and subsequent in-depth mechanistic characterization of RNAi in *C. elegans* helped established the entire RNAi field (HANNON 2002). RNAi in *C. elegans* is both easy and remarkably potent. The ease of dsRNA delivery is unmatched, including most notably by ingestion – so called environmental RNAi. However, a variety of enhanced RNAi (Eri) mutants show that even in *C. elegans*, RNAi can become even more potent (KENNEDY *et al.* 2004). Although not all nematodes in the *Caenorhabditis* genus are equally accessible for dsRNA delivery, most are capable of RNAi (FELIX 2008). Interestingly, the identified *eri* genes are conserved across *Caenorhabditis* and in many instances, widely conserved across evolution. This indicates independent selection for delivery and regulation of potency. Similar observations

have been made more broadly in the nematode phylum, as the *Haemonchus*, *Heterohabditis*, *Ostertagia*, *Heterodera*, *Globodera*, *Meloidogyne*, *Panagrolaimus*, and *Brugia* genera have all been shown to respond to at least some forms of RNAi delivery, though with different apparent potencies (FELIX 2008). These observations indicate that comparative analysis of RNAi in nematodes is likely to reveal much about the selective pressures that modify small RNA pathways. In this review of *C. elegans* RNAi genetics and methods, we pay particular attention to conserved genetic networks with the goal of leveraging the wealth of mechanistic information available in *C. elegans* to the application of RNAi in less accessible nematodes.

DISCUSSION

METHODS

The robustness of RNAi in *C. elegans* is likely due to both RdRP activity that amplifies silencing signals and the systemic nature of *C. elegans* RNAi that enables silencing signals to move between cells, tissues, and generations. Thus, small amounts of locally delivered dsRNA can cause robust silencing in any tissue in the treated animal as well as its progeny. Here, we compare the relative silencing potency of the three principal dsRNA delivery methods: microinjection, ingestion, and transgene expression (**Figure 1.1**).

Microinjection is the most direct and potent way to introduce RNAi triggers. Microinjection also provides control over dsRNA concentration and the cell or tissue to score for knockdown. Control of concentration is critical to maximize the effective dose while simultaneously avoiding non-specific toxicity or off-target effects. The concentration of dsRNA

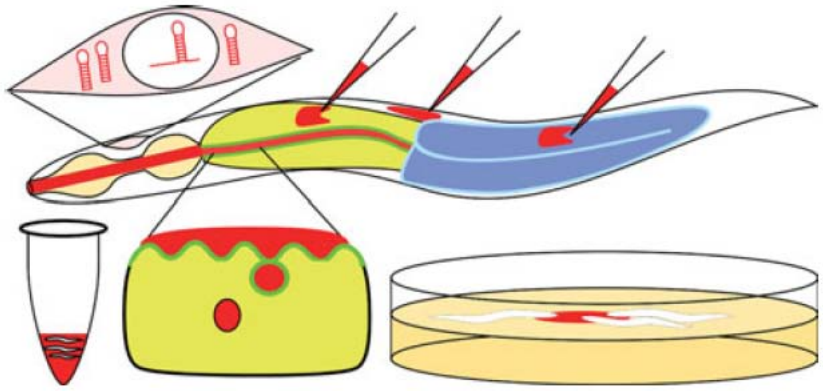

Figure 1.1: Double-stranded RNA delivery in *C. elegans*

Microinjection of concentrated dsRNA (red) into the large gut cells (yellow), the syncytial germline (blue), or the body cavity (white) affords the greatest control over delivery and the most potent response; however, throughput is limited. Throughput is improved by soaking whole animals in dsRNA, or feeding worms bacteria engineered to express dsRNA. Both soaking and feeding results in ingested dsRNA that requires the intestinal transmembrane protein SID-2 (green) for delivery into the animal. Finally, transgenic expression of double-stranded RNA or hairpin constructs can target dsRNA delivery to specific cell types not accessible by microinjection, and in *sid-1* mutant backgrounds, can limit the RNAi knock-down effect to the targeted cells.

to inject will vary from organism to organism (KUWABARA and COULSON 2000; NASEVICIUS and EKKER 2000; SVOBODA and STEIN 2009), from cell type to cell type (GRISHOK and MELLO 2002; WANG *et al.* 2005), and even from gene target to gene target (KRUEGER *et al.* 2007). Although in *C. elegans* silencing signals can spread from the injected cell or tissue, this is not true of other, even closely related species (WINSTON *et al.* 2007). Therefore, initial analysis of RNAi effectiveness should be limited to scoring the injected cell or syncytial tissue.

In some organisms, long dsRNA is toxic. For example, in vertebrates, long dsRNA triggers a non-sequence specific interferon response that leads to cell death (CULLEN 2006). Whether long dsRNA is toxic to invertebrates is largely unexplored. These toxic effects are avoided in mammalian cells by using siRNA to trigger RNAi; siRNAs are too short to trigger the non-specific effect (MITTAL 2004). Microinjection of siRNAs is effective in *C. elegans*, but the response is attenuated compared to long dsRNA (YANG *et al.* 2000).

Transgene-expressed dsRNA can also initiate RNAi and allows introduction of dsRNA into cells and tissues that are not accessible to microinjection, including neurons and muscle cells (SCHEPERS 2005). Another advantage is that transgenic lines can be maintained indefinitely and expanded to large populations that are not accessible by microinjection. In *C. elegans*, RNAi can be effectively triggered by either expressed hairpin RNA constructs or co-expressed sense and antisense RNA. However, the production of dsRNA-expressing transgenic animals is more complicated and less controllable than injecting dsRNA. First, it is difficult to avoid nonspecific expression of the transgene; the promoter may be active in unintended cells (GROVE *et al.* 2009). Second, it is difficult to assess the quality or quantity of RNAi trigger; unlike loading a microinjection needle with known concentrations of precisely defined dsRNA, endogenously

expressed dsRNA does not come with easily quantifiable measures. As a consequence, RNAi potency can vary between independent lines (PRAITIS *et al.* 2001) and from simple structural changes to the same hairpin construct (BOUDREAU *et al.* 2008). Third, transgenes in *C. elegans* are subject to spontaneous silencing via a mechanism that is at least in part dependent on RNAi silencing genes. Since RNAi silencing is saturable, expressed dsRNA may interfere with such silencing in a dose-dependent and variable way (KIM *et al.* 2005b) which adds a confounding factor when evaluating the presence, absence or penetrance of RNAi silencing.

Ingestion of dsRNA is the third principal means of introducing RNAi triggers into *C. elegans*. Ingestion can be accomplished either by soaking worms in a concentrated solution of purified dsRNA (MAEDA *et al.* 2001) or more simply by feeding worms bacteria engineered to expressed dsRNA (TIMMONS *et al.* 2001; TIMMONS and FIRE 1998). This mechanism of inducing effective RNAi is entirely dependent on systemic RNAi. However, systemic RNAi is not sufficient as specialized dsRNA uptake machinery is also required (WINSTON *et al.* 2007). In *C. elegans*, the transmembrane proteins SID-1 and SID-2 are required independently for ingestion mediated RNAi. SID-1 is required for the uptake of silencing signals into all cells, while SID-2 is required only for silencing initiated by ingested dsRNA. SID-2 is expressed exclusively in the intestine and localizes primarily to the apical membrane, suggesting that SID-2 may directly interact with ingested dsRNA for internalization (WINSTON *et al.* 2007).

SID-2 homologs are highly divergent, recognizable in only *Caenorhabditis* nematodes, and even among these, ingested dsRNA induces RNAi in only a few species (WINSTON *et al.* 2007). This molecular and functional divergence is consistent with the unpredictable distribution of organisms that are susceptible to ingested-dsRNA mediated RNAi (WHANGBO and HUNTER

2008). Consequently, absence of ingestion-mediated RNAi should not be interpreted as absence of RNAi or even systemic RNAi.

In organisms that are susceptible to ingestion mediated RNAi, the ability to easily subject animals to a large variety of dsRNA sequences has many advantages. In *C. elegans*, the construction and availability of libraries of engineered "RNAi foods" targeting the entire genome has made "feeding RNAi" an extremely powerful genetic tool (KAMATH and AHRINGER 2003; KAMATH *et al.* 2003; RUAL *et al.* 2004). Furthermore, feeding worms dsRNA expressing bacteria, like transgene-expressed dsRNA, enables large numbers of RNAi knock-down worms to be produced for genetic screens or biochemical assays; however, this conditional feeding RNAi has an advantage over transgene-expressed dsRNA when targeting genes important for growth, fertility, and viability. The apparent delivered dose of ingested dsRNA, however, is less than is achieved by microinjection, causing less penetrant phenotypes, which makes it often necessary to expose animals to ingested dsRNA for multiple generations (TIMMONS and FIRE 1998). Furthermore, different tissues respond differently to RNAi triggers, making it difficult to score the relative efficacy of RNAi (CALIXTO *et al.* 2010).

Other less frequently used means to introduce RNAi triggers into small metazoans include electroporation, transfection, and soaking in liposome-encapsulated dsRNA (GELDHOF *et al.* 2006; ISSA *et al.* 2005; KRAUTZ-PETERSON *et al.* 2007). These methods are not used in *C. elegans.*

MECHANISMS OF dsRNA TRANSPORT BY SID-1

Intercellular transport of dsRNA silencing signals in *C. elegans* requires the highly conserved dsRNA channel SID-1 (JOSE and HUNTER 2007). SID-1 is a transmembrane protein

with 11 predicted transmembrane domains, a 400+ amino acid extracellular N-terminal domain, and a short cytosolic C-terminal domain (FEINBERG and HUNTER 2003). Many recovered *sid-1* mutants have missense mutations in the transmembrane domains, suggesting that these sequences are essential for function. SID-1 is autonomously required for the import but not the export of RNAi triggers (JOSE *et al.* 2009). A *sid-1* promoter *gfp* construct was found to be expressed from the late embryo throughout adulthood in all non-neuronal tissues (WINSTON *et al.* 2002). Interestingly, neuronal cells are resistant to RNAi triggered by ingested or injected dsRNA, but sensitive to neuronally expressed dsRNA, indicating the defect is in delivery of dsRNA to neurons, not RNAi effectiveness in neurons; consistent with this, transgenic expression of SID-1 in neurons enables efficient systemic RNAi (CALIXTO *et al.* 2010). Furthermore, such expression enhances RNAi efficacy in these cells at the expense of wild-type cells (CALIXTO *et al.* 2010). These results suggest that SID-1 expression is limiting for systemic RNAi in *C. elegans.*

Mechanistic studies performed in *Drosophila* S2 cells indicate that SID-1 functions as a dsRNA-gated channel. *Drosophila* lacks a SID-1 homolog and endogenous mechanisms of dsRNA uptake in S2 cells are relatively inefficient, making these cells an ideal "blank slate" system to investigate SID-1 dsRNA transport properties. SID-1 activity in S2 cells has been primarily measured by uptake of radio-labeled dsRNA and by RNAi silencing of reporter genes. Recent studies have also used whole-cell patch-clamp analysis to characterize SID-1 channel properties. ^{32}P-labeled dsRNA added to the culture media of SID-1 expressing S2 cells is rapidly taken up, showing that SID-1 enables dsRNA transport (FEINBERG and HUNTER 2003; SHIH *et al.* 2009). To distinguish between active transport mechanisms that require continuous energy input (ATP) for dsRNA transport – i.e. pumps or receptors that require vesicle transport – versus

passive transport mechanisms that could transport dsRNA without additional energy input – i.e. channels or pores – the uptake assays were repeated in either ATP-depleted cells or in cells maintained at 4°C. For both treatments, the endogenous S2 cell RNA uptake was eliminated, while SID-1 dependent uptake was still very productive (FEINBERG and HUNTER 2003). These results indicate that SID-1 acts as a passive transporter, likely a channel or pore. Consistent with SID-1 functioning as a channel, whole-cell patch-clamp analysis showed that adding dsRNA to the cell media increased the conductance (opened channels) of SID-1 expressing cells and that washing the dsRNA away led to a return to baseline conductance (SHIH and HUNTER 2011). Together these results indicate that SID-1 is a dsRNA-gated channel.

These same transport and activity assays indicate that SID-1 nucleic acid transport is efficient, specific, and selective for dsRNA. SID-1 expression in S2 cells enabled detectable RNAi silencing at a 10^7-fold lower dsRNA concentration than in control cells (FEINBERG and HUNTER 2003; SHIH *et al.* 2009); this translates into less than one molecule of dsRNA per cell, indicating very efficient uptake. Similar results were obtained with cultured *C. elegans* cells (SHIH *et al.* 2009). Although initial studies using RNAi silencing of luciferase reporters indicated that *sid-1* dependent uptake efficiency is sensitive to dsRNA length (FEINBERG and HUNTER 2003), subsequent studies using radio-labeled 50 bp, 100 bp, and 500 bp dsRNAs showed indistinguishable results (SHIH *et al.* 2009). Similarly sized dsRNAs also indistinguishably open channels on whole-cell patched SID-1 expressing cells (SHIH and HUNTER 2011). Since size does not affect activation or transport, it is thought that longer dsRNA, when delivered systemically, is a more efficient silencing trigger. The whole-cell patch clamp analysis also indicates that nucleic acid transport by SID-1 is specific to dsRNA containing molecules. First, neither dsDNA nor a DNA-RNA heteroduplex can activate SID-1

expressing cells. Nucleotide substitution experiments indicate a requirement for the ribose 2'-OH. Although dsRNA is required for transport, molecules that contain single-stranded regions can be transported. Transport of hairpin molecules containing greater than 300 nucleotide single-stranded loops as well as pre-microRNA precursors were also detected. These results dramatically expand the possible repertoire of molecules transported by SID-1.

SID-1 homologs are present in nematodes, diverse invertebrate phyla, and all sequenced vertebrate genomes (ALTSCHUL *et al.* 1997; GRIMSON *et al.* 2008) (**Figure 1.2**). These proteins are highly conserved, which indicates a strongly selected function. Although *C. elegans* SID-1 has a demonstrated long-dsRNA transport activity, an activity or function remains unknown for all other homologs. *C. elegans* contains five SID-1 homologs (**Figure 1.3**) (GILLE 2004), some of which are more similar to vertebrate homologs than SID-1. However, alleles for none of these were recovered in the Sid screen. There are many reasons why mutations in these were not recovered in the Sid screen: these genes may not function in dsRNA transport, their dsRNA transport function may be redundant with another gene(s), or they may have additional essential functions such that mutations that disrupted dsRNA transport may be lethal. Because mutations in these genes have not yet been recovered, only RNAi is available to study their possible role in systemic RNAi or other functions. A serious limitation of this approach is illustrated by our analysis of *sid-1* by RNAi: repeated early attempts to produce an RNAi defect by *sid-1(RNAi)* failed. However, our certainty of the phenotype led us to continue pursuing RNAi of *sid-1* by injection of dsRNA, which ultimately caused a reduction in RNAi sensitivity in up to 50% of the progeny of an injected animal. We theorize that our difficulty in producing a RNAi-defective phenotype reflects both a necessity of SID-1 function for RNAi and the tremendous efficiency of dsRNA transport by SID-1: moderate *sid-1* knockdown may be sufficient to prevent further

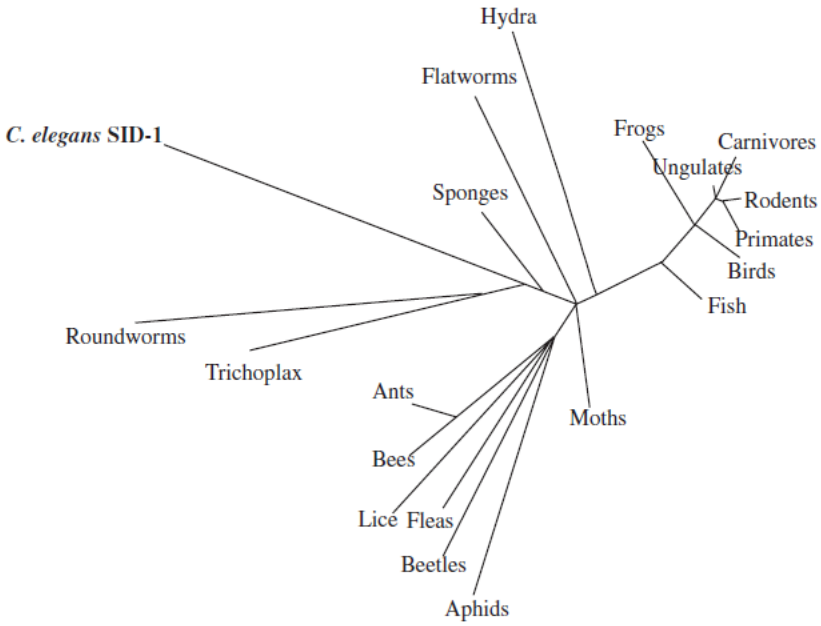

Figure 1.2: *C. elegans* SID-1 is widely conserved

SID-1 homologs are present in many taxonomic groups, suggesting widespread conservation of a protein which may support systemic RNAi in these other species. The taxonomic tree of *C. elegans* SID-1 was created using Grishin (protein) distance, with a max sequence difference of 0.85, a fast minimum evolution parameter, with radial display representing evolutionary distance.

Figure 1.3: SID-1 has five homologs in *C. elegans*

Amino acid alignment of the six *C. elegans* genes homologous to human *SidT2*. *sid-1*, *tag-130*, *C08A9.3*, and *Y37H2C.1* are similar in size and structure, while *C30E1.3* and *C30E1.4* are much more divergent. Yellow and orange indicate hydrophobic amino acids, green and purple indicate polar amino acids, red indicates acidic amino acids, cyan indicates basic amino acids, and brown indicates aromatic amino acids. Alignments are generated by Structure based Sequence Alignment Program (STRAP)'s built-in parameters (GILLE 2004).

Figure 1.3 (Continued): SID-1 has five homologs in *C. elegans*

knockdown of SID-1, but not sufficient to prevent detectable knock down of tester gene targets due to this high efficiency of transport for those SID-1 which remain.

The vertebrate SID-1 homologs are unlikely to transport long dsRNA due to the interferon response (BRIDGE *et al.* 2003). This raises the possibility that because the *C. elegans* SID-1 homologs are more similar to the vertebrate proteins, they may share a function and/or nucleic acid specificity different than that of SID-1. These considerations, along with the possibility of functional redundancy, challenge the mirror assumptions that the presence of a SID-1 homolog is evidence for systemic RNAi capacity and the absence of systemic defect when a SID-1 homolog is knocked-down or knocked-out demonstrates lack of dsRNA transport activity for that homolog.

ROLE OF SID-2 IN ENVIRONMENTAL RNAi

For ingested dsRNA to initiate RNAi, it must be first transported into the gut cells' cytoplasms. Because SID-1 expressed in Drosophila S2 cells is sufficient to enable uptake, one possibility is that SID-1 functions at the luminal membrane to transport ingested dsRNA across this membrane. However, in the worm, SID-1 is not sufficient, because *sid-2* mutants are specifically defective for environmental RNAi. Interestingly, SID-2 alone is also not sufficient, as *sid-1* mutants exposed to dsRNA fail to show silencing in gut cells. This indicates that these two proteins function together, either cooperatively or sequentially, to import ingested dsRNA (WINSTON *et al.* 2007).

SID-2 is a 311 amino acid single-pass transmembrane protein that is expressed in all gut cells and localizes strongly to the apical/luminal membrane. This indicates that SID-2 may be specialized to interact with ingested dsRNA. Curiously, the presumed dsRNA-interacting

extracellular domain is much less conserved that the intracellular domain. The *C. briggsae* species is unable to initiate RNAi from ingested dsRNA. However, *C. briggsae* expresses and localizes Cb-SID-2 indistinguishably from Ce-SID-2. Transgenic expression of Ce-SID-2 in *C. briggsae* enables environmental RNAi, suggesting either expression and/or functional differences between these two genes homologs. In contrast, expressing Cb-SID-2 in a *sid-2* mutant *C. elegans* strain failed to rescue environmental RNAi. The functional difference between the two SID-2 proteins has been mapped by domain swap experiments to the extracellular domain (MCEWAN *et al.* 2012). The *C. elegans* extracellular domain attached to the *C. briggsae* transmembrane and cytoplasmic domains functionally rescue *sid-2* mutants. The distribution of environmental RNAi-capable species within the known *Caenorhabditis* phylogeny is not consistent with either a simple loss or gain of ability. Furthermore, the linkage of environmental RNAi ability with SID-2 function has only been established for *C. elegans, C. briggsae,* and *C. remanei* (M. Felix, personal communication). These observations, combined with the non-predictable nature of which species are capable of taking up ingested dsRNA, suggest that gain and loss of this ability is rapid and likely encompasses many different proteins that can perform SID-2's function.

AUTONOMOUS VERSUS SYSTEMIC RNA INTERFERENCE

Systemic RNAi is the organism-wide spread of silencing either via distribution of the initial RNAi trigger or its effectors (JOSE and HUNTER 2007). In contrast, cell autonomous RNAi silencing is restricted to the cells and their descendants that directly encounter dsRNA by injection, infection, transfection, or expression. In *C. elegans*, cell autonomous RNAi is the activity that remains in a *sid-1* mutant. In *sid-1* mutants, transgene-expressed dsRNA and dsRNA

injected directly into the syncytial germline or into single gut cells causes efficient silencing in the germline and injected cell respectively, but no detectable silencing in other cells.

The RNAi silencing machinery is highly conserved, yet not all organisms have been shown to be RNAi-capable. One explanation may be that the machinery is used for TGS or RNA directed DNA elimination (MOCHIZUKI 2010; PAL-BHADRA *et al.* 2002). However, the lack of systemic RNAi may impede the detection of experimentally induced silencing phenotypes in many situations. For *Caenorhaditis* nematode species that have systemic RNAi, either injection of dsRNA or transgenc expression of Ce-SID-2 enables whole-animal experimental RNAi and even transgenerational silencing. However, at least one *Caenorhabidits* species, *C. brenneri* (*Caenorhabditis* sp. CB5161), apparently lacks systemic RNAi. This was discovered when dsRNA targeting the large subunit of RNA polymerase caused the expected early embryonic lethal phenotype when injected directly into the syncytial germline, but in contrast to all other tested species, failed to cause any detectable phenotype when injected into intestinal cells in *C. brenneri* (WINSTON *et al.* 2007); thus *C. brenneri* appears to be naturally systemic-RNAi-defective. Interestingly, the *C. brenneri* genomic sequence indicates that SID-1 is intact, indicating that addtional components required for systemic RNAi may be disabled or missing in this species. The apparent selection for an intact SID-1 in the absence of systemic RNAi indicates that SID-1 may have an additional function(s). While an ecologicaly important function for systemic RNAi in animals has not yet been reported, systemic RNAi appears to provide protection against viral spread in plants (MOURRAIN *et al.* 2000); however, this will remain speculative until a mutant that specifically disrupts systemic RNAi is recovered.

The presence or absence of systemic RNAi in the target organism can have profound effects on both the determination of whether RNAi works in that organism and how dsRNA can

be effectively delivered. The wide-spread use of RNAi in *Drosophila* is illustrative of the challenges and solutions. Microinjection of dsRNA into early syncytial *Drosophila* embryo provides access to all nuclei and their transcripts, but the lack of a robust RdRP-based amplification coupled with cellularization restricts effective RNAi to genes that function in the early embryo. This can be overcome by transgene-expressed dsRNA, which bypasses the complete lack of systemic RNAi in this organism (PERRIMON *et al.* 2010). The lack of systemic RNAi is likely due to lack of a *sid-1* homolog as well as other components required for systemic RNAi (SID-1 expression in *Drosophila* has not yet been reported to enable systemic RNAi, despite many groups attempting this approach - personal communications). Complementing the *in vivo* approach, RNAi screens have been applied to a variety of *Drosophila*-derived cultured cell lines, like S2 cells, where dsRNA added to the culture medium is taken up via endogenous scavenging receptors that rely on the endocytosis machinery (SALEH *et al.* 2006; ULVILA *et al.* 2006) or via transgenic expression of *C. elegans* SID-1 (BARTSCHERER *et al.* 2006).

Organisms in which RNAi works very well have both systemic RNAi and RdRP enabled amplification of RNAi triggers, leading to speculation that they may be mutually dependent. In some organisms, like *Arabidopsis*, it is these amplified products that become systemically mobile (FAGARD and VAUCHERET 2000).

Viral defense has been proposed as an evolutionary explanation for systemic RNAi. In *Drosophila* and *C. elegans*, some RNAi-related genes have antiviral roles, reducing viral titers in infected cells and animals (DING 2010; LU *et al.* 2005; SCHOTT *et al.* 2005; WILKINS *et al.* 2005). However, cultured *sid-1* mutant *C. elegans* cells were not more susceptible to viral infections than wild-type cells (SCHOTT *et al.* 2005), suggesting that systemic RNAi may not play a vital role in viral defense. The recent identification of viruses that can naturally infect whole worms

will provide an opportunity to properly test this hypothesis (FELIX *et al.* 2011). However, the systemic antiviral interferon response in mammals, which is triggered in response to long dsRNA (SLEDZ *et al.* 2003), provides a contrapositive argument to this hypothesis. In plants, viral infection induces a strong anti-viral RNAi response, which includes RdRP amplification of RNAi triggers, which then spread systemically to provide viral immunity to as yet uninfected cells and tissues (VANCE and VAUCHERET 2001).

Whatever the evolutionary roles of systemic RNAi may be, it is widely regarded as a powerful addition to cell-autonomous RNAi. However, as stated previously, the absence of systemic RNAi is not evidence for the absence of RNAi in the organism. RNAi may simply be more difficult to trigger and therefore detect in the absence of efficient delivery to all cells. In the next section, as we describe the mechanism of cell autonomous RNAi, we make particular note of how understanding such mechanisms can help researchers enhance cell autonomous RNAi, and therefore increase the potency of experimentally-induced RNAi.

MECHANISM OF AUTONOMOUS RNA INTERFERENCE

Mechanism of Exogenous RNAi processing

In *C. elegans*, when exogenously introduced long dsRNA (>100 basepairs) is introduced into a cell, it is bound by a protein complex that contains RDE-4 and DCR-1. RDE-4 contains two copies of a conserved dsRNA binding motif and binds as a dimer to dsRNA (Knight and Bass, 2001; Tabara *et al.* 2002). DCR-1 is a well-conserved RNase III endoribonuclease that cleaves dsRNA into short (~22 nucleotide) interfering RNAs (siRNAs) (HABIG *et al.* 2008; KNIGHT and BASS 2001; PAK and FIRE 2007; ZAMORE *et al.* 2000). Biochemically, these

double-stranded siRNAs have on each strand a 5' monophosphate, a free 3' hydroxyl group, and 2 nucleotides of overhang at the 3' end (MACRAE *et al.* 2006).

The RDE-4/DCR-1 complex also includes two Dicer-related helicases of unknown function (DRH-1 and 2) (DUCHAINE *et al.* 2006) as well as various members of the large Argonaute (AGO) family, defined by signature PAZ and PIWI domains (SONG *et al.* 2004). The AGO proteins are thought to be the catalytic machinery of RNAi-based silencing (CZECH and HANNON 2011). The PAZ domain is hypothesized to interface with DCR-1 (PADDISON and VOGT 2008).

In *C. elegans*, the Ago protein RDE-1 binds to double-strand siRNA produced by the DCR-1 complex and cleaves the passenger strand to produce a single-stranded guide siRNA (STEINER *et al.* 2009; TOMARI *et al.* 2004). In most species, the primary Ago protein – like RDE-1 – uses the guide strand to identify cognate mRNAs, and once bound, the slicer activity cleaves the mRNA between the 10^{th} and 11^{th} positions of the siRNA-mRNA complementary region via the activity of the Ago's RNase H catalytic domain (HALL 2005); however this particular event seems to be absent in *C. elegans* (STEINER *et al.* 2009). In *C. elegans*, single-strand siRNA produced by the sequential action of DCR-1 and RDE-1 on the long triggering dsRNA is referred to as a primary siRNA. Through still-mysterious processes, an RdRP produces from the siRNA-mRNA complex many copies of so-called secondary siRNAs, that are principally anti-sense to and distributed towards the 5' end of the cognate mRNA (PAK and FIRE 2007). In *C. elegans* somatic cells, the primary RdRP is RRF-1, while in the germline the primary RdRP appears to be EGO-1. These RdRPs are at least partially functionally redundant (SMARDON *et al.* 2000). The 5' end of these RdRP dependent secondary siRNAs contain triphosphate residues, indicating that they represent primary synthesis products; that is, they are

not produced by DCR-1 cleavage reactions. The secondary siRNAs are both more abundant than primary siRNAs and target an expanded sequence region on the cognate mRNA. These abundant secondary siRNAs interact with so-called secondary Argonautes (SAGOs) (YIGIT *et al.* 2006). These secondary siRNA-SAGO complexes appear to be directly involved in sequence-dependent mRNA degradation. However, as many SAGOs lack an active RNase H domain, precisely how they degrade mRNA remains unclear. It has been suggested that in *C. elegans*, mRNA targeted for PTGS are preferentially transported to P bodies or GW bodies (DING *et al.* 2005; JAKYMIW *et al.* 2005; LIU *et al.* 2005). It has been recently shown that these SAGOs, who seem to responsible for the bulk of the silencing, are poorly conserved compared to the other RNAi components, possibly providing another reason why *C. elegans* RNAi is so efficient compared to that of other species (DALZELL *et al.* 2011).

While RDE-1 and most SAGOs function in the cytoplasm, recent work has shown that one of the SAGOs, NRDE-3, shuttles secondary siRNAs into the nucleus. NRDE-3 has the signature PIWI and PAZ domains of an Ago protein, but also contains a nuclear localization signal required for its function (GUANG *et al.* 2008). Once inside the nucleus, NRDE-3 interacts with a complex of nuclear RNAi silencing factors, including the well conserved novel protein NRDE-2 (GUANG *et al.* 2010). The nuclear RNAi complex is guided by the siRNA to nascent transcripts and effects transcriptional silencing by impeding RNA polymerase elongation and recruiting histone methyltransferase activity (GUANG *et al.* 2010). This mechanism is likely the basis for heterochromatin modifications and other transcriptional gene silencing phenomena phenotypically linked to RNAi (CLAYCOMB *et al.* 2009; GRISHOK *et al.* 2005; MOTAMEDI *et al.* 2004). The synergistic PTGS and TGS mechanisms are summarized in **Figure 1.4**.

Figure 1.4: Summary of the exogenous RNAi pathway in *C. elegans*

1) Post delivery *in vitro* synthesized long (>100 bp) dsRNA (red) with 5' triphosphate (yellow) ends is 2) bound by the RDE-4 (purple) and DCR-1 (cyan) complex. 3) The endonuclease DCR-1 dices the long dsRNA into of ~20 nucleotide ds-siRNAs with two nucleotide single stranded 3' ends. The dicer products have 5' monophosphate and 3' hydroxyl ends. 4) Interaction with the Argonaute RDE-1 (pink) leads to slicing of the passenger strange producing 5) a single-stranded guide siRNA bound to RDE-1. 6) This primary ss-siRNA guides RDE-1 to its cognate mRNA (black). 7) In a mechanistically unclear step, the RdRP RRF-1 (coffee) is recruited to the RDE-1-siRNA-mRNA complex 8) leading to the production of many unprimed secondary siRNAs with 5'triphosphate ends. 9) Most of these secondary siRNAs match the originally targeted region, but secondary siRNAs anti-sense to regions both 5' and 3' to the originally introduced long dsRNA are also produced. 10a) In a second mechanistically unclear step, these secondary siRNAs become associated with cytoplasmic secondary Argonautes (SAGOs – orange) or 10b) the nuclear localized Argonaute NRDE-3. 11a) The secondary siRNAs then guide the cytoplasmic SAGOs to cognate mRNAs and via yet another mechanistically unclear step lead to the elimination of the mRNAs. 11b) NRDE-3 shuttles the secondary siRNAs into the nucleus where they guide transcriptional gene silencing processes.

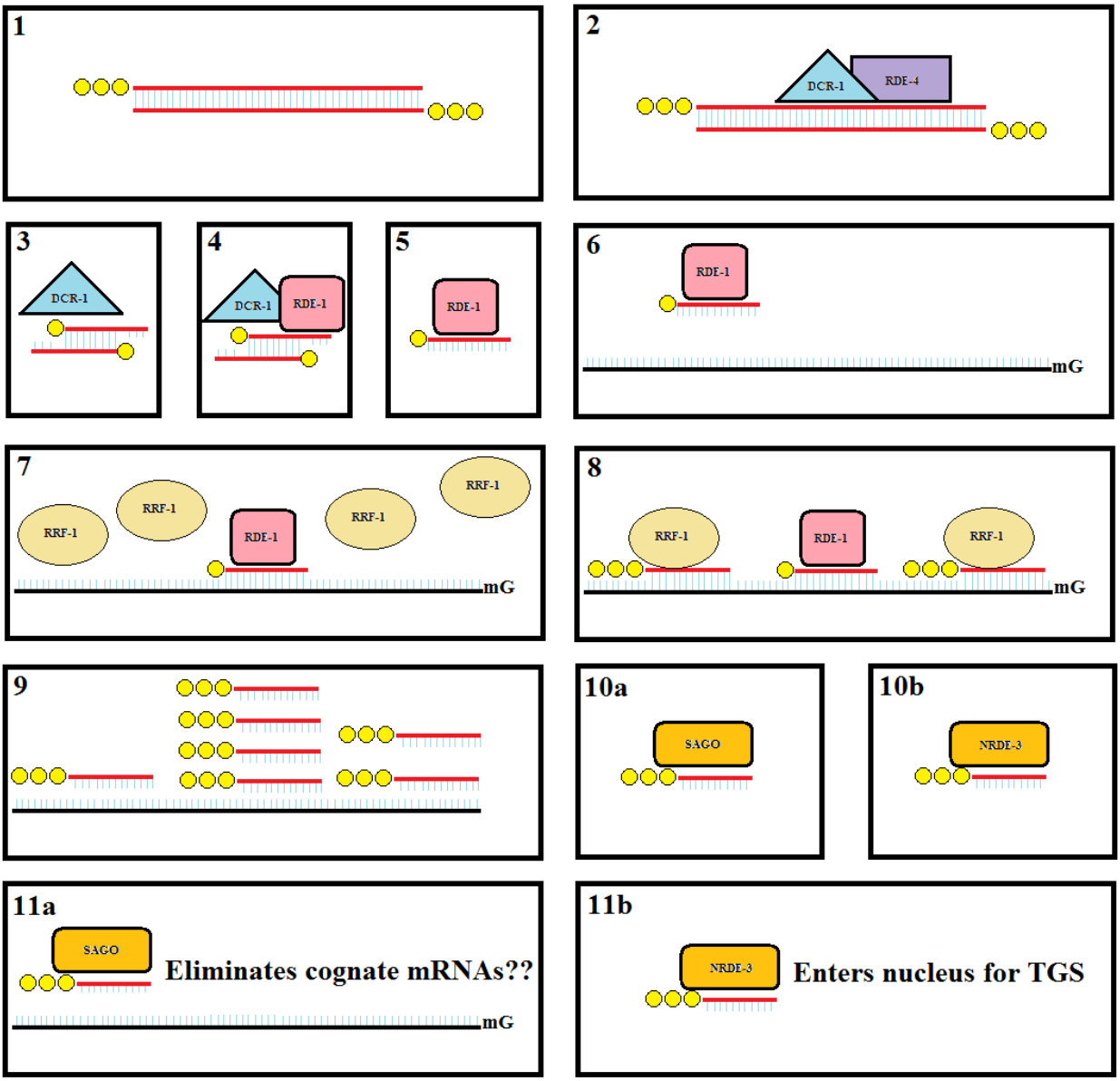

Figure 1.4 (Continued): Summary of the exogenous RNAi pathway in *C. elegans*

Regulators of Exogenous RNAi

Mutations that enhance RNAi silencing have been identified by various means. Mutations in genes required for production of endogenous siRNA silencing pathways were identified in screens for enhanced neuronal RNAi (Eri mutants) and discovered serendipitously when analyzing the phenotype of worms deleted for the RdRP *rrf-3* (KENNEDY *et al.* 2004; SIMMER *et al.* 2002). Another large class of mutants is in the worm Rb Tumor suppressor pathway, which appears to enhance RNAi by partial soma to germline transformation (WANG *et al.* 2005). It is not clear if this transformation replaces somatic RNAi with germline RNAi, which is particularly robust, or adds additional capacity to the somatic RNAi pathway. Eri mutants were initially sought for their ability to increase the discovery of RNAi phenotypes in large-scale feeding RNAi screens. For example, feeding wild-type worms 447 different RNAi foods resulted in only 307 expected loss-of-function phenotypes, while performing the same screen in the *rrf-3* mutant background resulted in 436 loss-of-function phenotypes (SIMMER *et al.* 2003). Because these mutants are enhanced for RNAi, it indicates that the wild-type *eri* genes function directly or indirectly to inhibit RNAi. Mechanistic investigations to date indicate that the enhanced RNAi phenotypes reflect indirect effects rather than the action of direct negative regulators.

The Eri class of enhancers are related by their facultative association with DCR-1 (DUCHAINE *et al.* 2006; GENT *et al.* 2009; PAVELEC *et al.* 2009). To date, nine Eri loci have been described (**Table 1.1**), including five in widely conserved genes (DUCHAINE *et al.* 2006; FISCHER *et al.* 2008; KENNEDY *et al.* 2004; PAVELEC *et al.* 2009; SIMMER *et al.* 2002). These genes are required for the production or stability of endogenous siRNAs. The current model for this *eri*-class is that the relatively abundant endogenous siRNAs compete with siRNAs produced from experimentally introduced dsRNA for limiting effector molecules, for example the SAGO

Table 1.1: Negative Regulators of RNA Interference in *C. elegans*

Gene Name	Conservation	Homologous Domains	Notes
eri-1	Wide	siRNase; RNA binding domains	Temperature sensitive sterile at 25ºC
rrf-3/eri-2	Wide	RdRP	Temperature sensitive sterile at 25ºC
eri-3	*Caenorhabditis*	Hydrolase	Temperature sensitive sterile at 25ºC
dcr-1/eri-4	Wide	Helicase domain of DCR-1	Temperature sensitive sterile at 25ºC; weak Eri phenotype
eri-5	Nematodes	Tudor domain	Germline-specific Eri phenotype
eri-6/7	Wide	Helicase	Retrotransposon homolog
ergo-1/eri-8	Wide	Argonaute	
eri-9	*Caenorhabditis*	RNA transferase	
eri-11	*Caenorhabditis*	Oligosaccharyl transferase	

proteins (LEE *et al.* 2006; YIGIT *et al.* 2006). Thus mutations in the Eri genes reduce the number of endogenous siRNAs and indirectly increase access to limiting components of silencing pathway(s). These limiting RNAi resources have been proposed to be secondary AGOs (YIGIT *et al.* 2006), DICER (MIKUMA *et al.* 2004), and even the dsRNA channel SID-1 (CALIXTO *et al.* 2010; WINSTON *et al.* 2002); in each case, over-expression increases RNAi efficacy.

Tissue-specific differences in RNAi sensitivity among the Eri mutants provides additional support for the competition model, and further suggest that the extent of competition differs among tissues (ZHUANG and HUNTER 2011). The tissue-specific differences can be explained by tissue-specific components of a competing small RNA pathway, by relative tissue-specific activities of multiple competing pathways, and even by multiple limiting resources, which may show tissue-specific biases. Interestingly, all nine Eri mutants show robust maternal rescue and showed enhanced RNAi in the germline. These observations indicate that not only are these Eri genes expressed and active in the germline, but that maternally synthesized product or the product(s) of their activity is apparently well distributed to somatic tissues in the progeny. This also suggests that the maternal contribution to the embryo directly or indirectly includes small RNAs (ZHUANG and HUNTER 2011).

These data indicate that exogenous RNAi capacity is regulated by or is responsive to endogenous small RNA silencing activity levels. Thus the sensitivity of the animal to exogenous dsRNA, whether experimentally introduced, the outcome of a viral infection, or other environmental or genomic stresses, may be tuned by intrinsic or extrinsic events (e.g. pathogens, DNA damage); for instance, systemic RNAi appears to be enhanced by starvation (WINSTON *et al.* 2002). This could reflect increased dsRNA transport or enhanced RNAi responsiveness mediated by changes in the level of endogenous siRNA levels. Analysis of the Eri class of genes

indicates that the endogenous siRNA pathways are important for maturation of sperm (GENT *et al.* 2009; PAVELEC *et al.* 2009), and proper chromosomal segregation cannot take place without the secondary Ago *csr-1* (CLAYCOMB et al. 2009). In contrast, *rde-4* and *rde-1* mutants, which appear to be specific to exogenous RNAi, do not seem to have any non-RNAi phenotypes (TABARA *et al.* 1999).

The nature of conservation among the *eri* genes should also be of interest in studying RNAi in other organisms (ALTSCHUL *et al.* 1997) (**Figure 1.5**; **Table 1.1**). ERI-1 is a well conserved nuclease with siRNase activity (KENNEDY *et al.* 2004); RRF-3 is a well conserved RdRP (CROMBACH and HOGEWEG 2011; SIJEN *et al.* 2001); the *dcr-1/eri-4(mg375)* mutant is a point mutation in the helicase domain of the well conserved DICER protein (MACRAE *et al.* 2006; PAVELEC *et al.* 2009); ERI-6/7 is a conserved helicase domain (FISCHER *et al.* 2008); and ERGO-1/ERI-8 (PAVELEC *et al.* 2009) is a well conserved Ago protein. Mutations to these conserved genes in other organisms have been shown to have some similar endogenous defects, such as general RNA processing defects (ANSEL *et al.* 2008), but assays in RNAi efficacy have not been thoroughly performed. This area of research holds vast potential for dramatically increasing RNAi applicability and technology. Even more interesting are the potential roles played by the non-conserved *eri* genes specific to *C. elegans* or *Caenorhabditis*; their predicted molecular identities (KELLEY and STERNBERG 2009) suggest that hydrolyases and transferases play a large role in small RNA production in *C. elegans* (**Table 1.1**). Perhaps such class-specific genes in other organisms hold the key to decreasing the competitive regulation of RNAi. Moreover, mutations to novel or non-conserved genes are less likely to have wide-ranging impacts, while maintaining similar degrees of RNAi hypersensitivity. Therefore, studying

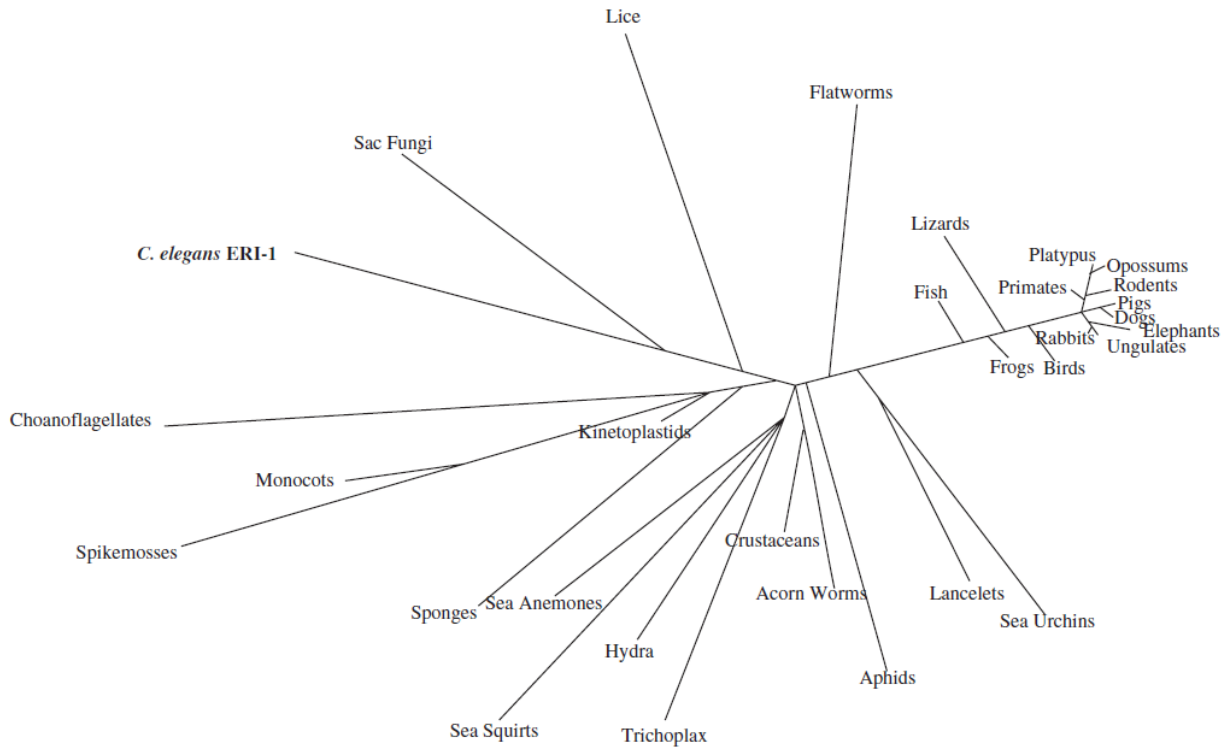

Figure 1.5: *C. elegans* ERI-1 is widely conserved

ERI-1, which is important for the production or stability of endogenous siRNA in *C. elegans*, has homologs in many taxonomic groups. Since it is likely that endogenous RNAi processes will compete with exogenous RNAi processes in these species, researchers should not only consider the possibility of enhancing RNAi, but the possibility that exogenous RNAi will interfere with essential endogenous processes (e.g. *eri-1* and *rrf-3* are required for sperm function). The taxonomic tree of *C. elegans* ERI-1 was created using Grishin (protein) distance, with a max sequence difference of 0.85, a fast minimum evolution parameter, and displayed with a forced equidistance representation.

organism-specific *eri* genes through genetic screens, if possible, holds tremendous promise for understanding (and pragmatically overcoming) RNAi regulation.

Finally, given that the products of *eri* pathway are effective competitors of the *rde* pathway, it is worthwhile to examine the chemical structures of small RNAs produced by the *eri* pathway. The *eri* gene products produce endogenous siRNAs of 22 or 26 nucleotides that usually begin with a G (22G or 26G siRNAs) and contain a 5' triphosphates (CONINE *et al.* 2010; GENT *et al.* 2010; VASALE *et al.* 2010; WELKER *et al.* 2010). Perhaps unknown chemical properties of these siRNAs are important for their relative enhanced activity. Attempting to introduce experimental siRNAs which share such properties may thus enhance RNAi efficacy as well (KIM *et al.* 2005a).

In *C. elegans*, the core of the RNAi machinery that interacts with experimentally introduced RNAi signals (whether long dsRNAs or siRNAs) is a relatively well-understood framework. Recent advances in deep sequencing revealed more and more of the intricacy and potency of the endogenous small RNA network, as well as its competitive regulation of the exogenous RNAi pathway. Researchers frustrated by the limited utility of RNAi in other species should examine the RNAi regulation perspective to perhaps overcome this seeming impasse. Once the RNAi silencing signal is inside the cell, most organisms from protists to fungi, and from plants to animals, all have some part of the conserved RNAi processing machinery, whether cytoplasmic PTGS or nuclear TGS (SHABALINA and KOONIN 2008). It is the relative effectiveness of RNAi that vastly differs (MAIDA and MASUTOMI 2011) and is possibly thwarting broader use of RNAi as a technological resource.

IMPLEMENTATION

The hallmarks of RNAi are specificity and potency. In *C. elegans*, dsRNA is not toxic and studies indicate that increasing dsRNA concentration can increase RNAi potency (REA 2007; ZHUANG and HUNTER 2011). Similarly, mutations in the Eri genes that reduce competition for limiting small RNA resources (LEE *et al.* 2006) and overexpression of these limiting resources can also increase RNAi potency (CALIXTO *et al.* 2010; MIKUMA *et al.* 2004; YIGIT *et al.* 2006). However, there is some possibility that these measures reduce specificity (PAVELEC *et al.* 2009). Furthermore, tissues differ in their relative sensitivity: for example, neurons are fairly refractory of RNAi (KAMATH and AHRINGER 2003; KAMATH *et al.* 2003) whereas the germline is hypersensitive to RNAi (SIJEN and PLASTERK 2003). Consequently, mutations that transform somatic cells towards germline can increase RNAi potency (WANG *et al.* 2005). Similarly, developmental stages or environmental conditions can also influence RNAi sensitivity: starved worms are slightly more sensitive to RNAi (JOSE and HUNTER 2007). Therefore, in assaying for RNAi efficacy, the gene target expression profile – both temporal and spatial – as well as environmental conditions need to be considered for optimal phenotypic output. These *C. elegans* tissue-specific and developmental sensitivities may be paralleled in other species and should be optimized when implementing RNAi. These considerations should be appropriately supplemented with the aforementioned methods for introducing RNAi to increase RNAi efficacy. For example, while microinjection of dsRNA into a mutant with a soma-to-germline transformation is an obvious means to increase the RNAi efficacy, transgenic expression of hairpin constructs under germline promoters – which are normally spontaneously suppressed (KIM *et al.* 2005b) – may become more effective as well in a soma-to-germline mutant.

Although RNAi potency increases with dsRNA dose, it is a common misperception that this relationship is linear. When RNAi potency (phenotypic penetrance) is plotted versus dsRNA

dose, one clearly observes a sigmoidal curve (**Figure 1.6**). Curiously, for most phenotypes, the expressivity (the severity of the phenotype) is nearly constant, thus the great variability at the empirically determined intermediate dose range reflects a mixture of strongly affected and non-affected individuals. This dose sensitivity likely underlies much of variation in reported RNAi effects, which in some cases are even contradictory (REA 2007). It is obvious best to use the maximum possible dose, but for potent foods, a simple dose response curve can determine an effective range with minimal variability.

Finally, the majority of the studies on *C. elegans* RNAi, including those referenced in this text, specifically refer to the N2 Bristol strain – the commonly used "wild type" strain for *C. elegans* research. However, there are variations in RNAi efficacy among wild isolates of *C. elegans* (FELIX *et al.* 2011). While the genetic basis for some of these variations is known, such as a polymorphism in a specific RNAi gene (SIMMER *et al.* 2002), other sources for such differences remain to be found. Future research into these population-specific RNAi efficacy differences for *C. elegans* and other species will be extremely relevant because it provides a clue as to the evolutionary scale at which changes in RNAi pathways may occur.

It seems reasonable to apply the lessons of the deep mechanistic and phenomenological observation made in *C. elegans*, as a first step towards enabling the highest probability of optimizing RNAi in other species. There will inevitably be species in which RNAi does not work, but the conservation of basal RNAi machinery suggests that more often than not, RNAi will function in most species.

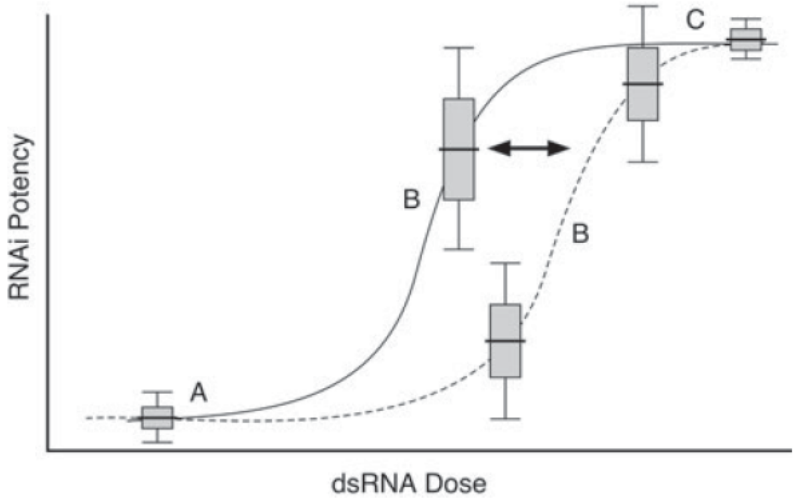

Figure 1.6: RNAi phenotypic penetrance is sensitive to dsRNA dose

Measurements of RNAi potency (penetrance) versus dsRNA dose show a sigmoidal relationship with high variability surround the inflection point (B). At low (A) and high (C) dsRNA dose, most worms do not at all or completely do respond. However, slight variations in delivered dsRNA dose at intermediate concentrations can have dramatic effects on perceived phenotypes. Mutations that enhance RNAi tend to shift such dose-response curves toward lower dsRNA dose (red) without noticeably affecting the shape of the curve.

AIMS AND QUESTIONS

Given what is known about enhanced RNAi in *C. elegans*, my research was driven by three main questions. First, aside from hypersensitivity to exogenous RNAi triggers, what are the characteristics of the known Eri mutants and how are they different from other classes of enhanced RNAi? Second, what is the genetic mechanism behind enhanced RNAi? That is, why is an Eri mutant Eri? And third, what are the broader physiological impacts, if any, of the loss of the *eri* pathway on *C. elegans*?

I answer the first question in chapters two and three by performing in-depth phenotypic analysis of the known Eri mutants and by analyzing screens for novel RNAi factors under different contexts. These findings contribute to the field's understanding of exogenous RNAi, especially for inducing more effective use of enhanced RNAi technology through deeper understanding of its characteristics.

I answer the second question in chapters four and five by examining the role of nuclear RNAi as the genetic mechanism behind enhanced RNAi. These findings contribute to the field's understanding of the *eri* pathway's endogenous gene regulatory roles, and further underscore the spatial complexity of competing cellular small RNA pathways.

I answer the third question in chapter six by examining developmental markers in Eri mutants. These findings contribute to the field's understanding of the general physiological impact caused by the loss of *eri* endo-siRNAs in *C. elegans*.

LITERATURE CITED

ALTSCHUL, S. F., T. L. MADDEN, A. A. SCHAFFER, J. ZHANG, Z. ZHANG *et al.*, 1997 Gapped BLAST and PSI-BLAST: a new generation of protein database search programs. Nucleic Acids Res **25:** 3389-3402.

ANSEL, K. M., W. A. PASTOR, N. RATH, A. D. LAPAN, E. GLASMACHER *et al.*, 2008 Mouse Eri1 interacts with the ribosome and catalyzes 5.8S rRNA processing. Nat Struct Mol Biol **15:** 523-530.

BARTSCHERER, K., N. PELTE, D. INGELFINGER and M. BOUTROS, 2006 Secretion of Wnt ligands requires Evi, a conserved transmembrane protein. Cell **125:** 523-533.

BOUDREAU, R. L., A. M. MONTEYS and B. L. DAVIDSON, 2008 Minimizing variables among hairpin-based RNAi vectors reveals the potency of shRNAs. RNA **14:** 1834-1844.

BRIDGE, A. J., S. PEBERNARD, A. DUCRAUX, A. L. NICOULAZ and R. IGGO, 2003 Induction of an interferon response by RNAi vectors in mammalian cells. Nat Genet **34:** 263-264.

CALIXTO, A., D. CHELUR, I. TOPALIDOU, X. CHEN and M. CHALFIE, 2010 Enhanced neuronal RNAi in C. elegans using SID-1. Nat Methods **7:** 554-559.

CHEKULAEVA, M., and W. FILIPOWICZ, 2009 Mechanisms of miRNA-mediated post-transcriptional regulation in animal cells. Current Opinion in Cell Biology **21:** 452-460.

CLAYCOMB, J. M., P. J. BATISTA, K. M. PANG, W. GU, J. J. VASALE *et al.*, 2009 The Argonaute CSR-1 and its 22G-RNA cofactors are required for holocentric chromosome segregation. Cell **139:** 123-134.

CONINE, C. C., P. J. BATISTA, W. GU, J. M. CLAYCOMB, D. A. CHAVES *et al.*, 2010 Argonautes ALG-3 and ALG-4 are required for spermatogenesis-specific 26G-RNAs and thermotolerant sperm in Caenorhabditis elegans. Proc Natl Acad Sci U S A **107:** 3588-3593.

CROMBACH, A., and P. HOGEWEG, 2011 Is RNA-dependent RNA polymerase essential for transposon control? BMC Syst Biol **5:** 104.

CULLEN, B. R., 2006 Is RNA interference involved in intrinsic antiviral immunity in mammals? Nat Immunol **7:** 563-567.

CZECH, B., and G. J. HANNON, 2011 Small RNA sorting: matchmaking for Argonautes. Nat Rev Genet **12:** 19-31.

DALZELL, J. J., P. MCVEIGH, N. D. WARNOCK, M. MITREVA, D. M. BIRD *et al.*, 2011 RNAi Effector Diversity in Nematodes. PLoS Negl Trop Dis **5:** e1176.

DING, L., A. SPENCER, K. MORITA and M. HAN, 2005 The developmental timing regulator AIN-1 interacts with miRISCs and may target the argonaute protein ALG-1 to cytoplasmic P bodies in C. elegans. Mol Cell **19:** 437-447.

DING, S. W., 2010 RNA-based antiviral immunity. Nat Rev Immunol **10:** 632-644.

DUCHAINE, T. F., J. A. WOHLSCHLEGEL, S. KENNEDY, Y. BEI, D. CONTE, JR. *et al.*, 2006 Functional proteomics reveals the biochemical niche of C. elegans DCR-1 in multiple small-RNA-mediated pathways. Cell **124:** 343-354.

FAGARD, M., and H. VAUCHERET, 2000 Systemic silencing signal(s). Plant Mol Biol **43:** 285-293.

FEINBERG, E. H., and C. P. HUNTER, 2003 Transport of dsRNA into cells by the transmembrane protein SID-1. Science **301:** 1545-1547.

FELIX, M. A., 2008 RNA interference in nematodes and the chance that favored Sydney Brenner. J Biol **7:** 34.

FELIX, M. A., A. ASHE, J. PIFFARETTI, G. WU, I. NUEZ *et al.*, 2011 Natural and experimental infection of Caenorhabditis nematodes by novel viruses related to nodaviruses. PLoS Biol **9:** e1000586.

FISCHER, S. E., M. D. BUTLER, Q. PAN and G. RUVKUN, 2008 Trans-splicing in C. elegans generates the negative RNAi regulator ERI-6/7. Nature **455:** 491-496.

GELDHOF, P., L. MURRAY, A. COUTHIER, J. S. GILLEARD, G. MCLAUCHLAN *et al.*, 2006 Testing the efficacy of RNA interference in Haemonchus contortus. Int J Parasitol **36:** 801-810.

GELDHOF, P., A. VISSER, D. CLARK, G. SAUNDERS, C. BRITTON *et al.*, 2007 RNA interference in parasitic helminths: current situation, potential pitfalls and future prospects. Parasitology **134:** 609-619.

GENT, J. I., A. T. LAMM, D. M. PAVELEC, J. M. MANIAR, P. PARAMESWARAN *et al.*, 2010 Distinct phases of siRNA synthesis in an endogenous RNAi pathway in C. elegans soma. Mol Cell **37:** 679-689.

GENT, J. I., M. SCHVARZSTEIN, A. M. VILLENEUVE, S. G. GU, V. JANTSCH *et al.*, 2009 A Caenorhabditis elegans RNA-directed RNA polymerase in sperm development and endogenous RNA interference. Genetics **183:** 1297-1314.

GILLE, C., 2004 Structural interpretation of mutations and SNPs using STRAP-NT pp. Medical School Charite Berlin.

GRIMSON, A., M. SRIVASTAVA, B. FAHEY, B. J. WOODCROFT, H. R. CHIANG *et al.*, 2008 Early origins and evolution of microRNAs and Piwi-interacting RNAs in animals. Nature **455:** 1193-1197.

GRISHOK, A., and C. C. MELLO, 2002 RNAi (Nematodes: Caenorhabditis elegans). Adv Genet **46:** 339-360.

GRISHOK, A., J. L. SINSKEY and P. A. SHARP, 2005 Transcriptional silencing of a transgene by RNAi in the soma of C. elegans. Genes Dev **19:** 683-696.

GROVE, C. A., F. DE MASI, M. I. BARRASA, D. E. NEWBURGER, M. J. ALKEMA *et al.*, 2009 A multiparameter network reveals extensive divergence between C. elegans bHLH transcription factors. Cell **138:** 314-327.

GUANG, S., A. F. BOCHNER, K. B. BURKHART, N. BURTON, D. M. PAVELEC *et al.*, 2010 Small regulatory RNAs inhibit RNA polymerase II during the elongation phase of transcription. Nature **465:** 1097-1101.

GUANG, S., A. F. BOCHNER, D. M. PAVELEC, K. B. BURKHART, S. HARDING *et al.*, 2008 An Argonaute transports siRNAs from the cytoplasm to the nucleus. Science **321:** 537-541.

HABIG, J. W., P. J. ARUSCAVAGE and B. L. BASS, 2008 In C. elegans, high levels of dsRNA allow RNAi in the absence of RDE-4. PLoS One **3:** e4052.

HALL, T. M., 2005 Structure and function of argonaute proteins. Structure **13:** 1403-1408.

HANNON, G. J., 2002 RNA interference. Nature **418:** 244-251.

ISSA, Z., W. N. GRANT, S. STASIUK and C. B. SHOEMAKER, 2005 Development of methods for RNA interference in the sheep gastrointestinal parasite, Trichostrongylus colubriformis. Int J Parasitol **35:** 935-940.

JAKYMIW, A., S. LIAN, T. EYSTATHIOY, S. LI, M. SATOH *et al.*, 2005 Disruption of GW bodies impairs mammalian RNA interference. Nat Cell Biol **7:** 1267-1274.

JOSE, A. M., and C. P. HUNTER, 2007 Transport of sequence-specific RNA interference information between cells. Annu Rev Genet **41:** 305-330.

JOSE, A. M., J. J. SMITH and C. P. HUNTER, 2009 Export of RNA silencing from C. elegans tissues does not require the RNA channel SID-1. Proc Natl Acad Sci U S A **106:** 2283-2288.

KAMATH, R. S., and J. AHRINGER, 2003 Genome-wide RNAi screening in Caenorhabditis elegans. Methods **30:** 313-321.

KAMATH, R. S., A. G. FRASER, Y. DONG, G. POULIN, R. DURBIN *et al.*, 2003 Systematic functional analysis of the Caenorhabditis elegans genome using RNAi. Nature **421:** 231-237.

KELLEY, L. A., and M. J. STERNBERG, 2009 Protein structure prediction on the Web: a case study using the Phyre server. Nat Protoc **4:** 363-371.

KENNEDY, S., D. WANG and G. RUVKUN, 2004 A conserved siRNA-degrading RNase negatively regulates RNA interference in C. elegans. Nature **427:** 645-649.

KIM, D. H., M. A. BEHLKE, S. D. ROSE, M. S. CHANG, S. CHOI *et al.*, 2005a Synthetic dsRNA Dicer substrates enhance RNAi potency and efficacy. Nat Biotechnol **23:** 222-226.

KIM, J. K., H. W. GABEL, R. S. KAMATH, M. TEWARI, A. PASQUINELLI *et al.*, 2005b Functional genomic analysis of RNA interference in C. elegans. Science **308:** 1164-1167.

KNIGHT, S. W., and B. L. BASS, 2001 A role for the RNase III enzyme DCR-1 in RNA interference and germ line development in Caenorhabditis elegans. Science **293:** 2269-2271.

KNOX, D. P., P. GELDHOF, A. VISSER and C. BRITTON, 2007 RNA interference in parasitic nematodes of animals: a reality check? Trends Parasitol **23:** 105-107.

KRAUTZ-PETERSON, G., M. RADWANSKA, D. NDEGWA, C. B. SHOEMAKER and P. J. SKELLY, 2007 Optimizing gene suppression in schistosomes using RNA interference. Mol Biochem Parasitol **153:** 194-202.

KRUEGER, U., T. BERGAUER, B. KAUFMANN, I. WOLTER, S. PILK *et al.*, 2007 Insights into effective RNAi gained from large-scale siRNA validation screening. Oligonucleotides **17:** 237-250.

KUWABARA, P. E., and A. COULSON, 2000 RNAi--prospects for a general technique for determining gene function. Parasitol Today **16:** 347-349.

LEE, R. C., C. M. HAMMELL and V. AMBROS, 2006 Interacting endogenous and exogenous RNAi pathways in Caenorhabditis elegans. RNA **12:** 589-597.

LIU, J., M. A. VALENCIA-SANCHEZ, G. J. HANNON and R. PARKER, 2005 MicroRNA-dependent localization of targeted mRNAs to mammalian P-bodies. Nat Cell Biol **7:** 719-723.

LU, R., M. MADURO, F. LI, H. W. LI, G. BROITMAN-MADURO *et al.*, 2005 Animal virus replication and RNAi-mediated antiviral silencing in Caenorhabditis elegans. Nature **436:** 1040-1043.

MACRAE, I. J., K. ZHOU, F. LI, A. REPIC, A. N. BROOKS *et al.*, 2006 Structural basis for double-stranded RNA processing by Dicer. Science **311:** 195-198.

MAEDA, I., Y. KOHARA, M. YAMAMOTO and A. SUGIMOTO, 2001 Large-scale analysis of gene function in Caenorhabditis elegans by high-throughput RNAi. Curr Biol **11:** 171-176.

MAIDA, Y., and K. MASUTOMI, 2011 RNA-dependent RNA polymerases in RNA silencing. Biol Chem **392:** 299-304.

MCEWAN, D. L., A. S. WEISMAN and C. P. HUNTER, 2012 Uptake of extracellular double-stranded RNA by SID-2. Mol Cell **47:** 746-754.

MIKUMA, T., H. KAWASAKI, Y. YAMAMOTO and K. TAIRA, 2004 Overexpression of Dicer enhances RNAi-mediated gene silencing by short-hairpin RNAs (shRNAs) in human cells. Nucleic Acids Symp Ser (Oxf)**:** 191-192.

MITTAL, V., 2004 Improving the efficiency of RNA interference in mammals. Nat Rev Genet **5:** 355-365.

MOAZED, D., 2009 Small RNAs in transcriptional gene silencing and genome defence. Nature **457:** 413-420.

MOCHIZUKI, K., 2010 RNA-directed epigenetic regulation of DNA rearrangements. Essays Biochem **48:** 89-100.

MOTAMEDI, M. R., A. VERDEL, S. U. COLMENARES, S. A. GERBER, S. P. GYGI *et al.*, 2004 Two RNAi complexes, RITS and RDRC, physically interact and localize to noncoding centromeric RNAs. Cell **119:** 789-802.

MOURRAIN, P., C. BECLIN, T. ELMAYAN, F. FEUERBACH, C. GODON *et al.*, 2000 Arabidopsis SGS2 and SGS3 genes are required for posttranscriptional gene silencing and natural virus resistance. Cell **101:** 533-542.

NASEVICIUS, A., and S. C. EKKER, 2000 Effective targeted gene 'knockdown' in zebrafish. Nat Genet **26:** 216-220.

PADDISON, P. J., and P. K. VOGT (Editors), 2008 *RNA Interference*. Springer.

PAK, J., and A. FIRE, 2007 Distinct populations of primary and secondary effectors during RNAi in C. elegans. Science **315:** 241-244.

PAL-BHADRA, M., U. BHADRA and J. A. BIRCHLER, 2002 RNAi related mechanisms affect both transcriptional and posttranscriptional transgene silencing in Drosophila. Mol Cell **9:** 315-327.

PAVELEC, D. M., J. LACHOWIEC, T. F. DUCHAINE, H. E. SMITH and S. KENNEDY, 2009 Requirement for the ERI/DICER complex in endogenous RNA interference and sperm development in Caenorhabditis elegans. Genetics **183:** 1283-1295.

PERRIMON, N., J. Q. NI and L. PERKINS, 2010 In vivo RNAi: today and tomorrow. Cold Spring Harb Perspect Biol **2:** a003640.

PRAITIS, V., E. CASEY, D. COLLAR and J. AUSTIN, 2001 Creation of low-copy integrated transgenic lines in Caenorhabditis elegans. Genetics **157:** 1217-1226.

REA, S. L., VENTURA, N., JOHNSON, T.E., 2007 Relationship between mitochondrial electron transport chain dysfunction, development, and life extension in Caenorhabditis elegans. PLoS Biology **5:** 2312-2329.

RUAL, J. F., J. CERON, J. KORETH, T. HAO, A. S. NICOT *et al.*, 2004 Toward improving Caenorhabditis elegans phenome mapping with an ORFeome-based RNAi library. Genome Res **14:** 2162-2168.

SALEH, M. C., R. P. VAN RIJ, A. HEKELE, A. GILLIS, E. FOLEY *et al.*, 2006 The endocytic pathway mediates cell entry of dsRNA to induce RNAi silencing. Nat Cell Biol **8:** 793-802.

SCHEPERS, U., 2005 *RNA interference in practice*. Wiley-VCH, Weinheim.

SCHOTT, D. H., D. K. CURETON, S. P. WHELAN and C. P. HUNTER, 2005 An antiviral role for the RNA interference machinery in Caenorhabditis elegans. Proc Natl Acad Sci U S A **102:** 18420-18424.

SHABALINA, S. A., and E. V. KOONIN, 2008 Origins and evolution of eukaryotic RNA interference. Trends Ecol Evol **23:** 578-587.

SHARP, P. A., 1999 RNAi and double-strand RNA. Genes & Development **13:** 139-141.

SHIH, J. D., M. C. FITZGERALD, M. SUTHERLIN and C. P. HUNTER, 2009 The SID-1 double-stranded RNA transporter is not selective for dsRNA length. RNA **15:** 384-390.

SHIH, J. D., and C. P. HUNTER, 2011 SID-1 is a dsRNA-selective dsRNA-gated channel. RNA.

SIJEN, T., J. FLEENOR, F. SIMMER, K. L. THIJSSEN, S. PARRISH *et al.*, 2001 On the role of RNA amplification in dsRNA-triggered gene silencing. Cell **107:** 465-476.

SIJEN, T., and R. H. PLASTERK, 2003 Transposon silencing in the Caenorhabditis elegans germ line by natural RNAi. Nature **426:** 310-314.

SILVA, J., K. CHANG, G. J. HANNON and F. V. RIVAS, 2004 RNA-interference-based functional genomics in mammalian cells: reverse genetics coming of age. Oncogene **23:** 8401-8409.

SIMMER, F., C. MOORMAN, A. M. VAN DER LINDEN, E. KUIJK, P. V. VAN DEN BERGHE *et al.*, 2003 Genome-wide RNAi of C. elegans using the hypersensitive rrf-3 strain reveals novel gene functions. PLoS Biol **1:** E12.

SIMMER, F., M. TIJSTERMAN, S. PARRISH, S. P. KOUSHIKA, M. L. NONET *et al.*, 2002 Loss of the putative RNA-directed RNA polymerase RRF-3 makes C. elegans hypersensitive to RNAi. Curr Biol **12:** 1317-1319.

SIOUD, M., 2011 Promises and challenges in developing RNAi as a research tool and therapy. Methods Mol Biol **703:** 173-187.

SLEDZ, C. A., M. HOLKO, M. J. DE VEER, R. H. SILVERMAN and B. R. WILLIAMS, 2003 Activation of the interferon system by short-interfering RNAs. Nat Cell Biol **5:** 834-839.

SMARDON, A., J. M. SPOERKE, S. C. STACEY, M. E. KLEIN, N. MACKIN *et al.*, 2000 EGO-1 is related to RNA-directed RNA polymerase and functions in germ-line development and RNA interference in C. elegans. Curr Biol **10:** 169-178.

SONG, J. J., S. K. SMITH, G. J. HANNON and L. JOSHUA-TOR, 2004 Crystal structure of Argonaute and its implications for RISC slicer activity. Science **305:** 1434-1437.

STEINER, F. A., K. L. OKIHARA, S. W. HOOGSTRATE, T. SIJEN and R. F. KETTING, 2009 RDE-1 slicer activity is required only for passenger-strand cleavage during RNAi in Caenorhabditis elegans. Nat Struct Mol Biol **16:** 207-211.

SVOBODA, P., and P. STEIN, 2009 RNAi experiments in mouse oocytes and early embryos. Cold Spring Harb Protoc **2009:** pdb top56.

TABARA, H., M. SARKISSIAN, W. G. KELLY, J. FLEENOR, A. GRISHOK *et al.*, 1999 The rde-1 gene, RNA interference, and transposon silencing in C. elegans. Cell **99:** 123-132.

TEIXEIRA, F. K., and V. COLOT, 2010 Repeat elements and the Arabidopsis DNA methylation landscape. Heredity **105:** 14-23.

TIMMONS, L., D. L. COURT and A. FIRE, 2001 Ingestion of bacterially expressed dsRNAs can produce specific and potent genetic interference in Caenorhabditis elegans. Gene **263:** 103-112.

TIMMONS, L., and A. FIRE, 1998 Specific interference by ingested dsRNA. Nature **395:** 854.

TOMARI, Y., C. MATRANGA, B. HALEY, N. MARTINEZ and P. D. ZAMORE, 2004 A protein sensor for siRNA asymmetry. Science **306:** 1377-1380.

ULVILA, J., M. PARIKKA, A. KLEINO, R. SORMUNEN, R. A. EZEKOWITZ *et al.*, 2006 Double-stranded RNA is internalized by scavenger receptor-mediated endocytosis in Drosophila S2 cells. J Biol Chem **281:** 14370-14375.

VANCE, V., and H. VAUCHERET, 2001 RNA silencing in plants--defense and counterdefense. Science **292:** 2277-2280.

VASALE, J. J., W. GU, C. THIVIERGE, P. J. BATISTA, J. M. CLAYCOMB *et al.*, 2010 Sequential rounds of RNA-dependent RNA transcription drive endogenous small-RNA biogenesis in the ERGO-1/Argonaute pathway. Proc Natl Acad Sci U S A **107:** 3582-3587.

WANG, D., S. KENNEDY, D. CONTE, JR., J. K. KIM, H. W. GABEL *et al.*, 2005 Somatic misexpression of germline P granules and enhanced RNA interference in retinoblastoma pathway mutants. Nature **436:** 593-597.

WELKER, N. C., D. M. PAVELEC, D. A. NIX, T. F. DUCHAINE, S. KENNEDY *et al.*, 2010 Dicer's helicase domain is required for accumulation of some, but not all, C. elegans endogenous siRNAs. RNA **16:** 893-903.

WHANGBO, J. S., and C. P. HUNTER, 2008 Environmental RNA interference. Trends Genet **24:** 297-305.

WHITE, S. A., and R. C. ALLSHIRE, 2008 RNAi-mediated chromatin silencing in fission yeast. Curr Top Microbiol Immunol **320:** 157-183.

WILKINS, C., R. DISHONGH, S. C. MOORE, M. A. WHITT, M. CHOW *et al.*, 2005 RNA interference is an antiviral defence mechanism in Caenorhabditis elegans. Nature **436:** 1044-1047.

WINSTON, W. M., C. MOLODOWITCH and C. P. HUNTER, 2002 Systemic RNAi in C. elegans requires the putative transmembrane protein SID-1. Science **295:** 2456-2459.

WINSTON, W. M., M. SUTHERLIN, A. J. WRIGHT, E. H. FEINBERG and C. P. HUNTER, 2007 Caenorhabditis elegans SID-2 is required for environmental RNA interference. Proc Natl Acad Sci U S A **104:** 10565-10570.

YANG, D., H. LU and J. W. ERICKSON, 2000 Evidence that processed small dsRNAs may mediate sequence-specific mRNA degradation during RNAi in Drosophila embryos. Curr Biol **10:** 1191-1200.

YIGIT, E., P. J. BATISTA, Y. BEI, K. M. PANG, C. C. CHEN *et al.*, 2006 Analysis of the C. elegans Argonaute family reveals that distinct Argonautes act sequentially during RNAi. Cell **127:** 747-757.

ZAMORE, P. D., T. TUSCHL, P. A. SHARP and D. P. BARTEL, 2000 RNAi: double-stranded RNA directs the ATP-dependent cleavage of mRNA at 21 to 23 nucleotide intervals. Cell **101:** 25-33.

ZHUANG, J. J., and C. P. HUNTER, 2011 Tissue Specificity of Caenorhabditis elegans Enhanced RNA Interference Mutants. Genetics **188:** 235-237.

Chapter Two

Tissue-specificity of *C. elegans* enhanced RNAi mutants

The contents were previously published in ZHUANG, J. J., and C. P. HUNTER, 2011. Tissue Specificity of *Caenorhabditis elegans* enhanced RNA interference mutants. *Genetics* **188**: 235-237. Permission to reuse was granted by the Genetics Society of America.

ABSTRACT

Gene knockdown by RNA interference (RNAi) in *Caenorhabditis elegans* is readily achieved by feeding bacteria expressing double-stranded RNA (dsRNA). Enhanced RNAi (Eri) mutants facilitate RNAi due to their hypersensitivity to dsRNA. Here, we compared eight Eri mutants for sensitivity to ingested dsRNA targeting a variety of tissue-specific genes.

INTRODUCTION

The effectiveness of double-strand RNA (dsRNA) delivery in *Caenorhabditis elegans* has made high-throughput RNA interference (RNAi) screens an essential research tool (MITANI 2009). For RNAi screens, dsRNA is usually administered via feeding RNAi, whereby worms ingest bacteria expressing gene-specific dsRNA (referred to as RNAi food). This is less potent than microinjecting dsRNAs, perhaps due to the lower amounts of internalized dsRNA (TIMMONS and FIRE 1998). The discovery of enhanced RNAi (Eri) mutants, which increases the sensitivity of worms to dsRNA, increases the discovery of RNAi phenotypes in large-scale screens. Nine Eri loci have been discovered thus far (DUCHAINE *et al.* 2006; FISCHER *et al.* 2008; KENNEDY *et al.* 2004; PAVELEC *et al.* 2009; SIMMER *et al.* 2002).

Although a variety of Eri mutants are used in RNAi screens, their selection has been *ad hoc*, as no systematic comparative analysis of the Eri strains has been reported. Such an analysis would provide a logical basis for selecting the most sensitive Eri mutant for general and tissue-specific screens. Here, we comprehensively characterize the tissue-specific RNAi sensitivities of eight Eri mutants.

RESULTS AND DISCUSSION

To characterize phenotypic differences among Eri mutants, we compared the relative penetrance of RNAi sensitivity at varying doses of dsRNA expressing bacteria (REA 2007). For each bacterial strain that expresses dsRNA targeting a *C. elegans* gene, we scored only one defined knockdown phenotype (**Table 2.1**). A representative dilution series is shown in **Figure 2.1** (**Table 2.2**). We sought to use this dose-response data to compare the enhanced silencing for each Eri mutant. For all strains, the variability in penetrance is greatest at intermediate dsRNA doses, suggesting a threshold effect. This variability, best observed via coefficient of variations (**Table 2.3**), strongly interferes with determining the onset of silencing. In contrast, the trend towards reduced variability at higher dsRNA doses provides a means to discriminate among Eri mutants. Based on this analysis, we developed a criterion for selecting the "most effective" Eri: one(s) that causes near complete (upper bound of 95% confidence interval at least 100% penetrant) and robust (less than 10% standard deviation) silencing at the lowest dsRNA dose.

We used the methods and criterion described to evaluate eight Eri mutants on 24 RNAi foods in eight tissues. The results of this analysis are presented in **Figure 2.2** (**Tables 2.4-2.27**). The majority of Eri mutants enhanced RNAi for nearly all tested tissues, but all showed relative differences in RNAi hypersensitivity for some foods. Our comprehensive phenotypic analysis of the Eri mutants indicates that they are not equivalent, consistent with the reported non-overlapping expression profiles of *eri-1* and *rrf-3* mutants (LEE *et al.* 2006).

In all experiments, we observed a sigmoidal curve for silencing penetrance versus RNAi concentration; at intermediate concentrations, the variance was highest. Therefore, to minimize variability associated with dose, all feeding RNAi assays should be preceded by a dilution series control to ensure that the RNAi food is not used at an "inflection point" concentration.

Table 2.1: Phenotypes scored for RNAi foods

The tissue-specific phenotype for each of the genes targeted by RNAi foods in **Figure 2.2** are listed and referenced. Single asterisk (*) indicates foods whose gene targets are grouped to a tissue due to high expression in that particular tissue. Double asterisks (**) indicate food whose gene target is grouped to a tissue due to phenotype scored resulting from defects within that particular tissue. The remaining foods are grouped to a tissue due to both expression and phenotype arising from a particular tissue's effects.

Table 2.1 (Continued): Phenotypes scored for RNAi foods

Tissue	Food	Phenotype	Reference
Epidermis	*bli-1*	Large blisters on animals	(MYLLYHARJU and KIVIRIKKO 2004)
Epidermis	*dpy-11*	Severely dumpy animals whose length is at most 3X its width	(KO and CHOW 2003)
Epidermis	*dpy-13*	Severely dumpy animals whose length is at most 3X its width	(BIRD 1992)
Gonad	*fkh-6*	Brood size reduction in developed L3s or older worms Affected animals are lethally absent	(CHANG *et al.* 2004)
Gonad	*gon-1*	Brood size reduction in developed L3s or older worms Affected animals are lethally absent	(TAMAI and NISHIWAKI 2007)
Gonad	*gon-4*	Severely protruding or absent gonad	(CHURCH and LAMBIE 2003)
Intestine	*act-5*	Brood size reduction in developed L3s or older worms Affected animals are lethally absent	(MACQUEEN *et al.* 2005)
Intestine	*gtl-1**	Brood size reduction in developed L3s or older worms Affected animals are significantly smaller in morphology	(XING *et al.* 2008)
Intestine	*ifc-2*	Bent posterior body morphology that paralyzes locomotion	(HUSKEN *et al.* 2008)
Muscle	*act-3*	Brood size reduction in developed L3s or older worms Affected animals are lethally absent	(MEISSNER *et al.* 2009)
Muscle	*myo-3*	Brood size reduction in developed L3s or older worms Affected animals are lethally absent	(AHNN and FIRE 1994)
Muscle	*unc-22*	Severe twitching that paralyzes locomotion	(FIRE *et al.* 1991)
Neuron	*hbl-1***	Paralysis	Thompson-Peer, K.L. 2009 *(unpublished)*
Neuron	*hmr-1**	Brood size reduction in developed L3s or older worms Affected animals are significantly smaller in morphology	(BROADBENT and PETTITT 2002)
Neuron	*unc-73*	Paralysis	(VANDERZALM *et al.* 2009)
Pharynx	*div-1**	Brood size reduction in developed L3s or older worms Affected animals are significantly smaller in morphology	(MCKAY *et al.* 2003)
Pharynx	*pbs-6**	Brood size reduction in developed L3s or older worms Affected animals are significantly smaller in morphology	(WANG *et al.* 2006)
Pharynx	*pha-4*	Brood size reduction in developed L3s or older worms Affected animals are lethally absent	(MANGO 2007)
Ubiquitous	*cdk-1*	Brood size reduction in developed L3s or older worms Affected animals are lethally absent	(SEYDOUX and FIRE 1994)
Ubiquitous	*knl-3*	Brood size reduction in developed L3s or older worms Affected animals are lethally absent	(CHEESEMAN *et al.* 2004)
Ubiquitous	*vha-15*	Brood size reduction in developed L3s or older worms Affected animals are lethally absent	(HUNT-NEWBURY *et al.* 2007)
Germline	*glp-1*	Absent germline in adult hermaphrodites	(VOUGHT *et al.* 2005)
Germline	*par-1*	Brood size reduction in developed L3s or older worms Affected animals are lethally absent	(BOWERMAN *et al.* 1997)
Germline	*pos-1*	Brood size reduction in developed L3s or older worms Affected animals are lethally absent	(TABARA *et al.* 1999)

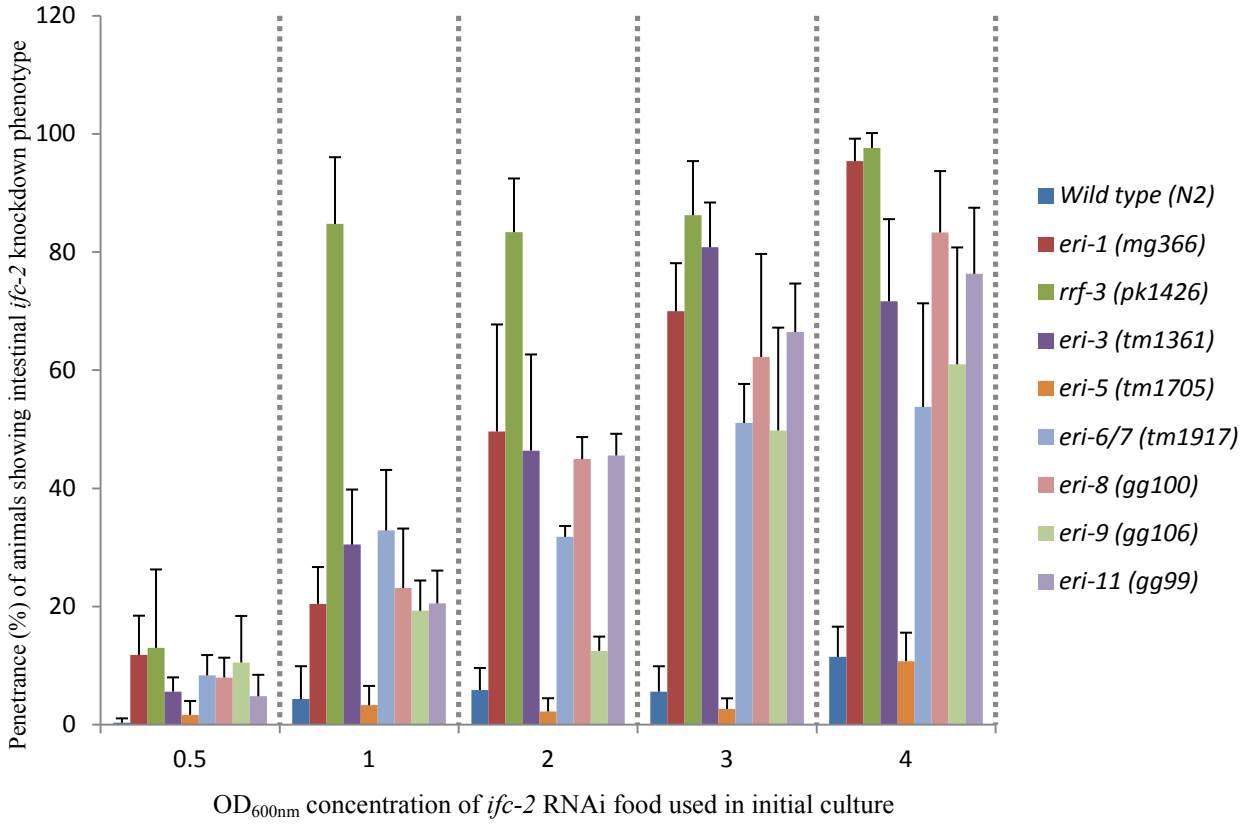

Figure 2.1: Dilution series of Eri responses by RNAi feeding against *ifc-2*

Single L3-stage larvae were placed on RNAi food targeting *ifc-2*; 4 days later, the percent of progeny showing the expected bent posterior and accompanying paralysis at each indicated concentration (OD at 600 nm) of initial bacterial culture were determined. For clarity, three bacterial culture concentrations (OD_{600nm} of 0.1, 0.25, and 0.75), which produced similar Eri penetrances as adjacent concentrations, are not included. Error bars represent standard deviation.

Table 2.2: Dilution series of Eri responses by RNAi feeding against *ifc-2*

Single L3-stage larvae were placed on RNAi food targeting *ifc-2*; 4 days later, the percent of progeny showing the expected bent posterior and accompanying paralysis at each indicated concentration (OD at 600 nm) of initial bacterial culture were determined. For clarity, three bacterial culture concentrations (OD_{600nm} of 0.1, 0.25, and 0.75), which produced similar Eri penetrances as adjacent concentrations, are not included. The tabulated mean (Avg) and standard deviation (SD) for N2 wild type were used as the basis to indicate an Eri or a Rde phenotype (Eri?), with $p<0.05$ as the criterion to denote significant difference from wild type response levels. A strain which fits the "best *eri*" criterion described in text is marked as "best", with asterisks indicating concentrations of RNAi food at which it fulfilled the criterion.

Table 2.2 (Continued): Dilution series results for *ifc-2* feeding

Strain	*OD_{600}*	*Penetrance readings*							*Avg*	*SD*	*Eri?*
Wild type (N2)	**0.5**	0/22	0/27	0/20	0/23	1/60			**0**	**0.01**	
	1	1/24	3/22	1/26	0/23	0/24			**0.04**	**0.06**	
	2	0/20	3/59	3/31	2/24	2/32			**0.06**	**0.04**	
	3	2/27	2/30	1/35	4/36	0/23			**0.06**	**0.04**	
	4	5/36	2/26	4/30	4/33	8/39	2/31	2/31	**0.11**	**0.05**	
eri-1 (mg366)	**0.5**	3/20	1/22	2/32	2/16	10/48			**0.12**	**0.07**	**Yes**
	1	6/21	8/34	5/29	4/33	5/24			**0.20**	**0.06**	**Yes**
	2	7/28	11/18	13/24	21/30	11/29			**0.50**	**0.18**	**Yes**
	3	17/24	20/31	19/32	22/29	23/29			**0.70**	**0.08**	**Yes**
	4	33/33	39/42	54/57	41/43	23/23	21/22	25/28	**0.95**	**0.04**	**Yes**
rrf-3 (pk1426) *Best*	**0.5**	5/25	0/38	4/28	0/10	12/39			**0.13**	**0.13**	
	1	20/28	25/28	35/46	20/23	33/33			**0.85**	**0.11**	**Yes**
	2**	32/39	24/25	22/25	13/18	22/28			**0.83**	**0.09**	**Yes**
	3**	15/19	22/23	16/21	45/47	33/39			**0.86**	**0.09**	**Yes**
	4**	29/30	28/30	10/10	29/30	20/20	40/40	29/30	**0.98**	**0.03**	**Yes**
eri-3 (tm1361)	**0.5**	6/80	2/90	5/60	1/20	2/40			**0.06**	**0.02**	**Yes**
	1	6/17	4/23	7/18	6/25	7/19			**0.30**	**0.09**	**Yes**
	2	12/16	5/14	12/30	7/16	6/16			**0.46**	**0.16**	**Yes**
	3	16/19	12/13	12/16	17/23	11/14			**0.81**	**0.08**	**Yes**
	4	15/20	17/19	11/17	12/15	8/17	17/26	16/20	**0.72**	**0.14**	**Yes**
eri-5 (tm1705)	**0.5**	4/80	2/60	0/20	0/20	0/20			**0.02**	**0.02**	
	1	0/44	3/60	0/20	3/40	2/50			**0.03**	**0.03**	
	2	0/20	2/80	3/80	0/20	2/40			**0.02**	**0.02**	
	3	0/28	1/40	1/40	2/60	4/80			**0.03**	**0.02**	
	4	1/31	4/30	3/48	3/22	5/33	7/54		**0.11**	**0.05**	
eri-6/7 (tm1917)	**0.5**	2/27	3/21	2/34	3/37	2/33			**0.08**	**0.03**	**Yes**
	1	13/26	8/26	6/25	5/19	9/27			**0.33**	**0.10**	**Yes**
	2	8/26	10/33	11/34	8/23	12/39			**0.32**	**0.02**	**Yes**
	3	9/22	13/22	16/30	10/20	13/25			**0.51**	**0.07**	**Yes**
	4	14/36	15/35	10/27	28/37	12/19	8/19	23/30	**0.54**	**0.18**	**Yes**
eri-8 (gg100)	**0.5**	3/23	2/28	4/42	2/39	2/39			**0.08**	**0.03**	**Yes**
	1	4/22	2/25	7/25	9/32	6/18			**0.23**	**0.10**	**Yes**
	2	9/23	12/26	13/27	10/23	11/23			**0.45**	**0.04**	**Yes**
	3	11/23	20/24	10/23	12/20	36/47			**0.62**	**0.17**	**Yes**
	4	17/24	24/27	24/28	20/30	31/36	31/34	45/48	**0.83**	**0.10**	**Yes**
eri-9 (gg106)	**0.5**	2/26	6/26	2/32	5/39	1/35			**0.04**	**0.08**	
	1	7/32	10/41	8/40	4/37	6/31			**0.09**	**0.05**	**Yes**
	2	3/20	3/27	3/32	4/27	5/41			**0.12**	**0.02**	**Yes**
	3	13/26	21/27	8/25	12/24	11/28			**0.50**	**0.17**	**Yes**
	4	9/21	10/21	14/30	16/28	17/24	13/21	10/10	**0.61**	**0.20**	**Yes**
eri-11 (gg99)	**0.5**	0/32	1/30	2/30	2/45	3/31			**0.05**	**0.04**	
	1	6/25	6/29	3/24	10/37	5/27			**0.21**	**0.06**	**Yes**
	2	13/31	13/26	13/28	11/23	10/24			**0.46**	**0.04**	**Yes**
	3	12/20	23/29	14/23	23/37	21/30			**0.66**	**0.08**	**Yes**
	4	18/26	24/25	30/35	19/27	21/30	22/28	18/28	**0.76**	**0.11**	**Yes**

Table 2.3: Coefficient of variation for Eri responses by RNAi feeding against *ifc-2*

Strains / OD_{600}	*Wild type (N2)*	*eri-1 (mg366)*	*rrf-3 (pk1426)*	*eri-3 (tm1361)*	*eri-5 (tm1705)*	*eri-6/7 (tm1917)*	*eri-8 (gg100)*	*eri-9 (gg106)*	*eri-11 (gg99)*
0.5	2.24	0.56	1.02	0.43	1.41	0.41	0.42	0.75	0.75
1	1.29	0.30	0.13	0.31	0.99	0.31	0.44	0.27	0.27
2	0.64	0.36	0.11	0.35	0.99	0.06	0.08	0.19	0.08
3	0.77	0.12	0.11	0.09	0.68	0.13	0.28	0.35	0.12
4	0.44	0.04	0.03	0.19	0.45	0.33	0.12	0.32	0.15

Variability strongly interferes with determining the onset of RNAi silencing. Therefore, those strains with the lowest coefficient of variation at the lowest dosage of RNAi triggers, such as *rrf-3(pk1426)* during *ifc-2(RNAi)* – highlighted in yellow – are deemed the "best" Eri strains.

Figure 2.2: Summary metric of tissue-specific Eri efficacy

Summary of Eri efficiency for the eight Eri strains tested on 24 RNAi foods representing eight tissues. A strain exhibiting significantly higher (*t* test $p<0.05$) penetrance than the N2 wild type strain's penetrance (green), at any tested bacterial RNAi food concentration, is marked as Eri (yellow or red). Strains exhibiting an Eri phenotype that have an upper bound of 95% confidence interval at least 100% penetrant with a less than 10% standard deviation are marked as the "best" Eri (red). "T.S. sterile" indicates strains that exhibit temperature-sensitive sterility at 25ºC.

	T.S. sterile	Epidermis			Gonad			Intestine			Muscle			Neuron			Pharynx			Ubiquitous			Germline		
		bli -1	*dpy -11*	*dpy -13*	*fkh -6*	*gon -1*	*gon -4*	*act -5*	*gtl -1*	*ifc -2*	*act - 3*	*myo -3*	*unc -22*	*hbl -1*	*hmr -1*	*unc -73*	*div -1*	*pbs -6*	*pha -4*	*cdk -1*	*knl -3*	*vha -15*	*glp -1*	*par -1*	*pos -1*
Wild type *(N2)*	No																							
eri-1 (mg366)	Yes																							
rrf-3 (pk1426)	Yes																							
eri-3 (tm1361)	Yes																							
eri-5 (tm1705)	No																							
eri-6/7 (tm1917)	No																							
ergo-1/eri-8 (gg100)	No																							
eri-9 (gg106)	No																							
eri-11 (gg99)	No																							

Figure 2.2 (Continued): Summary metric of tissue-specific Eri efficacy

Table 2.4: Dilution series of Eri responses by RNAi feeding against *bli-1*

Single L3-stage larvae were placed on RNAi food targeting *bli-1*; 4 days later, the percent of progeny showing the expected large blisters on the animals at each indicated concentration (OD at 600 nm) of initial bacterial culture were determined. For clarity, three bacterial culture concentrations (OD_{600nm} of 0.025, 0.25, and 4), which produced similar Eri penetrances as adjacent concentrations, are not included. The tabulated mean (Avg) and standard deviation (SD) for N2 wild type were used as the basis to indicate an Eri or a Rde phenotype (Eri?), with $p<0.05$ as the criterion to denote significant difference from wild type response levels. A strain which fits the "best *eri*" criterion described in text is marked as "best", with asterisks indicating concentrations of RNAi food at which it fulfilled the criterion.

Table 2.4 (Continued): Dilution series results for *bli-1* feeding

Strain	*OD_{600}*	*Penetrance readings*												*Avg*	*SD*	*Eri?*
Wildtype (N2)	**0.1**	1/86	0/32	1/64	2/80	0/20	0/20	0/20	0/20	0/20	0/20	0/20		**0**	**0.01**	
	0.5	23/83	30/123	23/102	23/97	0/20	0/20	0/20	0/20	1/45				**0.11**	**0.13**	
	1	24/124	2/18	6/38	5/47	9/47	4/26							**0.15**	**0.04**	
	2	81/163	98/178	78/164	46/134	39/113	45/109	45/107	19/40	27/41	9/26			**0.45**	**0.10**	
	3	16/27	131/196	132/212	45/53	38/52	46/57	60/70	43/53					**0.74**	**0.10**	
eri-1 (mg366) <u>*Best*</u>	**0.1**	9/80	13/73	12/61	11/79	24/76	0/64	0/40	0/20	0/20	0/20	1/60	0/20	**0.08**	**0.11**	
	0.5	37/82	12/29	37/90	59/116	51/93	48/90	23/58	10/34	10/38	12/51	21/34	6/23	**0.41**	**0.13**	**Yes**
	1	63/87	34/36	45/56	27/31	40/45	44/48	33/39						**0.86**	**0.07**	**Yes**
	2	71/84	59/73	43/60	69/82	86/102	44/51	31/37	44/53					**0.82**	**0.05**	**Yes**
	3**	57/59	95/110	66/80	68/74	20/20	84/92	68/85						**0.90**	**0.07**	**Yes**
rrf-3 (pk1426)	**0.1**	6/48	0/20	0/20	0/20	0/20	0/20							**0.02**	**0.05**	
	0.5	83/115	55/108	14/27	28/54	21/46	20/45	21/43						**0.52**	**0.09**	**Yes**
	1	88/121	66/84	37/73	70/123	18/35	60/70	58/84	45/60	78/91				**0.70**	**0.14**	**Yes**
	2	102/104	74/87	34/42	33/42	45/56	28/38	44/51	7/9					**0.83**	**0.07**	**Yes**
	3	110/112	73/79	5/7	31/43	39/46	37/42	42/50	60/65					**0.85**	**0.10**	**Yes**
eri-3 (tm1361)	**0.1**	16/81	23/69	22/92	5/87	16/119	17/58	7/57	1/40	0/20	0/20	0/20	0/20	**0.12**	**0.12**	
	0.5	88/128	63/64	97/139	32/93	66/126	26/76	24/65	1/30	7/20	10/31	30/47	17/30	**0.49**	**0.25**	**Yes**
	1	62/96	88/105	57/100	7/25	28/106	25/72	9/40	12/58	21/41	12/44	18/42	19/51	**0.41**	**0.19**	**Yes**
	2	76/102	54/68	84/108	41/54	51/55	27/30	35/43	40/45					**0.83**	**0.07**	**Yes**
	3	84/99	54/67	95/103	54/78	43/48	21/26	7/9	42/52	37/44				**0.82**	**0.07**	**Yes**
eri-5 (tm1705)	**0.1**	3/80	2/80	0/23	1/50	0/20	0/20	0/20	0/20	0/20				**0.01**	**0.01**	
	0.5	3/63	5/25	0/20	1/60	6/50	5/50	0/20						**0.07**	**0.07**	
	1	80/168	60/159	70/184	13/46	41/96	9/24	8/26	2/33	3/49	8/40	4/52	23/109	**0.27**	**0.15**	
	2	59/146	60/166	63/162	25/62	10/26	21/63	18/45	15/41					**0.38**	**0.02**	
	3	42/54	59/66	47/66	29/44	29/38								**0.76**	**0.09**	
eri-6/7 (tm1917)	**0.1**	20/138	14/115	7/59	0/20	0/20	0/20	0/20						**0.06**	**0.07**	
	0.5	46/146	74/191	14/59	22/53	11/54	14/49	1/7						**0.28**	**0.10**	**Yes**
	1	40/156	45/145	24/122	1/5	11/64	21/69	14/44	15/33	10/27	13/41	14/45		**0.29**	**0.08**	**Yes**
	2	79/121	29/40	16/35	17/34	16/36								**0.56**	**0.13**	**Yes**
	3	30/48	49/61	19/28	22/29	32/42								**0.73**	**0.07**	**Yes**
eri-8 (gg100)	**0.1**	6/90	12/120	24/123	11/120	33/128	17/120	10/80	0/20	0/20	0/20	0/20	0/20	**0.08**	**0.09**	
	0.5	51/134	54/130	54/120	43/105	59/133	41/95	36/117	10/90	0/90	2/90	12/32		**0.30**	**0.17**	**Yes**
	1	76/164	84/188	94/193	48/142	100/181	34/88	5/11	38/79	14/52	3/18	4/19	9/19	**0.39**	**0.12**	**Yes**
	2	66/135	59/126	6/12	33/55	33/54	23/32	24/39	22/32					**0.59**	**0.09**	**Yes**
	3	34/44	29/34	29/39	24/32	39/48								**0.79**	**0.05**	**Yes**
eri-9 (gg106)	**0.1**	7/90	5/69	2/56	0/20	0/20	0/20	0/20	0/20					**0.02**	**0.03**	
	0.5	90/202	51/154	32/143	49/130	57/124	32/80	42/105	11/34	19/45	6/22			**0.37**	**0.08**	**Yes**
	1	17/29	33/52	31/48	19/28	33/45								**0.66**	**0.05**	**Yes**
	2	65/128	103/181	86/172	46/52	53/60	48/57	32/42	24/39					**0.70**	**0.17**	**Yes**
	3	40/44	54/58	7/8	6/7	23/29								**0.87**	**0.05**	**Yes**
eri-11 (gg99)	**0.1**	6/95	2/107	16/132	13/97	16/75	3/90	11/105	0/20	0/20	0/20	0/20	0/20	**0.06**	**0.07**	
	0.5	68/170	72/188	52/153	25/91	37/96	37/118	19/112	5/20	7/20	3/22	0/20	13/50	**0.27**	**0.12**	**Yes**
	1	74/189	68/139	25/38	16/27	12/24	15/31	21/36						**0.53**	**0.09**	**Yes**
	2	3/5	6/8	26/32	15/19	32/38								**0.76**	**0.09**	**Yes**
	3	17/22	7/9	20/24	13/24	32/43								**0.73**	**0.11**	**Yes**

Table 2.5: Dilution series of Eri responses by RNAi feeding against *dpy-11*

Single L3-stage larvae were placed on RNAi food targeting *dpy-11*; 4 days later, the percent of progeny showing the expected severe dumpiness, in which an animal's length is at most three times its width, at each indicated concentration (OD at 600 nm) of initial bacterial culture were determined. For clarity, one bacterial culture concentration (OD_{600nm} of 4), which produced similar Eri penetrances as adjacent concentrations, is not included. The tabulated mean (Avg) and standard deviation (SD) for N2 wild type were used as the basis to indicate an Eri or a Rde phenotype (Eri?), with $p<0.05$ as the criterion to denote significant difference from wild type response levels. A strain which fits the "best *eri*" criterion described in text is marked as "best", with asterisks indicating concentrations of RNAi food at which it fulfilled the criterion.

Table 2.5 (Continued): Dilution series results for *dpy-11* feeding

Strain	*OD_{600}*	*Penetrance readings*							*Avg*	*SD*	*Eri?*
Wildtype (N2)	**0.05**	0/20	0/20	0/40	1/70	0/20	0/20	0/20	**0**	**0.01**	
	0.1	0/20	0/60	0/20	0/20	0/20	0/20	1/45	**0**	**0.01**	
	0.5	4/78	16/78	8/49	6/38	3/20	11/27	4/30	**0.18**	**0.11**	
	1	27/43	13/20	18/28	13/27	13/25	29/59	14/29	**0.56**	**0.08**	
	3	41/42	36/38	14/19	20/20	20/20	18/20	29/31	**0.93**	**0.09**	
eri-1 (mg366) *Best*	**0.05**	9/38	14/32	11/47	9/30	4/31	7/47	12/37	**0.26**	**0.11**	**Yes**
	0.1	6/62	15/75	19/29	20/44	22/49	5/16	9/29	**0.35**	**0.18**	**Yes**
	0.5**	39/49	51/54	49/50	20/20	63/75	20/20	20/20	**0.94**	**0.08**	**Yes**
	1**	20/20	20/20	20/20	20/20	40/40	20/20	20/20	**1.00**	**0**	**Yes**
	3	20/20	20/20	20/20	20/20	59/60	20/20	20/20	**1.00**	**0.01**	
rrf-3 (pk1426)	**0.05**	2/30	2/41	4/57	4/47	3/53	5/52	7/46	**0.08**	**0.03**	**Yes**
	0.1	31/82	35/96	9/35	14/46	11/32	14/39	10/28	**0.34**	**0.04**	**Yes**
	0.5	38/53	26/27	20/20	20/20	20/20	20/20		**0.95**	**0.11**	**Yes**
	1	20/20	20/20	30/30	20/20	20/21	20/20		**0.99**	**0.02**	**Yes**
	3	20/20	20/20	20/20	20/20	20/20	20/20		**1.00**	**0**	
eri-3 (tm1361)	**0.05**	3/29	2/32	9/52	6/41	3/30	5/52	9/66	**0.12**	**0.04**	**Yes**
	0.1	5/25	6/74	14/60	11/35	23/71	9/39	7/39	**0.22**	**0.08**	**Yes**
	0.5	36/52	32/43	15/22	27/34	15/24	18/23	24/29	**0.74**	**0.07**	**Yes**
	1	20/20	20/20	20/20	20/20	29/30	20/20	20/20	**1.00**	**0.01**	**Yes**
	3	20/20	20/20	20/20	20/20	59/60	20/20	20/20	**1.00**	**0.01**	
eri-5 (tm1705)	**0.05**	0/20	0/20	0/20	0/20	0/20	0/20	0/20	**0**	**0**	
	0.1	0/60	0/60	0/28	0/20	0/20	0/30	0/20	**0**	**0**	
	0.5	18/69	10/74	11/34	7/25	10/28	14/37	13/40	**0.29**	**0.08**	
	1	15/29	25/40	11/38	11/19	12/26	14/40	15/31	**0.47**	**0.12**	
	3	79/80	80/80	20/20	20/20	20/20	39/40	54/60	**0.98**	**0.04**	
eri-6/7 (tm1917)	**0.05**	2/40	0/20	0/20	9/70	3/30	0/20	7/40	**0.06**	**0.07**	
	0.1	0/8	16/35	8/35	7/27	9/27	6/24	9/29	**0.26**	**0.14**	**Yes**
	0.5	27/43	27/35	20/20	20/20	30/35	20/20	40/45	**0.88**	**0.14**	**Yes**
	1	20/20	20/20	60/60	30/30	39/40	77/80	20/20	**0.99**	**0.02**	**Yes**
	3	42/42	18/19	20/20	20/20	20/20	20/20	20/20	**0.99**	**0.02**	
eri-8 (gg100)	**0.05**	3/21	3/17	10/39	8/27	3/19	6/28	7/34	**0.21**	**0.05**	**Yes**
	0.1	4/79	29/107	3/14	15/18	8/18	13/31	6/24	**0.35**	**0.25**	**Yes**
	0.5	65/82	44/58	20/20	20/20	20/20	20/20	36/40	**0.92**	**0.11**	**Yes**
	1	20/20	20/20	20/20	39/40	20/20	20/20	69/70	**0.99**	**0.01**	**Yes**
	3	20/20	20/20	20/20	20/20	20/20	20/20	20/20	**1.00**	**0**	
eri-9 (gg106) *Best*	**0.05**	9/24	8/21	6/29	4/15	2/35	11/34	17/37	**0.30**	**0.13**	**Yes**
	0.1	19/84	4/73	12/21	23/33	20/34	13/26	24/38	**0.47**	**0.24**	**Yes**
	0.5**	50/59	38/38	20/20	19/20	20/20	20/20	40/40	**0.97**	**0.06**	**Yes**
	1**	20/20	20/20	20/20	74/80	20/20	20/20	20/20	**0.99**	**0.03**	**Yes**
	3	20/20	20/20	20/20	20/20	20/20	20/20	20/20	**1.00**	**0**	
eri-11 (gg99)	**0.05**	5/19	5/25	4/25	3/20	2/18	3/25	7/34	**0.17**	**0.05**	**Yes**
	0.1	14/98	4/22	4/21	6/18	8/19	5/18	3/21	**0.24**	**0.11**	**Yes**
	0.5	27/37	20/26	20/20	20/20	20/20	20/20	48/53	**0.91**	**0.12**	**Yes**
	1	16/20	20/20	20/20	20/20	20/20	20/20	20/20	**0.97**	**0.08**	**Yes**
	3	20/20	20/20	20/20	20/20	20/20	20/20	20/20	**1.00**	**0**	

Table 2.6: Dilution series of Eri responses by RNAi feeding against *dpy-13*

Single L3-stage larvae were placed on RNAi food targeting *dpy-13*; 4 days later, the percent of progeny showing the expected severe dumpiness, in which an animal's length is at most three times its width, at each indicated concentration (OD at 600 nm) of initial bacterial culture were determined. For clarity, four bacterial culture concentrations (OD_{600nm} of 0.01, 0.02, 1.5, and 4), which produced similar Eri penetrances as adjacent concentrations, are not included. The tabulated mean (Avg) and standard deviation (SD) for N2 wild type were used as the basis to indicate an Eri or a Rde phenotype (Eri?), with $p<0.05$ as the criterion to denote significant difference from wild type response levels. A strain which fits the "best *eri*" criterion described in text is marked as "best", with asterisks indicating concentrations of RNAi food at which it fulfilled the criterion.

Table 2.6 (Continued): Dilution series results for *dpy-13* feeding

Strain	*OD_{600}*	*Penetrance readings*									*Avg*	*SD*	*Eri?*
Wildtype (N2)	**0.04**	0/20	0/20	0/20	0/20	0/20	0/20	0/20			**0**	**0**	
	0.1	0/20	0/20	0/20	0/20	0/20	1/37	0/20			**0**	**0.01**	
	0.25	0/20	0/20	0/20	0/20	0/20	0/20	0/20			**0**	**0**	
	0.75	0/20	0/20	0/20	0/20	1/105	0/20	0/20			**0**	**0.01**	
	3	5/98	22/122	4/84	14/165	4/131	4/103	1/112	3/119	6/116	**0.06**	**0.05**	
eri-1 (mg366) *Best*	**0.04**	0/12	0/8	0/36	0/73	0/20	0/20	0/20			**0**	**0**	
	0.1	4/46	12/30	8/68	36/68	35/60	13/82	22/54	31/50		**0.36**	**0.22**	**Yes**
	0.25	17/28	44/44	9/19	67/78	60/73	4/5	20/20	20/20	20/20	**0.84**	**0.19**	**Yes**
	0.75**	34/35	20/20	58/60	51/51	20/20	20/20	20/20			**0.99**	**0.02**	**Yes**
	3**	9/9	6/6	12/12	58/58	20/20	20/22	20/20			**0.99**	**0.03**	**Yes**
rrf-3 (pk1426)	**0.04**	0/20	0/20	0/20	0/20	0/20	0/20				**0**	**0**	
	0.1	0/20	0/20	0/20	7/62	10/96	2/44	4/54	2/50	2/61	**0.05**	**0.04**	**Yes**
	0.25	3/58	6/57	80/115	71/78	37/48	25/56	38/65	23/61		**0.49**	**0.31**	**Yes**
	0.75	51/80	36/56	43/100	44/45	20/20	20/20	66/70	56/57	58/59	**0.84**	**0.21**	**Yes**
	3	67/67	20/20	42/44	20/20	20/20	20/20	20/20			**0.99**	**0.02**	**Yes**
eri-3 (tm1361)	**0.04**	0/20	0/20	0/20	0/20	0/20	0/20				**0**	**0**	
	0.1	3/62	0/55	3/77	13/88	5/80	3/44	1/14	7/55		**0.07**	**0.05**	**Yes**
	0.25	6/52	3/54	6/52	22/54	38/51	32/87	41/74	17/64	24/58	**0.34**	**0.23**	**Yes**
	0.75	37/75	64/80	48/81	76/89	87/94	94/101	62/84	86/90	43/52	**0.79**	**0.16**	**Yes**
	3	62/67	80/85	48/49	20/20	20/20	20/20				**0.97**	**0.03**	**Yes**
eri-5 (tm1705)	**0.04**	0/20	0/20	0/20	0/20	0/20	0/20	0/20			**0**	**0**	
	0.1	0/20	0/20	0/20	0/20	0/27	0/20				**0**	**0**	
	0.25	0/20	0/20	0/20	0/20	0/20	0/20	0/20			**0**	**0**	
	0.75	0/52	0/67	0/42	0/20	0/20	0/20	2/50			**0.01**	**0.02**	
	3	3/80	2/67	8/90	17/95	11/80	6/61	24/88	10/103		**0.12**	**0.08**	
eri-6/7 (tm1917)	**0.04**	0/25	0/22	0/20	0/20	0/20					**0**	**0**	
	0.1	2/63	1/60	1/84	3/74	0/58	1/82	0/20			**0.02**	**0.02**	
	0.25	1/60	4/56	2/51	23/101	29/129	33/144	22/111	8/81	17/95	**0.14**	**0.09**	**Yes**
	0.75	102/103	30/87	75/102	71/80	136/154	94/105	125/155	80/126	70/137	**0.74**	**0.21**	**Yes**
	3	94/96	88/91	61/70	20/20	96/100					**0.96**	**0.05**	**Yes**
eri-8 (gg100)	**0.04**	0/29	0/33	1/120	0/20	0/20	2/100				**0**	**0.01**	
	0.1	2/68	1/86	0/70	8/101	20/113	16/82	9/99	1/85		**0.07**	**0.08**	
	0.25	6/106	4/83	11/72	82/100	49/94	52/94	110/131	91/128	36/37	**0.52**	**0.35**	**Yes**
	0.75	55/60	57/80	52/57	118/120	117/120	20/20	20/20	114/161	20/20	**0.91**	**0.12**	**Yes**
	3	102/105	77/81	99/106	20/20	99/100					**0.97**	**0.03**	**Yes**
eri-9 (gg106)	**0.04**	0/64	0/55	0/57	0/20	0/20					**0**	**0**	
	0.1	0/67	0/58	0/49	5/76	8/86	3/109	8/103	2/63	5/74	**0.04**	**0.04**	
	0.25	7/79	10/106	4/79	24/126	39/109	35/108	22/131	14/98	68/122	**0.22**	**0.16**	**Yes**
	0.75	76/114	81/108	82/130	20/20	20/20	103/108	116/120	80/95	95/103	**0.86**	**0.14**	**Yes**
	3	95/100	74/78	89/94	20/20	99/100					**0.97**	**0.03**	**Yes**
eri-11 (gg99) *Best*	**0.04**	0/20	0/20	0/20	4/77	2/70	0/20	0/20			**0.01**	**0.02**	
	0.1	4/85	9/77	6/65	55/64	53/83	39/75	3/80	1/80		**0.29**	**0.33**	
	0.25	53/72	40/60	37/58	67/97	77/95	45/67	57/91	54/73	35/60	**0.68**	**0.07**	**Yes**
	0.75**	20/20	20/20	125/130	20/20	20/20	99/100	56/60	73/76		**0.98**	**0.03**	**Yes**
	3**	20/20	94/100	20/20	20/20	20/20	20/20	20/20	98/100	20/20	**0.99**	**0.02**	**Yes**

Table 2.7: Dilution series of Eri responses by RNAi feeding against *fkh-6*

Single L1-stage larvae were placed on RNAi food targeting *fkh-6*; 5 days later, the number of progeny surviving to L3-stage larvae or older at each indicated concentration (OD at 600 nm) of initial bacterial culture was determined. For clarity, two bacterial culture concentrations (OD_{600nm} of 0.25 and 0.5), which produced similar Eri penetrances as adjacent concentrations, are not included. The tabulated mean (Avg) and standard deviation (SD) were normalized to the brood sizes of each strain fed empty RNAi vector (**Table 2.27**), to obtain the normalized mean (N.Avg) and standard error of the mean (SEM). The normalized mean and the standard error of the mean for N2 wild type were used as the basis to indicate an Eri or a Rde phenotype (Eri?), with $p<0.05$ as the criterion to denote significant difference from wild type response levels. A strain which fits the "best *eri*" criterion described in text is marked as "best", with asterisks indicating concentrations of RNAi food at which it fulfilled the criterion.

Table 2.7 (Continued): Dilution series results for *fkh-6* feeding

Strain	*OD_{600}*	*Brood Size*						*Avg*	*SD*	*N.Avg*	*SEM*	*Eri?*
Wildtype (N2)	**0.002**	207	230	208	233	220		**220**	**12**	**0.03**	**0.10**	
	0.01	200	184	232	184	248	240	**215**	**29**	**0.05**	**0.15**	
	0.02	120	224	160	232	272	176	**197**	**55**	**0.13**	**0.26**	
	0.04	167	128	103	55	106	80	**107**	**39**	**0.53**	**0.18**	
	0.1	2	4	7	4	59	0	**13**	**23**	**0.94**	**0.10**	
eri-1 (mg366)	**0.002**	46	67	25	42	56		**47**	**16**	**0.70**	**0.10**	**Yes**
	0.01	57	37	43	31	24	22	**36**	**13**	**0.77**	**0.08**	**Yes**
	0.02	38	21	1	27	23	22	**22**	**12**	**0.86**	**0.08**	**Yes**
	0.04	0	38	55	35	6	33	**28**	**21**	**0.82**	**0.13**	**Yes**
	0.1	3	0	6	28	8	4	**8**	**10**	**0.95**	**0.06**	
rrf-3 (pk1426) *Best*	**0.002**	36	33	21	19	41	23	**29**	**9**	**0.78**	**0.07**	**Yes**
	0.01**	14	18	29	16	10	43	**22**	**12**	**0.84**	**0.09**	**Yes**
	0.02**	27	13	0	28	30	17	**19**	**12**	**0.86**	**0.09**	**Yes**
	0.04**	20	16	5	22	18	0	**14**	**9**	**0.90**	**0.07**	**Yes**
	0.1**	0	0	13	0	0	0	**2**	**5**	**0.98**	**0.04**	
eri-3 (tm1361)	**0.002**	112	171	140	128	108	148	**135**	**24**	**0.14**	**0.17**	
	0.01	120	125	88	104	42	68	**91**	**32**	**0.41**	**0.21**	**Yes**
	0.02	15	96	15	41	46	15	**38**	**32**	**0.76**	**0.20**	**Yes**
	0.04	68	43	45	37	31	1	**38**	**22**	**0.76**	**0.14**	**Yes**
	0.1	26	2	16	0	0	9	**9**	**10**	**0.94**	**0.07**	
eri-5 (tm1705)	**0.002**	152	154	192	184	203		**177**	**23**	**0**	**0.17**	
	0.01	188	199	184	205	152	167	**183**	**20**	**0**	**0.16**	
	0.02	148	120	112	114	125	137	**126**	**14**	**0.26**	**0.11**	
	0.04	70	97	71	79	112	84	**86**	**16**	**0.50**	**0.11**	
	0.1	1	17	5	3	33	4	**11**	**12**	**0.94**	**0.07**	
eri-6/7 (tm1917)	**0.002**	184	156	184	160	148		**166**	**17**	**0**	**0.14**	
	0.01	75	90	144	160	88	168	**121**	**41**	**0.22**	**0.27**	
	0.02	192	160	64	45	92		**111**	**63**	**0.29**	**0.41**	
	0.04	80	58	27	81	105	20	**62**	**33**	**0.60**	**0.22**	
	0.1	0	0	0	0	0	0	**0**	**0**	**1.00**	**0**	
eri-8 (gg100)	**0.002**	215	162	162	182	160	152	**172**	**23**	**0.23**	**0.11**	**Yes**
	0.01	148	160	203	154	159	158	**164**	**20**	**0.26**	**0.09**	**Yes**
	0.02	162	92	112	152	192	136	**141**	**36**	**0.37**	**0.16**	
	0.04	136	128	144	120	120	125	**129**	**10**	**0.42**	**0.05**	
	0.1	1	7	20	1	0	0	**5**	**8**	**0.98**	**0.04**	
eri-9 (gg106)	**0.002**	208	217	188	272	211	216	**219**	**28**	**0.09**	**0.13**	
	0.01	175	216	180	184	171	153	**180**	**21**	**0.25**	**0.10**	**Yes**
	0.02	184	248	224	205	153	168	**197**	**36**	**0.18**	**0.16**	
	0.04	32	136	200	168	154	198	**148**	**62**	**0.38**	**0.26**	
	0.1	0	39	0	7	46	3	**16**	**21**	**0.93**	**0.09**	
eri-11 (gg99)	**0.002**	216	224	270	233	312		**251**	**40**	**0.08**	**0.16**	
	0.01	109	82	115	120	192	152	**128**	**38**	**0.53**	**0.14**	**Yes**
	0.02	86	85	156	160	64	96	**108**	**40**	**0.61**	**0.15**	**Yes**
	0.04	140	76	108	9	35	30	**66**	**51**	**0.76**	**0.19**	
	0.1	1	0	0	1	39	4	**8**	**16**	**0.97**	**0.06**	**Yes**

Table 2.8: Dilution series of Eri responses by RNAi feeding against *gon-1*

Single L1-stage larvae were placed on RNAi food targeting *gon-1*; 5 days later, the number of progeny surviving to L3-stage larvae or older at each indicated concentration (OD at 600 nm) of initial bacterial culture was determined. For clarity, one bacterial culture concentration (OD_{600nm} of 0.1), which produced similar Eri penetrances as adjacent concentrations, is not included. The tabulated mean (Avg) and standard deviation (SD) were normalized to the brood sizes of each strain fed empty RNAi vector (**Table 2.27**), to obtain the normalized mean (N.Avg) and standard error of the mean (SEM). The normalized mean and the standard error of the mean for N2 wild type were used as the basis to indicate an Eri or a Rde phenotype (Eri?), with $p<0.05$ as the criterion to denote significant difference from wild type response levels. A strain which fits the "best *eri*" criterion described in text is marked as "best", with asterisks indicating concentrations of RNAi food at which it fulfilled the criterion.

Table 2.8 (Continued): Dilution series results for *gon-1* feeding

Strain	*OD_{600}*	*Brood Size*							*Avg*	*SD*	*N.Avg*	*SEM*	*Eri?*
Wildtype (N2)	**0.25**	238	259	208	160	216	240	168	**213**	**37**	**0.06**	**0.19**	
	0.5	208	192	162	120	246	208	171	**187**	**40**	**0.18**	**0.19**	
	1	66	59	101	166	160	150	152	**122**	**46**	**0.46**	**0.21**	
	2	35	75	120	132	138	118		**103**	**40**	**0.55**	**0.18**	
	3	4	19	28	21	39	60	0	**24**	**21**	**0.89**	**0.09**	
eri-1 (mg366) *Best*	**0.25**	102	72	20	32	43	11		**47**	**34**	**0.71**	**0.22**	**Yes**
	0.5	2	4	11	42	25	2		**14**	**16**	**0.91**	**0.10**	**Yes**
	1**	0	5	14	1	1	3	9	**5**	**5**	**0.97**	**0.03**	**Yes**
	2**	1	2	1	10	3	11	1	**4**	**4**	**0.97**	**0.03**	**Yes**
	3**	4	3	1	0	20	20	2	**7**	**9**	**0.95**	**0.06**	
rrf-3 (pk1426) *Best*	**0.25**	54	40	43	0	11	13		**27**	**22**	**0.80**	**0.16**	**Yes**
	0.5	53	31	40	15	8	2	11	**23**	**19**	**0.83**	**0.14**	**Yes**
	1**	1	0	0	1	1	11	2	**2**	**4**	**0.98**	**0.03**	**Yes**
	2**	1	5	1	0	1	18	2	**4**	**6**	**0.97**	**0.05**	**Yes**
	3**	0	0	0	0	0	2	0	**0**	**1**	**1.00**	**0.01**	**Yes**
eri-3 (tm1361)	**0.25**	44	61	4	72	40	64		**48**	**25**	**0.70**	**0.16**	**Yes**
	0.5	95	72	5	49	37	18		**46**	**34**	**0.70**	**0.22**	**Yes**
	1	74	42	8	39	80	30		**46**	**27**	**0.71**	**0.18**	**Yes**
	2	54	64	8	36	33	13		**35**	**22**	**0.78**	**0.14**	**Yes**
	3	5	4	2	1	1	0	0	**2**	**2**	**0.99**	**0.01**	**Yes**
eri-5 (tm1705)	**0.25**	152	144	166	168	125	136		**149**	**17**	**0.13**	**0.13**	
	0.5	144	126	137	90	128			**125**	**21**	**0.27**	**0.14**	
	1	11	78	1	78	87			**51**	**41**	**0.70**	**0.24**	
	2	100	10	2	28	82	76	66	**52**	**38**	**0.69**	**0.23**	
	3	1	1	1	40	0			**9**	**18**	**0.95**	**0.10**	
eri-6/7 (tm1917)	**0.25**	97	139	188	70	104	99		**116**	**42**	**0.25**	**0.27**	
	0.5	141	190	86	92	88	80	99	**111**	**40**	**0.29**	**0.27**	
	1	1	26	30	40	64	98	64	**46**	**32**	**0.70**	**0.21**	
	2	1	0	0	0	9	1	1	**2**	**3**	**0.99**	**0.02**	**Yes**
	3	0	2	2	2	1	2	2	**2**	**1**	**0.99**	**0.01**	**Yes**
eri-8 (gg100)	**0.25**	192	162	184	96	144			**156**	**38**	**0.30**	**0.17**	**Yes**
	0.5	64	108	30	81	54	47	97	**69**	**28**	**0.69**	**0.13**	**Yes**
	1	2	0	4	80	56	43	52	**34**	**32**	**0.85**	**0.14**	**Yes**
	2	1	0	2	1	1	49	12	**9**	**18**	**0.96**	**0.08**	**Yes**
	3	30	0	1	0	2	3	0	**5**	**11**	**0.98**	**0.05**	
eri-9 (gg106)	**0.25**	144	160	148	88	97			**127**	**33**	**0.47**	**0.14**	**Yes**
	0.5	114	120	80	71	94			**96**	**21**	**0.60**	**0.09**	**Yes**
	1	4	0	1	63	104	42		**36**	**42**	**0.85**	**0.18**	**Yes**
	2	1	0	1	42	58	0		**17**	**26**	**0.93**	**0.11**	**Yes**
	3	0	1	0	8	23	2	57	**13**	**21**	**0.95**	**0.09**	
eri-11 (gg99)	**0.25**	102	112	112	57	120	144		**108**	**29**	**0.61**	**0.11**	**Yes**
	0.5	94	128	3	47	0	2		**46**	**55**	**0.83**	**0.20**	**Yes**
	1	1	60	62	46	47	85	87	**55**	**29**	**0.80**	**0.11**	**Yes**
	2	0	1	0	1	58	34	34	**18**	**24**	**0.93**	**0.09**	**Yes**
	3	1	0	34	0	0	0	0	**5**	**13**	**0.98**	**0.05**	**Yes**

Table 2.9: Dilution series of Eri responses by RNAi feeding against *gon-4*

Single L3-stage larvae were placed on RNAi food targeting *gon-4*; 5 days later, the percent of progeny showing the expected severely protruding or absent gonads at each indicated concentration (OD at 600 nm) of initial bacterial culture were determined. The tabulated mean (Avg) and standard deviation (SD) for N2 wild type were used as the basis to indicate an Eri or a Rde phenotype (Eri?), with $p<0.05$ as the criterion to denote significant difference from wild type response levels. A strain which fits the "best *eri*" criterion described in text is marked as "best", with asterisks indicating concentrations of RNAi food at which it fulfilled the criterion.

Table 2.9 (Continued): Dilution series results for *gon-4* feeding

Strain	*OD_{600}*	*Penetrance readings*							*Avg*	*SD*	*Eri?*
Wildtype (N2)	**0.5**	1/29	1/39	0/40	0/20	0/20	1/40		**0.01**	**0.02**	
	1	0/22	0/18	2/43	0/20	2/40	0/20	1/30	**0.02**	**0.02**	
	2	2/24	2/30	2/21	0/20	2/60			**0.06**	**0.04**	
	3	6/19	5/24	1/18	5/56	0/47	2/28	5/64	**0.12**	**0.11**	
	4	1/6	11/76	2/30	1/5	1/20			**0.13**	**0.06**	
eri-1 (mg366)	**0.5**	2/22	3/32	1/23	0/20	0/20	1/30		**0.04**	**0.04**	
	1	9/18	6/30	3/28	0/20	0/20	2/12		**0.16**	**0.19**	
	2	22/26	24/24	15/18	4/25	0/20	6/18		**0.53**	**0.42**	**Yes**
	3	34/47	17/17	28/32	5/12	7/17	7/21		**0.63**	**0.28**	**Yes**
	4	19/20	10/21	20/22	7/16	11/13			**0.72**	**0.25**	**Yes**
rrf-3 (pk1426) *Best*	**0.5**	2/20	1/20	0/20	1/30	1/13	0/20		**0.04**	**0.04**	
	1	0/20	0/20	0/20	1/20	0/20	0/20		**0.01**	**0.02**	
	2	21/40	21/25	18/32	11/19	0/20	17/40		**0.49**	**0.28**	**Yes**
	3	28/35	29/34	29/41	17/20	15/21	22/23		**0.81**	**0.09**	**Yes**
	4**	20/20	20/20	19/23	7/9	20/20	17/19		**0.92**	**0.10**	**Yes**
eri-3 (tm1361)	**0.5**	0/20	1/20	1/16	0/20	1/24	0/20		**0.03**	**0.03**	
	1	4/30	3/20	1/30	1/20	0/20	1/30		**0.07**	**0.06**	
	2	9/20	17/31	19/31	10/20	18/55			**0.49**	**0.11**	**Yes**
	3	27/30	27/28	17/20	5/15	9/20	18/20		**0.73**	**0.27**	**Yes**
	4	33/35	21/25	32/35	26/30	12/14	39/50	26/35	**0.85**	**0.07**	**Yes**
eri-5 (tm1705)	**0.5**	2/20	2/20	3/20	0/20	0/8	0/62	0/20	**0.05**	**0.06**	
	1	3/40	6/50	0/20	0/20	0/20	1/40		**0.04**	**0.05**	
	2	3/22	10/25	6/21	0/20	0/20	1/20	0/20	**0.12**	**0.16**	
	3	3/15	8/24	8/34	4/39	0/20	0/20	11/56	**0.15**	**0.12**	
	4	0/20	5/34	4/42	0/20	0/20	4/20	3/42	**0.07**	**0.08**	
eri-6/7 (tm1917)	**0.5**	2/33	2/26	2/43	0/20	0/20	1/40	1/50	**0.03**	**0.03**	
	1	2/40	1/80	3/27	0/20	4/60	13/34	11/80	**0.11**	**0.13**	
	2	3/31	2/22	6/30	2/40	14/90	11/80		**0.12**	**0.05**	
	3	5/14	8/20	10/19	2/8	13/18	8/22		**0.44**	**0.17**	**Yes**
	4	11/20	7/9	16/19	21/29	3/8			**0.65**	**0.19**	**Yes**
eri-8 (gg100)	**0.5**	0/20	0/20	1/40	0/20	2/40	0/20	0/20	**0.01**	**0.02**	
	1	3/40	0/20	0/20	0/20	1/60	0/20	0/20	**0.01**	**0.03**	
	2	15/45	24/46	13/33	0/20	1/11	0/20	0/20	**0.19**	**0.22**	
	3	7/20	10/23	28/35	4/10	14/64	9/39		**0.41**	**0.21**	**Yes**
	4	8/12	9/19	19/24	12/15	5/8			**0.67**	**0.13**	**Yes**
eri-9 (gg106)	**0.5**	1/60	1/20	0/20	0/20	1/20	0/20	0/20	**0.02**	**0.02**	
	1	1/20	4/30	0/15	2/8	12/90	2/30		**0.11**	**0.09**	
	2	14/17	11/15	15/19	11/19	20/35	30/65		**0.66**	**0.14**	**Yes**
	3	10/13	10/14	20/27	11/16	20/38			**0.69**	**0.10**	**Yes**
	4	24/35	24/36	20/25	10/14	11/15			**0.72**	**0.05**	**Yes**
eri-11 (gg99)	**0.5**	0/20	1/40	1/40	0/20	0/20	1/30	0/20	**0.01**	**0.02**	
	1	0/20	1/40	0/20	0/20	1/10	0/20		**0.02**	**0.04**	
	2	7/55	14/56	6/32	11/30	8/28			**0.24**	**0.09**	**Yes**
	3	6/29	7/27	12/36	6/12	15/40			**0.33**	**0.11**	**Yes**
	4	7/14	19/20	20/22	6/20	7/31			**0.58**	**0.34**	**Yes**

Table 2.10: Dilution series of Eri responses by RNAi feeding against *act-5*

Single L3-stage larvae were placed on RNAi food targeting *act-5*; 4 days later, the number of progeny surviving to L3-stage larvae or older at each indicated concentration (OD at 600 nm) of initial bacterial culture was determined. The tabulated mean (Avg) and standard deviation (SD) were normalized to the brood sizes of each strain fed empty RNAi vector (**Table 2.27**), to obtain the normalized mean (N.Avg) and standard error of the mean (SEM). The normalized mean and the standard error of the mean for N2 wild type were used as the basis to indicate an Eri or a Rde phenotype (Eri?), with $p<0.05$ as the criterion to denote significant difference from wild type response levels. A strain which fits the "best *eri*" criterion described in text is marked as "best", with asterisks indicating concentrations of RNAi food at which it fulfilled the criterion.

Table 2.10 (Continued): Dilution series results for *act-5* feeding

Strain	*OD_{600}*	*Brood Size*							*Avg*	*SD*	*N.Avg*	*SEM*	*Eri?*
Wildtype (N2)	**0.001**	288	264	248	216	224	198		**240**	**32**	**0**	**0.18**	
	0.002	175	160	157	166	94	134	172	**151**	**29**	**0.33**	**0.14**	
	0.005	112	118	71	61	69	118	66	**88**	**27**	**0.61**	**0.12**	
	0.01	79	97	76	82	118			**90**	**17**	**0.60**	**0.09**	
	0.02	76	80	0	0	3	41		**33**	**38**	**0.85**	**0.17**	
eri-1 (mg366)	**0.001**	99	108	81	85	107	102		**97**	**11**	**0.39**	**0.08**	**Yes**
	0.002	57	91	97	50	44	65	59	**66**	**20**	**0.58**	**0.13**	**Yes**
	0.005	65	77	23	41	24	86	65	**54**	**25**	**0.66**	**0.16**	
	0.01	18	29	26	23	25			**24**	**4**	**0.85**	**0.03**	**Yes**
	0.02	1	0	4	21	0	8		**6**	**8**	**0.96**	**0.05**	
rrf-3 (pk1426) *Best*	**0.001**	66	85	89	76	115	88		**87**	**16**	**0.35**	**0.13**	**Yes**
	0.002	1	8	39	0	15	12	18	**13**	**13**	**0.90**	**0.10**	**Yes**
	0.005**	0	0	1	26	0	1	5	**5**	**10**	**0.96**	**0.07**	**Yes**
	0.01**	30	5	0	0	1	1	6	**6**	**11**	**0.95**	**0.08**	**Yes**
	0.02**	0	1	0	2	0	1	0	**1**	**1**	**1.00**	**0.01**	**Yes**
eri-3 (tm1361)	**0.001**	47	84	51	80	69			**66**	**17**	**0.57**	**0.11**	**Yes**
	0.002	52	74	30	42	31	41	62	**47**	**16**	**0.70**	**0.11**	**Yes**
	0.005	40	18	26	6	40	54	27	**30**	**16**	**0.81**	**0.10**	**Yes**
	0.01	12	8	25	22	18	25		**18**	**7**	**0.88**	**0.05**	**Yes**
	0.02	0	2	1	1	22	14	15	**8**	**9**	**0.95**	**0.06**	
eri-5 (tm1705)	**0.001**	192	168	180	164	204			**182**	**17**	**0**	**0.15**	
	0.002	168	87	142	164	134	144		**140**	**29**	**0.18**	**0.19**	
	0.005	73	92	108	93	78			**89**	**14**	**0.48**	**0.10**	
	0.01	114	17	17	69	92	89		**66**	**41**	**0.61**	**0.24**	
	0.02	55	39	0	0	0	18	3	**16**	**22**	**0.90**	**0.13**	
eri-6/7 (tm1917)	**0.001**	158	151	189	157	144			**160**	**17**	**0**	**0.14**	
	0.002	85	90	61	109	119			**93**	**23**	**0.40**	**0.15**	
	0.005	40	99	111	55	46			**70**	**32**	**0.55**	**0.21**	
	0.01	17	3	20	11	26			**15**	**9**	**0.90**	**0.06**	**Yes**
	0.02	1	7	8	32	0	42	5	**14**	**17**	**0.91**	**0.11**	
eri-8 (gg100)	**0.001**	144	120	104	148	168	256	153	**156**	**49**	**0.30**	**0.22**	**Yes**
	0.002	57	78	154	97	97	125		**101**	**34**	**0.54**	**0.15**	**Yes**
	0.005	34	82	103	38	95	29	74	**65**	**31**	**0.71**	**0.14**	
	0.01	28	1	38	16	17			**20**	**14**	**0.91**	**0.06**	**Yes**
	0.02	1	67	37	0	9	27	0	**20**	**25**	**0.91**	**0.11**	
eri-9 (gg106)	**0.001**	128	128	138	103	125			**124**	**13**	**0.48**	**0.06**	**Yes**
	0.002	125	118	99	69	109	110	95	**104**	**18**	**0.57**	**0.08**	**Yes**
	0.005	42	140	84	97	47	100		**85**	**37**	**0.65**	**0.15**	
	0.01	18	0	0	1	1	1		**4**	**7**	**0.99**	**0.03**	**Yes**
	0.02	81	0	1	1	0	25	21	**18**	**30**	**0.92**	**0.12**	
eri-11 (gg99)	**0.001**	128	216	152	232	140	168	212	**178**	**41**	**0.35**	**0.16**	**Yes**
	0.002	75	111	99	88	98	176		**108**	**36**	**0.61**	**0.13**	**Yes**
	0.005	68	62	71	18	52	122	97	**70**	**33**	**0.74**	**0.12**	
	0.01	11	0	88	85	55	22		**44**	**38**	**0.84**	**0.14**	**Yes**
	0.02	0	16	1	4	1	31	29	**12**	**14**	**0.96**	**0.05**	

Table 2.11: Dilution series of Eri responses by RNAi feeding against *gtl-1*

Single L3-stage larvae were placed on RNAi food targeting *gtl-1*; 4 days later, the number of progeny surviving to L3-stage larvae or older at each indicated concentration (OD at 600 nm) of initial bacterial culture was determined. For clarity, two bacterial culture concentrations (OD_{600nm} of 0.01 and 0.02), which produced similar Eri penetrances as adjacent concentrations, are not included. The tabulated mean (Avg) and standard deviation (SD) were normalized to the brood sizes of each strain fed empty RNAi vector (**Table 2.27**), to obtain the normalized mean (N.Avg) and standard error of the mean (SEM). The normalized mean and the standard error of the mean for N2 wild type were used as the basis to indicate an Eri or a Rde phenotype (Eri?), with $p<0.05$ as the criterion to denote significant difference from wild type response levels. A strain which fits the "best *eri*" criterion described in text is marked as "best", with asterisks indicating concentrations of RNAi food at which it fulfilled the criterion.

Table 2.11 (Continued): Dilution series results for *gtl-1* feeding

Strain	*OD_{600}*	*Brood Size*							*Avg*	*SD*	*N.Avg*	*SEM*	*Eri?*
Wildtype (N2)	**0.04**	216	216	207	162	189	200	192	**197**	**19**	**0.13**	**0.12**	
	0.1	190	220	240	224	64	112	128	**168**	**67**	**0.26**	**0.30**	
	0.5	224	210	232	207	189	180	187	**204**	**20**	**0.10**	**0.12**	
	1	204	168	160	128	144	84	88	**139**	**43**	**0.38**	**0.20**	
	2	189	168	160	22	28	40	52	**94**	**74**	**0.58**	**0.33**	
eri-1 (mg366)	**0.04**	192	144	76	80	136	112	176	**131**	**45**	**0.17**	**0.29**	
	0.1	144	96	104	81	88	80	72	**95**	**24**	**0.40**	**0.16**	
	0.5	128	104	128	56	72	64	79	**90**	**30**	**0.43**	**0.19**	**Yes**
	1	36	7	60	37	13	35	35	**32**	**17**	**0.80**	**0.11**	**Yes**
	2	40	48	45	48	54	39	40	**45**	**6**	**0.72**	**0.04**	
rrf-3 (pk1426) *Best*	**0.04**	36	77	62	65	108	65	71	**69**	**21**	**0.48**	**0.16**	**Yes**
	0.1	49	42	63	38	63	73	62	**56**	**13**	**0.58**	**0.10**	**Yes**
	0.5	39	45	54	40	24	34	45	**40**	**9**	**0.70**	**0.07**	**Yes**
	1**	19	8	16	30	30	0	28	**19**	**12**	**0.86**	**0.09**	**Yes**
	2**	7	16	8	22	15	18	38	**18**	**10**	**0.87**	**0.08**	**Yes**
eri-3 (tm1361)	**0.04**	152	128	135	88	112	102	68	**112**	**29**	**0.28**	**0.20**	
	0.1	21	136	96	76	44	72	72	**74**	**37**	**0.53**	**0.24**	
	0.5	25	95	15	68	6	72	40	**46**	**33**	**0.71**	**0.21**	**Yes**
	1	80	27	56	20	15	35	20	**36**	**24**	**0.77**	**0.15**	**Yes**
	2	20	45	17	40	32	40	10	**29**	**13**	**0.81**	**0.09**	
eri-5 (tm1705)	**0.04**	184	240	231	168	216	153	160	**193**	**36**	**0**	**0.24**	
	0.1	174	176	200	128	112	128	144	**152**	**32**	**0.11**	**0.21**	
	0.5	204	210	176	88	184	160	125	**164**	**44**	**0.04**	**0.28**	
	1	148	94	141	84	81	72	96	**102**	**30**	**0.40**	**0.19**	
	2	152	144	182	52	48	44	42	**95**	**61**	**0.44**	**0.37**	
eri-6/7 (tm1917)	**0.04**	60	76	75	176	136	184	202	**130**	**59**	**0.16**	**0.39**	
	0.1	47	43	74	61	62	104	90	**69**	**22**	**0.56**	**0.15**	**Yes**
	0.5	44	36	84	82	79	100	67	**70**	**23**	**0.55**	**0.15**	**Yes**
	1	16	20	22	65	34	42	17	**31**	**18**	**0.80**	**0.12**	**Yes**
	2	4	9	22	29	21	9	15	**16**	**9**	**0.90**	**0.06**	**Yes**
eri-8 (gg100)	**0.04**	120	136	85	137	88	104	120	**113**	**21**	**0.49**	**0.10**	**Yes**
	0.1	104	112	114	52	51	82		**86**	**29**	**0.61**	**0.13**	**Yes**
	0.5	44	44	68	68	79	72	80	**65**	**15**	**0.71**	**0.07**	**Yes**
	1	39	28	23	42	43	64	27	**38**	**14**	**0.83**	**0.06**	**Yes**
	2	12	20	20	12	17	14	24	**17**	**5**	**0.92**	**0.02**	**Yes**
eri-9 (gg106)	**0.04**	232	296	248	128	160	120	152	**191**	**68**	**0.20**	**0.29**	
	0.1	48	246	120	50	64	100	81	**101**	**69**	**0.58**	**0.29**	
	0.5	144	175	128	64	80	104		**116**	**41**	**0.52**	**0.17**	**Yes**
	1	32	39	49	84	72	68	98	**63**	**24**	**0.74**	**0.10**	**Yes**
	2	16	19	32	14	20	25	14	**20**	**7**	**0.92**	**0.03**	**Yes**
eri-11 (gg99) *Best*	**0.04**	192	160	196	120	104	104	192	**153**	**42**	**0.44**	**0.16**	**Yes**
	0.1	98	168	128	96	72	90	88	**106**	**32**	**0.61**	**0.12**	**Yes**
	0.5	80	96	104	48	56	104	60	**78**	**24**	**0.71**	**0.09**	**Yes**
	1**	70	72	68	20	45	9	41	**46**	**25**	**0.83**	**0.09**	**Yes**
	2**	35	43	85	21	28	14	16	**35**	**25**	**0.87**	**0.09**	**Yes**

Table 2.12: Dilution series of Eri responses by RNAi feeding against *act-3*

Single L3-stage larvae were placed on RNAi food targeting *act-3*; 4 days later, the number of progeny surviving to L3-stage larvae or older at each indicated concentration (OD at 600 nm) of initial bacterial culture was determined. For clarity, three bacterial culture concentrations (OD_{600nm} of 0.1, 0.25, and 0.5), which produced similar Eri penetrances as adjacent concentrations, are not included. The tabulated mean (Avg) and standard deviation (SD) were normalized to the brood sizes of each strain fed empty RNAi vector (**Table 2.27**), to obtain the normalized mean (N.Avg) and standard error of the mean (SEM). The normalized mean and the standard error of the mean for N2 wild type were used as the basis to indicate an Eri or a Rde phenotype (Eri?), with $p<0.05$ as the criterion to denote significant difference from wild type response levels. A strain which fits the "best *eri*" criterion described in text is marked as "best", with asterisks indicating concentrations of RNAi food at which it fulfilled the criterion.

Table 2.12 (Continued): Dilution series results for *act-3* feeding

Strain	*OD_{600}*	*Brood Size*							*Avg*	*SD*	*N.Avg*	*SEM*	*Eri?*
Wildtype (N2)	**0.002**	200	208	232	200	192	216		**208**	**14**	**0.08**	**0.10**	
	0.005	206	234	198	184	210	208		**207**	**16**	**0.09**	**0.11**	
	0.01	176	216	207	203	180	210	216	**201**	**17**	**0.11**	**0.11**	
	0.02	230	234	54	165	80	204	154	**160**	**71**	**0.29**	**0.32**	
	0.05	9	19	28	6	9	58	18	**21**	**18**	**0.91**	**0.08**	
eri-1 (mg366)	**0.002**	132	144	148	120	136	104	136	**131**	**15**	**0.17**	**0.11**	
	0.005	24	53	132	102	84	90	82	**81**	**35**	**0.49**	**0.22**	**Yes**
	0.01	36	63	57	34	69	37	88	**55**	**20**	**0.65**	**0.13**	**Yes**
	0.02	2	5	32	5	37	77	0	**23**	**28**	**0.86**	**0.18**	**Yes**
	0.05	0	4	0	1	0	12	0	**2**	**4**	**0.98**	**0.03**	
rrf-3 (pk1426) *Best*	**0.002**	200	56	116	78	117	129	112	**115**	**45**	**0.13**	**0.34**	
	0.005	65	28	49	93	67	104	88	**71**	**27**	**0.47**	**0.20**	**Yes**
	0.01	17	31	39	66	21	18	23	**31**	**17**	**0.77**	**0.13**	**Yes**
	0.02**	2	19	2	0	0	0	0	**3**	**7**	**0.98**	**0.05**	**Yes**
	0.05**	0	0	0	0	1	0	0	**0**	**0**	**1.00**	**0**	**Yes**
eri-3 (tm1361)	**0.002**	73	32	128	133	104	94	89	**93**	**34**	**0.40**	**0.23**	**Yes**
	0.005	40	31	33	101	58	66	100	**61**	**30**	**0.61**	**0.19**	**Yes**
	0.01	59	43	37	89	83	39	66	**59**	**21**	**0.62**	**0.14**	**Yes**
	0.02	46	9	8	0	59	16	1	**20**	**23**	**0.87**	**0.15**	**Yes**
	0.05	0	0	0	0	62	39	0	**14**	**26**	**0.91**	**0.16**	
eri-5 (tm1705)	**0.002**	222	203	116	176	144	150	168	**168**	**36**	**0.01**	**0.23**	
	0.005	180	188	210	200	126	140	130	**168**	**35**	**0.02**	**0.23**	
	0.01	123	116	136	144	152	112		**131**	**16**	**0.23**	**0.12**	
	0.02	148	72	36	41	133	28		**76**	**52**	**0.55**	**0.31**	
	0.05	0	3	21	26	12	4		**11**	**11**	**0.94**	**0.06**	
eri-6/7 (tm1917)	**0.002**	184	168	31	115	128	62	71	**108**	**57**	**0.30**	**0.37**	
	0.005	189	147	55	114	61	115	114	**114**	**47**	**0.27**	**0.31**	
	0.01	135	34	64	88	16	27	104	**67**	**44**	**0.57**	**0.29**	**Yes**
	0.02	81	3	4	2	3	1	2	**14**	**30**	**0.91**	**0.19**	**Yes**
	0.05	1	0	0	1	0	0	0	**0**	**0**	**1.00**	**0**	**Yes**
eri-8 (gg100) *Best*	**0.002**	272	264	112	160	128	96	136	**167**	**72**	**0.25**	**0.32**	
	0.005	63	42	112	160	160	162	174	**125**	**53**	**0.44**	**0.24**	**Yes**
	0.01	121	69	144	56	72	51	128	**92**	**38**	**0.59**	**0.17**	**Yes**
	0.02**	34	2	1	1	11	15	35	**14**	**15**	**0.94**	**0.07**	**Yes**
	0.05**	0	1	1	0	1	1	3	**1**	**1**	**1.00**	**0**	**Yes**
eri-9 (gg106)	**0.002**	205	192	180	170	190	192	66	**171**	**47**	**0.29**	**0.20**	**Yes**
	0.005	176	186	176	174	161	152	168	**170**	**11**	**0.29**	**0.06**	**Yes**
	0.01	164	56	141	156	174	210	155	**151**	**47**	**0.37**	**0.20**	**Yes**
	0.02	88	60	152	0	70	23	95	**70**	**50**	**0.71**	**0.21**	**Yes**
	0.05	1	28	1	12	4	5	0	**7**	**10**	**0.97**	**0.04**	
eri-11 (gg99)	**0.002**	195	224	188	232	276	152	216	**212**	**39**	**0.23**	**0.15**	
	0.005	155	160	288	176	248	203	176	**201**	**50**	**0.27**	**0.19**	
	0.01	138	152	152	160	208	162	41	**145**	**51**	**0.47**	**0.19**	**Yes**
	0.02	172	23	72	6	59	100	76	**73**	**54**	**0.73**	**0.20**	**Yes**
	0.05	5	0	8	17	16	12	46	**15**	**15**	**0.95**	**0.05**	

Table 2.13: Dilution series of Eri responses by RNAi feeding against *myo-3*

Single L3-stage larvae were placed on RNAi food targeting *myo-3*; 4 days later, the number of progeny surviving to L3-stage larvae or older at each indicated concentration (OD at 600 nm) of initial bacterial culture was determined. For clarity, three bacterial culture concentrations (OD_{600nm} of 0.05, 0.1, and 0.25), which produced similar Eri penetrances as adjacent concentrations, are not included. The tabulated mean (Avg) and standard deviation (SD) were normalized to the brood sizes of each strain fed empty RNAi vector (**Table 2.27**), to obtain the normalized mean (N.Avg) and standard error of the mean (SEM). The normalized mean and the standard error of the mean for N2 wild type were used as the basis to indicate an Eri or a Rde phenotype (Eri?), with $p<0.05$ as the criterion to denote significant difference from wild type response levels. A strain which fits the "best *eri*" criterion described in text is marked as "best", with asterisks indicating concentrations of RNAi food at which it fulfilled the criterion.

Table 2.13 (Continued): Dilution series results for *myo-3* feeding

Strain	*OD_{600}*	*Brood Size*							*Avg*	*SD*	*N.Avg*	*SEM*	*Eri?*
Wildtype (N2)	**0.5**	241	205	164	170	228	181	226	**202**	**31**	**0.11**	**0.16**	
	0.75	248	256	196	193	259	168	202	**217**	**36**	**0.04**	**0.18**	
	1	220	230	201	183	147	129	127	**177**	**43**	**0.22**	**0.20**	
	2	176	165	146	139	196	128	90	**149**	**35**	**0.34**	**0.16**	
	3	102	91	69	94	65	78	106	**86**	**16**	**0.62**	**0.08**	
eri-1 (mg366)	**0.5**	92	98	68	74	85	55	58	**76**	**17**	**0.52**	**0.11**	**Yes**
	0.75	82	54	49	55	42	42	78	**57**	**16**	**0.64**	**0.10**	**Yes**
	1	13	58	9	25	18	19	40	**26**	**17**	**0.84**	**0.11**	**Yes**
	2	0	2	2	5	12	0		**4**	**5**	**0.98**	**0.03**	**Yes**
	3	0	0	0	1	0	0	0	**0**	**0**	**1.00**	**0**	**Yes**
rrf-3 (pk1426) *Best*	**0.5**	74	58	68	18	42	55	19	**48**	**22**	**0.64**	**0.17**	**Yes**
	0.75	31	0	0	2	45	0	5	**12**	**18**	**0.91**	**0.14**	**Yes**
	1**	0	0	2	3	0	0	1	**1**	**1**	**0.99**	**0.01**	**Yes**
	2**	0	0	0	0	2	0	9	**2**	**3**	**0.99**	**0.03**	**Yes**
	3**	1	2	0	0	0	4	0	**1**	**2**	**0.99**	**0.01**	**Yes**
eri-3 (tm1361)	**0.5**	105	122	78	105	84	100	99	**99**	**15**	**0.36**	**0.11**	**Yes**
	0.75	76	122	66	75	74	64	47	**75**	**23**	**0.52**	**0.15**	**Yes**
	1	12	95	94	69	29	24	90	**59**	**36**	**0.62**	**0.24**	**Yes**
	2	3	25	0	2	0	5	0	**5**	**9**	**0.97**	**0.06**	**Yes**
	3	0	0	0	0	0	1	0	**0**	**0**	**1.00**	**0**	**Yes**
eri-5 (tm1705)	**0.5**	176	192	196	180	188	204		**189**	**10**	**0**	**0.10**	
	0.75	174	118	176	180	130	120	112	**144**	**31**	**0.15**	**0.31**	
	1	168	176	84	146	192	188		**159**	**40**	**0.07**	**0.40**	
	2	166	167	168	76	144	132	132	**141**	**33**	**0.17**	**0.33**	
	3	96	45	40	32	30	48	58	**50**	**22**	**0.71**	**0.22**	
eri-6/7 (tm1917)	**0.5**	196	186	206	218	180	206	196	**198**	**13**	**0**	**0.13**	
	0.75	82	111	96	94	114	110	120	**104**	**13**	**0.33**	**0.10**	**Yes**
	1	104	49	106	46	106	80	101	**85**	**27**	**0.46**	**0.18**	**Yes**
	2	0	0	2	0	10	0	0	**2**	**4**	**0.99**	**0.02**	**Yes**
	3	0	0	0	2	0	0	1	**0**	**1**	**1.00**	**0.01**	**Yes**
eri-8 (gg100)	**0.5**	238	216	222	216	196	184	206	**211**	**18**	**0.05**	**0.09**	
	0.75	224	240	206	196	180	206		**209**	**21**	**0.06**	**0.10**	
	1	112	120	96	80	76	86	90	**94**	**16**	**0.58**	**0.07**	**Yes**
	2	0	0	0	1	0	2	11	**2**	**4**	**0.99**	**0.02**	**Yes**
	3	0	0	1	2	0	0		**1**	**1**	**1.00**	**0**	**Yes**
eri-9 (gg106)	**0.5**	264	272	240	232	232	222		**244**	**20**	**0**	**0.10**	
	0.75	224	264	260	196	208	220	201	**225**	**27**	**0.06**	**0.13**	
	1	11	160	90	5	60	40	55	**60**	**53**	**0.75**	**0.22**	**Yes**
	2	0	12	2	11	7	0	5	**5**	**5**	**0.98**	**0.02**	**Yes**
	3	1	3	0	0	0	0	1	**1**	**1**	**1.00**	**0**	**Yes**
eri-11 (gg99)	**0.5**	272	230	216	224	230	270		**240**	**24**	**0**	**0.11**	
	0.75	232	208	196	238	240	216	208	**220**	**17**	**0**	**0.08**	
	1	156	181	144	144	106	134	98	**138**	**29**	**0.50**	**0.11**	**Yes**
	2	0	2	18	35	30	0	14	**14**	**14**	**0.95**	**0.05**	**Yes**
	3	0	0	0	5	0	5	6	**2**	**3**	**0.99**	**0.01**	**Yes**

Table 2.14: Dilution series of Eri responses by RNAi feeding against *unc-22*

Single L3-stage larvae were placed on RNAi food targeting *unc-22*; 4 days later, the percent of progeny showing the expected paralysis due to severe twitching at each indicated concentration (OD at 600 nm) of initial bacterial culture were determined. For clarity, two bacterial culture concentrations (OD_{600nm} of 3 and 4), which produced similar Eri penetrances as adjacent concentrations, are not included. The tabulated mean (Avg) and standard deviation (SD) for N2 wild type were used as the basis to indicate an Eri or a Rde phenotype (Eri?), with $p<0.05$ as the criterion to denote significant difference from wild type response levels. A strain which fits the "best *eri*" criterion described in text is marked as "best", with asterisks indicating concentrations of RNAi food at which it fulfilled the criterion.

Table 2.14 (Continued): Dilution series results for *unc-22* feeding

Strain	OD_{600}	*Penetrance readings*							*Avg*	*SD*	*Eri?*
Wildtype (N2)	**0.1**	3/28	3/18	1/16	5/31	0/13	3/25	1/17	**0.10**	**0.06**	
	0.25	8/30	9/35	8/29	5/30	5/22	5/20		**0.24**	**0.04**	
	0.5	8/31	8/36	10/28	8/27	8/27	8/30	11/26	**0.30**	**0.07**	
	1	7/24	7/25	12/21	11/22	6/16	10/19	11/27	**0.42**	**0.11**	
	2	26/31	27/36	22/26	25/27	29/36	26/29	28/33	**0.84**	**0.06**	
eri-1 (mg366)	**0.1**	3/26	3/35	1/22	4/32	2/27	0/30	2/19	**0.08**	**0.04**	
	0.25	8/42	5/23	9/21	8/19	6/25	6/21	10/23	**0.32**	**0.11**	
	0.5	18/33	27/33	8/17	19/41	26/37	19/34	19/22	**0.63**	**0.16**	**Yes**
	1	46/55	6/7	20/22	31/32	45/50	19/21	24/30	**0.88**	**0.06**	**Yes**
	2	47/50	37/39	20/20	20/20	19/20	48/50	18/20	**0.96**	**0.04**	**Yes**
rrf-3 (pk1426) *Best*	**0.1**	15/37	18/27	12/41	2/41	7/33	2/36	6/36	**0.26**	**0.22**	
	0.25	20/32	27/37	36/48	24/31	18/24	30/35	34/36	**0.78**	**0.10**	**Yes**
	0.5**	36/41	51/58	37/41	46/51	32/34	39/46	44/44	**0.91**	**0.05**	**Yes**
	1**	31/33	45/49	20/20	46/50	20/20	20/20	19/21	**0.95**	**0.04**	**Yes**
	2**	54/56	20/20	20/20	40/40	20/20	46/47	20/20	**0.99**	**0.01**	**Yes**
eri-3 (tm1361)	**0.1**	4/15	9/19	2/30	3/54	6/36	2/31	2/37	**0.16**	**0.16**	
	0.25	3/30	5/24	5/24	5/31	9/40	10/35	6/31	**0.20**	**0.06**	
	0.5	28/31	20/31	29/46	30/40	14/18	24/34	17/22	**0.74**	**0.09**	**Yes**
	1	42/46	48/52	40/42	20/20	19/20	20/20	31/33	**0.95**	**0.03**	**Yes**
	2	24/26	46/52	20/20	20/20	19/20	20/20	21/23	**0.95**	**0.05**	**Yes**
eri-5 (tm1705)	**0.1**	3/28	3/37	2/28	4/30	5/47	4/35	3/26	**0.10**	**0.02**	
	0.25	5/49	3/21	1/25	6/25	7/36	7/27	6/34	**0.17**	**0.08**	
	0.5	4/33	11/48	19/39	8/29	10/19	4/37		**0.29**	**0.18**	
	1	22/47	9/29	19/34	14/28	24/44	19/40	13/30	**0.47**	**0.08**	
	2	37/47	26/38	27/30	19/23	20/22	24/27	46/49	**0.85**	**0.09**	
eri-6/7 (tm1917)	**0.1**	2/21	13/34	4/39	6/33	13/39	14/30	5/24	**0.25**	**0.14**	**Yes**
	0.25	14/42	15/37	17/36	10/19	6/20	14/29	11/24	**0.43**	**0.08**	**Yes**
	0.5	29/40	22/29	28/32	25/28	30/33	32/37		**0.84**	**0.08**	**Yes**
	1	51/55	20/20	39/40	78/80	30/30	20/20		**0.98**	**0.03**	**Yes**
	2	20/20	29/30	20/20	20/20	20/20	20/20	38/41	**0.98**	**0.03**	**Yes**
eri-8 (gg100)	**0.1**	4/30	4/25	5/27	1/27	1/35	3/25		**0.11**	**0.06**	
	0.25	9/22	11/31	6/23	14/34	8/18	5/16	10/27	**0.37**	**0.06**	**Yes**
	0.5	22/30	30/38	26/32	22/30	28/36	12/16	14/17	**0.77**	**0.04**	**Yes**
	1	46/49	44/47	20/20	20/20	37/40	63/69	19/20	**0.95**	**0.03**	**Yes**
	2	17/18	23/25	58/60	20/20	68/70	28/29	20/20	**0.97**	**0.03**	**Yes**
eri-9 (gg106)	**0.1**	5/38	3/34	1/22	0/22	1/14	1/19	1/17	**0.06**	**0.04**	
	0.25	3/14	3/20	4/21	3/16	14/28	12/30	8/29	**0.27**	**0.13**	
	0.5	12/22	18/27	20/26	20/27	14/19	29/37	14/19	**0.71**	**0.08**	**Yes**
	1	10/11	37/41	37/41	20/20	20/20	70/72	31/32	**0.95**	**0.04**	**Yes**
	2	51/56	44/46	20/20	20/20	44/47	40/40	20/20	**0.97**	**0.04**	**Yes**
eri-11 (gg99)	**0.1**	6/37	12/26	2/31	8/33	6/26	6/21	6/31	**0.23**	**0.12**	**Yes**
	0.25	13/37	9/29	6/18	11/21	11/30	12/19	10/30	**0.41**	**0.12**	**Yes**
	0.5	13/18	10/19	22/30	18/29	31/33	17/22	20/26	**0.73**	**0.13**	**Yes**
	1	10/24	18/23	22/23	41/42	20/20	17/20		**0.83**	**0.22**	**Yes**
	2	29/33	37/41	38/40	37/42	20/20	20/20	69/72	**0.94**	**0.05**	**Yes**

Table 2.15: Dilution series of Eri responses by RNAi feeding against *hbl-1*

Single L3-stage larvae were placed on RNAi food targeting *hbl-1*; 4 days later, the percent of progeny showing the expected paralysis at each indicated concentration (OD at 600 nm) of initial bacterial culture were determined. For clarity, two bacterial culture concentrations (OD_{600nm} of 0.02 and 0.5), which produced similar Eri penetrances as adjacent concentrations, are not included. The tabulated mean (Avg) and standard deviation (SD) for N2 wild type were used as the basis to indicate an Eri or a Rde phenotype (Eri?), with $p<0.05$ as the criterion to denote significant difference from wild type response levels. A strain which fits the "best *eri*" criterion described in text is marked as "best", with asterisks indicating concentrations of RNAi food at which it fulfilled the criterion.

Table 2.15 (Continued): Dilution series results for *hbl-1* feeding

Strain	*OD_{600}*	*Penetrance readings*								*Avg*	*SD*	*Eri?*
Wildtype (N2)	**0.1**	0/20	0/20	0/20	0/20	0/20	0/20	0/20	0/20	**0**	**0**	
	0.25	0/20	0/20	2/78	1/98	0/62	0/20			**0.01**	**0.01**	
	0.75	0/20	2/100	1/100	12/89	16/104	16/83	1/80	4/90	**0.07**	**0.08**	
	1.5	5/95	6/80	4/83	43/110	14/93	17/81	12/124	16/135	**0.14**	**0.11**	
	3	16/59	15/76	22/91	24/105	23/109	34/108	46/143	21/140	**0.24**	**0.06**	
eri-1 (mg366)	**0.1**	3/50	2/50	0/50	0/20	0/20	0/20	3/74	1/56	**0.02**	**0.02**	
	0.25	7/62	10/44	0/20	6/90	2/50	68/71	20/60		**0.25**	**0.33**	
	0.75	8/13	13/33	34/53	24/67	20/20	17/21	16/29	17/33	**0.61**	**0.21**	**Yes**
	1.5	11/14	37/45	25/27	74/78	84/88	65/100	37/41	21/32	**0.83**	**0.12**	**Yes**
	3	17/22	8/10	6/8	51/56	69/75	46/50	48/70	14/16	**0.83**	**0.09**	**Yes**
rrf-3 (pk1426) <u>*Best*</u>	**0.1**	4/50	6/60	6/60	1/50	0/20	0/20	7/79		**0.06**	**0.05**	
	0.25	15/38	16/52	16/75	13/82	10/72	26/64	12/54		**0.26**	**0.11**	**Yes**
	0.75	37/57	31/72	51/99	20/20	27/30	26/30	34/43	34/55	**0.72**	**0.20**	**Yes**
	1.5**	20/20	20/20	20/20	20/20	28/30	20/20	33/35	27/29	**0.98**	**0.03**	**Yes**
	3**	20/20	20/20	20/20	20/20	20/20	20/20	20/20		**1.00**	**0**	**Yes**
eri-3 (tm1361)	**0.1**	9/81	1/15	5/78	0/20	5/80	0/20	3/68	4/60	**0.05**	**0.04**	
	0.25	12/56	13/38	11/58	0/53	9/77	14/79	20/73	19/80	**0.19**	**0.10**	**Yes**
	0.75	15/27	13/18	28/54	19/20	29/30	159/174	34/40	24/36	**0.77**	**0.18**	**Yes**
	1.5	20/20	20/20	20/20	20/20	20/20	145/155	20/20	20/20	**0.99**	**0.02**	**Yes**
	3	20/20	20/20	20/20	18/19	20/20	90/127	20/20	20/20	**0.96**	**0.10**	**Yes**
eri-5 (tm1705)	**0.1**	0/20	0/20	0/20	0/20	0/20	0/20	0/20	0/20	**0**	**0**	
	0.25	0/20	0/20	0/20	0/20	0/20	0/20	2/50	1/50	**0.01**	**0.01**	
	0.75	3/100	3/100	5/100	5/93	17/107	28/149	2/31	10/68	**0.09**	**0.06**	
	1.5	19/107	20/100	23/81	9/111	1/12	8/79	16/50	15/46	**0.20**	**0.10**	
	3	27/87	31/109	25/71	14/111	13/80	24/132	10/57	24/56	**0.25**	**0.11**	
eri-6/7 (tm1917)	**0.1**	9/66	0/20	1/50	3/50	1/50	1/15	1/58		**0.05**	**0.06**	
	0.25	23/118	16/86	7/89	11/56	10/120	16/84	8/54	24/63	**0.18**	**0.09**	**Yes**
	0.75	23/89	5/69	28/59	20/20	59/82	79/90	36/50	20/20	**0.64**	**0.34**	**Yes**
	1.5	24/88	30/32	20/20	34/43	20/20	50/90	24/48	38/40	**0.75**	**0.28**	**Yes**
	3	20/20	20/20	20/20	73/80	20/20	28/30	20/20		**0.98**	**0.04**	**Yes**
eri-8 (gg100) <u>*Best*</u>	**0.1**	3/100	9/100	7/150	4/70	5/150	1/90			**0.04**	**0.03**	
	0.25	16/95	9/91	38/143	24/111	26/129	29/105	21/92		**0.21**	**0.06**	**Yes**
	0.75	20/21	20/21	27/27	138/148	28/30	43/47	48/104	68/98	**0.86**	**0.18**	**Yes**
	1.5**	20/20	20/20	20/20	26/29	20/20	27/29	20/20	140/150	**0.97**	**0.04**	**Yes**
	3**	20/20	20/20	20/20	20/20	20/20	78/89	20/20	20/20	**0.98**	**0.04**	**Yes**
eri-9 (gg106)	**0.1**	5/100	5/100	6/100	0/20	0/20	0/20	0/53	0/20	**0.02**	**0.03**	
	0.25	20/115	13/85	19/96	7/103	9/160	14/180	34/168	2/6	**0.16**	**0.09**	**Yes**
	0.75	67/78	57/91	39/97	117/147	116/166	96/121	35/124	40/87	**0.61**	**0.21**	**Yes**
	1.5	62/69	49/50	159/178	26/165	27/151	49/69	104/115		**0.67**	**0.36**	**Yes**
	3	22/22	14/14	99/100	81/135	47/50	20/20	96/103		**0.92**	**0.15**	**Yes**
eri-11 (gg99)	**0.1**	1/100	0/20	0/20	4/150	2/120	0/20	4/150	2/80	**0.01**	**0.01**	
	0.25	8/86	10/54	7/56	12/105	8/82	9/113	9/61	11/63	**0.13**	**0.04**	**Yes**
	0.75	12/55	8/22	43/85	63/133	55/91	34/66	21/88		**0.42**	**0.15**	**Yes**
	1.5	18/18	20/22	44/77	85/108	76/114	76/129			**0.75**	**0.18**	**Yes**
	3	13/14	14/14	17/19	115/137	20/20	103/143	20/20	20/20	**0.92**	**0.10**	**Yes**

Table 2.16: Dilution series of Eri responses by RNAi feeding against *hmr-1*

Single L3-stage larvae were placed on RNAi food targeting *hmr-1*; 4 days later, the number of progeny surviving to L3-stage larvae or older at each indicated concentration (OD at 600 nm) of initial bacterial culture was determined. For clarity, three bacterial culture concentrations (OD_{600nm} of 0.01, 1, and 2), which produced similar Eri penetrances as adjacent concentrations, are not included. The tabulated mean (Avg) and standard deviation (SD) were normalized to the brood sizes of each strain fed empty RNAi vector (**Table 2.27**), to obtain the normalized mean (N.Avg) and standard error of the mean (SEM). The normalized mean and the standard error of the mean for N2 wild type were used as the basis to indicate an Eri or a Rde phenotype (Eri?), with $p<0.05$ as the criterion to denote significant difference from wild type response levels. A strain which fits the "best *eri*" criterion described in text is marked as "best", with asterisks indicating concentrations of RNAi food at which it fulfilled the criterion.

Table 2.16 (Continued): Dilution series results for *hmr-1* feeding

Strain	*OD_{600}*	*Brood Size*							*Avg*	*SD*	*N.Avg*	*SEM*	*Eri?*
Wildtype (N2)	**0.02**	224	208	240	198	232	248		**225**	**19**	**0.01**	**0.12**	
	0.05	184	200	240	272	248	256		**233**	**34**	**0**	**0.18**	
	0.1	252	224	200	240	256	220	238	**233**	**20**	**0**	**0.13**	
	0.25	288	264	200	210	225	252	224	**238**	**32**	**0**	**0.17**	
	0.5	225	240	264	259	224	208	228	**235**	**20**	**0**	**0.13**	
eri-1 (mg366)	**0.02**	104	128	120	114	144	88	80	**111**	**22**	**0.30**	**0.15**	**Yes**
	0.05	72	56	78	96	70	84	72	**75**	**12**	**0.52**	**0.08**	**Yes**
	0.1	53	25	71	58	83	53	61	**58**	**18**	**0.64**	**0.12**	**Yes**
	0.25	54	0	23	14	8	22	0	**17**	**19**	**0.89**	**0.12**	**Yes**
	0.5	13	0	0	20	19	0	60	**16**	**21**	**0.90**	**0.13**	**Yes**
rrf-3 (pk1426) *Best*	**0.02**	78	101	85	48	80	63	71	**75**	**17**	**0.44**	**0.13**	**Yes**
	0.05	89	42	49	53	45	63	100	**63**	**23**	**0.53**	**0.17**	**Yes**
	0.1**	0	0	1	1	0	6	21	**4**	**8**	**0.97**	**0.06**	**Yes**
	0.25**	22	0	1	2	24	0	18	**10**	**11**	**0.93**	**0.08**	**Yes**
	0.5**	0	0	0	0	0	0	0	**0**	**0**	**1.00**	**0**	**Yes**
eri-3 (tm1361)	**0.02**	72	102	72	85	120	128		**97**	**24**	**0.38**	**0.17**	**Yes**
	0.05	120	108	128	144	90			**118**	**20**	**0.24**	**0.15**	**Yes**
	0.1	29	23	37	25	13	17	40	**26**	**10**	**0.83**	**0.07**	**Yes**
	0.25	0	19	12	3	0	3		**6**	**8**	**0.96**	**0.05**	**Yes**
	0.5	0	0	0	0	1	6	3	**1**	**2**	**0.99**	**0.01**	**Yes**
eri-5 (tm1705)	**0.02**	144	184	203	217	152	168	193	**180**	**27**	**0**	**0.19**	
	0.05	216	168	216	192	152			**189**	**29**	**0**	**0.20**	
	0.1	152	168	152	176	184	184	128	**163**	**21**	**0.04**	**0.15**	
	0.25	168	144	116	156	170	125	136	**145**	**21**	**0.15**	**0.15**	
	0.5	192	184	156	160	176	152	175	**171**	**15**	**0**	**0.13**	
eri-6/7 (tm1917)	**0.02**	132	105	93	84	108	90	98	**101**	**16**	**0**	**0.11**	
	0.05	136	160	128	168	104	168	136	**143**	**24**	**0.08**	**0.17**	
	0.1	33	26	20	46	35	112	68	**49**	**32**	**0.69**	**0.21**	**Yes**
	0.25	46	29	0	36	42	45		**33**	**17**	**0.79**	**0.11**	**Yes**
	0.5	10	0	0	4	3	0	1	**3**	**4**	**0.98**	**0.02**	**Yes**
eri-8 (gg100) *Best*	**0.02**	96	168	136	142	153	160	169	**146**	**25**	**0**	**0.12**	
	0.05	128	72	144	104	128	56	128	**109**	**33**	**0.51**	**0.15**	**Yes**
	0.1**	3	25	17	25	5	16	12	**15**	**9**	**0.93**	**0.04**	**Yes**
	0.25**	1	1	0	4	0	8	3	**2**	**3**	**0.99**	**0.01**	**Yes**
	0.5**	0	1	0	0	0	1	0	**0**	**0**	**1.00**	**0**	**Yes**
eri-9 (gg106)	**0.02**	180	232	168	168	176	196	187	**187**	**22**	**0.22**	**0.10**	**Yes**
	0.05	160	176	120	200	112	128	204	**157**	**38**	**0.34**	**0.16**	**Yes**
	0.1	15	168	160	72	114	104	71	**101**	**54**	**0.58**	**0.23**	**Yes**
	0.25	37	87	33	52	27	67	72	**54**	**23**	**0.78**	**0.09**	**Yes**
	0.5	8	12	0	9	34	0	15	**11**	**12**	**0.95**	**0.05**	**Yes**
eri-11 (gg99)	**0.02**	256	184	208	200	168	184	180	**197**	**29**	**0.28**	**0.12**	**Yes**
	0.05	152	160	180	205	200	198		**183**	**22**	**0.33**	**0.09**	**Yes**
	0.1	64	66	95	56	96	162	80	**88**	**36**	**0.68**	**0.13**	**Yes**
	0.25	48	0	15	80	30	50	52	**39**	**27**	**0.86**	**0.10**	**Yes**
	0.5	6	0	11	0	0	0	7	**3**	**5**	**0.99**	**0.02**	**Yes**

Table 2.17: Dilution series of Eri responses by RNAi feeding against *unc-73*

Single L3-stage larvae were placed on RNAi food targeting *unc-73*; 4 days later, the percent of progeny showing the expected paralysis at each indicated concentration (OD at 600 nm) of initial bacterial culture were determined. For clarity, three bacterial culture concentrations (OD_{600nm} of 0.03, 0.25, and 1), which produced similar Eri penetrances as adjacent concentrations, are not included. The tabulated mean (Avg) and standard deviation (SD) for N2 wild type were used as the basis to indicate an Eri or a Rde phenotype (Eri?), with $p<0.05$ as the criterion to denote significant difference from wild type response levels. A strain which fits the "best *eri*" criterion described in text is marked as "best", with asterisks indicating concentrations of RNAi food at which it fulfilled the criterion.

Table 2.17 (Continued): Dilution series results for *unc-73* feeding

Strain	*OD_{600}*	*Penetrance readings*							*Avg*	*SD*	*Eri?*
Wildtype (N2)	**0.1**	0/20	0/20	0/20	0/20	0/20	0/20	0/20	**0**	**0**	
	0.5	0/20	0/20	0/20	0/20	1/30	0/20	1/40	**0.01**	**0.01**	
	0.75	0/20	0/20	0/20	0/20	0/20	0/20	0/20	**0**	**0**	
	2	0/20	0/20	0/20	2/50	0/30	0/20	2/80	**0.01**	**0.02**	
	3	0/20	0/20	0/20	6/90	3/80	0/20	0/20	**0.01**	**0.03**	
eri-1 (mg366)	**0.1**	0/20	0/20	0/20	0/26	0/35	0/20	0/20	**0**	**0**	
	0.5	5/50	8/67	13/61	17/47	6/27	14/32	12/33	**0.26**	**0.13**	**Yes**
	0.75	12/40	14/50	9/47	13/35	20/57	27/48	26/54	**0.36**	**0.13**	**Yes**
	2	21/23	74/78	22/38	21/31	73/84	30/53		**0.76**	**0.17**	**Yes**
	3	20/20	103/112	20/20	28/30	20/20	42/47		**0.96**	**0.05**	**Yes**
rrf-3 (pk1426)	**0.1**	0/20	0/20	0/20	1/29	2/60	0/20	0/20	**0.01**	**0.02**	
	0.5	1/60	4/50	3/70	4/15	13/67	6/48		**0.12**	**0.10**	**Yes**
	0.75	3/6	10/42	10/31	13/37	38/61	44/61	21/48	**0.46**	**0.17**	**Yes**
	2	18/39	19/77	22/58	46/54	43/55	81/91	88/97	**0.65**	**0.27**	**Yes**
	3	18/64	18/47	25/54	27/30	88/90	58/68		**0.64**	**0.30**	**Yes**
eri-3 (tm1361)	**0.1**	0/20	0/20	0/12	0/20	1/30	0/20	0/20	**0**	**0.01**	
	0.5	2/50	3/60	5/50	1/15	2/23	12/56	15/40	**0.13**	**0.12**	**Yes**
	0.75	18/52	16/48	13/32	13/35	11/22	26/36	13/30	**0.44**	**0.13**	**Yes**
	2	11/44	22/46	16/65	19/46	6/10	32/36	80/82	**0.55**	**0.29**	**Yes**
	3	29/46	25/44	26/48	53/60	18/20	22/24	43/44	**0.77**	**0.19**	**Yes**
eri-5 (tm1705)	**0.1**	0/20	0/20	2/30	0/20	0/20	0/20	1/108	**0.01**	**0.02**	
	0.5	0/20	0/20	0/20	0/20	0/20	0/20		**0**	**0**	
	0.75	1/40	0/20	0/20	0/20	1/30	12/120	4/120	**0.03**	**0.04**	
	2	0/20	0/20	1/20	1/30	0/20	2/89	0/20	**0.02**	**0.02**	
	3	1/20	2/30	4/50	2/60	1/30	5/103	0/20	**0.04**	**0.03**	
eri-6/7 (tm1917)	**0.1**	0/20	0/20	0/20	0/67	1/53	1/90	0/20	**0**	**0.01**	
	0.5	3/40	7/50	2/60	4/57	6/78	1/32	8/69	**0.08**	**0.04**	**Yes**
	0.75	6/22	17/77	17/69	26/39	10/17	11/90	17/83	**0.33**	**0.21**	**Yes**
	2	34/43	47/50	44/50	23/40	38/66	34/40	14/60	**0.69**	**0.25**	**Yes**
	3	46/50	47/50	20/20	20/20	20/20	30/33	50/53	**0.96**	**0.04**	**Yes**
eri-8 (gg100) <u>*Best*</u>	**0.1**	0/20	0/20	2/50	2/50	3/60	0/23	0/29	**0.02**	**0.02**	
	0.5	8/90	8/60	4/70	14/73	28/78	34/82	17/68	**0.21**	**0.14**	**Yes**
	0.75	56/73	86/101	46/53	41/51	29/45	32/57	30/65	**0.71**	**0.16**	**Yes**
	2**	20/20	20/20	20/20	19/24	20/20	117/122	81/81	**0.96**	**0.08**	**Yes**
	3**	20/20	20/20	20/20	20/20	20/20	124/133	20/20	**0.99**	**0.03**	**Yes**
eri-9 (gg106)	**0.1**	1/50	0/20	0/20	4/71	5/57	1/130	0/20	**0.02**	**0.03**	
	0.5	3/100	8/100	2/80	9/54	24/83	13/51		**0.14**	**0.11**	**Yes**
	0.75	9/60	8/69	25/78	11/62	6/48	34/64	15/47	**0.25**	**0.15**	**Yes**
	2	40/48	43/65	35/46	29/94	19/71	52/57	31/72	**0.60**	**0.26**	**Yes**
	3	48/50	83/90	89/90	67/88	107/115	41/49		**0.90**	**0.09**	**Yes**
eri-11 (gg99)	**0.1**	0/20	1/40	0/20	0/20	1/30	0/20	2/80	**0.01**	**0.02**	
	0.5	11/122	6/72	10/87	7/50	4/72	6/44	21/53	**0.15**	**0.11**	**Yes**
	0.75	24/55	7/64	21/73	36/79	21/66	27/84	29/86	**0.32**	**0.11**	**Yes**
	2	32/79	20/71	22/67	11/59	53/72	12/35	35/66	**0.40**	**0.18**	**Yes**
	3	51/83	112/118	20/20	20/20	56/66	91/107	61/67	**0.88**	**0.13**	**Yes**

Table 2.18: Dilution series of Eri responses by RNAi feeding against *div-1*

Single L3-stage larvae were placed on RNAi food targeting *div-1*; 4 days later, the number of progeny surviving to L3-stage larvae or older at each indicated concentration (OD at 600 nm) of initial bacterial culture was determined. The tabulated mean (Avg) and standard deviation (SD) were normalized to the brood sizes of each strain fed empty RNAi vector (**Table 2.27**), to obtain the normalized mean (N.Avg) and standard error of the mean (SEM). The normalized mean and the standard error of the mean for N2 wild type were used as the basis to indicate an Eri or a Rde phenotype (Eri?), with $p<0.05$ as the criterion to denote significant difference from wild type response levels. A strain which fits the "best *eri*" criterion described in text is marked as "best", with asterisks indicating concentrations of RNAi food at which it fulfilled the criterion.

Table 2.18 (Continued): Dilution series results for *div-1* feeding

Strain	*OD_{600}*	*Brood Size*							*Avg*	*SD*	*N.Avg*	*SEM*	*Eri?*
Wildtype (N2)	**0.5**	95	104	128	105	128	160	146	**124**	**24**	**0.45**	**0.12**	
	1	86	57	69	72	33	37	56	**59**	**19**	**0.74**	**0.09**	
	2	88	53	50	47	79	33	37	**55**	**21**	**0.76**	**0.09**	
	3	59	62	49	54	84	33	50	**56**	**16**	**0.75**	**0.07**	
	4	63	50	58	83	50	34	32	**53**	**18**	**0.77**	**0.08**	
eri-1 (mg366)	**0.5**	98	100	64	120	66	99	80	**90**	**20**	**0.43**	**0.13**	
	1	60	96	78	68	36	48	46	**62**	**21**	**0.61**	**0.13**	
	2	29	63	59	10	55	31	40	**41**	**19**	**0.74**	**0.12**	
	3	50	50	56	44	23	35	59	**45**	**13**	**0.71**	**0.08**	
	4	51	74	19	64	39	10	47	**43**	**23**	**0.73**	**0.15**	
rrf-3 (pk1426)	**0.5**	64	96	63	84	102	57	54	**74**	**19**	**0.44**	**0.15**	
	1	36	65	75	35	34	41	26	**45**	**18**	**0.67**	**0.14**	
	2	36	42	66	27	25	10	11	**31**	**19**	**0.77**	**0.15**	
	3	26	23	1	25	10	27	15	**18**	**10**	**0.86**	**0.07**	**Yes**
	4	20	24	17	17	19	43	15	**22**	**10**	**0.83**	**0.07**	
eri-3 (tm1361) *Best*	**0.5**	47	54	79	55	51	55	37	**54**	**13**	**0.65**	**0.09**	
	1	94	34	47	25	45	27	50	**46**	**23**	**0.70**	**0.15**	
	2**	18	36	13	10	14	19		**18**	**9**	**0.88**	**0.06**	**Yes**
	3**	10	24	32	18	15	17	8	**18**	**8**	**0.89**	**0.05**	**Yes**
	4**	8	16	9	10	15	32	12	**15**	**8**	**0.91**	**0.05**	**Yes**
eri-5 (tm1705)	**0.5**	46	72	88	104	112	120	81	**89**	**26**	**0.48**	**0.16**	
	1	32	28	40	7	48	39	13	**30**	**15**	**0.83**	**0.09**	
	2	23	25	26	22	18	23	18	**22**	**3**	**0.87**	**0.02**	**Yes**
	3	18	20	18	23	9	21	16	**18**	**5**	**0.90**	**0.03**	**Yes**
	4	30	25	20	9	22	25	19	**21**	**7**	**0.87**	**0.04**	**Yes**
eri-6/7 (tm1917)	**0.5**	106	108	90	88	72	84	105	**93**	**13**	**0.40**	**0.10**	
	1	38	34	31	36	44	37	61	**40**	**10**	**0.74**	**0.07**	
	2	52	38	26	29	34	2	30	**30**	**15**	**0.81**	**0.10**	
	3	44	14	23	51	31	27	48	**34**	**14**	**0.78**	**0.09**	
	4	19	25	29	28	16	6	33	**22**	**9**	**0.86**	**0.06**	**Yes**
eri-8 (gg100)	**0.5**	104	108	135	162	166	180	168	**146**	**31**	**0.34**	**0.14**	
	1	192	86	102	60	78	76		**99**	**48**	**0.56**	**0.21**	
	2	128	108	90	36	32	56	33	**69**	**40**	**0.69**	**0.18**	
	3	29	70	106	39	44	36	39	**52**	**27**	**0.77**	**0.12**	
	4	74	78	25	30	27	19		**42**	**26**	**0.81**	**0.12**	
eri-9 (gg106)	**0.5**	114	148	120	76	122	88	98	**109**	**24**	**0.54**	**0.10**	
	1	72	130	112	30	24	18	24	**59**	**47**	**0.76**	**0.19**	
	2	72	42	114	31	26	29	22	**48**	**34**	**0.80**	**0.14**	
	3	75	88	65	30	35	20	21	**48**	**28**	**0.80**	**0.12**	
	4	25	43	33	29	23	24	20	**28**	**8**	**0.88**	**0.03**	**Yes**
eri-11 (gg99)	**0.5**	112	232	160	136	162	200	176	**168**	**40**	**0.39**	**0.15**	
	1	98	102	118	37	72	96	82	**86**	**26**	**0.68**	**0.10**	
	2	104	44	90	33	45	28	34	**54**	**30**	**0.80**	**0.11**	
	3	44	98	96	40	35	34	35	**55**	**29**	**0.80**	**0.11**	
	4	31	42	34	25	37	37		**34**	**6**	**0.87**	**0.02**	**Yes**

Table 2.19: Dilution series of Eri responses by RNAi feeding against *pbs-6*

Single L3-stage larvae were placed on RNAi food targeting *pbs-6*; 4 days later, the number of progeny surviving to L3-stage larvae or older at each indicated concentration (OD at 600 nm) of initial bacterial culture was determined. For clarity, three bacterial culture concentrations (OD_{600nm} of 0.005, 0.01, and 1), which produced similar Eri penetrances as adjacent concentrations, are not included. The tabulated mean (Avg) and standard deviation (SD) were normalized to the brood sizes of each strain fed empty RNAi vector (**Table 2.27**), to obtain the normalized mean (N.Avg) and standard error of the mean (SEM). The normalized mean and the standard error of the mean for N2 wild type were used as the basis to indicate an Eri or a Rde phenotype (Eri?), with $p<0.05$ as the criterion to denote significant difference from wild type response levels. A strain which fits the "best *eri*" criterion described in text is marked as "best", with asterisks indicating concentrations of RNAi food at which it fulfilled the criterion.

Table 2.19 (Continued): Dilution series results for *pbs-6* feeding

Strain	*OD_{600}*	*Brood Size*							*Avg*	*SD*	*N.Avg*	*SEM*	*Eri?*
Wildtype (N2)	**0.02**	205	227	224	244	207	240	207	**222**	**16**	**0.02**	**0.11**	
	0.05	244	256	216	134	264	200	160	**211**	**49**	**0.07**	**0.23**	
	0.1	172	190	84	53	210	41	93	**120**	**69**	**0.47**	**0.31**	
	0.25	62	50	39	20	21	60		**42**	**19**	**0.81**	**0.08**	
	0.5	32	12	15	13	23	20	22	**20**	**7**	**0.91**	**0.03**	
eri-1 (mg366)	**0.02**	107	137	120	72	80	80	80	**97**	**25**	**0.39**	**0.16**	**Yes**
	0.05	134	88	84	64	44	60	75	**78**	**29**	**0.50**	**0.18**	**Yes**
	0.1	110	33	56	66	40	33	36	**53**	**28**	**0.66**	**0.18**	
	0.25	20	48	6	9	4	3	11	**14**	**16**	**0.91**	**0.10**	
	0.5	4	1	2	11	4	4	0	**4**	**4**	**0.98**	**0.02**	**Yes**
rrf-3 (pk1426)	**0.02**	122	152	120	128	120	138	112	**127**	**14**	**0.04**	**0.12**	
	0.05	144	135	96	104	126	84	78	**110**	**26**	**0.18**	**0.20**	
	0.1	51	85	38	25	96	43	84	**60**	**28**	**0.55**	**0.21**	
	0.25	0	2	2	7	9	87	23	**19**	**31**	**0.86**	**0.23**	
	0.5	0	1	1	0	0	0	3	**1**	**1**	**0.99**	**0.01**	**Yes**
eri-3 (tm1361) *Best*	**0.02**	152	176	42	144	104	156	75	**121**	**49**	**0.22**	**0.32**	
	0.05	156	99	32	45	19	84	31	**67**	**49**	**0.57**	**0.32**	**Yes**
	0.1	41	25	72	22	56	80	72	**53**	**24**	**0.66**	**0.15**	
	0.25**	16	4	2	3	7	8	2	**6**	**5**	**0.96**	**0.03**	**Yes**
	0.5**	2	11	0	0	1	0	3	**2**	**4**	**0.98**	**0.03**	**Yes**
eri-5 (tm1705)	**0.02**	170	162	160	152	90	112	95	**134**	**34**	**0.21**	**0.22**	
	0.05	165	144	66	48	62	49	49	**83**	**50**	**0.51**	**0.29**	**Yes**
	0.1	56	133	71	42	30	21	33	**55**	**38**	**0.68**	**0.23**	
	0.25	16	18	6	20	13	23	13	**16**	**6**	**0.91**	**0.03**	**Yes**
	0.5	2	3	4	2	5	2	2	**3**	**1**	**0.98**	**0.01**	**Yes**
eri-6/7 (tm1917) *Best*	**0.02**	176	192	168	184	232	190	112	**179**	**36**	**0**	**0.25**	
	0.05	150	162	96	96	100	104	126	**119**	**27**	**0.23**	**0.19**	
	0.1	40	35	23	112	66	40		**53**	**32**	**0.66**	**0.21**	
	0.25**	24	11	3	9	2	3	6	**8**	**8**	**0.95**	**0.05**	**Yes**
	0.5**	0	0	2	3	4	3	1	**2**	**2**	**0.99**	**0.01**	**Yes**
eri-8 (gg100)	**0.02**	234	232	266	248	240	224	232	**239**	**14**	**0**	**0.07**	
	0.05	280	272	144	192	152	193		**206**	**58**	**0.08**	**0.26**	
	0.1	105	28	77	75	45	120		**75**	**35**	**0.66**	**0.16**	
	0.25	18	19	11	56	22	19	16	**23**	**15**	**0.90**	**0.07**	
	0.5	2	3	13	0	3	7	3	**4**	**4**	**0.98**	**0.02**	**Yes**
eri-9 (gg106)	**0.02**	216	192	250	210	192	208	222	**213**	**20**	**0.11**	**0.10**	
	0.05	217	227	190	160	192	184	170	**191**	**24**	**0.20**	**0.11**	
	0.1	124	66	160	167	126	112	44	**114**	**45**	**0.52**	**0.19**	
	0.25	26	69	14	16	27	32	16	**29**	**19**	**0.88**	**0.08**	
	0.5	2	0	2	8	9	13	22	**8**	**8**	**0.97**	**0.03**	**Yes**
eri-11 (gg99)	**0.02**	161	227	116	146	136	168	135	**156**	**36**	**0.43**	**0.14**	**Yes**
	0.05	192	224	126	88	112	128		**145**	**52**	**0.47**	**0.19**	**Yes**
	0.1	26	158	136	128	128	67	33	**97**	**54**	**0.65**	**0.20**	
	0.25	51	66	26	24	8	37		**35**	**21**	**0.87**	**0.08**	
	0.5	0	3	12	7	7	8	8	**6**	**4**	**0.98**	**0.01**	**Yes**

Table 2.20: Dilution series of Eri responses by RNAi feeding against *pha-4*

Single L3-stage larvae were placed on RNAi food targeting *pha-4*; 4 days later, the number of progeny surviving to L3-stage larvae or older at each indicated concentration (OD at 600 nm) of initial bacterial culture was determined. For clarity, two bacterial culture concentrations (OD_{600nm} of 0.05 and 0.5), which produced similar Eri penetrances as adjacent concentrations, are not included. The tabulated mean (Avg) and standard deviation (SD) were normalized to the brood sizes of each strain fed empty RNAi vector (**Table 2.27**), to obtain the normalized mean (N.Avg) and standard error of the mean (SEM). The normalized mean and the standard error of the mean for N2 wild type were used as the basis to indicate an Eri or a Rde phenotype (Eri?), with $p<0.05$ as the criterion to denote significant difference from wild type response levels. A strain which fits the "best *eri*" criterion described in text is marked as "best", with asterisks indicating concentrations of RNAi food at which it fulfilled the criterion.

Table 2.20 (Continued): Dilution series results for *pha-4* feeding

Strain	*OD_{600}*	*Brood Size*							*Avg*	*SD*	*N.Avg*	*SEM*	*Eri?*
Wildtype (N2)	**0.01**	208	199	210	233	240	264	260	**231**	**26**	**0**	**0.15**	
	0.02	210	272	280	256	252	244		**252**	**25**	**0**	**0.15**	
	0.04	176	189	240	255	224	234	200	**217**	**29**	**0.04**	**0.16**	
	0.1	149	160	176	168	152	140		**158**	**13**	**0.30**	**0.09**	
	0.25	147	158	164	168	136	174		**158**	**14**	**0.30**	**0.09**	
eri-1 (mg366)	**0.01**	98	133	160	128	152	130	176	**140**	**25**	**0.12**	**0.17**	
	0.02	70	85	61	100	73	130	47	**81**	**27**	**0.49**	**0.18**	**Yes**
	0.04	11	0	57	46	73	94	108	**56**	**40**	**0.65**	**0.25**	**Yes**
	0.1	0	45	28	71	61	62		**45**	**27**	**0.72**	**0.17**	**Yes**
	0.25	31	15	47	12	17	13		**23**	**14**	**0.86**	**0.09**	**Yes**
rrf-3 (pk1426)	**0.01**	114	101	120	112	104	106		**110**	**7**	**0.18**	**0.08**	**Yes**
	0.02	76	81	47	92	64	90		**75**	**17**	**0.44**	**0.13**	**Yes**
	0.04	6	54	49	61	43	10		**37**	**23**	**0.72**	**0.18**	**Yes**
	0.1	1	0	7	19	34	44	57	**23**	**22**	**0.83**	**0.17**	**Yes**
	0.25	6	1	0	0	16	9	0	**5**	**6**	**0.97**	**0.05**	**Yes**
eri-3 (tm1361) <u>*Best*</u>	**0.01**	162	142	115	54	45	42	82	**92**	**49**	**0.41**	**0.32**	**Yes**
	0.02	46	87	72	74	54	75	29	**62**	**20**	**0.60**	**0.13**	**Yes**
	0.04	60	79	15	23	7	4	53	**34**	**29**	**0.78**	**0.19**	**Yes**
	0.1**	28	25	23	14	3	16	33	**20**	**10**	**0.87**	**0.07**	**Yes**
	0.25**	10	15	3	5	17	3	3	**8**	**6**	**0.95**	**0.04**	**Yes**
eri-5 (tm1705)	**0.01**	194	192	170	178	190	176	184	**183**	**9**	**0**	**0.12**	
	0.02	192	182	160	200	170	160	167	**176**	**16**	**0**	**0.14**	
	0.04	168	144	184	168	152	168		**164**	**14**	**0.04**	**0.13**	
	0.1	100	86	100	133	132	93	65	**101**	**24**	**0.41**	**0.16**	
	0.25	55	62	35	57	33	50	20	**45**	**15**	**0.74**	**0.09**	**Yes**
eri-6/7 (tm1917)	**0.01**	216	240	169	200	205	163	162	**194**	**30**	**0**	**0.22**	
	0.02	217	266	156	132	172	182		**188**	**48**	**0**	**0.32**	
	0.04	179	126	73	62	112	114	88	**108**	**39**	**0.31**	**0.26**	**Yes**
	0.1	52	74	41	63	56	63	41	**56**	**12**	**0.64**	**0.08**	**Yes**
	0.25	60	0	28	30	64	54	47	**40**	**23**	**0.74**	**0.15**	**Yes**
eri-8 (gg100)	**0.01**	236	248	232	224	216	235		**232**	**11**	**0**	**0.06**	
	0.02	86	164	144	176	176	154	160	**151**	**31**	**0.32**	**0.14**	**Yes**
	0.04	61	82	64	84	92	63	100	**78**	**16**	**0.65**	**0.07**	**Yes**
	0.1	7	3	28	4	3	47	30	**17**	**18**	**0.92**	**0.08**	**Yes**
	0.25	25	10	52	55	63	32	9	**35**	**22**	**0.84**	**0.10**	**Yes**
eri-9 (gg106)	**0.01**	244	246	272	240	256	256		**252**	**12**	**0**	**0.08**	
	0.02	216	176	216	240	280	278		**234**	**40**	**0.02**	**0.18**	
	0.04	164	171	208	248	224	170	220	**201**	**33**	**0.16**	**0.14**	
	0.1	36	57	114	92	90	123		**85**	**33**	**0.64**	**0.14**	**Yes**
	0.25	89	107	87	106	74	146		**102**	**25**	**0.58**	**0.11**	**Yes**
eri-11 (gg99)	**0.01**	292	260	320	264	274	312		**287**	**25**	**0**	**0.11**	
	0.02	264	254	240	248	341	324	304	**282**	**40**	**0**	**0.16**	
	0.04	153	116	216	216	200	209	226	**191**	**41**	**0.30**	**0.16**	**Yes**
	0.1	85	81	228	200	240	256	176	**181**	**72**	**0.34**	**0.27**	
	0.25	65	72	80	93	96	112		**86**	**17**	**0.68**	**0.07**	**Yes**

Table 2.21: Dilution series of Eri responses by RNAi feeding against *cdk-1*

Single L3-stage larvae were placed on RNAi food targeting *cdk-1*; 4 days later, the number of progeny surviving to L3-stage larvae or older at each indicated concentration (OD at 600 nm) of initial bacterial culture was determined. For clarity, three bacterial culture concentrations (OD_{600nm} of 0.025, 0.25, and 0.75), which produced similar Eri penetrances as adjacent concentrations, are not included. The tabulated mean (Avg) and standard deviation (SD) were normalized to the brood sizes of each strain fed empty RNAi vector (**Table 2.27**), to obtain the normalized mean (N.Avg) and standard error of the mean (SEM). The normalized mean and the standard error of the mean for N2 wild type were used as the basis to indicate an Eri or a Rde phenotype (Eri?), with $p<0.05$ as the criterion to denote significant difference from wild type response levels. A strain which fits the "best *eri*" criterion described in text is marked as "best", with asterisks indicating concentrations of RNAi food at which it fulfilled the criterion.

Table 2.21 (Continued): Dilution series results for *cdk-1* feeding

Strain	*OD_{600}*	*Brood Size*							*Avg*	*SD*	*N.Avg*	*SEM*	*Eri?*
Wildtype (N2)	**0.1**	248	284	222	192	248	248		**240**	**31**	**0**	**0.17**	
	0.5	194	244	224	239	157			**212**	**36**	**0.07**	**0.18**	
	1	124	4	9	17	0			**31**	**52**	**0.86**	**0.23**	
	2	87	137	4	6	3	51	3	**42**	**53**	**0.82**	**0.23**	
	3	0	11	0	6	2	2	3	**3**	**4**	**0.98**	**0.02**	
eri-1 (mg366)	**0.1**	13	127	192	120	123	84	148	**115**	**56**	**0.27**	**0.35**	
	0.5	77	75	65	36	47			**60**	**18**	**0.62**	**0.12**	**Yes**
	1	22	0	2	0	1	0		**4**	**9**	**0.97**	**0.06**	
	2	2	40	0	0	0	0	0	**6**	**15**	**0.96**	**0.09**	
	3	1	0	0	1	0	1	0	**0**	**1**	**1.00**	**0**	
rrf-3 (pk1426) <u>*Best*</u>	**0.1**	50	76	123	156	160	192	160	**131**	**51**	**0.02**	**0.39**	
	0.5**	2	0	3	0	0	0	0	**1**	**1**	**0.99**	**0.01**	**Yes**
	1**	1	0	0	0	0	0		**0**	**0**	**1.00**	**0**	
	2**	0	0	0	0	0	0	1	**0**	**0**	**1.00**	**0**	
	3**	0	0	0	1	0	0	0	**0**	**0**	**1.00**	**0**	
eri-3 (tm1361)	**0.1**	134	6	126	108	104	120	120	**103**	**44**	**0.34**	**0.29**	
	0.5	67	5	0	0	11	38		**20**	**27**	**0.87**	**0.17**	**Yes**
	1	26	65	0	1	0	14	34	**20**	**24**	**0.87**	**0.15**	
	2	0	0	1	1	0	0	0	**0**	**0**	**1.00**	**0**	
	3	9	1	0	0	0	0	0	**1**	**3**	**0.99**	**0.02**	
eri-5 (tm1705)	**0.1**	189	210	174	186	140	148	195	**177**	**25**	**0**	**0.18**	
	0.5	106	126	58	8	99			**79**	**47**	**0.53**	**0.28**	**Yes**
	1	58	72	0	0	0	0	0	**19**	**32**	**0.89**	**0.19**	
	2	81	5	0	0	0	0	0	**12**	**30**	**0.93**	**0.18**	
	3	0	1	0	0	0	0	0	**0**	**0**	**1.00**	**0**	
eri-6/7 (tm1917)	**0.1**	99	220	182	216	176	240	168	**186**	**47**	**0**	**0.31**	
	0.5	51	9	4	3	11			**16**	**20**	**0.90**	**0.13**	**Yes**
	1	33	0	0	0	0	0		**6**	**13**	**0.96**	**0.09**	
	2	4	1	0	1	0	0	0	**1**	**1**	**0.99**	**0.01**	
	3	0	2	0	1	0	0	0	**0**	**1**	**1.00**	**0.01**	
eri-8 (gg100)	**0.1**	262	276	194	248	240	240	272	**247**	**28**	**0**	**0.13**	
	0.5	24	93	1	0	6			**25**	**39**	**0.89**	**0.18**	**Yes**
	1	8	19	0	0	0	44	17	**13**	**16**	**0.94**	**0.07**	
	2	0	2	0	0	0	0	0	**0**	**1**	**1.00**	**0**	
	3	1	0	0	0	0	2	1	**1**	**1**	**1.00**	**0**	
eri-9 (gg106)	**0.1**	282	270	224	184	214	240	248	**237**	**34**	**0.01**	**0.15**	
	0.5	20	0	4	9	3	0		**6**	**8**	**0.97**	**0.03**	**Yes**
	1	124	0	0	0	2	2		**21**	**50**	**0.91**	**0.21**	
	2	3	127	0	0	3	1	1	**19**	**48**	**0.92**	**0.20**	
	3	0	0	0	0	0	0	1	**0**	**0**	**1.00**	**0**	
eri-11 (gg99)	**0.1**	272	298	264	216	272	224	260	**258**	**29**	**0.06**	**0.12**	
	0.5	181	282	64	78	38	104	192	**134**	**87**	**0.51**	**0.32**	**Yes**
	1	47	0	0	2	5	4	3	**9**	**17**	**0.97**	**0.06**	
	2	32	2	3	0	0	0	0	**5**	**12**	**0.98**	**0.04**	
	3	0	0	0	0	0	0	0	**0**	**0**	**1.00**	**0**	

Table 2.22: Dilution series of Eri responses by RNAi feeding against *knl-3*

Single L3-stage larvae were placed on RNAi food targeting *knl-3*; 4 days later, the number of progeny surviving to L3-stage larvae or older at each indicated concentration (OD at 600 nm) of initial bacterial culture was determined. For clarity, three bacterial culture concentrations (OD_{600nm} of 2, 3, and 4), which produced similar Eri penetrances as adjacent concentrations, are not included. The tabulated mean (Avg) and standard deviation (SD) were normalized to the brood sizes of each strain fed empty RNAi vector (**Table 2.27**), to obtain the normalized mean (N.Avg) and standard error of the mean (SEM). The normalized mean and the standard error of the mean for N2 wild type were used as the basis to indicate an Eri or a Rde phenotype (Eri?), with $p<0.05$ as the criterion to denote significant difference from wild type response levels. A strain which fits the "best *eri*" criterion described in text is marked as "best", with asterisks indicating concentrations of RNAi food at which it fulfilled the criterion.

Table 2.22 (Continued): Dilution series results for *knl-3* feeding

Strain	*OD_{600}*	*Brood Size*							*Avg*	*SD*	*N.Avg*	*SEM*	*Eri?*
Wildtype (N2)	**0.1**	256	242	184	210	180	232	200	**215**	**29**	**0.05**	**0.16**	
	0.25	264	240	237	216	260	235	224	**239**	**18**	**0**	**0.12**	
	0.5	240	192	148	168	208	191		**191**	**32**	**0.16**	**0.16**	
	0.75	212	200	176	162	180	169	203	**186**	**19**	**0.18**	**0.11**	
	1	99	63	84	47	77			**74**	**20**	**0.67**	**0.09**	
eri-1 (mg366)	**0.1**	63	40	168	155	162	151		**123**	**56**	**0.22**	**0.36**	
	0.25	100	152	96	120	120	184	156	**133**	**32**	**0.16**	**0.21**	
	0.5	50	1	55	111	81	114	77	**70**	**39**	**0.56**	**0.25**	**Yes**
	0.75	81	74	50	54	75	56	49	**63**	**13**	**0.60**	**0.09**	**Yes**
	1	1	0	0	0	0	66	13	**11**	**25**	**0.93**	**0.15**	**Yes**
rrf-3 (pk1426) *Best*	**0.1**	108	62	97	97	113	91	115	**98**	**18**	**0.27**	**0.14**	**Yes**
	0.25	68	130	110	89	78	105	100	**97**	**21**	**0.27**	**0.16**	**Yes**
	0.5	96	62	108	58	96	72	81	**82**	**19**	**0.39**	**0.15**	**Yes**
	0.75	69	64	102	93	80	109	89	**87**	**17**	**0.35**	**0.13**	**Yes**
	1**	0	0	15	0	10	5	1	**4**	**6**	**0.97**	**0.04**	**Yes**
eri-3 (tm1361)	**0.1**	99	91	210	200	195	208	220	**175**	**55**	**0**	**0.37**	
	0.25	85	184	89	189	78	170		**133**	**54**	**0.15**	**0.35**	
	0.5	62	83	185	168	76	82		**109**	**53**	**0.30**	**0.35**	
	0.75	128	123	126	101	96	113	103	**113**	**13**	**0.28**	**0.11**	
	1	0	22	12	16	59	36	10	**22**	**20**	**0.86**	**0.13**	**Yes**
eri-5 (tm1705)	**0.1**	224	184	243	216	236	200	168	**210**	**27**	**0**	**0.20**	
	0.25	240	244	198	232	200	168	180	**209**	**30**	**0**	**0.22**	
	0.5	82	109	132	144	157	187	136	**135**	**34**	**0.21**	**0.22**	
	0.75	114	121	113	132	128	104	117	**118**	**10**	**0.30**	**0.09**	**Yes**
	1	0	0	28	22	44	0	23	**17**	**17**	**0.90**	**0.10**	**Yes**
eri-6/7 (tm1917)	**0.1**	133	151	170	210	216	214	203	**185**	**34**	**0**	**0.24**	
	0.25	180	188	216	198	232	232		**208**	**22**	**0**	**0.18**	
	0.5	105	86	160	155	168	222		**149**	**48**	**0.04**	**0.32**	
	0.75	133	164	168	144	160	184		**159**	**18**	**0**	**0.14**	
	1	0	31	1	8	20	0	40	**14**	**16**	**0.91**	**0.11**	**Yes**
eri-8 (gg100) *Best*	**0.1**	194	256	292	252	272	216	240	**246**	**33**	**0**	**0.15**	
	0.25	215	220	210	210	214	243	241	**222**	**14**	**0**	**0.07**	
	0.5	176	186	200	186	200	202		**192**	**11**	**0.14**	**0.06**	
	0.75	131	157	142	131	152	140	156	**144**	**11**	**0.35**	**0.05**	**Yes**
	1**	0	0	0	13	11	9	7	**6**	**6**	**0.97**	**0.03**	**Yes**
eri-9 (gg106)	**0.1**	234	240	280	272	288	244		**260**	**23**	**0**	**0.11**	
	0.25	192	240	264	240	248	232	225	**234**	**22**	**0.02**	**0.11**	
	0.5	216	224	137	149	168	174	150	**174**	**34**	**0.27**	**0.15**	
	0.75	132	126	126	138	131	159	146	**137**	**12**	**0.43**	**0.06**	**Yes**
	1	10	5	40	38	19	12	78	**29**	**26**	**0.88**	**0.11**	**Yes**
eri-11 (gg99) *Best*	**0.1**	292	280	272	320	258	288	304	**288**	**20**	**0**	**0.10**	
	0.25	248	256	280	264	224	254	320	**264**	**30**	**0.04**	**0.13**	
	0.5	236	248	156	288	224	235	256	**235**	**40**	**0.14**	**0.16**	
	0.75	68	81	116	92	109	97	83	**92**	**17**	**0.66**	**0.06**	**Yes**
	1**	1	1	15	0	3	21	6	**7**	**8**	**0.98**	**0.03**	**Yes**

Table 2.23: Dilution series of Eri responses by RNAi feeding against *vha-15*

Single L3-stage larvae were placed on RNAi food targeting *vha-15*; 4 days later, the number of progeny surviving to L3-stage larvae or older at each indicated concentration (OD at 600 nm) of initial bacterial culture was determined. For clarity, two bacterial culture concentrations (OD_{600nm} of 0.1 and 0.5), which produced similar Eri penetrances as adjacent concentrations, are not included. The tabulated mean (Avg) and standard deviation (SD) were normalized to the brood sizes of each strain fed empty RNAi vector (**Table 2.27**), to obtain the normalized mean (N.Avg) and standard error of the mean (SEM). The normalized mean and the standard error of the mean for N2 wild type were used as the basis to indicate an Eri or a Rde phenotype (Eri?), with $p<0.05$ as the criterion to denote significant difference from wild type response levels. A strain which fits the "best *eri*" criterion described in text is marked as "best", with asterisks indicating concentrations of RNAi food at which it fulfilled the criterion.

Table 2.23 (Continued): Dilution series results for *vha-15* feeding

Strain	*OD_{600}*	*Brood Size*							*Avg*	*SD*	*N.Avg*	*SEM*	*Eri?*
Wildtype (N2)	**0.03**	231	205	185	216	179	229	208	**208**	**20**	**0.08**	**0.12**	
	0.25	170	181	190	288	127	136	183	**182**	**53**	**0.20**	**0.24**	
	1	73	128	127	97	222	135	122	**129**	**46**	**0.43**	**0.21**	
	2	117	79	79	164	78	122		**107**	**35**	**0.53**	**0.16**	
	3	30	66	97	100	65	105		**77**	**29**	**0.66**	**0.13**	
eri-1 (mg366)	**0.03**	155	173	77	128	140	151	156	**140**	**31**	**0.12**	**0.20**	
	0.25	45	69	77	41	83	97	68	**69**	**20**	**0.57**	**0.13**	**Yes**
	1	3	18	3	42	51	44	30	**27**	**20**	**0.83**	**0.12**	**Yes**
	2	0	6	0	40	7	10	12	**11**	**14**	**0.93**	**0.09**	**Yes**
	3	1	2	0	0	1	12	0	**2**	**4**	**0.99**	**0.03**	**Yes**
rrf-3 (pk1426) <u>*Best*</u>	**0.03**	144	59	196	148	195	97		**140**	**54**	**0**	**0.41**	
	0.25	29	3	77	57	34	33	0	**33**	**27**	**0.75**	**0.21**	**Yes**
	1**	0	1	0	24	1			**5**	**11**	**0.96**	**0.08**	**Yes**
	2**	0	0	0	0	0	0	0	**0**	**0**	**1.00**	**0**	**Yes**
	3**	0	0	0	0	0	0	0	**0**	**0**	**1.00**	**0**	**Yes**
eri-3 (tm1361)	**0.03**	135	155	164	133	162	86	145	**140**	**27**	**0.10**	**0.19**	
	0.25	63	40	66	52	62	9	19	**44**	**23**	**0.71**	**0.15**	**Yes**
	1	0	18	1	0	1	0	46	**9**	**17**	**0.94**	**0.11**	**Yes**
	2	0	0	0	0	0	17	0	**2**	**6**	**0.98**	**0.04**	**Yes**
	3	0	0	0	0	0	1	1	**0**	**0**	**1.00**	**0**	**Yes**
eri-5 (tm1705)	**0.03**	97	126	163	195	208	102	153	**149**	**43**	**0.12**	**0.27**	
	0.25	127	238	106	165	173	114	85	**144**	**52**	**0.15**	**0.32**	
	1	34	64	43	11	102	65		**53**	**31**	**0.69**	**0.19**	**Yes**
	2	5	7	204	26	34	23	45	**49**	**70**	**0.71**	**0.41**	
	3	24	19	12	67	113	34		**45**	**39**	**0.74**	**0.23**	
eri-6/7 (tm1917)	**0.03**	219	143	148	226	127	161		**171**	**42**	**0**	**0.28**	
	0.25	127	78	51	113	128	78		**96**	**31**	**0.38**	**0.21**	
	1	0	22	51	9	60	16	5	**23**	**23**	**0.85**	**0.15**	**Yes**
	2	2	1	0	15	46	9	26	**14**	**17**	**0.91**	**0.11**	**Yes**
	3	1	0	1	1	0	1	15	**3**	**5**	**0.98**	**0.04**	**Yes**
eri-8 (gg100) <u>*Best*</u>	**0.03**	180	256	209	242	251	273		**235**	**34**	**0**	**0.16**	
	0.25	48	46	27	125	154	49	25	**68**	**51**	**0.70**	**0.23**	**Yes**
	1**	1	0	20	1	2	0	0	**3**	**7**	**0.98**	**0.03**	**Yes**
	2**	0	0	0	1	1	1	4	**1**	**1**	**1.00**	**0.01**	**Yes**
	3**	0	2	0	3	0	0	0	**1**	**1**	**1.00**	**0.01**	**Yes**
eri-9 (gg106)	**0.03**	219	238	284	246	233	257	237	**245**	**21**	**0**	**0.11**	
	0.25	192	150	179	55	167	150	114	**144**	**46**	**0.40**	**0.20**	
	1	102	114	62	6	101	53	49	**70**	**38**	**0.71**	**0.16**	**Yes**
	2	3	0	1	34	105	46	28	**31**	**37**	**0.87**	**0.16**	**Yes**
	3	1	0	0	1	10	1	0	**2**	**4**	**0.99**	**0.02**	**Yes**
eri-11 (gg99)	**0.03**	292	246	239	247	258	285	228	**256**	**24**	**0.06**	**0.11**	
	0.25	123	135	220	224	189	249	185	**189**	**47**	**0.31**	**0.18**	
	1	24	8	2	50	1	66	43	**28**	**26**	**0.90**	**0.09**	**Yes**
	2	5	60	0	125	1	43	15	**36**	**46**	**0.87**	**0.17**	**Yes**
	3	0	1	0	1	0	82	0	**12**	**31**	**0.96**	**0.11**	**Yes**

Table 2.24: Dilution series of Eri responses by RNAi feeding against *glp-1*

Single L3-stage larvae were placed on RNAi food targeting *glp-1*; 4 days later, the percent of progeny showing the expected absent germline at each indicated concentration (OD at 600 nm) of initial bacterial culture were determined. The tabulated mean (Avg) and standard deviation (SD) for N2 wild type were used as the basis to indicate an Eri or a Rde phenotype (Eri?), with $p<0.05$ as the criterion to denote significant difference from wild type response levels. A strain which fits the "best *eri*" criterion described in text is marked as "best", with asterisks indicating concentrations of RNAi food at which it fulfilled the criterion.

Table 2.24 (Continued): Dilution series results for *glp-1* feeding

Strain	OD_{600}	*Penetrance readings*							*Avg*	*SD*	*Eri?*
Wildtype (N2)	**1**	2/56	2/67	1/80	0/20	0/20	0/20	1/60	**0.01**	**0.01**	
	2	3/67	1/18	2/40	0/20	2/60			**0.04**	**0.02**	
	3	9/31	6/25	8/27	6/25	10/31	12/39	8/24	**0.29**	**0.04**	
	4	26/61	24/52	7/14	9/28	9/25	9/26	12/36	**0.39**	**0.07**	
	5	11/29	26/53	16/31	13/25	18/28	20/34	19/36	**0.52**	**0.08**	
eri-1 (mg366)	**1**	4/49	5/46	6/42	8/47	3/25	3/20	8/45	**0.14**	**0.03**	**Yes**
	2	12/38	13/33	17/39	9/32	8/23	11/30	18/41	**0.37**	**0.06**	**Yes**
	3	14/28	17/33	14/43	16/32	13/28	24/48	22/39	**0.48**	**0.07**	**Yes**
	4	23/34	29/41	38/52	16/23	24/40			**0.68**	**0.05**	**Yes**
	5	24/28	21/27	28/37	25/35	24/31	32/42	31/38	**0.78**	**0.05**	**Yes**
rrf-3 (pk1426)	**1**	7/47	8/61	12/39	4/39	3/38	5/37		**0.15**	**0.08**	**Yes**
	2	10/41	16/50	26/47	39/54	15/34	14/27	18/38	**0.47**	**0.16**	**Yes**
	3	53/57	41/51	18/36	21/28	41/57	29/39		**0.74**	**0.14**	**Yes**
	4	31/33	42/54	21/27	29/40	36/49	27/40	39/50	**0.77**	**0.08**	**Yes**
	5	31/37	25/30	33/38	28/42	23/25	28/34	28/33	**0.83**	**0.08**	**Yes**
eri-3 (tm1361)	**1**	3/36	5/45	7/25	2/28	2/29	5/37	4/35	**0.12**	**0.07**	**Yes**
	2	10/36	6/19	19/37	22/63	21/47	12/27	11/35	**0.38**	**0.09**	**Yes**
	3	17/39	22/48	14/30	25/37	15/26	19/36	27/49	**0.53**	**0.08**	**Yes**
	4	14/18	39/48	22/33	40/47	22/30	19/24	44/47	**0.80**	**0.09**	**Yes**
	5	19/24	8/9	27/38	17/22	22/30	23/27	21/25	**0.80**	**0.07**	**Yes**
eri-5 (tm1705) *Best*	**1**	3/29	4/28	4/37	3/30	2/60	3/50	0/20	**0.08**	**0.05**	**Yes**
	2	21/34	13/20	10/21	10/30	10/22	12/22		**0.51**	**0.12**	**Yes**
	3	7/11	7/14	11/28	8/21	5/14	25/40	12/28	**0.47**	**0.12**	**Yes**
	4	27/36	25/32	20/29	22/27	14/22	22/29	23/28	**0.75**	**0.07**	**Yes**
	5**	11/13	12/13	34/35	27/29	30/33	19/21	13/13	**0.93**	**0.05**	**Yes**
eri-6/7 (tm1917)	**1**	2/36	4/61	7/32	5/30	5/34	6/40	6/46	**0.13**	**0.06**	**Yes**
	2	12/28	11/27	9/35	8/33	8/35	6/28	12/26	**0.32**	**0.11**	**Yes**
	3	18/31	24/34	20/29	14/25	11/19	26/37		**0.64**	**0.07**	**Yes**
	4	30/35	24/37	24/31	23/29	13/17	27/36	23/29	**0.77**	**0.06**	**Yes**
	5	19/26	18/21	14/25	23/27	26/30	18/20	24/30	**0.80**	**0.12**	**Yes**
eri-8 (gg100)	**1**	7/79	8/78	7/29	9/50	6/42	2/23	3/35	**0.13**	**0.06**	**Yes**
	2	17/38	7/18	9/54	8/24	10/29	18/47	15/49	**0.34**	**0.09**	**Yes**
	3	17/32	15/29	16/30	29/47	20/43	35/58	27/44	**0.55**	**0.06**	**Yes**
	4	20/23	49/68	26/36	24/40	33/47	12/17	32/54	**0.70**	**0.09**	**Yes**
	5	20/32	33/40	22/25	25/30	24/30	23/26	25/34	**0.80**	**0.09**	**Yes**
eri-9 (gg106)	**1**	8/75	1/48	8/60	2/28	4/46	6/63	11/93	**0.09**	**0.04**	**Yes**
	2	13/39	8/24	11/39	12/39	18/53	5/32	4/16	**0.29**	**0.07**	**Yes**
	3	12/28	20/39	20/36	19/34	21/35	14/25	24/45	**0.54**	**0.05**	**Yes**
	4	28/31	30/40	17/27	20/23	17/28	30/39	15/22	**0.74**	**0.11**	**Yes**
	5	43/65	40/51	16/28	34/38	16/18	24/28	26/32	**0.78**	**0.12**	**Yes**
eri-11 (gg99)	**1**	4/69	5/53	0/20	0/20	2/40	0/20	0/20	**0.03**	**0.04**	
	2	17/53	11/37	5/19	3/10	9/28	7/24		**0.30**	**0.02**	**Yes**
	3	24/39	16/25	7/20	23/49	10/19	12/28	27/55	**0.50**	**0.10**	**Yes**
	4	44/57	36/44	27/41	27/39	17/27	41/49	19/25	**0.74**	**0.08**	**Yes**
	5	31/36	52/58	16/20	34/39	13/16	24/26	29/37	**0.85**	**0.05**	**Yes**

Table 2.25: Dilution series of Eri responses by RNAi feeding against *par-1*

Single L3-stage larvae were placed on RNAi food targeting *par-1*; 4 days later, the number of progeny surviving to L3-stage larvae or older at each indicated concentration (OD at 600 nm) of initial bacterial culture was determined. For clarity, two bacterial culture concentrations (OD_{600nm} of 0.25 and 0.75), which produced similar Eri penetrances as adjacent concentrations, are not included. The tabulated mean (Avg) and standard deviation (SD) were normalized to the brood sizes of each strain fed empty RNAi vector (**Table 2.27**), to obtain the normalized mean (N.Avg) and standard error of the mean (SEM). The normalized mean and the standard error of the mean for N2 wild type were used as the basis to indicate an Eri or a Rde phenotype (Eri?), with $p<0.05$ as the criterion to denote significant difference from wild type response levels. A strain which fits the "best *eri*" criterion described in text is marked as "best", with asterisks indicating concentrations of RNAi food at which it fulfilled the criterion.

Table 2.25 (Continued): Dilution series results for *par-1* feeding

Strain	*OD_{600}*	*Brood Size*							*Avg*	*SD*	*N.Avg*	*SEM*	*Eri?*
Wildtype (N2)	**0.1**	196	248	256	220	216	232		**228**	**22**	**0**	**0.13**	
	0.5	196	184	200	160	212			**190**	**20**	**0.16**	**0.12**	
	1	133	109	130	108	94			**115**	**16**	**0.49**	**0.09**	
	2	97	49	65	192	36			**88**	**63**	**0.61**	**0.28**	
	3	10	14	17	18	17	9	6	**13**	**5**	**0.94**	**0.02**	
eri-1 (mg366)	**0.1**	130	208	184	168	192	216		**183**	**31**	**0**	**0.21**	
	0.5	79	95	31	131	104	116	128	**98**	**35**	**0.38**	**0.22**	
	1	35	57	87	34	6	41		**43**	**27**	**0.73**	**0.17**	**Yes**
	2	4	19	6	18	9	18		**12**	**7**	**0.92**	**0.04**	**Yes**
	3	7	26	15	12	9	23	5	**14**	**8**	**0.91**	**0.05**	
rrf-3 (pk1426)	**0.1**	18	38	176	112	104	87	118	**93**	**53**	**0.30**	**0.40**	
	0.5	11	10	10	18	21	14		**14**	**5**	**0.90**	**0.04**	**Yes**
	1	7	19	12	12	16	12	2	**11**	**6**	**0.91**	**0.04**	**Yes**
	2	7	12	5	13	10	12	9	**10**	**3**	**0.93**	**0.02**	**Yes**
	3	8	10	10	6	7	3	4	**7**	**3**	**0.95**	**0.02**	
eri-3 (tm1361)	**0.1**	27	5	19	90	69	90	144	**63**	**49**	**0.59**	**0.32**	**Yes**
	0.5	18	18	11	8	11	4	54	**18**	**17**	**0.89**	**0.11**	**Yes**
	1	5	8	3	10	6	40	18	**13**	**13**	**0.92**	**0.08**	**Yes**
	2	12	3	1	1	2	1	5	**4**	**4**	**0.98**	**0.03**	**Yes**
	3	15	7	21	17	3	2	6	**10**	**7**	**0.93**	**0.05**	
eri-5 (tm1705) *Best*	**0.1**	8	94	77	47	248	136	184	**113**	**82**	**0.33**	**0.49**	
	0.5**	4	15	10	14	19	11	28	**14**	**8**	**0.92**	**0.05**	**Yes**
	1**	5	10	7	6	10	11	4	**8**	**3**	**0.96**	**0.02**	**Yes**
	2**	4	14	9	8	3	4	7	**7**	**4**	**0.96**	**0.02**	**Yes**
	3	18	21	10	2	10	9	7	**11**	**6**	**0.94**	**0.04**	
eri-6/7 (tm1917)	**0.1**	159	168	200	208	232	186		**192**	**27**	**0**	**0.20**	
	0.5	15	12	35	232	13	31	12	**50**	**81**	**0.68**	**0.52**	
	1	3	3	5	11	10	8		**7**	**4**	**0.96**	**0.02**	**Yes**
	2	45	19	11	12	5	13	11	**17**	**13**	**0.89**	**0.09**	**Yes**
	3	6	3	6	5	8	3	8	**6**	**2**	**0.96**	**0.01**	**Yes**
eri-8 (gg100)	**0.1**	228	184	220	243	248	208	270	**229**	**28**	**0**	**0.13**	
	0.5	9	27	268	173	159	100	176	**130**	**91**	**0.41**	**0.41**	
	1	119	80	188	40	39	64	20	**79**	**58**	**0.65**	**0.26**	
	2	16	21	8	11	60	12	17	**21**	**18**	**0.91**	**0.08**	**Yes**
	3	6	16	9	14	10	26	10	**13**	**7**	**0.94**	**0.03**	
eri-9 (gg106)	**0.1**	272	244	232	219	255	244		**244**	**18**	**0**	**0.10**	
	0.5	14	26	148	137	172	200	196	**128**	**77**	**0.47**	**0.32**	
	1	137	144	86	150	176			**139**	**33**	**0.42**	**0.14**	
	2	23	17	48	117	13	121	140	**68**	**55**	**0.71**	**0.23**	
	3	2	8	97	40	12	15	5	**26**	**34**	**0.89**	**0.14**	
eri-11 (gg99)	**0.1**	280	292	216	252	270	260	243	**259**	**25**	**0.05**	**0.11**	
	0.5	96	20	113	132	248	164		**129**	**76**	**0.53**	**0.28**	**Yes**
	1	86	62	200	196	51	121	99	**116**	**60**	**0.57**	**0.22**	
	2	60	62	17	10	22	17		**31**	**23**	**0.89**	**0.09**	**Yes**
	3	11	6	8	4	16	9	8	**9**	**4**	**0.97**	**0.01**	**Yes**

Table 2.26: Dilution series of Eri responses by RNAi feeding against *pos-1*

Single L3-stage larvae were placed on RNAi food targeting *pos-1*; 4 days later, the number of progeny surviving to L3-stage larvae or older at each indicated concentration (OD at 600 nm) of initial bacterial culture was determined. For clarity, two bacterial culture concentrations (OD_{600nm} of 0.03 and 2), which produced similar Eri penetrances as adjacent concentrations, are not included. The tabulated mean (Avg) and standard deviation (SD) were normalized to the brood sizes of each strain fed empty RNAi vector (**Table 2.27**), to obtain the normalized mean (N.Avg) and standard error of the mean (SEM). The normalized mean and the standard error of the mean for N2 wild type were used as the basis to indicate an Eri or a Rde phenotype (Eri?), with $p<0.05$ as the criterion to denote significant difference from wild type response levels. A strain which fits the "best *eri*" criterion described in text is marked as "best", with asterisks indicating concentrations of RNAi food at which it fulfilled the criterion.

Table 2.26 (Continued): Dilution series results for *pos-1* feeding

Strain	*OD_{600}*	*Brood Size*							*Avg*	*SD*	*N.Avg*	*SEM*	*Eri?*
Wildtype (N2)	**0.1**	216	205	272	180	196	232	205	**217**	**30**	**0.04**	**0.17**	
	0.25	184	168	10	248	231	240		**180**	**89**	**0.20**	**0.40**	
	0.5	201	170	169	150	153			**169**	**20**	**0.26**	**0.11**	
	0.75	147	37	3	2	133	74	118	**66**	**61**	**0.71**	**0.28**	
	1	30	0	3	2	0	4	71	**7**	**27**	**0.97**	**0.05**	
eri-1 (mg366)	**0.1**	123	128	154	164	164	171	192	**151**	**24**	**0.05**	**0.14**	
	0.25	132	107	130	188	220	133	168	**152**	**40**	**0.04**	**0.28**	
	0.5	39	0	7	6	10			**13**	**15**	**0.92**	**0.11**	**Yes**
	0.75	74	0	2	0	0	0	22	**13**	**28**	**0.92**	**0.19**	
	1	64	55	2	0	1	0	0	**20**	**29**	**0.87**	**0.19**	
rrf-3 (pk1426)	**0.1**	91	176	162	126	168	184	186	**151**	**35**	**0**	**0.28**	
	0.25	138	61	8	204	8	82		**84**	**77**	**0.37**	**0.64**	
	0.5	0	50	1	2	0	0	1	**8**	**19**	**0.93**	**0.15**	**Yes**
	0.75	0	0	0	0	0	0	0	**0**	**0**	**1.00**	**0**	**Yes**
	1	0	0	0	0	0	0	0	**0**	**0**	**1.00**	**0**	
eri-3 (tm1361)	**0.1**	109	90	124	140	125	192	144	**130**	**32**	**0.17**	**0.24**	
	0.25	142	136	100	27	10	36	25	**75**	**56**	**0.52**	**0.38**	
	0.5	11	32	41	2	7	5	7	**16**	**15**	**0.90**	**0.10**	**Yes**
	0.75	0	0	0	8	4	0	17	**2**	**6**	**0.99**	**0.02**	**Yes**
	1	0	2	2	1	18			**5**	**8**	**0.97**	**0.05**	
eri-5 (tm1705) *Best*	**0.1**	129	174	192	228	85	244	200	**175**	**56**	**0**	**0.37**	
	0.25	78	85	208	184	35	252	136	**140**	**79**	**0.18**	**0.51**	
	0.5**	1	5	3	0	0	2	16	**2**	**6**	**0.99**	**0.01**	**Yes**
	0.75**	0	0	0	1	0	0	0	**0**	**0**	**1.00**	**0**	**Yes**
	1	10	0	0	0	0	0	0	**2**	**4**	**0.99**	**0.02**	
eri-6/7 (tm1917)	**0.1**	166	156	144	128	164	167		**154**	**15**	**0.01**	**0.13**	
	0.25	186	200	15	97	128	168	184	**132**	**66**	**0.15**	**0.45**	
	0.5	68	0	20	0	23	22		**22**	**25**	**0.86**	**0.18**	**Yes**
	0.75	1	1	0	0	2	0	0	**1**	**1**	**1.00**	**0.01**	**Yes**
	1	0	0	1	1	0	0	0	**0**	**0**	**1.00**	**0**	
eri-8 (gg100)	**0.1**	232	256	184	252	304	240	204	**245**	**39**	**0**	**0.18**	
	0.25	168	264	99	75	29	129	236	**127**	**85**	**0.43**	**0.37**	
	0.5	40	0	1	50	84	2		**35**	**34**	**0.84**	**0.16**	**Yes**
	0.75	32	11	0	0	0	0	1	**7**	**12**	**0.97**	**0.06**	**Yes**
	1	44	30	0	1	1	1	0	**13**	**18**	**0.94**	**0.09**	
eri-9 (gg106)	**0.1**	224	248	252	200	168	228	210	**220**	**29**	**0.08**	**0.14**	
	0.25	144	172	164	62	128	192		**134**	**46**	**0.44**	**0.19**	
	0.5	47	71	4	2	0	1	2	**21**	**29**	**0.91**	**0.13**	**Yes**
	0.75	5	0	0	1	0	0	21	**1**	**8**	**1.00**	**0.01**	**Yes**
	1	0	0	0	0	0	0	9	**0**	**3**	**1.00**	**0**	
eri-11 (gg99)	**0.1**	240	208	250	244	256	224	216	**237**	**18**	**0.13**	**0.09**	
	0.25	252	214	272	258	228	243	192	**245**	**28**	**0.11**	**0.10**	
	0.5	212	230	296	77	202	128		**191**	**78**	**0.30**	**0.29**	
	0.75	64	67	0	0	1	3		**26**	**33**	**0.90**	**0.13**	
	1	0	0	6	0	0	37	8	**7**	**14**	**0.97**	**0.05**	

Table 2.27: Different Eri strains' brood sizes upon L4440 vector feeding

Strain	Brood Size										Avg	SD
Wildtype (N2)	185	218	237	242	208	247	248	222	215	244	**227**	**21**
eri-1 (mg366)	168	156	151	162	149	167	167	147			**158**	**9**
rrf-3 (pk1426)	137	137	142	135	143	138	139	117	127	119	**133**	**9**
eri-3 (tm1361)	169	160	146	134	151	176	167	143			**156**	**16**
eri-5 (tm1705)	150	188	189	144	173	177	186	172	177	147	**170**	**17**
eri-6/7 (tm1917)	145	143	154	176	143	168	168	148	152		**155**	**12**
eri-8 (gg100)	226	229	208	230	219	234	219	221	218		**223**	**8**
eri-9 (gg106)	221	249	233	231	237	227	262	254	241		**239**	**13**
eri-11 (gg99)	285	242	274	284	297	279	268	285	249		**274**	**18**
sid-1 (qt9)	178	206	214	238	211	224	218	260	243	231	**222**	**23**

The presented means and standard deviations were used for normalized means and standard errors of the means in RNAi feeding assays that caused lethality phenotypes.

When dsRNA doses cannot be controlled, using the most appropriate Eri mutant maximizes robustness and sensitivity.

We selected RNAi targets based on tissue-specific gene expression and/or phenotypes, and interpreted the data based on these differences, but it's important to consider that the differences in responses might relate to unknown relationships between the genes. Consistent with our goal, most sets of tissue-specific genes show consistent phenotypes within Eri mutant classes. For *rrf-3* and *ergo-1/eri-8*, we analyzed a second independent allele, finding similar tissue specificity. Therefore, the observed tissue specificity is likely a property of the *eri* genes rather than a consequence of unique alleles (**Figure 2.3**).

To further document tissue-specific Eri phenotypes, we crossed all the Eri mutants into a *sur-5::gfp* strain that ubiquitously expresses GFP in all cells (GU *et al.* 1998). All the *eri(-);sur-5::gfp* doubles exhibited spontaneous transgene silencing (**Figure 2.4**), which interfered with the effect of *gfp* dsRNA. However, consistent with the tissue-specific effects described above, the relative differences in spontaneous *gfp* silencing in the intestinal nuclei among *eri-1;sur-5::gfp*, *rrf-3;sur-5::gfp,* and *ergo-1/eri-8;sur-5::gfp* strains corresponded with their relative differences in RNAi efficacy against endogenous intestinal targets (**Table 2.28**).

A limited comparison of the Eri phenotypes of retinoblastoma pathway mutants *lin-15b(n744)* and *lin-35(n745)* (Wang *et al*. 2005) with *eri-1* and *rrf-3* showed that their sensitivity and robustness were less than the Eri mutants' (**Figure 2.5**).

We also found that all the Eri mutants show strong maternal rescue (**Figures 2.6, 2.7; Tables 2.29-2.32**). However, there is no maternal rescue for the temperature-sensitive (T.S.) sterility phenotype of T.S. Eri mutants (**Table 2.33**). This is not due to a perdurance problem in which the maternally-loaded products are depleted before *eri*-related spermatogenesis begins,

Figure 2.3: Dilution series of Eri responses of different *rrf-3* and *eri-8* alleles by RNAi feeding against *act-3*, *hmr-1*, and *vha-15*

Single L3-stage larvae were placed on RNAi food targeting *act-3* (A), *hmr-1* (B), and *vha-15* (C); 4 days later, the percent of progeny showing the expected knockdown phenotypes, as listed in **Table 2.1**, at each indicated concentration (OD at 600 nm) of initial bacterial culture were determined. Error bars represent 95% confidence intervals.

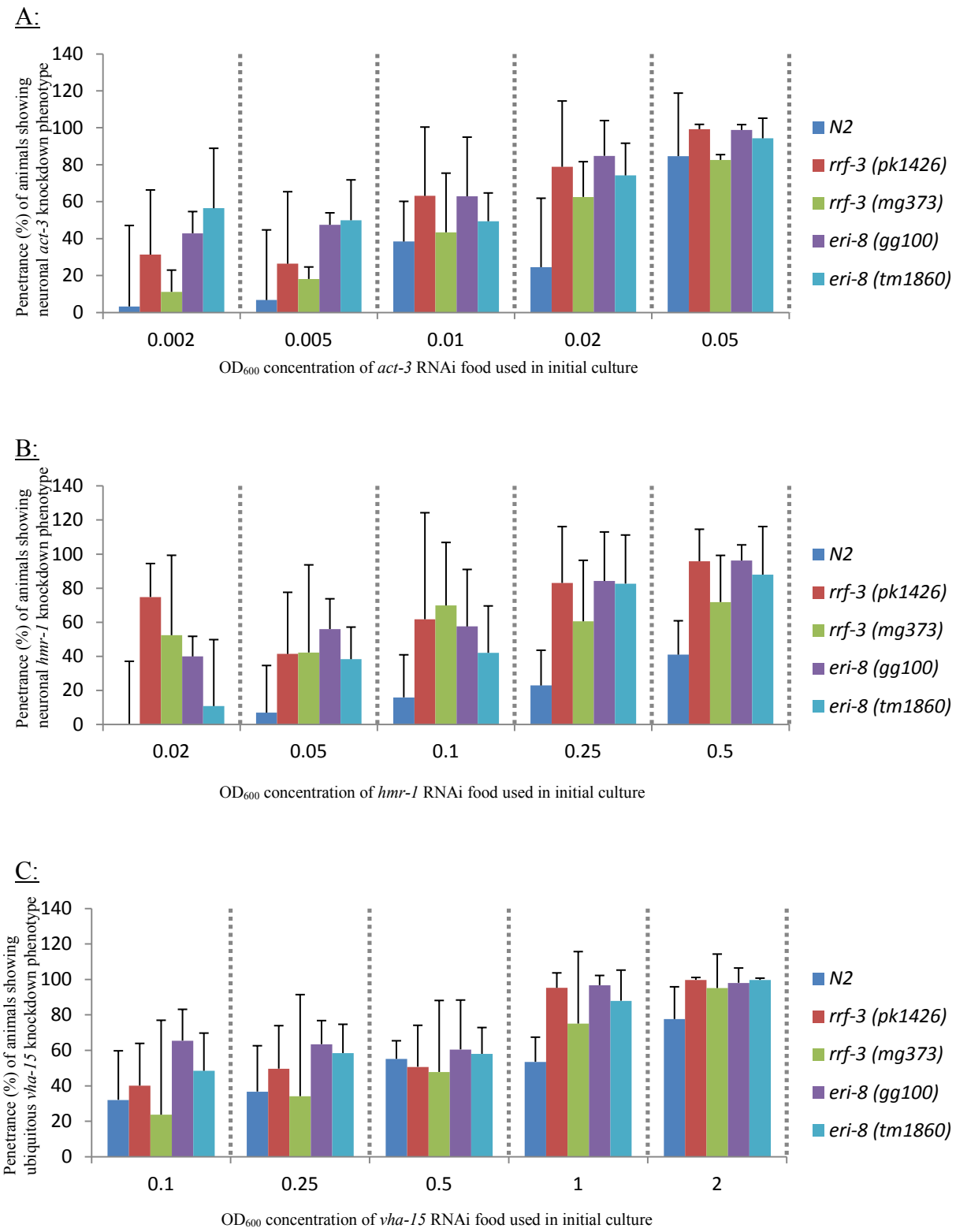

Figure 2.3 (Continued): Dilution series of Eri responses of different *rrf-3* and *eri-8* alleles by RNAi feeding against *act-3*, *hmr-1*, and *vha-15*

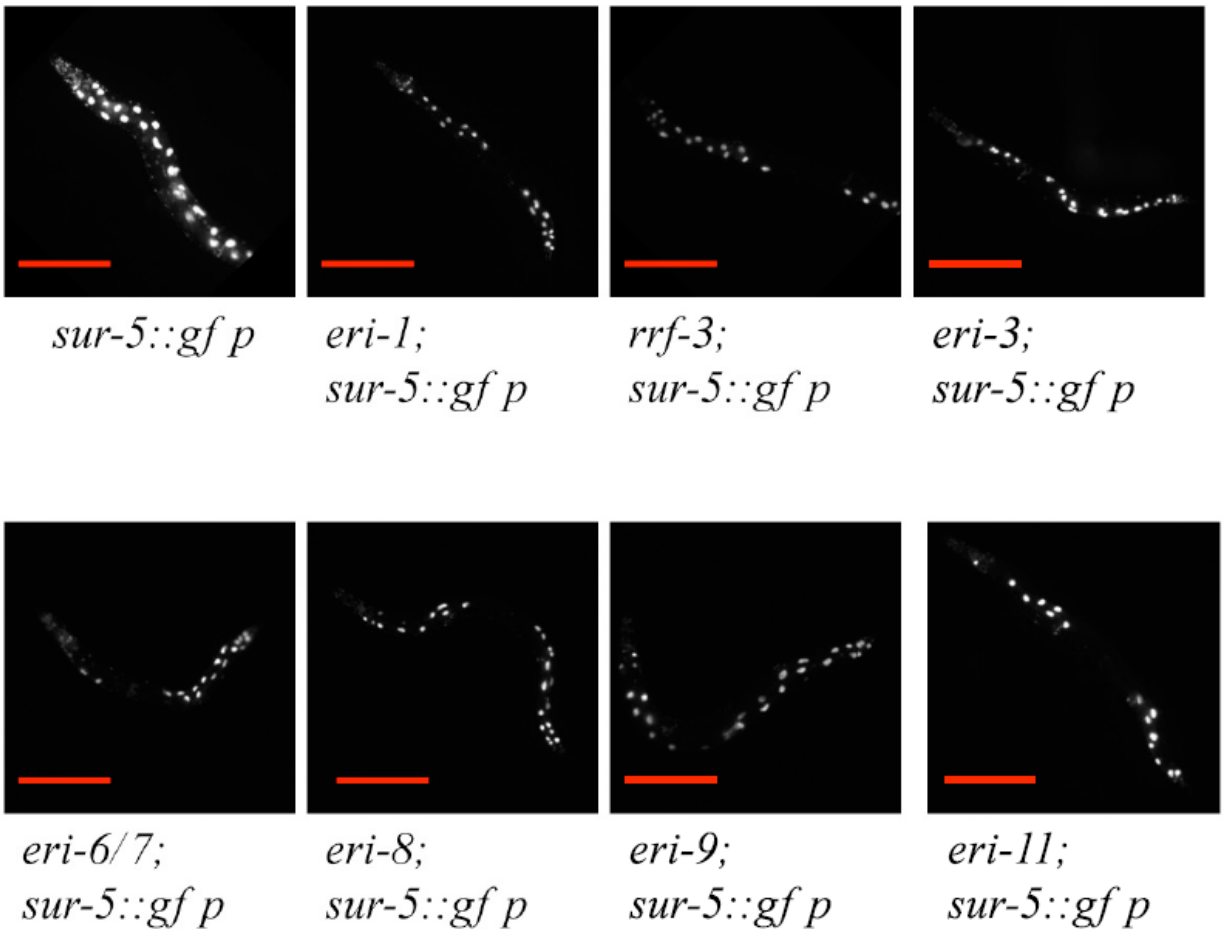

Figure 2.4: All Eri mutants enhance transgene silencing

Eri mutants enhance transgene silencing in a *sur-5::gfp* background. GFP images were exposed for 100 milliseconds. Red scale bar indicates 0.2 mm.

Table 2.28: Transgene silencing penetrance of *eri-1*, *rrf-3*, and *eri-8* in the *sur-5::gfp* background

Strain	Penetrance of spontaneous intestinal TGS at 20ºC					Mean	STD
N2 wild type	3/98	1/88	2/109	1/19	0/82	0.02	0.02
eri-1 (mg366)	48/62	28/46	31/54			0.65	0.11
rrf-3 (pk1426)	73/83	76/91	38/45	39/57	97/107	0.83	0.09
eri-8 (gg100)	30/38	24/42	25/35	42/53	28/40	0.71	0.09

Single L3-stage larvae were placed on OP50 food; 4 days later, the percent of progeny showing spontaneous transgene silencing in the intestinal nuclei was determined. For consistency, only worms with distinctly absent *gfp* expression in intestinal nuclei, as shown in **Figure 2.4**, are scored as having spontaneous transgene silencing.

Figure 2.5: Dilution series of Eri responses of *eri-1* and *rrf-3* versus *lin-15b* and *lin-35* by RNAi feeding against *dpy-13*, *unc-22*, and *unc-73*

Single L3-stage larvae were placed on RNAi food targeting *dpy-13* (A), *unc-22* (B), and *unc-73* (C); 4 days later, the percent of progeny showing the expected knockdown phenotypes, as listed in **Table 2.1**, at each indicated concentration (OD at 600 nm) of initial bacterial culture were determined. Error bars represent 95% confidence intervals.

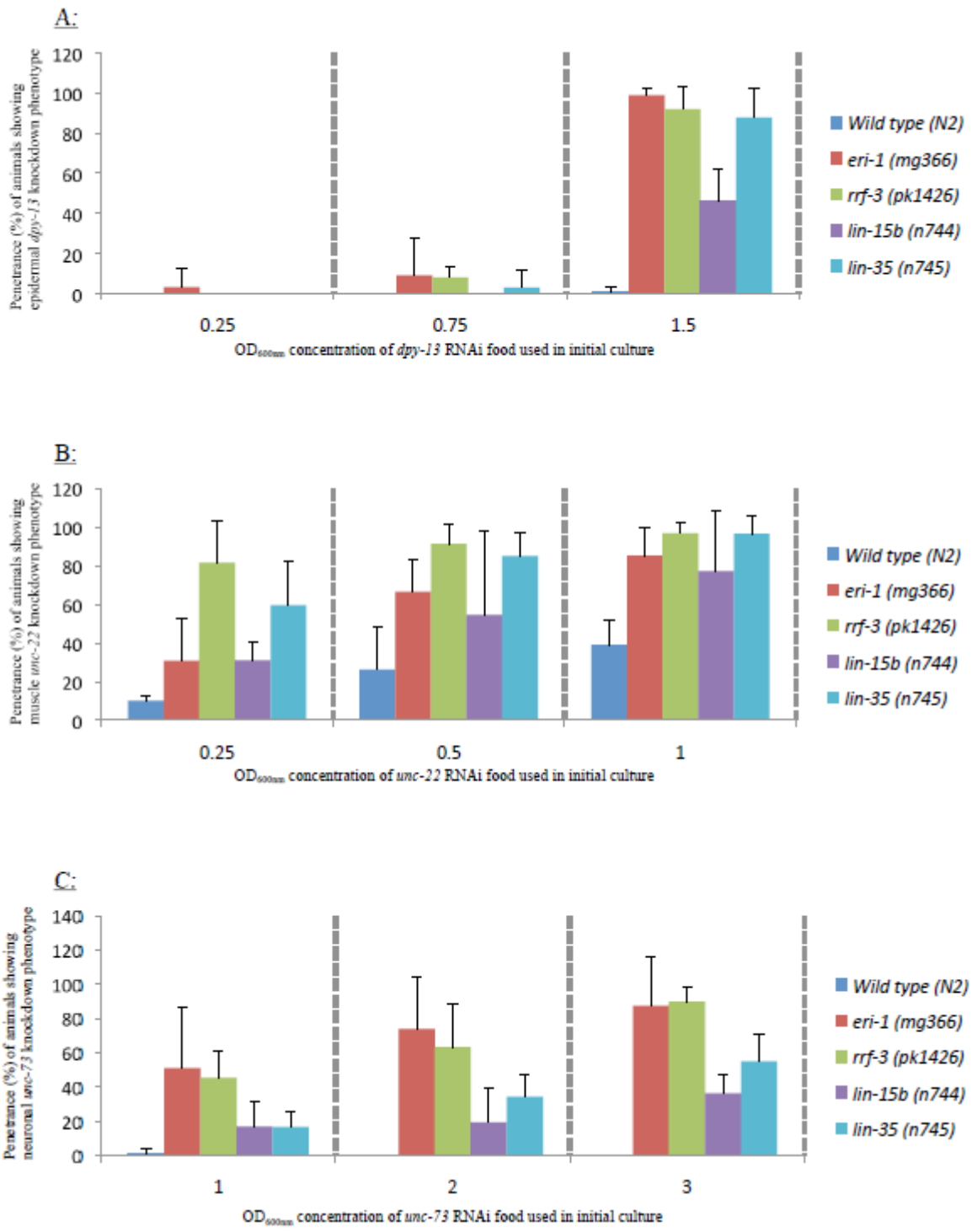

Figure 2.5 (Continued): Dilution series of Eri responses of *eri-1* and *rrf-3* versus *lin-15b* and *lin-35* by RNAi feeding against *dpy-13*, *unc-22*, and *unc-73*

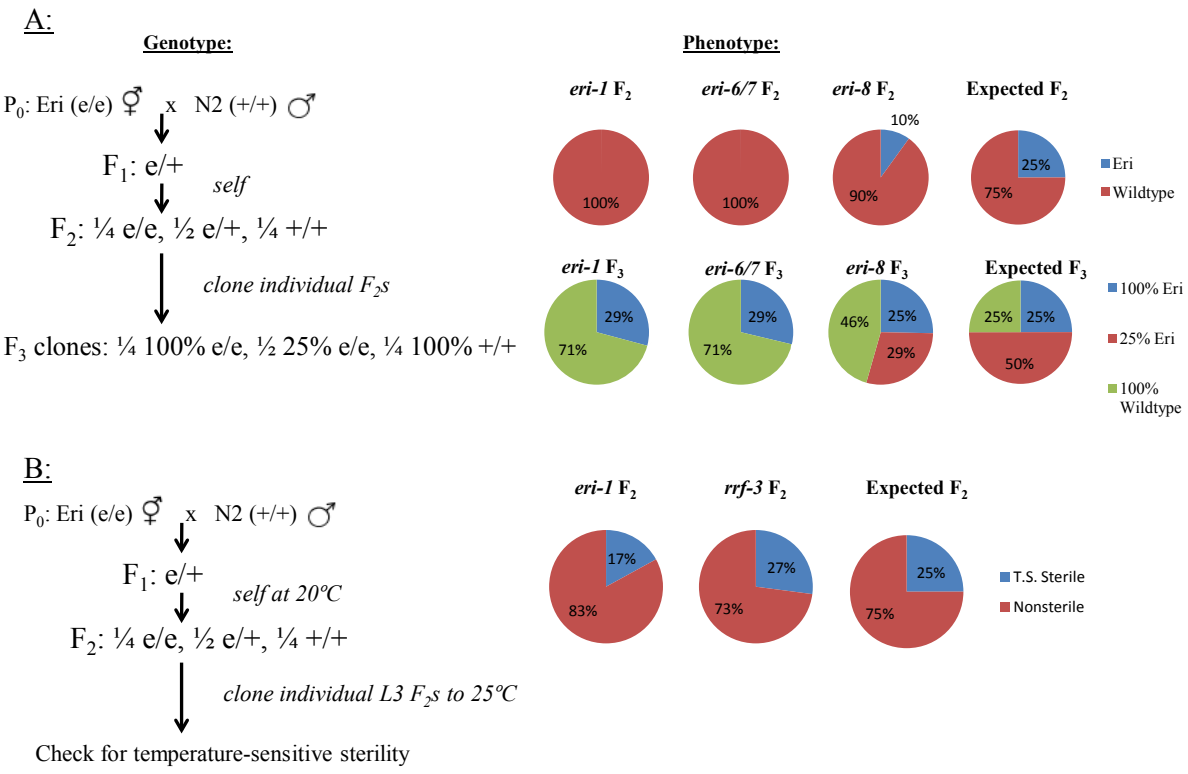

Figure 2.6: Somatic maternal rescue of the Eri phenotype

An outcross between an Eri (e/e) hermaphrodite and a N2 wild type (+/+) male begets a 1:2:1 (e/e):(e/+):(+/+) genotypic ratio at the F_2. Assuming a single-locus recessive trait, the expectation is that one quarter of the F2 progeny should be Eri. **(A)** Out-crossed *eri-1* (which is sterile at 25ºC), *eri-6/7*, and *eri-8* (which are not sterile at 25ºC) show significantly lower than expected levels ($p<10^{-9}$) of the Eri phenotype at the F_2. Similarly, the F_3 progeny of the F_2 show significantly higher than expected levels ($p<10^{-5}$) of wild-type progeny. **(B)** Out-crossed *eri-1* and *rff-3* (which are both sterile at 25ºC) show expected levels ($p>0.18$) of the temperature-sensitive sterile progeny at the F_2. **Figure 2.7** eliminates other possible parental rescue/effect mechanisms. **Tables 2.29** and **2.32** show data used for *p* values.

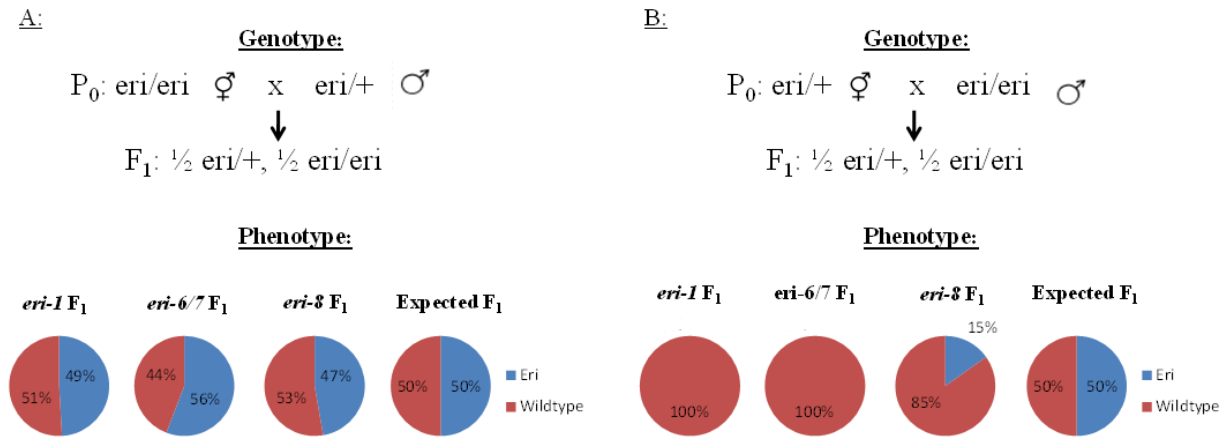

Figure 2.7: Somatic maternal rescue of the Eri phenotype

The progeny of a heterozygous Eri male crossed to homozygous Eri hermaphrodite versus a homozygous Eri male crossed to a heterozygous Eri hermaphrodite are compared for Eri phenotypes. Assuming a single-locus recessive trait, the expectation is that the F_1 should be 50% Eri in both reciprocal crosses. **(A)** The cross progeny of *eri-1*, *eri-6/7*, and *eri-8* show expected levels (p>0.48) of Eri phenotype when the mother is homozygous Eri. **(B)** The cross progeny of *eri-1*, *eri-6/7*, and *eri-8* show significantly lower than expected levels ($p<10^{-13}$) of Eri phenotype when the mother is heterozygous Eri. See **Tables 2.30** and **2.31** for data used in determining p values.

Table 2.29: Maternal rescue of Eri phenotype on *dpy-13* feeding via outcrossing

Strain	**F_2 Dpy:Non-Dpy**						**χ2 value**
eri-1 (mg366)	0:60	0:30	0:40	0:80	0:50		1.5e-23
rrf-3 (pk1426)	0:120	0:80	0:80				4.4e-22
eri-3 (tm1361)	0:50	0:40	0:50	0:80	0:80		1.5e-23
eri-6/7 (tm1917)	0:80	0:100	0:100	0:80	0:60		2.7e-32
eri-8 (gg100)	4:29	2:34	4:48	4:25			9.4e-9
eri-9 (gg106)	1:59	0:40	2:78	0:80	1:49	0:60	2.3e-26
eri-11 (gg99)	0:40	3:32	2:31	2:38	0:60		5.8e-13
Strain	**F_3 100% Dpy: 25% Dpy: 100% Non-Dpy**						**χ2 value**
eri-1 (mg366)	6:0:10	5:0:11	3:0:13				9.1e-15
rrf-3 (pk1426)	6:0:10	2:0:12	4:0:12				2.8e-15
eri-3 (tm1361)	2:0:14	4:0:12	3:0:13				2.2e-20
eri-6/7 (tm1917)	5:0:11	5:0:11	5:0:11	3:0:13	5:0:11		2.3e-24
eri-8 (gg100)	5:8:3	4:7:5	2:8:5	3:0:13	6:0:10		4.0e-5
eri-9 (gg106)	4:0:12	3:0:13	2:0:14	5:0:11	3:0:13		1.4e-29
eri-11 (gg99)	5:0:11	5:0:11	3:0:13	4:0:12	6:0:10		2.3e-24

Corresponding to **Figure 2.6A**, the observed phenotypic ratios of the outcross progeny in the F_2 and F_3 are as indicated. At the F_2, the expected phenotypic ratio of 1:3 Dpy:non-Dpy is used as the basis for chi-squared test calculations; at the F_3, the expected phenotypic ratio of 1:2:1 100% Dpy: 25% Dpy:100% Non-Dpy is used as the basis for chi-squared test calculations. Observed results are summed for chi-squared test calculations.

Table 2.30: Maternal rescue of Eri phenotype on *dpy-13* feeding via a heterozygous Eri male crossed with a homozygous Eri hermaphrodite

Strain	F_1 Dpy:Non-Dpy					$\chi 2$ value
eri-1 (mg366)	18:20	24:25	10:8	13:16	18:17	0.82
rrf-3 (pk1426)	11:10	6:8	13:14			0.80
eri-3 (tm1361)	5:8	4:6	13:10			0.77
eri-6/7 (tm1917)	14:9	6:4	4:6			0.45
eri-8 (gg100)	21:28	12:11	20:18	16:18	8:11	0.48
eri-9 (gg106)	12:18	18:13	10:14	15:15		0.64
eri-11 (gg99)	11:16	10:14	12:10	10:7	13:10	0.93

Corresponding to **Figure 2.7A**, the observed phenotypic ratios of the cross progeny are as indicated. The expected phenotypic ratio of 1:1 Dpy:non-Dpy is used as the basis for chi-squared test calculations. Observed results are summed for chi-squared test calculations.

Table 2.31: Maternal rescue of Eri phenotype on *dpy-13* feeding via a homozygous Eri male crossed with a heterozygous Eri hermaphrodite

Strain	F_1 Dpy:Non-Dpy					χ2 value
eri-1 (mg366)	0:16	0:14	0:33			2.1e-15
rrf-3 (pk1426)	0:18	0:13	0:23	0:16		5.9e-17
eri-3 (tm1361)	0:40	0:20	0:20			3.7e-19
eri-6/7 (tm1917)	0:60	0:60	0:80	0:80	0:50	9.6e-74
eri-8 (gg100)	1:14	5:14	4:17	5:28	2:22	1.7e-13
eri-9 (gg106)	0:25	0:29	0:16			5.9e-17
eri-11 (gg99)	0:19	0:20	0:21	0:24		4.9e-20

Corresponding to **Figure 2.7B**, the observed phenotypic ratios of the cross progeny are as indicated. The expected phenotypic ratio of 1:1 Dpy:non-Dpy is used as the basis for chi-squared test calculations. Observed results are summed for chi-squared test calculations.

Table 2.32: Maternal rescue of Eri phenotype on *hmr-1* and *unc-73* feeding via outcrossing

Strain	**Food**	**F_2 Phenotype:No-Phenotype**					**χ2 value**
eri-1 (mg366)	*unc-73*	0:76	0:45	0:35	0:45		2.7e-16
rrf-3 (pk1426)	*unc-73*	0:34	0:36	0:23			2.6e-8
eri-8 (gg100)	*unc-73*	8:24	3:27	3:28	3:38	2:34	3.1e-5
Strain	**Food**	**F_3 100% Phenotype: 25%Phenotype:No-Phenotype**					**χ2 value**
eri-1 (mg366)	*unc-73*	4:0:12	5:0:11	4:0:12	3:0:13		1.4e-21
rrf-3 (pk1426)	*unc-73*	5:0:11	5:0:11	2:0:14	3:0:13		1.8e-22
eri-3 (tm1361)	*hmr-1*	6:0:10	2:0:14	3:0:13	4:0:12		1.8e-22
eri-6/7 (tm1917)	*hmr-1*	3:0:13	3:0:13	2:0:14			2.1e-20
eri-8 (gg100)	*hmr-1*	2:0:14	1:0:15	3:0:13			7.1e-23

Corresponding to **Figure 2.6A**, the observed phenotypic ratios of the outcross progeny in the F_2 and F_3 are as indicated when fed the three respective RNAi foods. At the F_2, the expected phenotypic ratio of 1:3 with-phenotype:without-phenotype is used as the basis for chi-squared test calculations; at the F_3, the expected phenotypic ratio of 1:2:1 100% with-phenotype: 25% with-phenotype: 100% without-phenotype is used as the basis for chi-squared test calculations. Observed results are summed for chi-squared test calculations.

Table 2.33: No maternal rescue of Eri phenotype-related spermatogenesis defects

Strain	F_2 Sterile:Non-sterile			$\chi 2$ value
eri-1 (mg366)	2:14	3:13	3:12	0.18
rrf-3 (pk1426)	5:11	3:13	5:11	0.74
eri-3 (tm1361)	3:13	4:12	3:13	0.50

Corresponding to **Figure 2.6B**, the observed phenotypic ratios of the outcross progeny are as indicated. The expected phenotypic ratio of 1:3 sterile:not-sterile is used as the basis for chi-squared test calculations. Observed results are summed for chi-squared test calculations.

because we utilized *bli-1* RNAi – whose target is expressed only during the fourth larval stage (PAGE 1997) when spermatogenesis begins – and found penetrant maternal rescue of the Eri phenotype (**Table 2.34**). Eri maternal rescue could suggest that part of the maternal contribution to the embryo includes small RNAs or their associates.

The described tissue-specific RNAi sensitivities, T.S. sterility data, maternal rescue penetrance, brood size (**Table 2.27**), and effect on transgenes provide a practical guide to the selection of Eri mutants. There are other weaker enhanced RNAi mutants, including *dcr-1/eri-4(mg375)* (PAVELEC *et al.* 2009), tissue-specific *sid-1* overexpressers (CALIXTO *et al.* 2010), and transgene-specific silencers (KNIGHT and BASS 2002). Though these may not be versatile genetic tools, their future phenotypic analysis is equally important, because understanding the interactions amongst all *eri* genes provides insights about small RNA pathways.

SUPPLEMENTAL RESULTS AND DISCUSSION

As listed in **Table 2.1**, some RNAi foods had relatively extreme loss-of-function phenotypes scored for the sake of more explicit precision. For example, *unc-22* RNAi is usually scored just for the mere presence of twitching (FIRE *et al.* 1991). However, *unc-22* RNAi still causes twitching down to a 1/200,000 dilution of bacterial RNAi food in both N2 and *eri-1* (data not shown), at which point, errors from dilution is probably more variable than the phenotypic penetrance. Therefore, the more extreme phenotype of twitching to the point of paralysis is more appropriate for our dilution series' scoring purposes. Knockdown assays in general should therefore similarly consider the relationship between expressivity and penetrance at the concentrations of RNAi foods used. Although expressivity is another factor usually

Table 2.34: Maternal rescue of Eri phenotype on *bli-1* feeding via outcrossing

Strain	Penetrance of Bli at F_2				Mean	STD	*p* value
N2 wild type	39/86	63/144	58/119		0.46	0.03	
eri-1 (mg366)	78/87	66/97	65/70		0.84	0.13	0.008
rrf-3 (pk1426)	46/51	34/41	38/41		0.89	0.05	0.0002
eri-8 (gg100)	46/67	45/69	47/80		0.64	0.05	0.006
N2 x *eri-1*	63/134	51/116	74/139	34/80	0.47	0.05	0.78
N2 x *rrf-3*	36/73	64/123	15/37	32/74	0.46	0.05	1
N2 x *eri-8*	75/145	48/101	36/72	52/97	0.51	0.03	0.11

Corresponding to **Figure 2.6A**, the observed phenotypic penetrances of the outcross progeny in the F_2 are as indicated. The N2 wild type penetrance was used as the basis for a *t* test, to compare an Eri mutant's or an outcrossed-Eri mutant's penetrance, with a two-tailed *p* value as indicated.

considered for RNAi efficacy, it is much harder to quantify objectively. Penetrance of one very specific phenotype was therefore used as the sole measure of knockdown efficacy.

RNAi phenotypes were scored in the next generation for of three reasons. One, this practice is more common in the field for reverse genetics applications, so our method would serve as a more fitting guideline. Two, putting L3s on RNAi food and scoring the next generation versus putting embryos on RNAi food and scoring the same generation results in almost identical phenotypic penetrance (data not shown; (VASTENHOUW *et al.* 2006)). Three, scoring in the next generation allows for a more consistent method across all the to-be tested RNAi foods, including those with germline phenotypes that cannot be assayed in the same generation.

The data in **Figure 2.2** and **Tables 2.2-2.26** should not be construed as an absolute scale (that feeding a particular Eri mutant on a particular RNAi food concentration will result in the listed penetrance), due to differences between protocols. Rather, the relative differences between conditions (that one particular Eri mutant has different penetrance on different concentrations of an RNAi food) are the trends that should be robust.

Previous reports showed that a portion of the spontaneous transgene silencing is due to mobile silencing signals (JOSE *et al.* 2009) and the silenced cells in the gut correspond to the position of the developing gonad, suggestive that silencing signals emanate from the germline. We tested this by ablating the gonad of L1 animals and found that the extent of silencing was unchanged (**Figure 2.8**). Thus the silencing is either entirely of somatic origin or is initiated in the embryo.

The strong germline-specific *eri-5(tm1705)* phenotype was unexpected. This may reflect the incomplete penetrance *eri-5* has on small RNA metabolism; *eri-5* mutants show reduced but

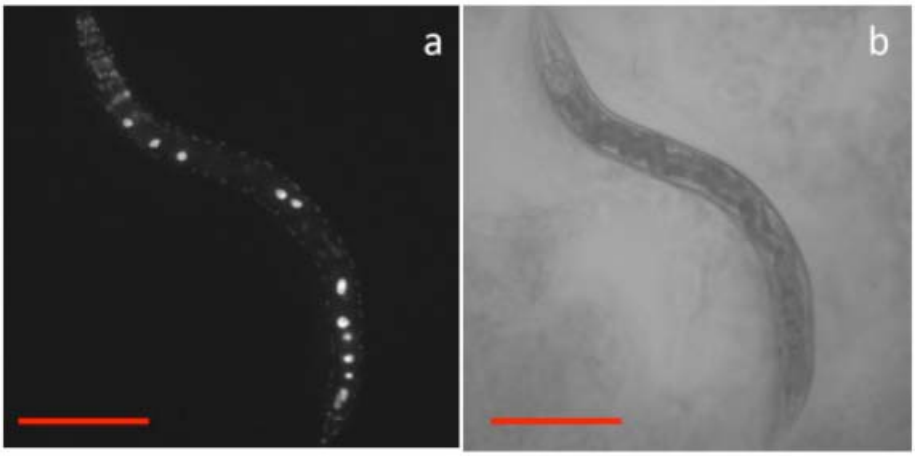

eri-8; sur-5::gf p germline laser ablated

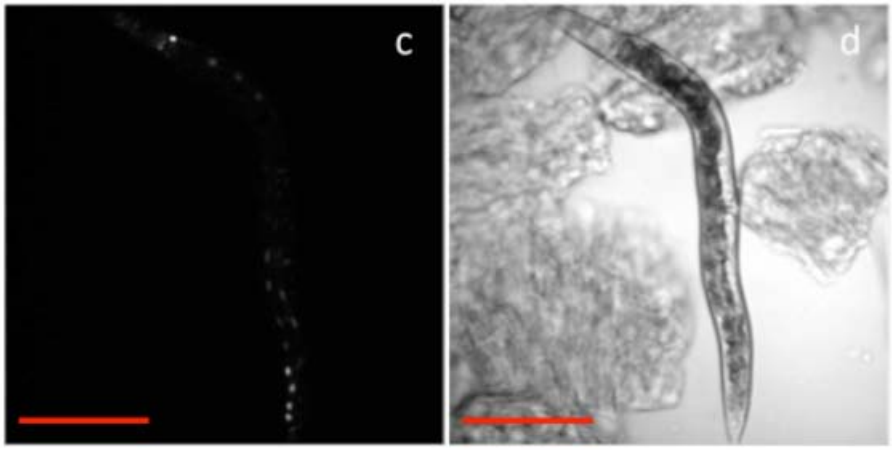

eri-8; sur-5::gf p glp-1 RNAi

Figure 2.8: Transgene silencing seen in Eri mutants is not from a germline source

eri-8 (gg100); sur-5::gfp animals exhibit spontaneous transgene silencing **(A)** even with a laser ablated germline **(B)** (see Supplemental Materials and Methods). *eri-8 (gg100); sur-5::gfp* animals fed RNAi targeting *glp-1* still exhibit spontaneous transgene silencing **(C)**, despite also lacking germlines **(D)**. GFP images were exposed for 100 milliseconds. Red scale bar indicates 0.2 mm.

not eliminated endo-siRNA processing (DUCHAINE *et al.* 2006). To date, no screens have been performed for germline-specific Eri mutants; such a screen could reveal the different requirements for endogenous small RNA pathways.

Duchaine *et al*. 2006 reported a rather weak Eri phenotype for *eri-5(mg392)* for some somatic targets, whereas we generally did not see a somatic Eri phenotype for *eri-5(tm1705)*. This difference could be due to the fact that we systemically enumerated the RNAi food concentrations at which we scored our animals, whereas Duchaine *et al*. did not; it is quite likely that when they scored their animals, they were at a concentration of food that may have produced a weak Eri phenotype. Furthermore, we scored only penetrance of a strict phenotype, whereas Duchaine *et al*. scored a combination of expressivity and penetrance, also possibly accounting for our differences.

MATERIALS AND METHODS

Strains

Strains used in this study are listed in **Table 2.3**5. All strains and their assays were maintained and performed at 20ºC, except heat shift experiments for temperature-sensitive alleles, which were performed at 25ºC.

Dilution series procedure

Single colonies from the Ahringer library (KAMATH and AHRINGER 2003) were inoculated and grown using previously described methods (TIMMONS *et al.* 2001). The final optical density (OD) of bacteria was determined by spectrometry at 600 nm. For dilution series, the bacteria were diluted in either LB media for final OD of 1.0 or greater, or in neutral carrier bacteria

Table 2.35: Strains used in this study

Strain	Allele	Reference
N2 Bristol	Wild type	
GR1373	*eri-1(mg366)*	Kennedy *et al*. 2004
NL2099	*rrf-3(pk1426)*	Simmer *et al*. 2002
YY13	*rrf-3(mg373)*	Pavelec *et al*. 2009
WM172	*eri-3(tm1361)*	Duchaine *et al*. 2006
WM171	*eri-5(tm1705)*	Duchaine *et al*. 2006
FX01917	*eri-6/7(tm1917)*	Fischer *et al*. 2008
YY168	*eri-8(gg100)*	Pavelec *et al*. 2009
WM158	*eri-8(tm1860)*	Pavelec *et al*. 2009
YY216	*eri-9(gg106)*	Pavelec *et al*. 2009
YY209	*eri-11 (gg99)*	Unpublished. S. Kennedy
MT2495	*lin-15b(n744)*	Wang *et al*. 2005
MT10430	*lin-35(n745)*	Wang *et al*. 2005
HC195	*nrIs20[sur-5::gfp]*	Jose *et al*. 2009
HC745	*eri-1(mg366); nrIs20 [sur-5::gfp]*	
HC746	*rrf-3(pk1426); nrIs20 [sur-5::gfp]*	
HC747	*eri-3(tm1316); nrIs20 [sur-5::gfp]*	
HC748	*eri-6/7(tm1917); nrIs20 [sur-5::gfp]*	
HC749	*ergo-1/eri-8(gg100); nrIs20 [sur-5::gfp]*	
HC750	*eri-9(gg106); nrIs20 [sur-5::gfp]*	
HC751	*eri-11(gg99); nrIs20 [sur-5::gfp]*	

(*E.coli* HT115(DE3) containing an empty L4440 vector) to maintain a minimal total bacteria concentration of 1.0 OD. This minimal bacterial concentration was found necessary to maintain worm growth. In each case 20 μL of RNAi food (which is enough to support the progeny from one worm) at the desired concentrations were seeded onto and grown overnight at room temperature onto 1mM isopropyl-β-D-thiogalactopyranoside (GoldBio), 1mM carbenicillin (EMD Biosciences) NG plates (BRENNER 1974) in 30mm petri dishes (Greiner Bio-One) to induce dsRNA production. Non-starved third-larval stage single *C. elegans* worms of the desired strain were placed onto each seeded plate at 20ºC, with the exception of *fkh-6*, *gon-1*, and *gon-4* RNAi foods, which required first-larval stage single worms to be placed to ensure the elimination of the gonad.

Observed knockdown phenotypes were similar to previously observed RNAi experiments with the same gene targets, as reported in WormBase Release WS217. A single scored phenotype, as listed in **Table 2.1**, was scored for penetrance in the progeny generation of each plate's single worm four days later. HC196:*sid-1(qt9)* was used as a negative control and, as expected, did not show any RNAi knockdown phenotypes across all foods tested (WINSTON *et al.* 2002). Each Eri strain on each concentration of RNAi food was replicated between five to 12 times, as indicated in **Tables 2.2** & **2.4-2.26**.

Means and standard deviations were calculated for each Eri strain on each RNAi food concentration for nonlethal/non-growth-defective phenotypes. Normalized mean and standard errors of the mean were calculated for each Eri strain on each RNAi food concentration for lethal/growth-defective phenotypes, with brood sizes of each Eri strain feeding on vector RNAi food (**Table 2.27**) – which agreed very well with previously published data (DUCHAINE *et al.* 2006; PAVELEC *et al.* 2009) – used for normalization. A *t* test analysis of the N2 wild-type

response on each RNAi food concentration is the basis for determining an Eri phenotype on that RNAi food concentration, with a two-tailed *p* value less than 0.05 indicating significant difference. Coefficients of variation were tabulated by dividing the standard deviation by the mean.

Maternal rescue analysis:

Genetic cross analysis for an Eri phenotype on *dpy-13* RNAi food was tested at OD_{600nm} 1.5, on *hmr-1* RNAi food at OD_{600nm} 0.5, and on *unc-73* RNAi food at OD_{600nm} 3.0, using the same aforementioned setup for inoculating, growing, and seeding the RNAi plates. The shift to 25ºC to test for maternal rescue of temperature-sensitive sterility was made at the third-larval stage to ensure that spermatogenesis occurred at 25ºC.

Imaging:

All images were initially analyzed on an Olympus dissecting scope, with Illumatool Tunable Lighting System, attached to an EXFO X-Cite Fluorescence Illumination System for fluorescent detection assays. All presented images were captured on a Zeiss Axiophot, attached to a Zeiss AttoArc for fluorescent detection assays, using a Hamamatsu Digital Camera, with Openlab software. Scale bar was measured using a 0.01 mm stage micrometer (Olympus). After initial image capture, all subsequent analysis of images was performed using ImageJ software (National Institutes of Health, USA).

Laser ablation:

The *eri-8*; *sur-5::gfp* strain underwent germline removal via laser ablation as described in Bargmann and Avery 1995. Technical assistance courtesy of Stephen A. Banse.

LITERATURE CITED

AHNN, J., and A. FIRE, 1994 A screen for genetic loci required for body-wall muscle development during embryogenesis in Caenorhabditis elegans. Genetics **137:** 483-498.

BIRD, D. M., 1992 Sequence comparison of the Caenorhabditis elegans dpy-13 and col-34 genes, and their deduced collagen products. Gene **120:** 261-266.

BOWERMAN, B., M. K. INGRAM and C. P. HUNTER, 1997 The maternal par genes and the segregation of cell fate specification activities in early Caenorhabditis elegans embryos. Development **124:** 3815-3826.

BRENNER, S., 1974 The genetics of Caenorhabditis elegans. Genetics **77:** 71-94.

BROADBENT, I. D., and J. PETTITT, 2002 The C. elegans hmr-1 gene can encode a neuronal classic cadherin involved in the regulation of axon fasciculation. Curr Biol **12:** 59-63.

CALIXTO, A., D. CHELUR, I. TOPALIDOU, X. CHEN and M. CHALFIE, 2010 Enhanced neuronal RNAi in C. elegans using SID-1. Nat Methods **7:** 554-559.

CHANG, W., C. TILMANN, K. THOEMKE, F. H. MARKUSSEN, L. D. MATHIES *et al.*, 2004 A forkhead protein controls sexual identity of the C. elegans male somatic gonad. Development **131:** 1425-1436.

CHEESEMAN, I. M., S. NIESSEN, S. ANDERSON, F. HYNDMAN, J. R. YATES, 3RD *et al.*, 2004 A conserved protein network controls assembly of the outer kinetochore and its ability to sustain tension. Genes Dev **18:** 2255-2268.

CHURCH, D. L., and E. J. LAMBIE, 2003 The promotion of gonadal cell divisions by the Caenorhabditis elegans TRPM cation channel GON-2 is antagonized by GEM-4 copine. Genetics **165:** 563-574.

DUCHAINE, T. F., J. A. WOHLSCHLEGEL, S. KENNEDY, Y. BEI, D. CONTE, JR. *et al.*, 2006 Functional proteomics reveals the biochemical niche of C. elegans DCR-1 in multiple small-RNA-mediated pathways. Cell **124:** 343-354.

FIRE, A., D. ALBERTSON, S. W. HARRISON and D. G. MOERMAN, 1991 Production of antisense RNA leads to effective and specific inhibition of gene expression in C. elegans muscle. Development **113:** 503-514.

FISCHER, S. E., M. D. BUTLER, Q. PAN and G. RUVKUN, 2008 Trans-splicing in C. elegans generates the negative RNAi regulator ERI-6/7. Nature **455:** 491-496.

GU, T., S. ORITA and M. HAN, 1998 Caenorhabditis elegans SUR-5, a novel but conserved protein, negatively regulates LET-60 Ras activity during vulval induction. Mol Cell Biol **18:** 4556-4564.

HUNT-NEWBURY, R., R. VIVEIROS, R. JOHNSEN, A. MAH, D. ANASTAS *et al.*, 2007 High-throughput in vivo analysis of gene expression in Caenorhabditis elegans. PLoS Biol **5:** e237.

HUSKEN, K., T. WIESENFAHRT, C. ABRAHAM, R. WINDOFFER, O. BOSSINGER *et al.*, 2008 Maintenance of the intestinal tube in Caenorhabditis elegans: the role of the intermediate filament protein IFC-2. Differentiation **76:** 881-896.

JOSE, A. M., J. J. SMITH and C. P. HUNTER, 2009 Export of RNA silencing from C. elegans tissues does not require the RNA channel SID-1. Proc Natl Acad Sci U S A **106:** 2283-2288.

KAMATH, R. S., and J. AHRINGER, 2003 Genome-wide RNAi screening in Caenorhabditis elegans. Methods **30:** 313-321.

KENNEDY, S., D. WANG and G. RUVKUN, 2004 A conserved siRNA-degrading RNase negatively regulates RNA interference in C. elegans. Nature **427:** 645-649.

KNIGHT, S. W., and B. L. BASS, 2002 The role of RNA editing by ADARs in RNAi. Mol Cell **10:** 809-817.

KO, F. C., and K. L. CHOW, 2003 A mutation at the start codon defines the differential requirement of dpy-11 in Caenorhabditis elegans body hypodermis and male tail. Biochem Biophys Res Commun **309:** 201-208.

LEE, R. C., C. M. HAMMELL and V. AMBROS, 2006 Interacting endogenous and exogenous RNAi pathways in Caenorhabditis elegans. RNA **12:** 589-597.

MACQUEEN, A. J., J. J. BAGGETT, N. PERUMOV, R. A. BAUER, T. JANUSZEWSKI *et al.*, 2005 ACT-5 is an essential Caenorhabditis elegans actin required for intestinal microvilli formation. Mol Biol Cell **16:** 3247-3259.

MANGO, S. E., 2007 The C. elegans pharynx: a model for organogenesis, pp. 1-26 in *WormBook*.

MCKAY, S. J., R. JOHNSEN, J. KHATTRA, J. ASANO, D. L. BAILLIE *et al.*, 2003 Gene expression profiling of cells, tissues, and developmental stages of the nematode C. elegans. Cold Spring Harb Symp Quant Biol **68:** 159-169.

MEISSNER, B., A. WARNER, K. WONG, N. DUBE, A. LORCH *et al.*, 2009 An integrated strategy to study muscle development and myofilament structure in Caenorhabditis elegans. PLoS Genet **5:** e1000537.

MITANI, S., 2009 Nematode, an experimental animal in the national BioResource project. Exp Anim **58:** 351-356.

MYLLYHARJU, J., and K. I. KIVIRIKKO, 2004 Collagens, modifying enzymes and their mutations in humans, flies and worms. Trends Genet **20:** 33-43.

PAGE, A. P., JOHNSTONE, I.L., 1997 The cuticle (March 19, 2007), pp. WormBook, ed. The C. elegans Research Community, WormBook, doi/10.1895/wormbook.1.138.1, http://www.wormbook.org.

PAVELEC, D. M., J. LACHOWIEC, T. F. DUCHAINE, H. E. SMITH and S. KENNEDY, 2009 Requirement for the ERI/DICER complex in endogenous RNA interference and sperm development in Caenorhabditis elegans. Genetics **183:** 1283-1295.

REA, S. L., VENTURA, N., JOHNSON, T.E., 2007 Relationship between mitochondrial electron transport chain dysfunction, development, and life extension in Caenorhabditis elegans. PLoS Biology **5:** 2312-2329.

SEYDOUX, G., and A. FIRE, 1994 Soma-germline asymmetry in the distributions of embryonic RNAs in Caenorhabditis elegans. Development **120:** 2823-2834.

SIMMER, F., M. TIJSTERMAN, S. PARRISH, S. P. KOUSHIKA, M. L. NONET *et al.*, 2002 Loss of the putative RNA-directed RNA polymerase RRF-3 makes C. elegans hypersensitive to RNAi. Curr Biol **12:** 1317-1319.

TABARA, H., R. J. HILL, C. C. MELLO, J. R. PRIESS and Y. KOHARA, 1999 pos-1 encodes a cytoplasmic zinc-finger protein essential for germline specification in C. elegans. Development **126:** 1-11.

TAMAI, K. K., and K. NISHIWAKI, 2007 bHLH transcription factors regulate organ morphogenesis via activation of an ADAMTS protease in C. elegans. Dev Biol **308:** 562-571.

TIMMONS, L., D. L. COURT and A. FIRE, 2001 Ingestion of bacterially expressed dsRNAs can produce specific and potent genetic interference in Caenorhabditis elegans. Gene **263:** 103-112.

TIMMONS, L., and A. FIRE, 1998 Specific interference by ingested dsRNA. Nature **395:** 854.

VANDERZALM, P. J., A. PANDEY, M. E. HURWITZ, L. BLOOM, H. R. HORVITZ *et al.*, 2009 C. elegans CARMIL negatively regulates UNC-73/Trio function during neuronal development. Development **136:** 1201-1210.

VASTENHOUW, N. L., K. BRUNSCHWIG, K. L. OKIHARA, F. MULLER, M. TIJSTERMAN *et al.*, 2006 Gene expression: long-term gene silencing by RNAi. Nature **442:** 882.

VOUGHT, V. E., M. OHMACHI, M. H. LEE and E. M. MAINE, 2005 EGO-1, a putative RNA-directed RNA polymerase, promotes germline proliferation in parallel with GLP-1/notch signaling and regulates the spatial organization of nuclear pore complexes and germline P granules in Caenorhabditis elegans. Genetics **170:** 1121-1132.

WANG, P., J. ZHAO and A. K. CORSI, 2006 Identification of novel target genes of CeTwist and CeE/DA. Dev Biol **293:** 486-498.

WINSTON, W. M., C. MOLODOWITCH and C. P. HUNTER, 2002 Systemic RNAi in C. elegans requires the putative transmembrane protein SID-1. Science **295:** 2456-2459.

XING, J., X. YAN, A. ESTEVEZ and K. STRANGE, 2008 Highly Ca2+-selective TRPM channels regulate IP3-dependent oscillatory Ca2+ signaling in the C. elegans intestine. J Gen Physiol **131:** 245-255.

Chapter Three

Analyses of three screens for novel RNAi mutants

Some contents were previously presented as a part of the Ph.D. qualification report and its accompanying preliminary data (May, 2010).

INTRODUCTION

The identification of the currently known enhanced RNAi mutants was a result of a variety of approaches, many of which were mutually confirmatory. Of the canonical *eri* mutants described in Chapter Two, *rrf-3* was the first discovered, and characterized completely fortuitously during an analysis of the four *C. elegans* RNA-dependent RNA polymerases (RdRPs) (SIMMER *et al.* 2002). It was re-discovered along with *eri-1*, *eri-3*, *eri-4/dcr-1*, *eri-5*, and *eri-6/7* in a forward genetic screen for enhanced neuronal silencing (KENNEDY *et al.* 2004). In this screen, *gfp* was driven by the neuronal promoter of *unc-47*, and because *C. elegans* neurons are normally recalcitrant to RNAi, mutant strains exhibiting knockdown of *gfp* were thus deemed enhanced for RNAi. Around the same time, another group was attempting to analyze the biochemical interactions of *dicer*; because *C. elegans* only has one *dicer* homolog in its genome, this "chokepoint" analysis was extremely insightful (DUCHAINE *et al.* 2006). In this study, although most DCR-1-interacting genes were expectedly RNAi-defective (Rde) when mutated, ERI-3 and ERI-5 were found to interact as well. Finally, *eri-6/7* was re-discovered along with *eri-8/ergo-1*, *eri-9*, and *eri-11* in a forward genetic screen for enhanced pan-operon silencing (PAVELEC *et al.* 2009). In this screen, *lin-15b(RNAi)* was fed to worms, and while wild type strains exhibited no effect, enhanced RNAi animals knocked down both *lin-15b* and *lin-15a* transcripts because the two are in an operon, which causes a multi-vulva phenotype.

Besides these canonical *eri* mutants, the *lin-15(n765)* mutant was discovered to be enhanced for RNAi *ad hoc* (WANG *et al.* 2005). Subsequently, large portions of the *C. elegans* synMuv *rb* pathway were similarly implicated as Eri, including *hpl-2*, *lin-35*, *dpl-1*, *lin-13*, *lin-9*, *lin-38*, *lin-56*, *let-60*, and *efl-1* (LEHNER *et al.* 2006; WANG *et al.* 2005). Recently, small RNA sequencing of some *rb* mutants found that many RNAi components, especially those in the

germline, like worm-specific secondary Argonautes (WAGOs), are overexpressed in these *rb* mutants (WU *et al.* 2012), thus partially explaining their mechanism of action.

Both the *eri* and *rb* class not only enhance RNAi against exogenous double-stranded RNA (dsRNA), but also enhance spontaneous transgene silencing (ZHUANG and HUNTER 2011). If the definition of enhanced RNAi is extended to include enhanced transgene silencing, then transcriptional regulators such as components of the DRM/dREAM protein complex or the nucleosome remodeling and deacetylase complex can also be classified as Eri mutants (WU *et al.* 2012). However, the exact nature of how these genes affect responses to small RNAs is still unclear. A fascinating example of enhanced transgene silencing not corresponding to enhanced exogenous RNAi is the case of the *adr* mutants. *C. elegans* adenosine deaminases (ADAR-1, ADAR-2) deaminate adenosines to inosines in dsRNAs in order to prevent transgenes from being somatically silenced. In *adr-1* and *adr-2* mutants, there is enhanced transgene silencing, but no changes in sensitivity to exogenous dsRNA (KNIGHT and BASS 2002).

While enhanced RNAi is the focus of my research, it's noteworthy to point out that many screens for what was expected to be an Rde phenotype turned up Eri mutants, such as the aforementioned cases of *rrf-3*, *eri-3*, and *eri-5*, and the candidate screen I performed in Chapter 5 (**Table 5.1**). Thus, discussing the nature of the Rde screens performed to date is similarly important for examining the potential landscape of enhanced RNAi. The first screen performed for Rde mutants fed worms dsRNA against *pos-1*, a germline gene target, and selected for survivors (TABARA *et al.* 1999). Based on a hypothesis presented in the first screen, another group performed a candidate screen of strains unable to repress *Tc1* transposition, and some turned out to also be RNAi-insensitive (KETTING *et al.* 1999). Biochemical analysis of DCR-1 and its interacting components also yielded many factors whose loss expectedly caused an Rde

phenotype (DUCHAINE *et al.* 2006; KNIGHT and BASS 2001). Another forward genetic screen performed for systemic RNAi defective (Sid) mutants examined worms with body-wall muscle *gfp* (*myo-3::gfp*), pharyngeal *gfp* (*myo-2::gfp*), and a pharyngeal dsRNA source (*myo-2::pfg-gfp*). A worm that is Sid but not Rde will have desilencing of the bodywall muscle *gfp*, but maintain silencing of the pharyngeal *gfp* (WINSTON *et al.* 2002). The most recent forward genetic screen for Rde mutants used a neuronal dsRNA source (*snb-1::pfg-gfp*) and the ubiquitous *sur-5::gfp* marker. An Rde worm in this screen will remain *gfp* positive (ZHANG *et al.* 2012). Finally, fortuitous discoveries of background mutations (ZHANG *et al.* 2011) and natural variations among *C. elegans* strains (TIJSTERMAN *et al.* 2002) that cause an Rde phenotype also occurred over the years.

With the recent advances in small RNA sequencing technology and the observations that *eri* mutants are defective for endogenous small RNA production, more and more approaches for understanding all the genes implicated in RNAi rely on genome-scale analysis. Many RNAi genes with weak phenotypes, which were perhaps previously bypassed in the genetic screens, are now having redoubled efforts devoted to their analysis because of confirmation through deep-sequencing. For example, mutation to the RdRP *rrf-2* was initially thought to be absent of any RNAi phenotypes; however, the fact that it was found to be misexpressed in a *rb* mutant made it a promising candidate for reexamination. And indeed, it was found to be very weakly Rde upon reanalysis (WU *et al.* 2012).

However, despite these advances, completely novel mechanisms for RNAi or its regulation may still be missed if deep sequencing is performed mostly in the context of already-known RNAi mutants. Therefore, it'd be informative to examine areas that the published screens may have missed to possibly elucidate truly novel RNAi components.

SCREEN FOR ENHANCED SYSTEMIC RNAi

The systemic effect of RNAi in *C. elegans*, whereby silencing spreads between cells and tissues, contributes significantly to its potency (FIRE *et al.* 1998). Because of this potency, unintended silencing must be avoided, suggesting significant levels of negative regulation; however, no known Eri mutant fits this model, especially at the systemic RNAi level. Furthermore, the distinction between regulating cell autonomous RNAi and systemic transport of silencing signals has not been characterized for any known Eri mutant, even though studies in plant RNAi transport have discovered roles played by proteins molecularly similar to the *C. elegans* ERIs (BROSNAN *et al.* 2007; DUNOYER *et al.* 2007; DUNOYER *et al.* 2005; HIMBER *et al.* 2003; SCHWACH *et al.* 2005; SMITH *et al.* 2007; VOINNET 2008; YOO *et al.* 2004).

A pilot screen of ~2,000 animals from 2002 (performed by W.M. Winston and C. Molodowitch) identified 13 enhanced RNAi spreader (Ersr) mutants. This screen was similar in design to the screen that identified the dsRNA channel *sid-1* (FEINBERG and HUNTER 2003; WINSTON *et al.* 2002). In the pilot screen (**Figure 3.1A**), a pharyngeally-expressed *gfp* reporter (*myo-2::gfp*) and a bodywall muscle-expressed GFP reporter (*myo-3::gfp*) were silenced by a pharyngeally-expressed hairpin *gfp* (*myo-2::pfg-gfp*). In wild-type animals, the hairpin silences pharyngeal GFP modestly and bodywall muscle GFP along a gradient (**Figure 3.1B**); in Ersr mutants, pharyngeal GFP silenced at wild-type levels but bodywall muscle GFP was silenced to a greater extent, possibly because of greater spread of silencing.

My analysis of these 13 Ersr mutants identified three classes (**Figure 3.1C**). In the first class, eight strong Ersr alleles failed to complement each other, mapped to a region near *eri-6/7*, and representative alleles failed to complement *eri-6/7*. The preponderance of *eri-6/7* alleles may

Figure 3.1: Screen for enhanced RNAi spreader (Ersr) mutations and analysis of mutant alleles (**A**) Schematic of strain construction and expected phenotypes of RNAi defective (Rde) mutants, wild-type animals, and Ersr mutants. **(B)** GFP expression pattern of a wild-type animal in the screen background. Red arrow points to *myo-2::gfp* (pharyngeal) expression. White arrows point to *myo-3::gfp* (bodywall muscle) expression. There is increasing GFP expression with increasing distance away from the pharyngeal silencing source *myo-2::pfg-gfp*. **(C)** Alleles of each of the three classes of Ersrs found in the screen, the results of complementation analysis, and their phenotype by feeding RNAi. The three class II *ersr*s were independent, complementing alleles, whereas complementation between the two class III *ersr*s was not performed. **(D)** GFP expression pattern of a class I or class II *ersr* animal; qt71 was used as the representative allele. Red arrow points to *myo-2::gfp* (pharyngeal) expression. White arrows point to the weak remaining *myo-3::gfp* (bodywall muscle) expression. **(E)** GFP expression pattern of a class III *ersr* animal; qt74 was used as the representative allele. Red arrow points to *myo-2::gfp* (pharyngeal) expression. The was almost no *myo-3::gfp* (bodywall muscle) expression. All images are representative. Pharynx of worms are all pointing towards the upper left corner.

A

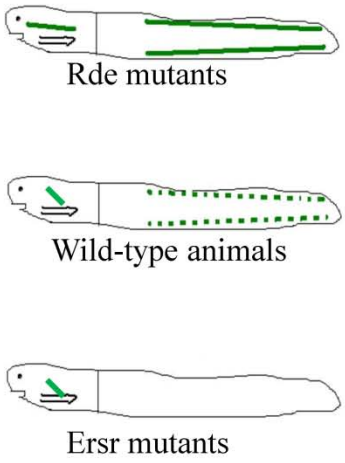

B

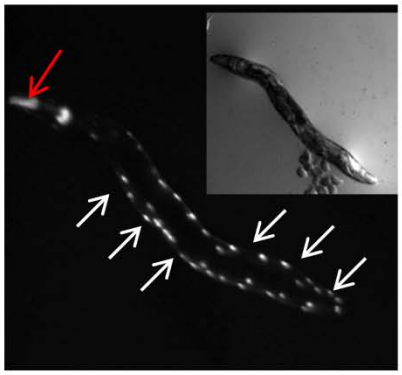

C

Alleles found in Ersr screen	Complements *eri-6/7*	Enhanced for RNAi feeding
Class I: qt65, qt66, qt67, qt68, qt71, qt72, qt75, qt76	No	Yes
Class II: qt64, qt69, qt70	Yes	Weak
Class III: qt73, qt74	Yes	No

D

myo-3::gfp; myo-2::pfg-gfp; myo-2::gfp; ersr (class I/classII)

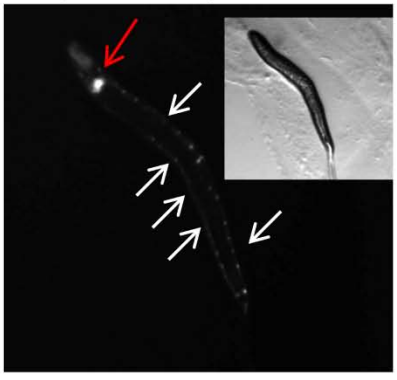

E

myo-3::gfp; myo-2::pfg-gfp; myo-2::gfp; ersr (class III)

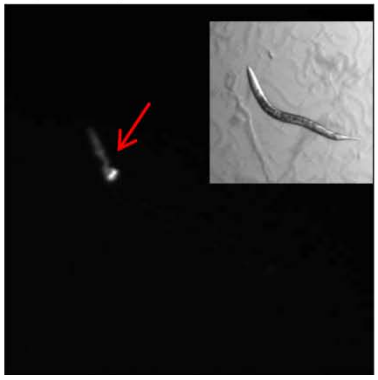

Figure 3.1 (Continued): Screen for enhanced RNAi spreader (Ersr) mutations and analysis of mutant alleles

be expected, as the screen was performed at 25ºC, where most other *eri*s are sterile (FISCHER *et al.* 2008). In the second class, three independent alleles became successively weaker after outcrossing; after three outcrosses, their phenotypic penetrance decreased to ~5%, making analysis difficult. **Figure 3.1D** shows representative *gfp*-reporter phenotypes of class 1 and 2 Ersr alleles. The two remaining alleles in the third class strongly enhanced silencing of the *gfp* reporter (**Figure 3.1E**), but did not enhance RNAi for endogenous genes by feeding. An independent *gfp* reporter (*sur-5::gfp*) crossed into these two alleles showed similarly enhanced silencing. It's likely that these alleles enhance only transgene silencing, a process actively involving RNAi (GRISHOK *et al.* 2005). Absence of a non-reporter phenotype again makes subsequent analysis difficult. However, it's promising that a small screen captured a variety of Eris/Ersrs, encouraging future larger screen for unidentified RNAi regulators.

Even though eight out the 13 candidates isolated did not complement *eri-6/7(tm1917)*, surprisingly, we were not able to identify a molecular lesion by sequencing the genomic region of both *eri-6* and *eri-7* for the strongest mutant *qt66*. However, because *eri-6/7* is a trans-spliced product, defects outside of the genomic region could still impact the complete assembly of a functional gene product (FISCHER *et al.* 2008). Interestingly enough, four of the six splice forms of *eri-6* (c-f) contain three sets of direct repeats and a region with 99.3% nucleotide identity to *K09B11.4*, a paralog of *retr-1*; in fact, *eri-6* was even initially annotated as *rag-1*-related. Furthermore, *C. briggsae*'s *eri-6/7* is a fused (not trans-spliced) product while it has no *K09B11.4* homolog. These facts suggest a possibility that *C. elegans eri-6/7* evolved its structure in response to an adjacent insertion of a retrotransposon-like element. If true, the lack of molecular lesions within the *eri-6/7* genomic region in our eight candidates could be related to the intricate assembly *C. elegans eri-6/7* requires.

CANDIDATE SCREEN FOR ENHANCED SYSTEMIC TRANSGENE SILENCING

Analysis of the Ersr mutants from the pilot screen failed to identify new regulators, but the effort highlighted the subtlety of enhanced RNAi spreading phenotypes, suggesting a platform for analysis of Eri mutants that might regulate transport. To determine whether any of the published Eri mutants affect specific transport steps, I crossed each available *eri* mutant (and *sid-1* as a control) into a *sur-5::gfp* background which expresses ubiquitous *gfp* (*eri-x; sur-5::gfp*). I then crossed in a pharyngeally-expressed hairpin GFP (*myo-2::pfg-gfp*) and examined the silencing patterns to identify candidates for detailed analysis.

Ubiquitous *gfp* expression in *sur-5::gfp* worms is silenced in a gradient fashion when the *myo-2::pfg-gfp* hairpin is present (**Figure 3.2A, B**). The *gfp* expression is weakest near the source of the hairpin and gradually increases along the anterior-posterior axis of the worm. As expected, *sid-1; myo-2::pfg-gfp*; *sur-5::gfp* (**Figure 3.2S, T**) did not show any silencing spreading from the pharynx. This transgenic platform makes RNAi spreading visually accessible.

For all the *eri*s in the *sur-5::gfp* background (with or without the *gfp* hairpin), there is spontaneous transgene silencing near the middle of the worm (**Figure 3.2C**). This spontaneous silencing seems to be another competing RNAi pathway for limited resources because knocking out the endogenous RNAi pathway (*eri* mutants) or knocking down the exogenous RNAi pathway (**Figure 3.3**) increases its potency. Because this silencing "hole" is present in all *eri*s, it somewhat impedes visualizing RNAi spreading, but patterns of *gfp* expression can still be examined in the remainder of the worm.

eri-1, *rrf-3*, *eri-4*, *eri-6/7*, and *eri-8* in the *myo-2::pfg-gfp*; *sur-5::gfp* background caused uniformly decreased *gfp* expression throughout the worm. While this observation cannot

Figure 3.2: Eri mutants' effects on RNAi silencing spread

N2 wild type, *eri-1(mg366)*, *rrf-3(pk1426)*, *eri-3(tm1361)*, *eri-4/dcr-1(mg375)*, *eri-6/7(tm1917)*, *eri-8(gg100)*, *eri-9(gg106)*, *eri-11(gg99)*, and *sid-1(qt9)* in an ubiquitously expressed *sur-5::gfp* background (**A, C, E, G, I, K, M, O, Q, S**) and with the addition of a hairpin *pfg-gfp* expressed in the pharynx by the *myo-2* promoter (**B, D, F, H, J, L, N, P, R, T**). *eri-3* (**H**), *eri-9* (**P**), and e*ri-11*(**R**) show perturbed spreading patterns in the presence of the hairpin *gfp* (boxed in red), suggestive of enhanced transport. All other Eri strains show uniformly decreased *gfp* expression pattern in the presence of the hairpin *pgf-gfp*: images in **D, F, J, L, N** show at least 2x lower quantifiable GFP expression upon ImageJ analysis than images in **C, E, I, K, M**, respectively. All Eri strains show spontaneous transgene silencing near the middle of the worm – a "hole" of absent GFP expression – with boundaries demarcated by white arrows for *eri-1; sur-5::gfp* as illustration (**C**). All images are representative. All images are exposed for 100 milliseconds. Pharynx of worms are all pointing towards the upper left corner.

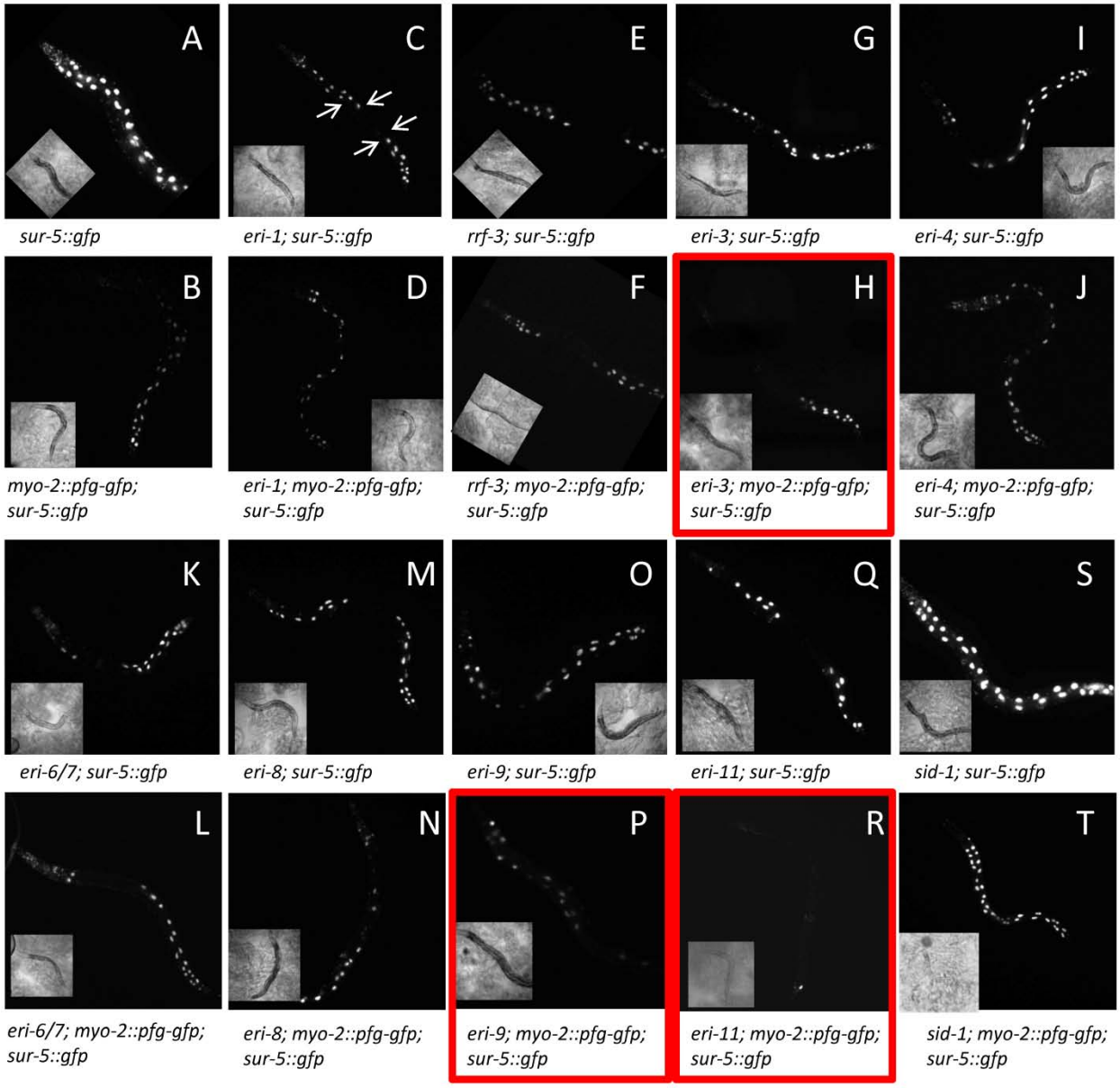

Figure 3.2 (Continued): Eri mutants' effects on RNAi silencing spread

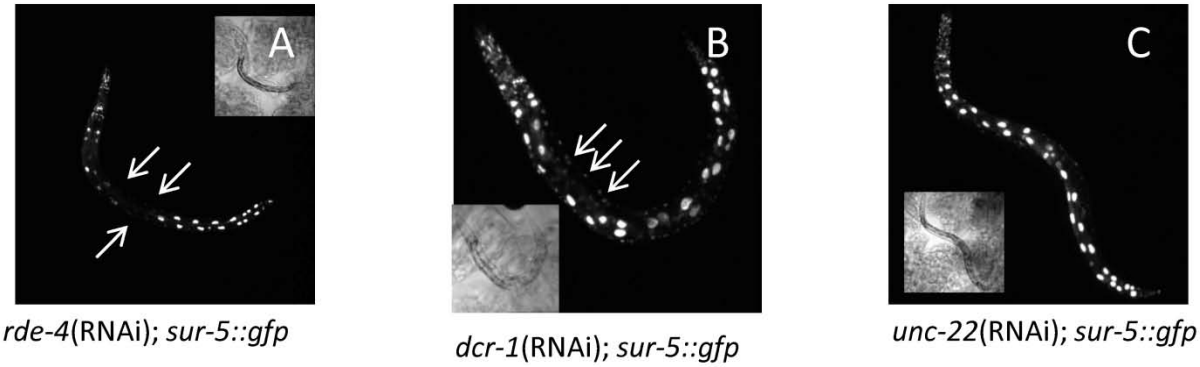

Figure 3.3: Knockdown of exogenous RNAi pathway genes *rde-4* and *dcr-1* causes spontaneous transgene silencing

(A) RDE-4 knockdown in wild-type *sur-5::gfp* animals causes spontaneous *gfp* silencing, indicated by the white arrows. **(B)** DCR-1 knockdown in wild-type *sur-5::gfp* animals also causes spontaneous *gfp* silencing, indicated by the white arrows. **(C)** UNC-22 knockdown in wild-type *sur-5::gfp* animals does not cause spontaneous gfp silencing. All images are representative. All images are exposed for 100 milliseconds. Pharynx of worms are all pointing towards the upper left corner.

preclude enhancing RNAi spreading, especially since the gradient seen in **Figure 3.2** seems to be absent (possibly due to lower signals overall), these *eri*s don't exhibit patently perturbed spreading patterns.

eri-3; sur-5::gfp with *myo-2::pfg-gfp* and *eri-11; sur-5::gfp* with *myo-2::pfg-gfp* (**Figure 3.2H, R**) show complete anterior silencing. The enhanced silencing phenotype of *eri-3* and *eri-11* varies from silencing just past the vulva (**Figure 3.4A**) to silencing of the entire worm except three tail cells (**Figure 3.4B**). *eri-3* and *eri-11* could potentially enhance uptake of RNAi silencing in the anterior of the worm.

eri-9; sur-5::gfp with *myo-2::pfg-gfp* (**Figure 3.2P**) shows an "inverse gradient" pattern: silencing is weakest near the hairpin GFP and increases towards the posterior of the animal. The "inverse gradient" phenotype is independent of the transgene silencing "hole" (**Figure 3.4C**). *eri-9* could potentially enhance export of RNAi silencing to the posterior of the worm.

~90% of *eri-3* worms and ~20-30% of *eri-9* worms exhibit these described phenotypes (**Figure 3.4D**); these penetrances increase at lower temperatures, consistent with previously reported *myo-2::pfg-gfp* potency (WINSTON *et al.* 2002). To confirm the enhanced RNAi phenotypes, feeding *E. coli* expressing dsRNA *gfp* was used as an alternate silencing source; upon diluted feeding, wild-type *sur-5::gfp* animals were partially silenced, but *eri-3; sur-5::gfp* and *eri-9; sur-5::gfp* became completely silenced (**Figures 3.4E, F, G**), suggesting that the unsilenced cells in **Figure 3.2H, P** are still RNAi responsive. The described phenotypes for *eri-3* and *eri-9* are present throughout larval development and adulthood (**Figures 3.4H-M**).

eri-3, *eri-9*, and *eri-11* are promising candidate negative regulators of RNA transport because of their interesting RNAi spreading patterns. *eri-3*, *eri-9*, and *eri-11* are all cloned novel genes, making them intriguing candidates to propose a transport role for. I attempted to dissect

Figure 3.4: Further characterization of *eri-3* and *eri-9*'s enhanced spreading phenotypes

(A) The "weakest" extreme of *eri-3* spreading, where silencing is only up to the vulva. **(B)** The "strongest" extreme of *eri-3* spreading, where silencing is the entire animal except 3 tail cells, indicated by the white arrow. **(C)** *eri-9* animals show the transgene silencing "hole", indicated by the white arrows, as well as the "inverse" silencing gradient; enhanced spreading seems independent of transgene silencing. (**D)** penetrance of *eri-3* and *eri-9* phenotypes is highest at 15 degrees and lowest at 25 degrees. (**E, F, G)** *eri-3* (**F**) and *eri-9* (**G**) animals without the *gfp* hairpin still silences *gfp* at a low concentration of *gfp(RNAi)* feeding compared to wild type (**E**). The enhanced silencing pertains generally to all RNAi sources. (**H, I, J)** The *eri-3* spreading phenotype is consistently present throughout larval development. (**K, L, M)** The *eri-9* spreading phenotype is consistently present through larval development. All images are exposed for 100 milliseconds, except **B**, which was exposed for 400 milliseconds. All images are representative. Pharynx of worms are all pointing towards the upper left corner.

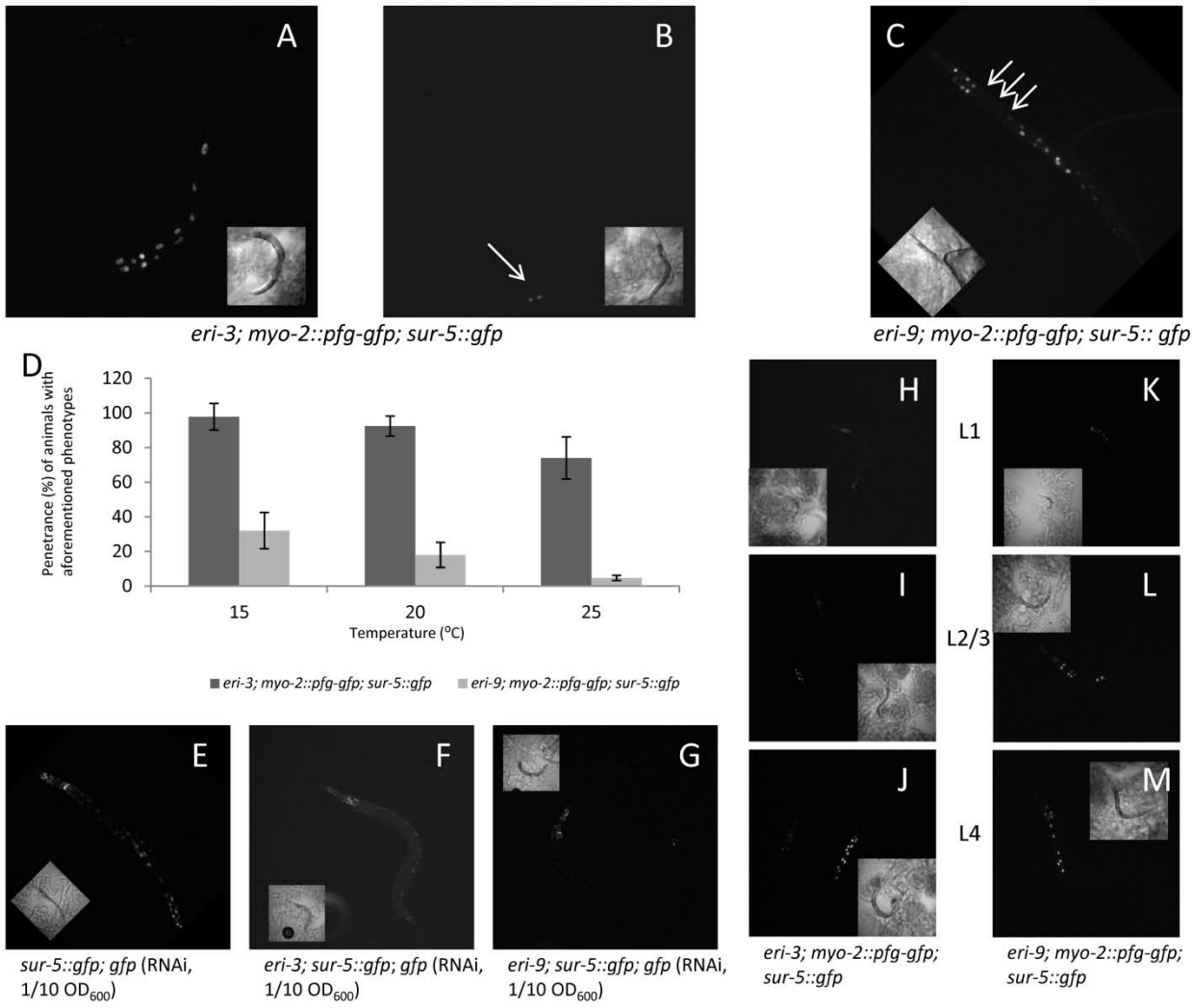

Figure 3.4 (Continued): Further characterization of *eri-3* and *eri-9*'s enhanced spreading phenotypes

their possible roles in transport regulation via mosaic analysis by using transcriptional and translational fusion constructs, which also elucidates the *in vivo* expression patterns for *eri-3*, *eri-9*, and *eri-11*. Mechanistically, there are broadly four possible mutations from which an Eri phenotype may result (**Figure 3.5**): first, cell autonomously, a mutation may increase sensitivity or decrease turnover of RNAi signals (i.e. deficiency in an exonuclease that degrades lingering dsRNA); second, a mutation may increase export of RNAi signals (i.e. deficiency in a regulator that gates dsRNA exit); third, a mutation may increase extracellular transport of RNAi signals (i.e. deficiency in a dsRNA binding protein that slows extracellular trafficking); fourth, a mutation may increase uptake of RNAi signals (i.e. deficiency in a SID-1 regulator). These mechanisms can be distinguished from one another by mosaic analysis.

My data suggest *eri-3*, *eri-9*, *eri-11* exert an effect on receiving cells along the anterior-posterior axis. Therefore, I was hoping to examine seam cells during mosaic analysis because they are also aligned along the A-P axis; their lineage is also ideal for mosaic analysis because many adjacent seam cells derive from early ancestors that diverged 7 to 11 cell divisions before their terminal differentiation (ALTUN and HALL 2005). I microinjected the wild-type copy *eri-3*, *eri-9*, or *eri-11* along with red fluorescent marker (DsRed), which are inherited as semi-stable extra-chromosomal arrays, with technical assistance courtesy of C. Roehrig. Theoretically, array loss during any of the 7 to 11 cell divisions before adjacent seam cells' terminal differentiation in one lineage but not the other will create adjacent red and non-red cells, indicative of adjacent mosaic ERI rescue.

However, the *gfp* and *dsRed* expression were both quite noisy. Expression was only detectable in the vulva, gonad sheath, some pharyngeal and epithelial cells, and the tail sphincter using transcriptional or translational reporters (**Figures 3.6-3.12**). This expression pattern

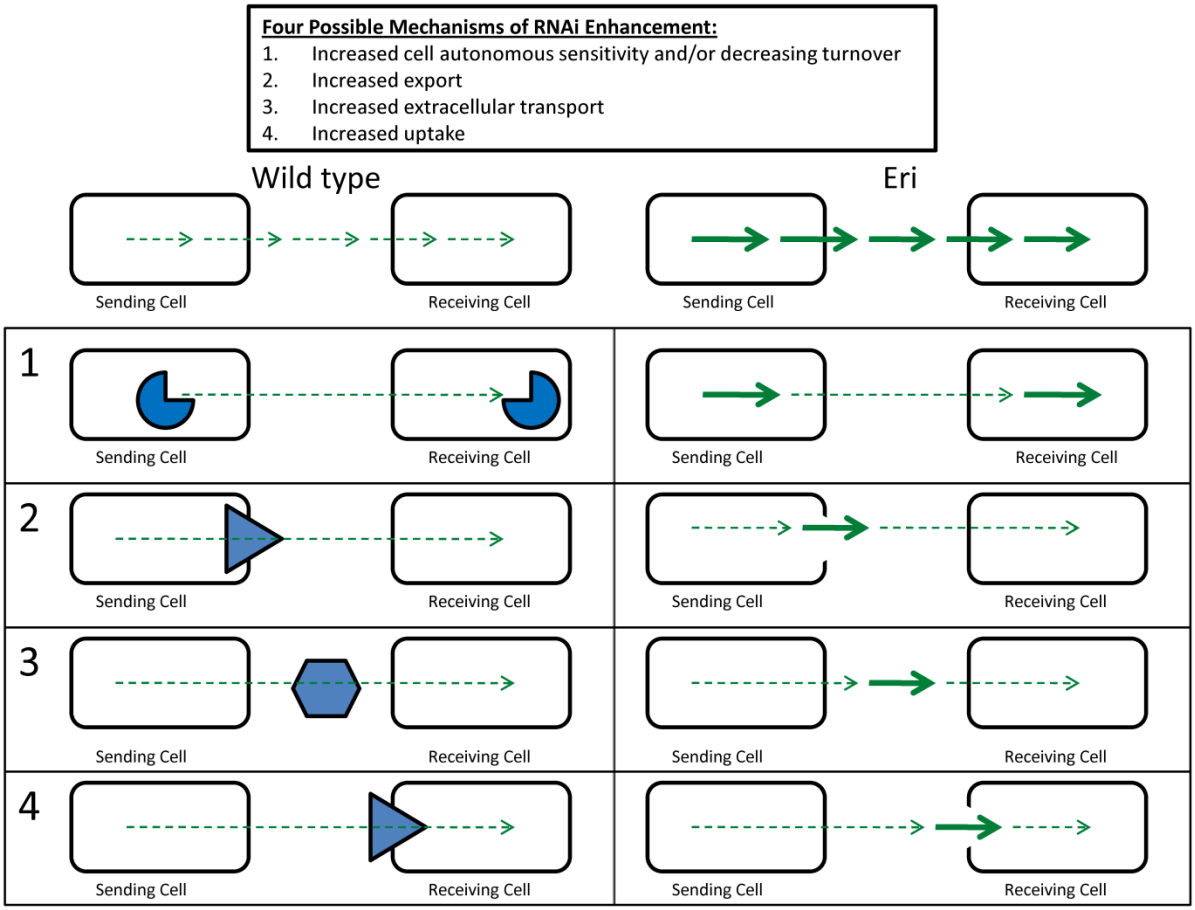

Figure 3.5: Schematic of the four possible mechanisms for RNAi enhancement and mutations which can cause an Eri phenotype

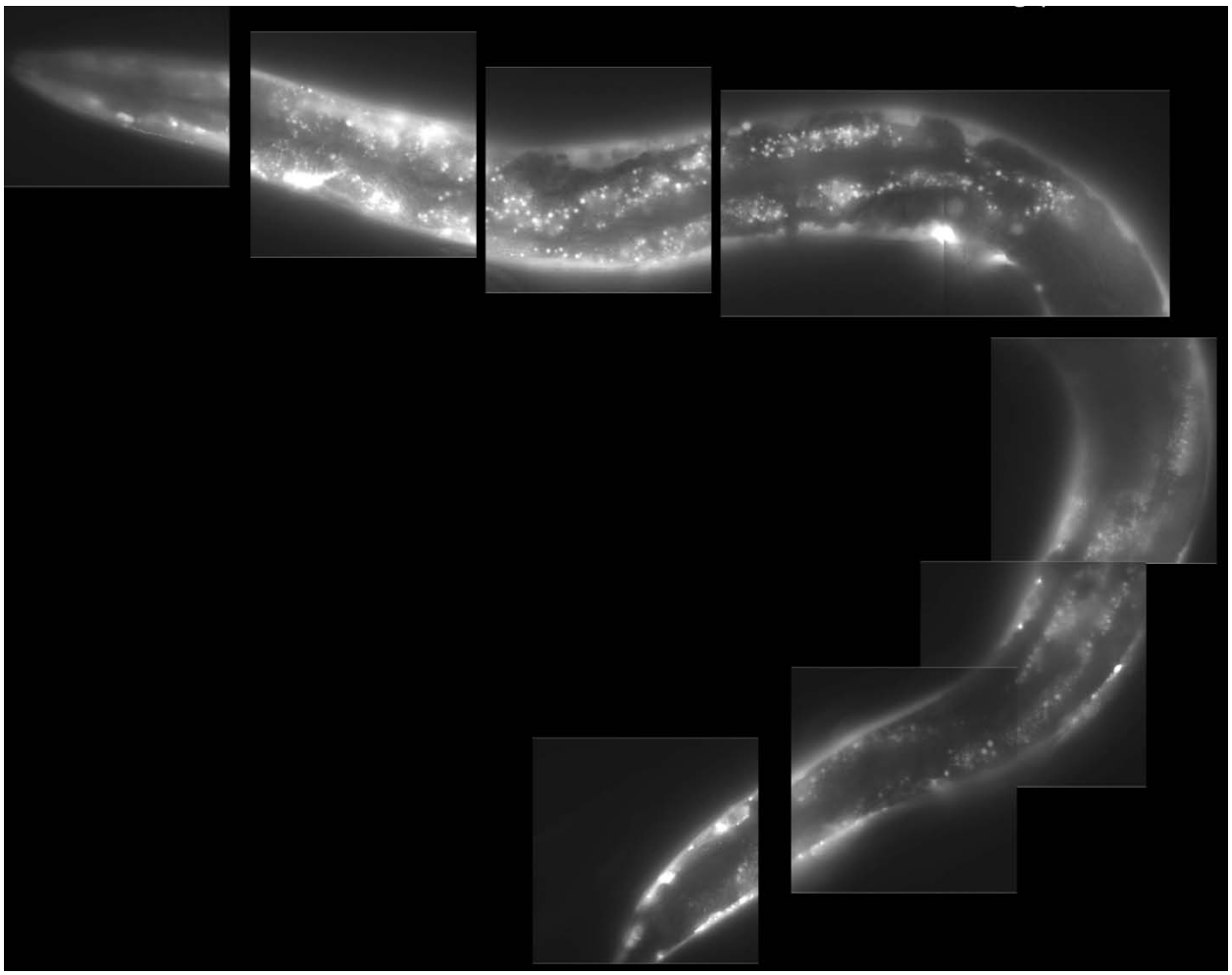

Figure 3.6: *eri-3-gfp* translational fusion expression – whole worm

All stitched images were exposed for the same amount of time, indicating perhaps that *eri-3* is more highly expressed in the anterior than the posterior. In the absence of the *gfp* marker, there is still robust gut autofluorescence, suggesting noise in the readout.

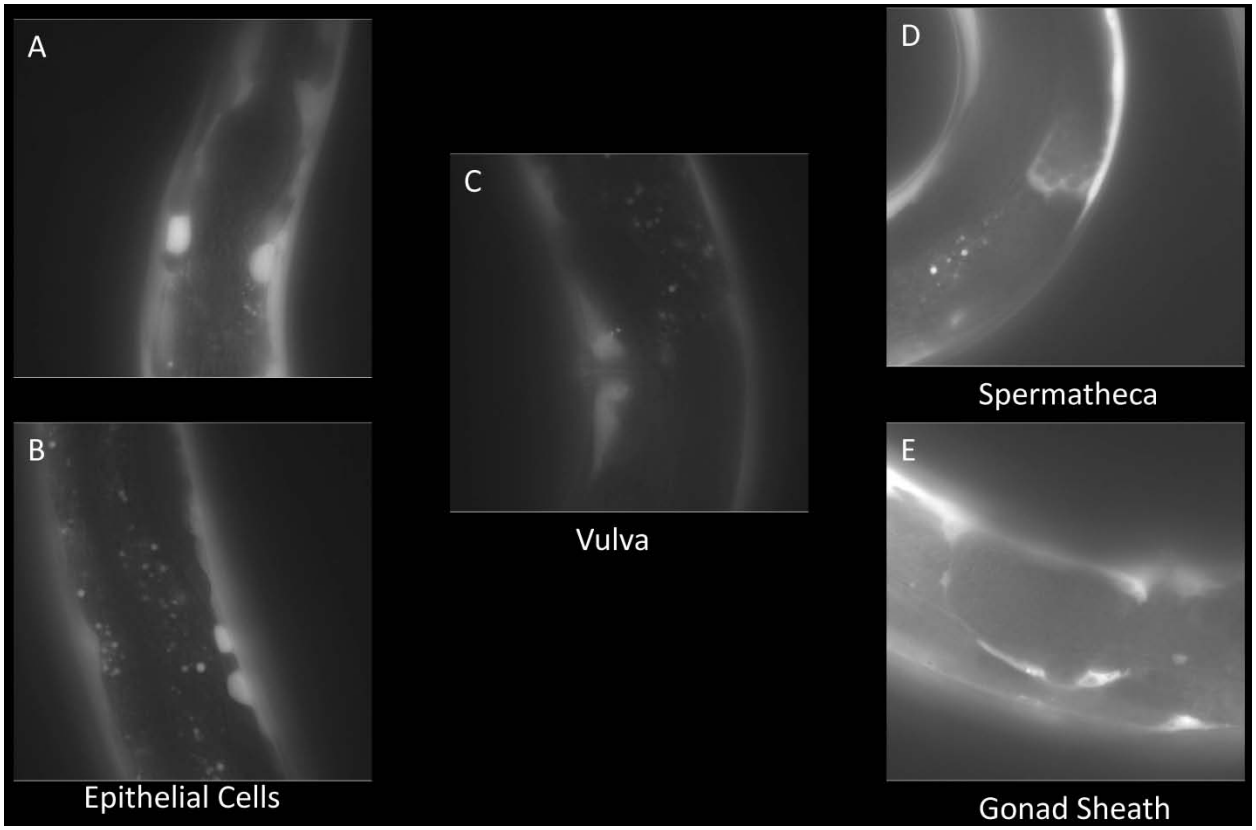

Figure 3.7: *eri-3-gfp* translational fusion expression – parts

There is robust *gfp* expression in the epithelial cells (**A**, **B**), faint expression in the vulva (**C**), and very robust expression in the spermatheca (**D**) and the gonad sheath (**E**), consistent perhaps with the *eri*s' roles in the germline. In the absence of the *gfp* marker, there is almost no autofluorescence in the vulva, gonad, or epithelial cells, suggesting a more genuine readout. All images were exposed for the same amount of time.

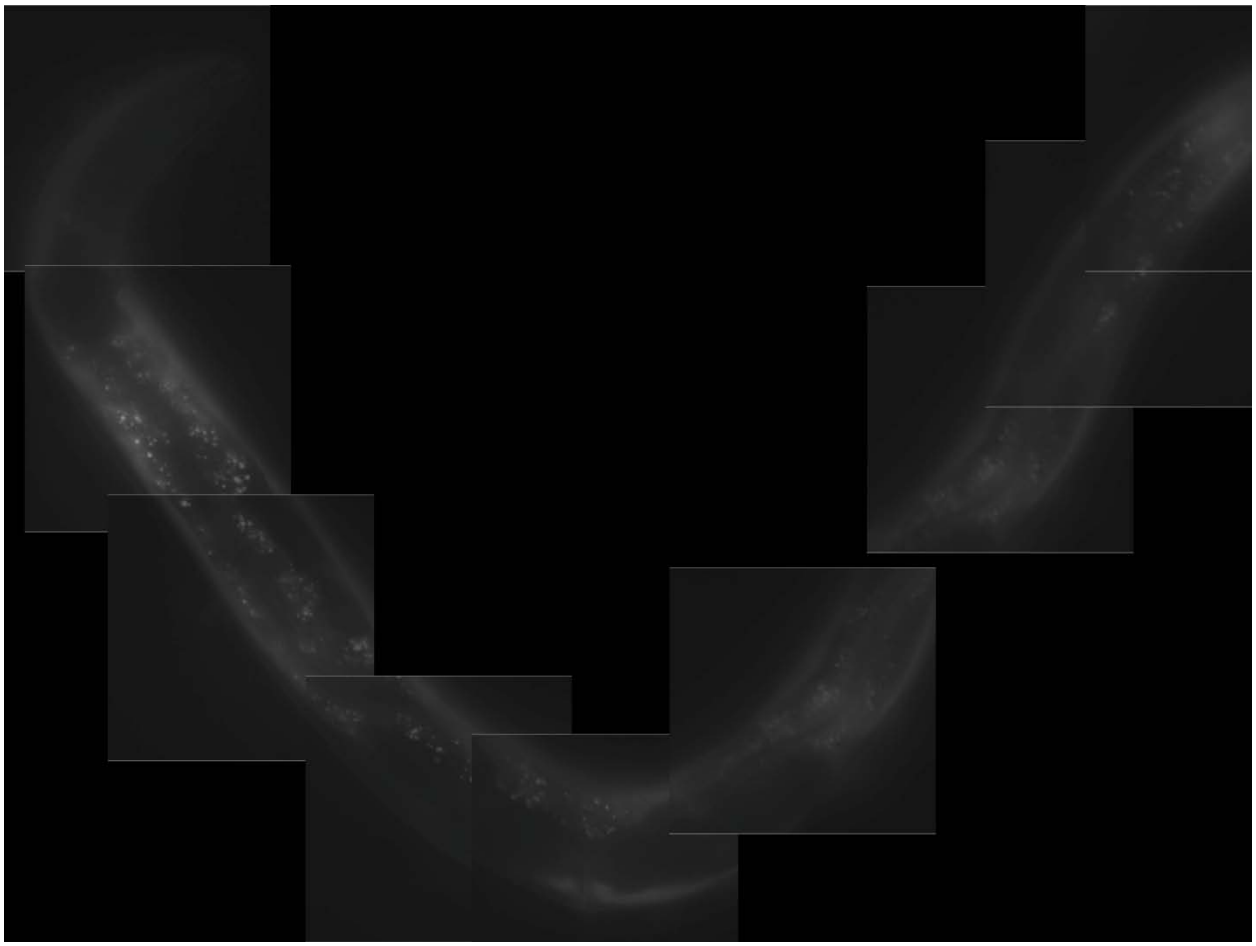

Figure 3.8: *eri-9p::gfp* transcriptional fusion expression – whole worm

All stitched images were exposed for the same amount of time, indicating perhaps that *eri-9* is more highly expressed in the anterior than the posterior. In the absence of the *gfp* marker, there is still robust gut autofluorescence, suggesting noise in the readout.

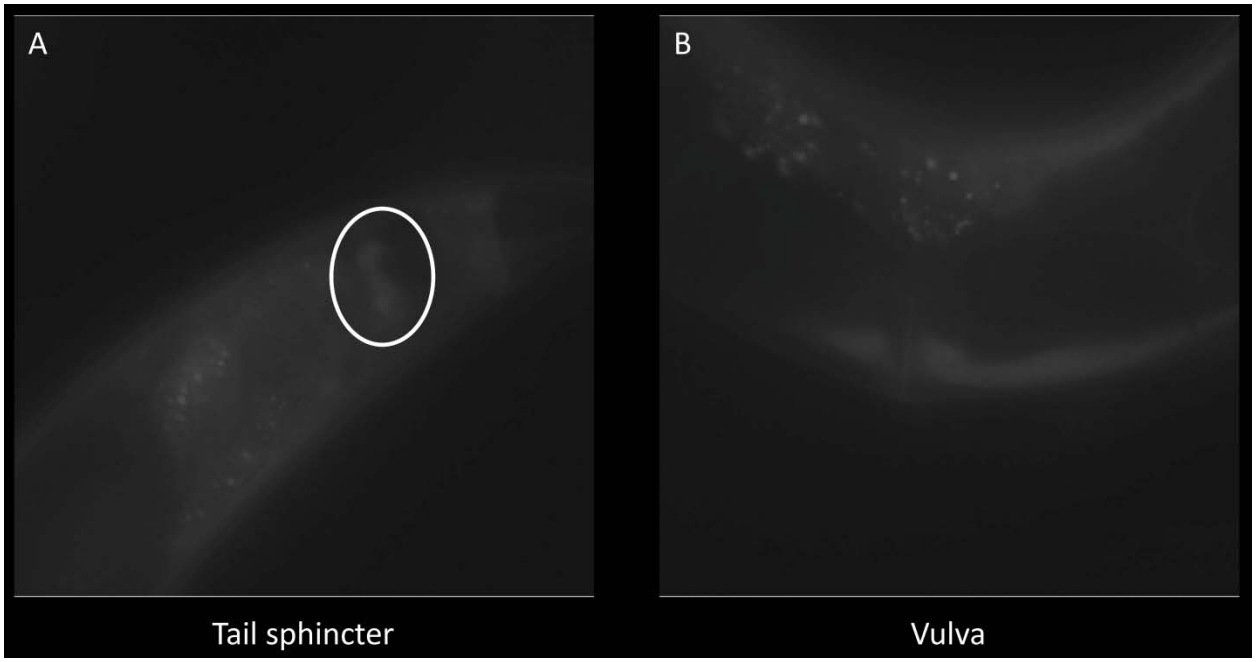

Figure 3.9: *eri-9p::gfp* transcriptional fusion expression – parts

There is faint *gfp* expression in the tail sphincter cells (**A**, **B**) and the vulva (**C**). In the absence of the *gfp* marker, there is almost no autofluorescence in the tail or vulva, suggesting a more genuine readout. All images were exposed for the same amount of time.

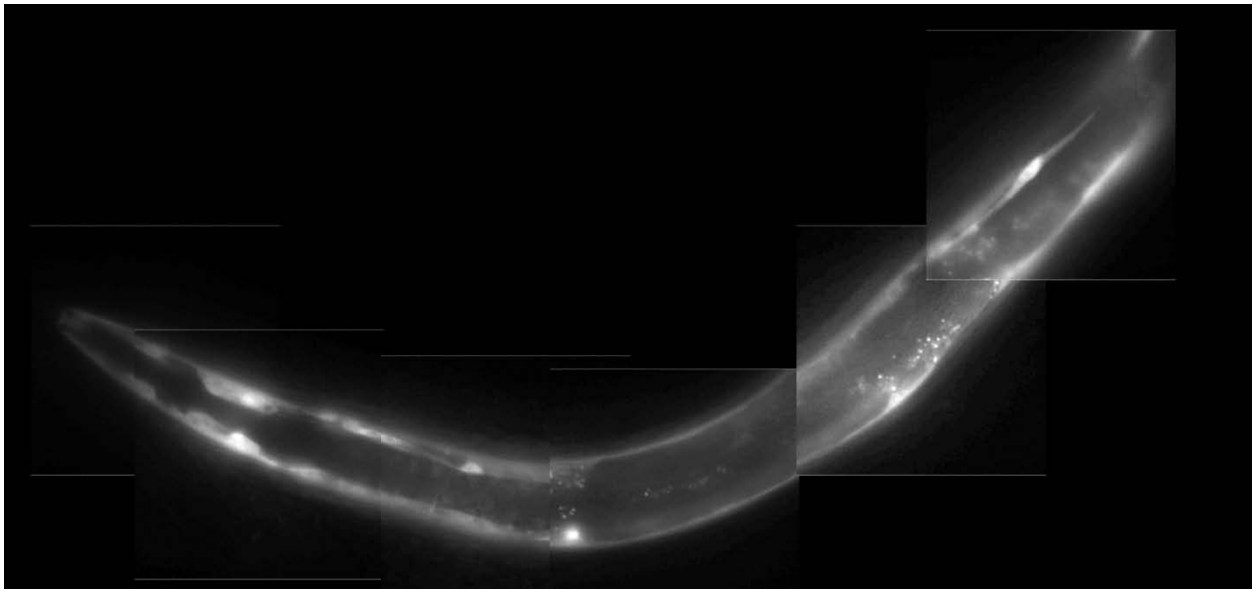

Figure 3.10: *eri-11-gfp* translational fusion expression – whole worm

All stitched images were exposed for the same amount of time, indicating perhaps that *eri-11* is slightly more highly expressed in the posterior than the anterior. In the absence of the *gfp* marker, there is still robust gut autofluorescence, suggesting noise in the readout.

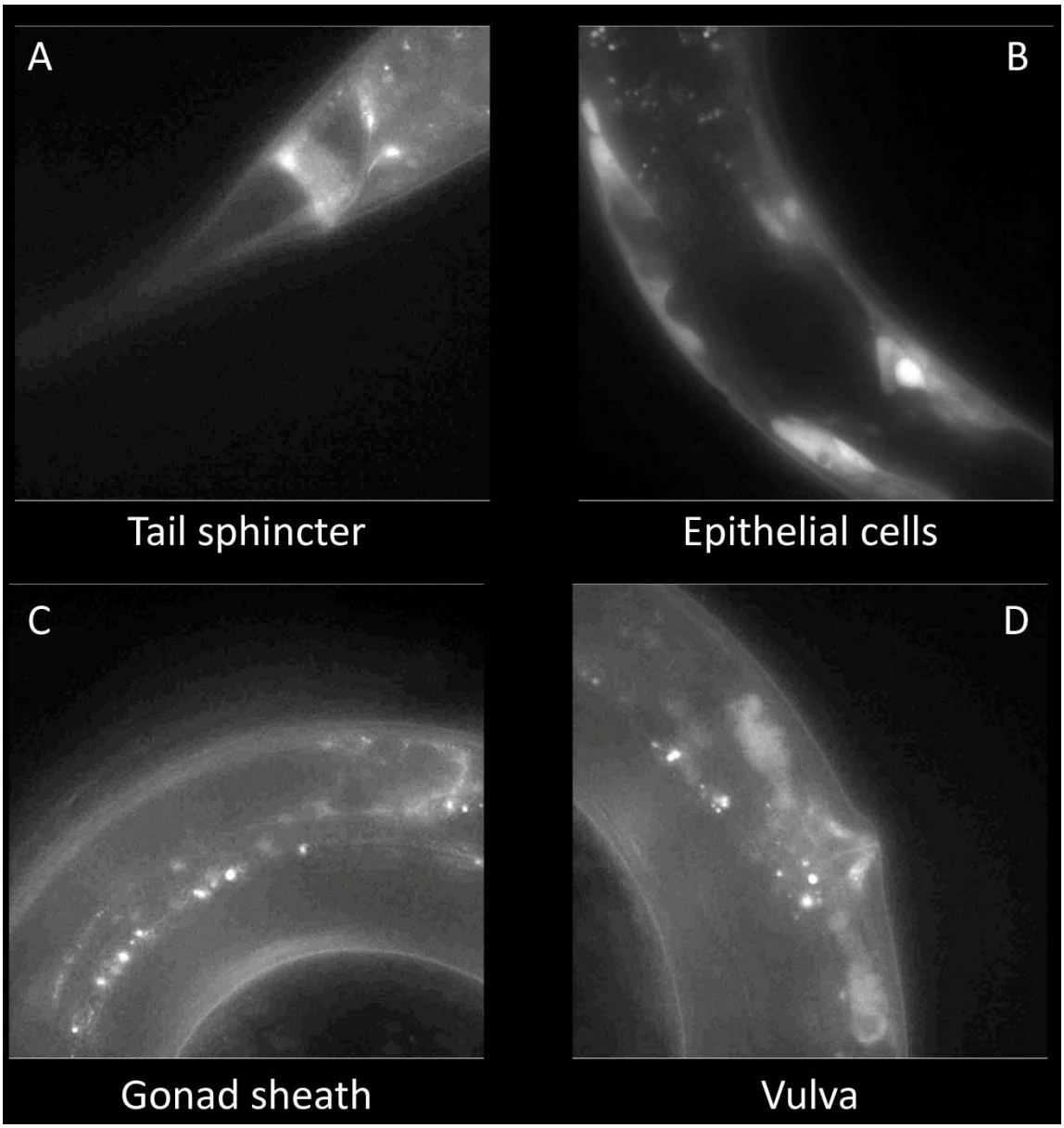

Figure 3.11: *eri-11-gfp* translational fusion expression – parts

There is robust *gfp* expression in the tail sphincter (**A**), some epithelial cells (**B**), and faint expression in the gonad sheath (**C**) and the vulva (**D**), consistent perhaps with the *eri*s' roles in the germline. In the absence of the *gfp* marker, there is almost no autofluorescence in the tail sphincter, epithelial cells, gonad sheaths, and the vulva, suggesting a more genuine readout. All images were exposed for the same amount of time.

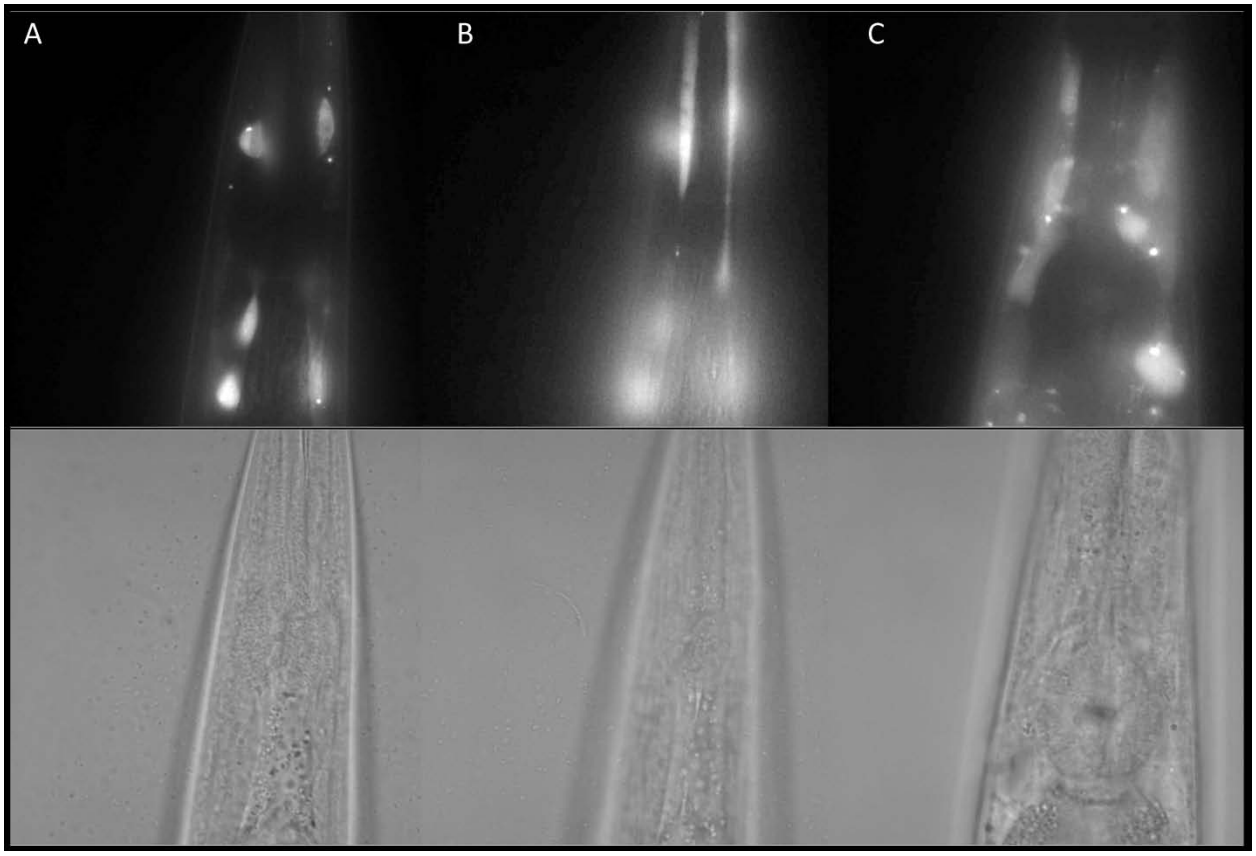

Figure 3.12: *eri-11-gfp* translational fusion expression – pharynx

There is robust *gfp* expression in the pharyngeal support cells (**A**), pharyngeal muscle cells (**B**), and around the bulbs of the pharynx (**C**). In the absence of the *gfp* marker, there is almost no autofluorescence in the pharyngeal area, suggesting a more genuine readout. All images were exposed for the same amount of time.

makes it difficult to compare adjacent *eri(+)* and *eri(-)* cells for discovery of specific transport functions, but to my knowledge this was the first reported expression profile for these genes.

More mosaic rescue lines could potentially generate defined *eri(+)* and *eri(-)* cells. Therefore, future experiments in which such lineage discriminations are possible should perform the following three experiments to discriminate amongst the potential mechanisms of enhanced systemic RNAi as outlined in **Figure 3.5**.

The first future experiment should discriminate mechanism 1 from 2 and those from 3 or 4 (**Figure 3.13**). I would express in an *eri* minus *sid-1* minus animal – which cannot import but can export RNAi signals – hairpin GFP and GFP in all cells, and mosaic rescue with ERI. I will compare level of GFP expression between an *eri*(+) versus *eri*(-) cell. If enhanced RNAi is caused by increased cell autonomous RNAi, then silencing should be lower in *eri*(+) cells. Conversely, if enhanced RNAi is due to enhanced export of silencing signals, then silencing should be higher in *eri*(+) cells because they would retain more silencing signals than *eri*(-) cells. Because this first experiment is performed in a *sid-1*(-) background, *eri* mutants that act via enhancing extracellular transport or import would not be affected by ERI rescue.

The second future experiment should discriminate mechanisms 1 or 4 from 2 or 3 (**Figure 3.14**). I would express in an *eri* minus animal hairpin GFP in one cell type ("sending") that's rescued with ERI, and GFP reporter in a different cell type ("receiving") which is mosaically rescued with ERI. I will compare the level of GFP expression between an *eri*(+) versus an *eri*(-) receiving cell. If enhanced RNAi is caused by increased cell autonomous RNAi, then silencing should be lower in *eri*(+) cells compared to *eri*(-) cells. Similarly, if enhanced RNAi is due to enhanced uptake of silencing signals, then silencing should be lower in *eri*(+) cells compared to *eri*(-) cells. Because this experiment is performed with *eri*(+) sending cells, *eri*

Four Possible Mechanisms of RNAi Enhancement:

1. Increased cell autonomous sensitivity and/or decreasing turnover
2. Increased export
3. Increased extracellular transport
4. Increased uptake

Mosaic Experiment I: Distinguish (1) from (2) and from (3 or 4)

**eri*(-) animal
***sid-1*(-) animal: cannot import, can export
***pfg-gfp* in all cells
*GFP target in all cells
*mosaic rescue ERI
*compare *eri*(+) versus *eri*(-) cells for GFP levels

Anticipated Results:

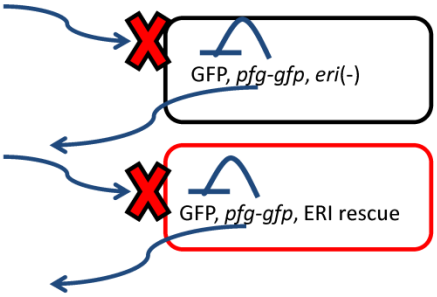

	1	2	3	4
eri(-):	+++	+	++	++
eri(+):	++	++	++	++

Figure 3.13: Schematic of the first hypothetical mosaic analysis experiment, its construct, and its expected results

Wild type baseline silencing of GFP is indicated by "++".

Four Possible Mechanisms of RNAi Enhancement:

1. Increased cell autonomous sensitivity and/or decreasing turnover
2. Increased export
3. Increased extracellular transport
4. Increased uptake

Mosaic Experiment II: Distinguish (1 or 4) from (2 or 3)

**eri*(-) animal
***pfg-gfp* in cell type 1 – sending cells
*rescue ERI in sending cells
*GFP target in cell type 2 – receiving cells
*mosaic ERI rescue in receiving cells
*compare *eri*(+) versus *eri*(-) receiving cells for GFP levels

Anticipated Results:

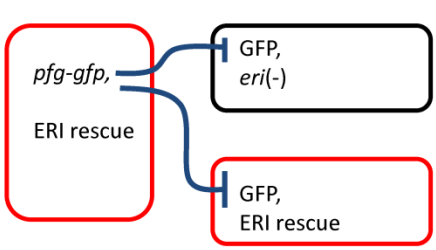

	1	2	3	4
eri(-):	+++	++	++	+++
eri(+):	++	++	++	++

Figure 3.14: Schematic of the second hypothetical mosaic analysis experiment, its construct, and its expected results

Wild type baseline silencing of GFP is indicated by "++".

mutants that act via enhancing export would not be affected by receiving cell ERI rescue. Similarly, because there is always expression of wild-type ERI somewhere in the animal in this experiment, *eri* mutants that act via enhancing extracellular transport would not be affected by receiving cell ERI rescue.

The third future experiment should discriminate mechanisms 1 or 4 from 2 and from 3 (**Figure 3.15**). I would express in an *eri* minus animal hairpin *gfp* in one cell type ("sending"), and *gfp* reporter in a different cell type ("receiving") which is mosaically rescued with ERI. I will compare the level of *gfp* expression between an *eri*(+) versus an *eri*(-) receiving cell. If enhanced RNAi is caused by increased cell autonomous RNAi, then silencing should be lower in *eri*(+) cells compared to *eri*(-) cells. Similarly, if enhanced RNAi is due to enhanced uptake of silencing signals, then silencing should be lower in *eri*(+) cells compared to *eri*(-) cells. However, because this experiment is performed with *eri*(-) sending cells, if enhanced RNAi is due to enhanced export of silencing signals, then silencing would be higher-than-wild-type regardless of receiving cell ERI rescue. Conversely, because there is always expression of wild-type ERI, upon mosaic rescue, somewhere in the animal in this experiment, *eri* mutants that act via enhancing extracellular transport would not be affected by receiving cell ERI rescue.

Nevertheless, the findings from this screen combined with the previous one are quite promising. Unlike the other *eri* genes, *eri-6/7* was not found in the DCR-1 immunoprecipitation (DUCHAINE *et al.* 2006); and unlike the other *eri* genes, *eri*-3, *eri-9*, and *eri-11* are not widely conserved. These unique features make them appropriate candidates for systemic RNAi enhancers, and perhaps they are regulators for *C. elegans'* especially sensitive systemic RNAi response. Therefore, reverse genetic analysis of systemic gene targets can perhaps utilize these *eri* mutants to optimize knockdown phenotypes.

Four Possible Mechanisms of RNAi Enhancement:

1. Increased cell autonomous sensitivity and/or decreasing turnover
2. Increased export
3. Increased extracellular transport
4. Increased uptake

Mosaic Experiment III: Distinguish (1 or 4) from (2) and from (3)

**eri*(-) animal
***pfg-gfp* in cell type 1 – sending cells
*no ERI rescue in any sending cells; *eri*(-) sending cells
*GFP target in cell type 2 – receiving cells
*mosaic ERI rescue in receiving cells
*compare *eri*(+) versus *eri*(-) receiving cells for GFP levels

Anticipated Results:

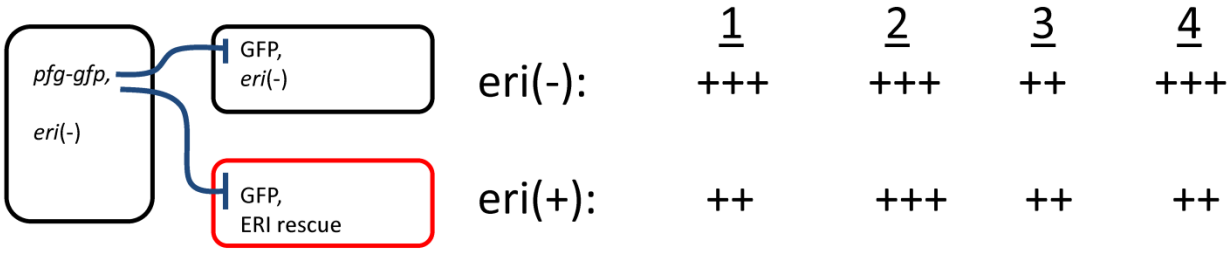

Figure 3.15: Schematic of the third hypothetical mosaic analysis experiment, its construct, and its expected results

Wild type baseline silencing of GFP is indicated by "++".

SCREEN FOR SOMATIC RNAi DEFECTIVE MUTANTS

Previously published screens for Rde mutants have used either RNAi against germline targets (TABARA *et al.* 1999) or relied on transgenes as the initial filter (WINSTON *et al.* 2002; ZHANG *et al.* 2012). Along with my advisor, I designed and taught a discovery-based laboratory course (Harvard College MCB153 Spring 2011) based on a genetic screen for Rde mutants challenged with dsRNA-based RNAi targeting somatic genes.

The students in the course screened 100,000 genomes mutated with EMS grown on *dpy-11(RNAi)* for non-Dpy F2 progeny at 20°C. These starting strain worms also contained *myo-2::pfg-gfp*, *myo-2::gfp*, and *myo-3::gfp* as a confirmation mechanism for ensuring that feeding RNAi phenotypes corresponded with RNAi silencing induced by transgenes. This background also allows easy distinction between Rde or Sid phenotypes.

The class discovered four candidate Rde mutants and one candidate Eri mutant. I followed up the class' analysis and confirmed one of the Rde mutants as insensitive to *bli-1(RNAi)*, *dpy-11(RNAi)*, and *unc-22(RNAi)* by feeding (**Figure 3.16**). Furthermore, there is a lack of *gfp* silencing for both *myo-2*- and *myo-3*- driven *gfp* in this mutant, suggesting that it's likely a true Rde and not a Sid. I also confirmed the Eri mutant as hypersensitive to *hmr-1(RNAi)* by feeding (**Figure 3.17**). I froze and archived the Rde candidate as HC785 and the Eri candidate as HC787 for future in-depth analysis.

This screen suggests that previous screens may not have been saturating in discovering the full landscape of RNAi pathway components. The unique conditions of a somatic RNAi target by feeding RNAi may have had advantages that previous screens did not, thus providing a proof-of-principle that future unique forward genetic screens for RNAi factors remain fruitful endeavors.

Figure 3.16: HC785 is Rde to feeding RNAi assays

Feeding N2 worms OD_{600nm} 3.5, 1.0, and 1.0 *bli-1(RNAi)*, *dpy-11(RNAi)*, *unc-22(RNAi)* induced very penetrant blisters that caused paralysis (**A**), extreme dumpiness (**C**), and muscle emaciation and paralysis (**E**) in N2 wild type worms, respectively. In the HC785 strains containing the candidate Rde mutant, these phenotypes are largely absent when the same RNAi dosages were fed to the worms (**B, D, F**).

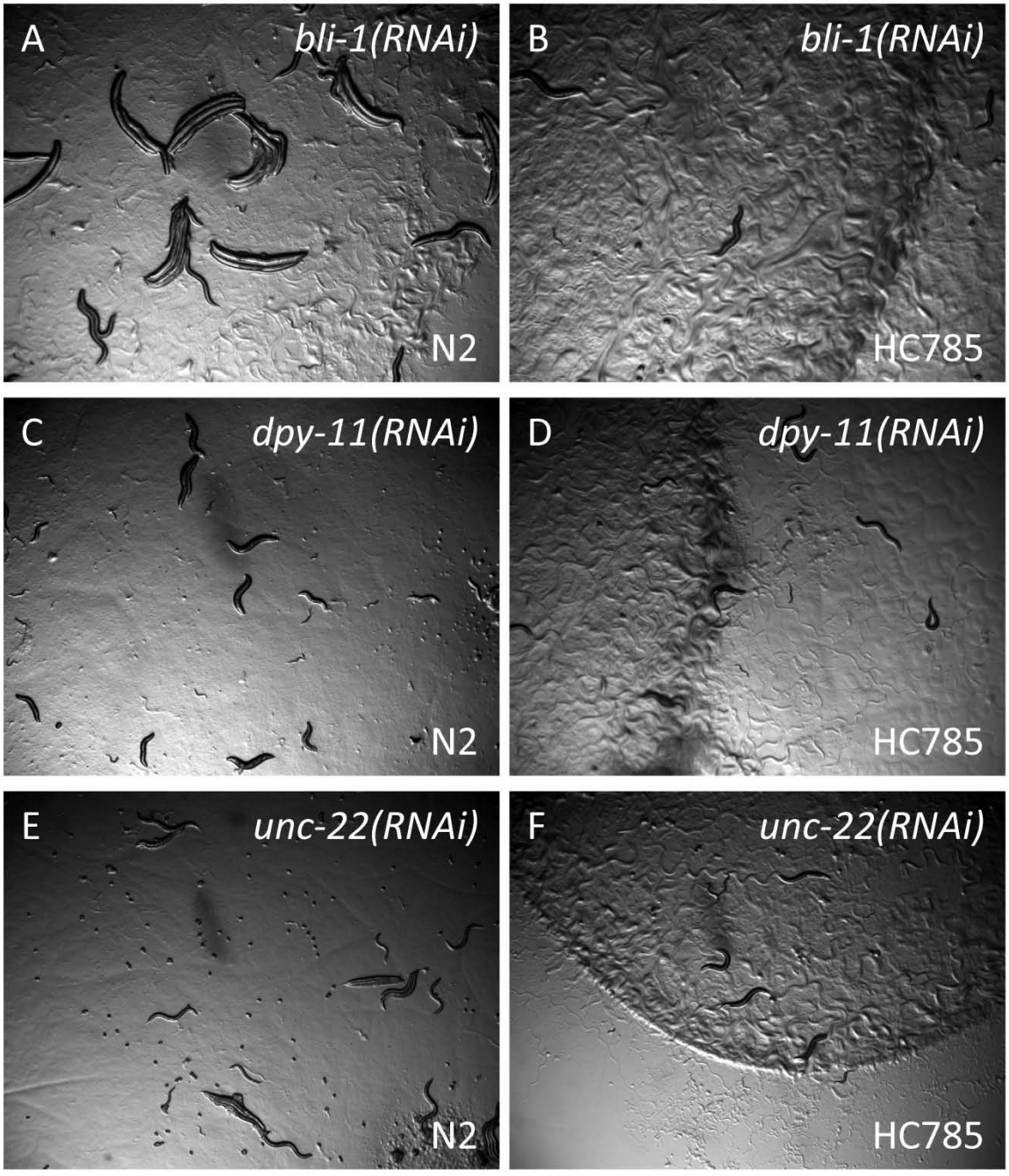

Figure 3.16 (Continued): HC785 is Rde to feeding RNAi assays

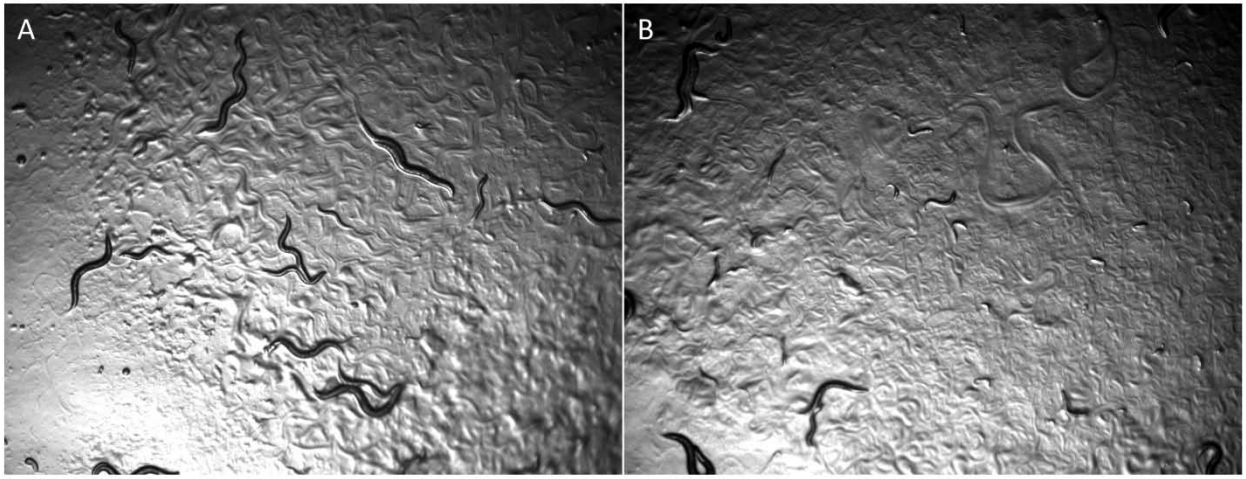

Figure 3.17: HC787 is Eri to *hmr-1* feeding RNAi assay

Feeding N2 worms OD_{600nm} 3.5 *hmr-1(RNAi)* induced no RNAi phenotypes (**A**), but very penetrant developmental delays in HC787 (**B**).

LITERATURE CITED

ALTUN, Z. F., and D. H. HALL, 2005 Seam Cells - postembryonic development of seam cells - cell list, pp. in *WormAtlas*.

BROSNAN, C. A., N. MITTER, M. CHRISTIE, N. A. SMITH, P. M. WATERHOUSE *et al.*, 2007 Nuclear gene silencing directs reception of long-distance mRNA silencing in Arabidopsis. Proceedings of the National Academy of Sciences of the United States of America **104:** 14741-14746.

DUCHAINE, T. F., J. A. WOHLSCHLEGEL, S. KENNEDY, Y. BEI, D. CONTE, JR. *et al.*, 2006 Functional proteomics reveals the biochemical niche of C. elegans DCR-1 in multiple small-RNA-mediated pathways. Cell **124:** 343-354.

DUNOYER, P., C. HIMBER, V. RUIZ-FERRER, A. ALIOUA and O. VOINNET, 2007 Intra- and intercellular RNA interference in Arabidopsis thaliana requires components of the microRNA and heterochromatic silencing pathways. Nature Genetics **39:** 848-856.

DUNOYER, P., C. HIMBER and O. VOINNET, 2005 DICER-LIKE 4 is required for RNA interference and produces the 21-nucleotide small interfering RNA component of the plant cell-to-cell silencing signal. Nat Genet **37:** 1356-1360.

FEINBERG, E. H., and C. P. HUNTER, 2003 Transport of dsRNA into cells by the transmembrane protein SID-1. Science **301:** 1545-1547.

FIRE, A., S. XU, M. K. MONTGOMERY, S. A. KOSTAS, S. E. DRIVER *et al.*, 1998 Potent and specific genetic interference by double-stranded RNA in Caenorhabditis elegans. Nature **391:** 806-811.

FISCHER, S. E., M. D. BUTLER, Q. PAN and G. RUVKUN, 2008 Trans-splicing in C. elegans generates the negative RNAi regulator ERI-6/7. Nature **455:** 491-496.

GRISHOK, A., J. L. SINSKEY and P. A. SHARP, 2005 Transcriptional silencing of a transgene by RNAi in the soma of C. elegans. Genes Dev **19:** 683-696.

HIMBER, C., P. DUNOYER, G. MOISSIARD, C. RITZENTHALER and O. VOINNET, 2003 Transitivity-dependent and -independent cell-to-cell movement of RNA silencing. Embo Journal **22:** 4523-4533.

KENNEDY, S., D. WANG and G. RUVKUN, 2004 A conserved siRNA-degrading RNase negatively regulates RNA interference in C. elegans. Nature **427:** 645-649.

KETTING, R. F., T. H. A. HAVERKAMP, H. G. A. M. VAN LUENEN and R. H. A. PLASTERK, 1999 mut-7 of C-elegans, required for transposon silencing and RNA interference, is a homolog of Werner syndrome helicase and RNaseD. Cell **99:** 133-141.

KNIGHT, S. W., and B. L. BASS, 2001 A role for the RNase III enzyme DCR-1 in RNA interference and germ line development in Caenorhabditis elegans. Science **293:** 2269-2271.

KNIGHT, S. W., and B. L. BASS, 2002 The role of RNA editing by ADARs in RNAi. Mol Cell **10:** 809-817.

LEHNER, B., A. CALIXTO, C. CROMBIE, J. TISCHLER, A. FORTUNATO *et al.*, 2006 Loss of LIN-35, the Caenorhabditis elegans ortholog of the tumor suppressor p105Rb, results in enhanced RNA interference. Genome Biology **7**.

PAVELEC, D. M., J. LACHOWIEC, T. F. DUCHAINE, H. E. SMITH and S. KENNEDY, 2009 Requirement for the ERI/DICER complex in endogenous RNA interference and sperm development in Caenorhabditis elegans. Genetics **183:** 1283-1295.

SCHWACH, F., F. E. VAISTIJ, L. JONES and D. C. BAULCOMBE, 2005 An RNA-dependent RNA polymerase prevents meristem invasion by potato virus X and is required for the activity but not the production of a systemic silencing signal. Plant Physiology **138:** 1842-1852.

SIMMER, F., M. TIJSTERMAN, S. PARRISH, S. P. KOUSHIKA, M. L. NONET *et al.*, 2002 Loss of the putative RNA-directed RNA polymerase RRF-3 makes C. elegans hypersensitive to RNAi. Curr Biol **12:** 1317-1319.

SMITH, L. M., O. PONTES, L. SEARLE, N. YELINA, F. K. YOUSAFZAI *et al.*, 2007 An SNF2 protein associated with nuclear RNA silencing and the spread of a silencing signal between cells in Arabidopsis. Plant Cell **19:** 1507-1521.

TABARA, H., M. SARKISSIAN, W. G. KELLY, J. FLEENOR, A. GRISHOK *et al.*, 1999 The rde-1 gene, RNA interference, and transposon silencing in C. elegans. Cell **99:** 123-132.

TIJSTERMAN, M., K. L. OKIHARA, K. THIJSSEN and R. H. A. PLASTERK, 2002 PPW-1, a PAZ/PIWI protein required for efficient germline RNAi, is defective in a natural isolate of C-elegans. Current Biology **12:** 1535-1540.

VOINNET, O., 2008 Use, tolerance and avoidance of amplified RNA silencing by plants. Trends in Plant Science **13:** 317-328.

WANG, D., S. KENNEDY, D. CONTE, JR., J. K. KIM, H. W. GABEL *et al.*, 2005 Somatic misexpression of germline P granules and enhanced RNA interference in retinoblastoma pathway mutants. Nature **436:** 593-597.

WINSTON, W. M., C. MOLODOWITCH and C. P. HUNTER, 2002 Systemic RNAi in C. elegans requires the putative transmembrane protein SID-1. Science **295:** 2456-2459.

WU, X., Z. SHI, M. CUI, M. HAN and G. RUVKUN, 2012 Repression of germline RNAi pathways in somatic cells by retinoblastoma pathway chromatin complexes. PLoS Genet **8:** e1002542.

YOO, B. C., F. KRAGLER, E. VARKONYI-GASIC, V. HAYWOOD, S. ARCHER-EVANS *et al.*, 2004 A systemic small RNA signaling system in plants. Plant Cell **16:** 1979-2000.

ZHANG, C., T. A. MONTGOMERY, S. E. FISCHER, S. M. GARCIA, C. G. RIEDEL *et al.*, 2012 The Caenorhabditis elegans RDE-10/RDE-11 complex regulates RNAi by promoting secondary siRNA amplification. Curr Biol **22:** 881-890.

ZHANG, C., T. A. MONTGOMERY, H. W. GABEL, S. E. FISCHER, C. M. PHILLIPS *et al.*, 2011 mut-16 and other mutator class genes modulate 22G and 26G siRNA pathways in Caenorhabditis elegans. Proc Natl Acad Sci U S A **108:** 1201-1208.

ZHUANG, J. J., and C. P. HUNTER, 2011 Tissue Specificity of Caenorhabditis elegans Enhanced RNA Interference Mutants. Genetics **188:** 235-237.

Chapter Four

Enhanced RNAi is dependent on *nrde-3*

The contents are a part of the in-press report ZHUANG, J. J., S.A. BANSE, and C. P. HUNTER, 2013. The Nuclear Argonaute NRDE-3 Contributes to Transitive RNAi in *Caenorhabditis elegans*. *Genetics* **doi: 10.1534/genetics. 113.149765**. Portions of the transitive RNAi studies were performed in collaboration with Dr. Stephen A. Banse, as denoted. Permission to reuse was granted by the Genetics Society of America.

ABSTRACT

The *Caenorhabditis elegans* nuclear RNAi defective (Nrde) mutants were identified by their inability to silence polycistronic transcripts in enhanced RNAi (Eri) mutant backgrounds. Here, we report additional *nrde-3*-dependent RNAi phenomena that extend the mechanisms, roles, and functions of nuclear RNAi. We show that *nrde-3* mutants are broadly RNAi deficient and that over-expressing NRDE-3 enhances RNAi. Consistent with NRDE-3 being a dose-dependent limiting resource for effective RNAi, we find that NRDE-3 is required for *eri*-dependent enhanced RNAi phenotypes, although only for a subset of target genes. These results suggest that *nrde-3* define a limiting RNAi resource pathway. Limiting RNAi resources are proposed to primarily act via endogenous RNA silencing pathways. Consistent with this, we find that *nrde-3* mutants mis-express genes regulated by endogenous siRNAs and incompletely silence repetitive transgene arrays. Finally, we find that *nrde-3* contributes to transitive RNAi, whereby amplified silencing triggers act *in trans* to silence sequence-similar genes. Because *nrde*-dependent silencing is thought to act *in cis* to limit the production of primary transcripts, this result reveals an unexpected role for nuclear processes in RNAi silencing.

INTRODUCTION

Genetic analysis of RNA interference (RNAi) in *C. elegans* initially identified and characterized genes and activities important for post-transcriptional gene silencing (PTGS) in response to exogenous double-stranded RNA (dsRNA) (TABARA *et al.* 1999; TABARA *et al.* 2002). Because these gene products target mature mRNAs, they were presumed to act in the cytoplasm (FIRE *et al.* 1998). However, a genetic screen for mutants specifically defective for pan-operon RNAi silencing (BOSHER *et al.* 1999) identified genes important for transcriptional gene silencing

(TGS) processes that operate in the nucleus (BURKHART *et al.* 2011; BURTON *et al.* 2011; GUANG *et al.* 2010; GUANG *et al.* 2008). These genes were termed nuclear RNAi defective (*nrde*).

The best-characterized *nrde* is NRDE-3, an Argonaute that shuttles secondary short-interfering RNAs (siRNAs) from the cytoplasm to the nucleus (GUANG *et al.* 2008). When siRNA are absent or reduced, NRDE-3 is primarily detected in the cytoplasm, and when siRNAs are abundant, NRDE-3 is readily detected in the nucleus. In the nucleus, the siRNA-bound NRDE-3 forms a complex with the nuclear restricted NRDE-1, 2, and 4 (BURTON *et al.* 2011). The associated siRNA guides the NRDE-complex to cognate nascent mRNA transcripts, which impedes RNA polymerase II transcription elongation and further initiates histone methylation dependent TGS (BURTON *et al.* 2011; GUANG *et al.* 2010). This RNA-directed epigenetic mechanism also enables multi-generational silencing (GU *et al.* 2012); the recently identified germline nuclear Argonaute HRDE-1 functions like the soma-restricted NRDE-3 to enable this multigenerational silencing (BUCKLEY *et al.* 2012). *hrde-1* is also important for germline immortality. As these enlightening studies on mechanisms and downstream endogenous roles of nuclear RNAi have progressed, broader identification of other nuclear RNAi dependent upstream processes and their interactions with cytoplasmic RNAi therefore becomes ever more important.

Enhanced RNAi (Eri) mutant backgrounds have been important for the discovery and characterization of *nrde* functions. Eri mutants identify genes important for the production or stability of endogenous short-interfering RNAs (endo-siRNAs) (DUCHAINE *et al.* 2006; FISCHER *et al.* 2008; KENNEDY *et al.* 2004; PAVELEC *et al.* 2009; SIMMER *et al.* 2002). Genes complementary to endo-siRNAs are mis-regulated in Eri mutants (GENT *et al.* 2010). Interestingly, these endo-siRNAs also make up the bulk of siRNAs associated with NRDE-3 *in vivo* (GUANG *et al.* 2008). Thus, a role for *nrde-3* in the enhanced RNAi silencing associated

with the *eri* mutants is expected, although the scope and significance of this role has not been investigated.

Here, we report our identification of additional *nrde-3*-dependent processes. We define a significant and broad contribution of *nrde-3* to exogenous RNAi silencing and determine that NRDE-3 is a distinct limiting RNAi resource. As expected, *nrde-3* is important for enhanced RNAi phenotypes, but unexpectedly only for a subset of targeted genes. We also provide evidence that *nrde-3* is important for endo-siRNA regulated gene expression and multi-copy transgene silencing. Finally, we show that *nrde-3* contributes to transitive RNAi, revealing an unexpected role for nuclear processes in exogenous RNAi.

RESULTS

Nuclear RNAi mutants are broadly deficient for dsRNA-induced silencing

RNAi effectiveness in wild-type animals is dependent on dsRNA dose. Consequently, high concentrations of dsRNA can compensate for, or mask, weak RNAi-defective (Rde) phenotypes (ZHUANG and HUNTER 2011). To determine whether *nrde-3* mutants have a weak Rde phenotype when dsRNA is limiting, we measured RNAi efficacy in *nrde-3* mutants in response to a dsRNA dilution series. We found that the silencing responses to *dpy-11(RNAi), par-1(RNAi)*, *qua-1(RNAi)*, and *unc-22(RNAi)* were significantly reduced in *nrde-3(gg66)* mutants (**Figure 4.1A; Tables 4.1, 4.2, 4.3**). Because reduced RNAi efficacy could be caused by background mutations (ZHANG *et al.* 2011), we confirmed the above results with a second *nrde-3* allele, *gg64*, (**Figure 4.2; Table 4.3**) and showed that an *nrde-3-gfp* transgene construct completely rescued the RNAi defects (**Figure 4.2**). Therefore, in addition to RNAi targeting operons, *nrde-3* is also required for efficient RNAi targeting conventionally transcribed and processed genes. However, RNAi

Figure 4.1: *nrde-3* is required for robust exogenous RNAi

(A) The penetrance of *dpy-11(RNAi)* relative to dose of feeding RNAi bacteria for the indicated strains is shown. The progeny of L3 larvae placed on the RNAi food were scored as L4 larvae. **(B)** Schematic of trans-generational RNAi assay. Dpy or Unc L4 larvae grown on either *dpy-11* or *unc-22* dsRNA expressing bacteria were transferred to non-RNAi bacteria. The non-exposed progeny were scored for Dpy-11 or Unc-22 phenotypes as L4 larvae. **(C-F)** The fraction of N2 and *nrde-3(gg66)* broods that transmitted *dpy-11(RNAi)* (**C**) or *unc-22(RNAi)* (**E**) silencing to non-exposed progeny and the penetrance of the Dpy **(D)** and Unc **(F)** phenotypes within individual N2 and *nrde-3(gg66)* broods. **(G-I)** The penetrance of Dpy phenotypes within individual broods from the indicated crosses. **(J)** The penetrance of *dpy-11(RNAi)* relative to dose of feeding RNAi bacteria for the indicated strains is shown. Embryos from unexposed mothers hatched in the presence of RNAi food and were scored as L4 larvae. The phenotypes scored for all assays are listed in **Table S1**. The *dpy-11(RNAi)* bacteria OD_{600nm}=2.0 and the *unc-22(RNAi)* bacteria OD_{600nm}=1.0. The numbers of animals scored for **(A)** and **(J)** are listed in **Table S2**. *p*-values calculated by *t*-test; * indicates $p<0.05$ and ** indicates $p<0.01$.

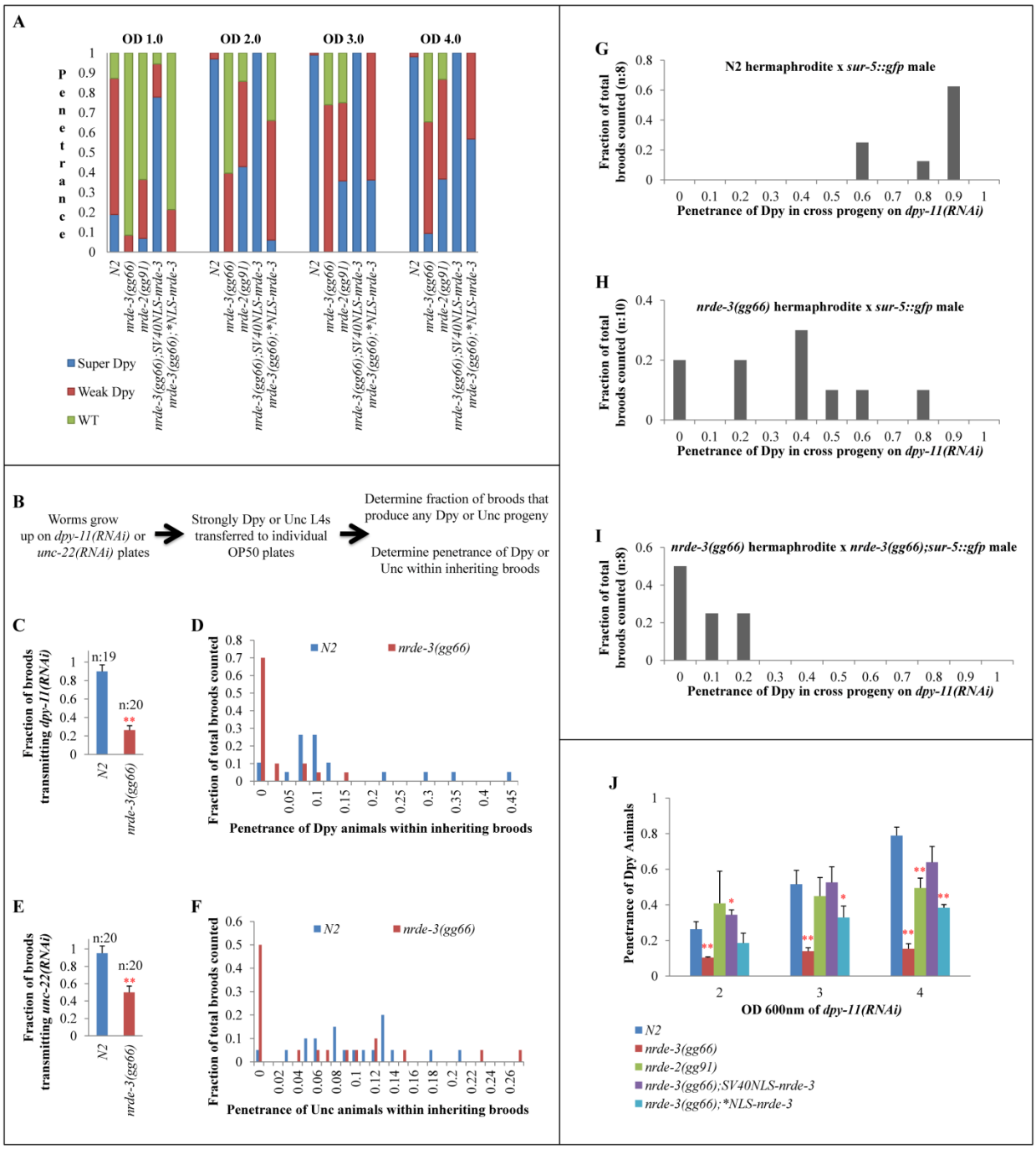

Figure 4.1 (Continued): *nrde-3* is required for robust exogenous RNAi

Table 4.1: Phenotypes and expressivities scored in various RNAi assays

RNAi Target	Phenotype Scored
dpy-11	-Super dumpy: severely dumpy animals whose length is at most 3X its width -Weak dumpy: mildly dumpy animals at most 80% the length of N2 worms *When not specified, both categories are scored as dumpy
dpy-13	I: no phenotype II: very slightly shorter than wild type animals (much less severe than *dpy-11* weak dumpy; see **Figure 4.6A**) III: Severely dumpy animals whose length is at most 3X its width
dpy-28	Mildly dumpy animals at most 80% the length of N2 worms
elt-1	-Embryonic lethal: dead embryos -Developmental defect: arrested larval growth and deformed tail morphologies
hmr-1	Dead embryos and animals with significantly smaller in morphology and head deformities
ifc-2	Bent posterior body morphology that paralyzes locomotion
lir-1	I: no phenotype, normal growth II: arrest during L1/L2 III: embryonic lethality
myo-3	Paralyzed worms with rigid columnar body morphologies
par-1	Dead embryos
qua-1	Abnormally rigid body morphology and paralyzed movement
unc-15	I: no phenotype, normal movement II: paralyzed movement III: abnormally rigid body morphology and paralyzed movement
unc-22	Abnormally rigid body morphology and paralyzed movement and/or twitching upon 10mM levamisole treatment
unc-73	Paralysis with bulging and curled body morphology

These phenotypes are the basis for the various penetrance recordings in all figures and tables for the indicated genes targeted by feeding RNAi assays. For representative phenotypes scored for *dpy-11(RNAi)*, *dpy-13(RNAi)*, and *ifc-2(RNAi)*, see **Figures 4.2, 4.3,** and **4.6**.

Table 4.2: n-values for *dpy-11(RNAi)* Rde penetrance for various strains shown in **Figure 4.1A, J**

Assay	OD_{600nm}	Strain	Number Tested
Feed from L3 (4.1A)	1.0	N2	117
Feed from L3 (4.1A)	1.0	*nrde-3(gg66)*	119
Feed from L3 (4.1A)	1.0	*nrde-2(gg91)*	44
Feed from L3 (4.1A)	1.0	*nrde-3(gg66); SV40NLS-nrde-3*	72
Feed from L3 (4.1A)	1.0	*nrde-3(gg66); *NLS-nrde-3*	61
Feed from L3 (4.1A)	2.0	N2	98
Feed from L3 (4.1A)	2.0	*nrde-3(gg66)*	91
Feed from L3 (4.1A)	2.0	*nrde-2(gg91)*	28
Feed from L3 (4.1A)	2.0	*nrde-3(gg66); SV40NLS-nrde-3*	50
Feed from L3 (4.1A)	2.0	*nrde-3(gg66); *NLS-nrde-3*	50
Feed from L3 (4.1A)	3.0	N2	93
Feed from L3 (4.1A)	3.0	*nrde-3(gg66)*	69
Feed from L3 (4.1A)	3.0	*nrde-2(gg91)*	56
Feed from L3 (4.1A)	3.0	*nrde-3(gg66); SV40NLS-nrde-3*	42
Feed from L3 (4.1A)	3.0	*nrde-3(gg66); *NLS-nrde-3*	47
Feed from L3 (4.1A)	4.0	N2	104
Feed from L3 (4.1A)	4.0	*nrde-3(gg66)*	75
Feed from L3 (4.1A)	4.0	*nrde-2(gg91)*	30
Feed from L3 (4.1A)	4.0	*nrde-3(gg66); SV40NLS-nrde-3*	60
Feed from L3 (4.1A)	4.0	*nrde-3(gg66); *NLS-nrde-3*	37
Bleached embryo (4.1J)	2.0	N2	259
Bleached embryo (4.1J)	2.0	*nrde-3(gg66)*	203
Bleached embryo (4.1J)	2.0	*nrde-2(gg91)*	164
Bleached embryo (4.1J)	2.0	*nrde-3(gg66); SV40NLS-nrde-3*	170
Bleached embryo (4.1J)	2.0	*nrde-3(gg66); *NLS-nrde-3*	190
Bleached embryo (4.1J)	3.0	N2	255
Bleached embryo (4.1J)	3.0	*nrde-3(gg66)*	215
Bleached embryo (4.1J)	3.0	*nrde-2(gg91)*	238
Bleached embryo (4.1J)	3.0	*nrde-3(gg66); SV40NLS-nrde-3*	191
Bleached embryo (41J)	3.0	*nrde-3(gg66); *NLS-nrde-3*	159
Bleached embryo (4.1J)	4.0	N2	280
Bleached embryo (4.1J)	4.0	*nrde-3(gg66)*	178
Bleached embryo (4.1J)	4.0	*nrde-2(gg91)*	201
Bleached embryo (4.1J)	4.0	*nrde-3(gg66); SV40NLS-nrde-3*	238
Bleached embryo (4.1J)	4.0	*nrde-3(gg66); *NLS-nrde-3*	177

Table 4.3: Penetrance readings for *nrde-3*'s decreased RNAi response of *gg64* and *gg66* alleles to various RNAi targets

RNAi Target	Method of RNAi	N2	*nrde-3 (gg66)*	*nrde-3 (gg64)*
dpy-11	Feed L3 of mom	0.93 n=28	**Figure 4.1A**	0.08 n=13
par-1	Feed L3 of mom	1.00 n=35	0.86 n=190	
qua-1	Feed L3 of mom	0.65 n=52	0.11 n=46	
unc-22	Feed L3 of mom	0.95 n=20	0.43 n=14	
qua-1	Bleached embryos	0.69 n=89	0.47 n=183	

Single L3-stage larvae ("feed L3 of mom") or bleached embryos were placed on RNAi food targeting *dpy-11* (at OD_{600nm} 1.0), *par-1* (at OD_{600nm} 1.0), *qua-1* (at OD_{600nm} 1.0), and *unc-22* (at OD_{600nm} 2.0); 4 days later, the percent of progeny showing the expected phenotypes described in **Table 4.1** were determined for the listed strains.

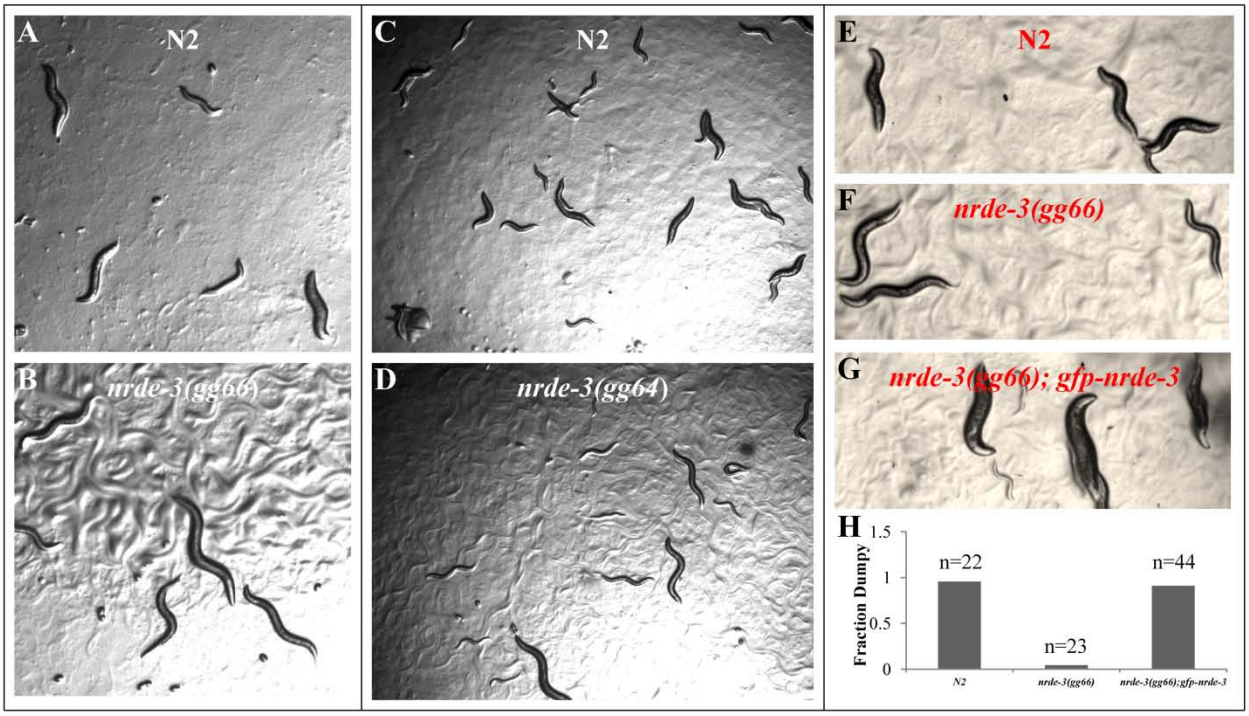

Figure 4.2: *nrde-3(gg64)* is Rde to *dpy-11(RNAi)* and *nrde-3(gg66)* is rescued by *nrde-3-gfp*

(A-B) Representative images of **(A)** wild type (N2) and **(B)** *nrde-3(gg66)* progeny from L3 hermaphrodites grown on *dpy-11(RNAi)* RNAi bacteria at OD_{600nm} 1.0. N2 worms were more sensitive to *dpy-11(RNAi)* by feeding than *nrde-3(gg66)* worms were. Penetrance differences between the strains are shown in **Figure 4.1A** and **Table 4.2**. **(C-D)** Representative images of **(C)** N2 wild type and **(D)** *nrde-3*(*gg64)* progeny from L3 hermaphrodites grown on *dpy-11(RNAi)* RNAi bacteria at OD_{600nm} 1.0. N2 worms were more sensitive to *dpy-11(RNAi)* by feeding than *nrde-3(gg66)* worms were. Penetrance differences between the strains are shown in **Table 4.3**. **(E-G)** Representative images of **(E)** N2 wild type, **(F)** *nrde-3*(*gg66)*, and **(G)** *nrde-3*(*gg66); nrde-3-gfp* progeny from L3 hermaphrodites grown on *dpy-11(RNAi)* RNAi bacteria at OD_{600nm} 1.0. Fewer *nrde-3(gg66)* animals are dumpy compared to N2 and *nrde-3*(*gg66); nrde-3-gfp* animals treated with the same dosage of dsRNA. **(H)** The penetrance of *dpy-11(RNAi)*'s expected phenotype described in **(E-G)** are indicated.

remains effective in *nrde-3* mutant backgrounds when the trigger dsRNA is not limiting (**Figure 4.1A**), indicating that nuclear-dependent RNAi silencing is particularly important when dsRNA is limited.

NRDE-3 is an Argonaute that has been proposed to shuttle siRNA from the cytoplasm to the nucleus where they associate with nuclear restricted factors, including NRDE-2, to effect transcriptional gene silencing (BURTON *et al.* 2011; GUANG *et al.* 2010).To determine whether these broad RNAi deficiencies reveal an undetected role for NRDE-3 in the cytoplasm, we similarly tested *nrde-2(gg91)* mutants. The results show that NRDE-2 is similarly required for an efficient response to exogenous RNAi (**Figure 4.1A, 4.3; Table 4.2**). Because NRDE-2 is thought to be completely nuclear localized (BURTON *et al.* 2011), these results support a nuclear-acting step for efficient exogenous RNAi. To provide additional support for this conclusion, we compared the rescue of *nrde-3(gg66)* mutant animals by *nrde-3-gfp* transgene constructs that either lack a nuclear localization signal ("**NLS-nrde-3*") or in which the NRDE-3 NLS has been replaced with a *Simian virus 40* nuclear localization signal ("*SV40NLS-nrde-3*") (GUANG *et al.* 2008). We found that the **NLS-nrde-3* construct failed to rescue the *nrde-3(gg66)* RNAi defect, while the *SV40NLS-nrde-3* construct provided at least a wild-type response to *dpy-11(RNAi)* (**Figure 4.1A**). These results show that nuclear localized activities broadly contribute to RNAi triggered by exogenous dsRNA.

nrde-3 contributes to inter- and intra-generational responses to exogenous RNAi

The *nrde* genes have recently been implicated in the transmission of silencing to the progeny (BURTON *et al.* 2011; GU *et al.* 2012). A remarkable feature of RNAi in *C. elegans* is that silencing initiated in the mother can be efficiently transmitted via the germline to the progeny,

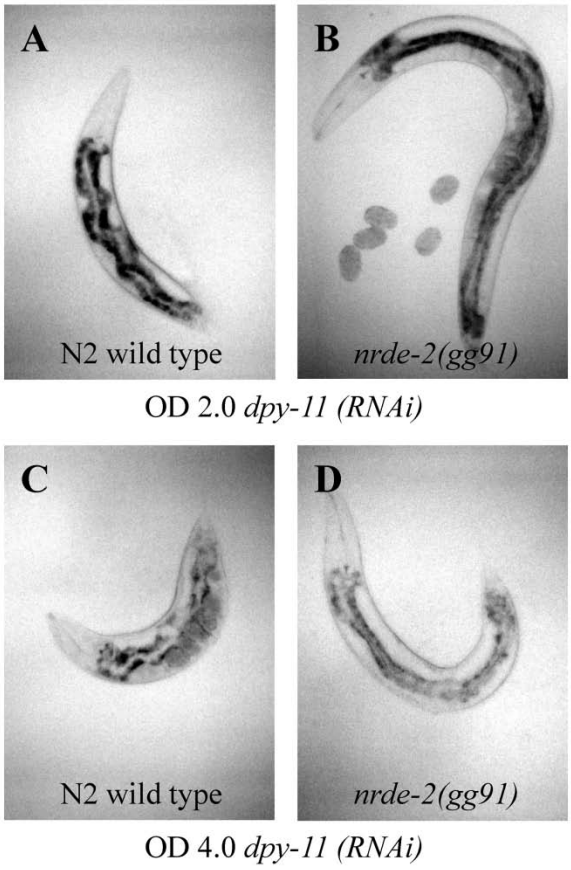

Figure 4.3: *nrde-2(gg91)* is less sensitive to *dpy-11(RNAi)* than N2

Representative images of N2 and *nrde-2*(*gg91)* from L3 hermaphrodites grown on *dpy-11(RNAi)* RNAi bacteria at OD_{600nm} 2.0 (**(A)** & **(B)**) and at OD_{600nm} 4.0 (**(D)** & **(E)**). Fewer *nrde-2(gg91)* animals are dumpy compared to N2 animals treated with the same dosage of dsRNA, although the difference is markedly larger at OD_{600nm} 2.0. The penetrance of *dpy-11(RNAi)*'s expected phenotype is shown in **Figure 4.1A** and **Table 4.2**.

and once established, can persist for at least 80 generations (VASTENHOUW *et al.* 2006). Analysis of this multigenerational silencing demonstrated that PTGS mechanisms are required to initiate silencing, and implicated TGS mechanisms in its maintenance (GRISHOK *et al.* 2000). The most convenient methods for performing exogenous RNAi in *C. elegans* involve exposing both the mother and her progeny to the silencing trigger: i.e. feeding dsRNA-expressing *E. coli* to a mother and scoring her progeny brood for phenotypes on that same plate. Therefore, the requirement for *nrde* function for efficient silencing (**Figure 4.1A**) may reflect a requirement for TGS-dependent maintenance mechanisms in the progeny rather than PTGS mechanisms in the mother. To investigate whether *nrde-3* function is required in the mother or the progeny for silencing, we exposed either mothers or their progeny to the dsRNA trigger, and compared in both cases RNAi silencing efficiency in the progeny.

First, we asked whether *nrde-3* is important for transmission of silencing from dsRNA-exposed mothers to non-exposed progeny. Specifically, we grew wild-type and *nrde-3(gg66)* worms from hatching to the fourth larval stage (L4) on either *dpy-11* or *unc-22* dsRNA expressing bacteria. We then transferred the RNAi-affected Dpy or Unc L4 worms to control bacteria and scored their non-exposed progeny for Dpy-11 or Unc-22 phenotypes (**Figure 4.1B**). We found that the fraction of broods inheriting RNAi silencing was two-to-four-fold higher in the wild-type background (**Figure 4.1C, E; Table 4.4**). Furthermore, the penetrance of Dpy or Unc within each RNAi-inheriting brood was also higher in the wild-type background (**Figure 4.1D, F; Table 4.4**). Thus, in the absence of continued exposure to the dsRNA trigger, NRDE-3 is important for the transmission of RNAi silencing.

We next asked whether introducing wild-type NRDE-3 to the progeny of *nrde-3(gg66)* mothers could restore the penetrance of the inherited silencing. Specifically, we crossed dsRNA-

Table 4.4: Penetrance readings of *nrde-3* contribution to trans-generational silencing shown in **Figure 4.1C-F**

Brood count for positive RNAi transmission (Figure 4.1C, 4.1E)								
Strain	RNAi Target	Broods transmitting RNAi				Average	SD	*p*-value
N2	*dpy-11*	19/20	19/20	16/20	17/19*	0.90	0.07	
nrde-3(gg66)	*dpy-11*	4/20	6/20	5/20	6/20*	0.26	0.05	<0.001
eri-1(mg366)	*dpy-11*	16/19	8/9	7/9	19/20*	0.86	0.07	
eri-1(mg366); nrde-3(gg66)	*dpy-11*	4/17	0/7	3/9	7/20*	0.23	0.16	<0.001
N2	*unc-22*	7/7*	6/7*	6/6*		0.95	0.08	
nrde-3(gg66)	*unc-22*	4/7*	3/7*	3/6*		0.50	0.07	0.002
eri-1(mg366)	*unc-22*	17/20	8/10	9/10	18/20*	0.86	0.05	
eri-1(mg366); nrde-3(gg66)	*unc-22*	9/19	4/10	5/9	9/20*	0.47	0.06	<0.001

Representative penetrances of in-brood RNAi phenotypes (from broods with * above) (Figure 4.1D, 4.1F)																					
Strain	RNAi Target	Penetrance																			
N2	*dpy-11*	5/81	3/77	5/63	6/70	5/57	0/34	6/62	0/54	2/37	6/89	5/70	12/40	10/99	5/80	4/39	23/51	15/67	30/81	3/30	
nrde-3(gg66)	*dpy-11*	4/62	12/94	0/75	1/84	0/24	0/41	0/35	0/77	0/79	0/31	0/74	6/62	0/44	0/46	1/54	0/31	0/24	0/35	4/66	0/43
eri-1(mg366)	*dpy-11*	38/62	14/41	19/30	17/23	50/78	7/12	0/21	7/11	19/46	36/68	31/66	9/58	6/29	9/52	23/63	29/36	40/41	49/63	29/70	33/79
eri-1(mg366); nrde-3(gg66)	*dpy-11*	0/11	0/16	0/37	4/60	6/78	0/48	0/32	0/60	0/32	5/65	3/62	0/43	4/57	7/37	0/31	0/23	0/25	2/48	0/36	0/41
N2 (three samples; shading)	*unc-22*	5/39	5/40	4/48	4/51	1/37	2/41	2/35	1/24	3/28	0/46	4/33	7/40	4/32	3/25	2/21	7/50	6/29	1/19	2/26	3/39
nrde-3(gg66) (three samples; shading)	*unc-22*	8/36	3/30	0/24	0/31	3/25	1/31	0/32	0/30	4/36	0/40	0/36	0/11	9/33	2/38	4/28	2/29	0/18	3/36	0/38	0/44
eri-1(mg366)	*unc-22*	6/21	5/11	6/18	0/19	3/21	3/21	0/18	6/26	3/19	3/16	6/26	4/26	7/30	4/18	12/27	17/24	10/41	9/33	15/42	10/35
eri-1(mg366); nrde-3(gg66)	*unc-22*	0/28	2/35	5/28	0/45	0/35	3/48	4/36	0/26	4/32	3/34	0/51	2/29	7/40	0/25	0/31	0/14	0/18	0/18	8/26	0/15

exposed *nrde-3(gg66)* hermaphrodites to wild-type males and scored the penetrance of inherited silencing in the heterozygous wild-type progeny. In wild-type by wild-type positive control crosses, almost all mothers transmitted the Dpy-11 RNAi phenotype to their progeny (**Figure 4.1G**), while in *nrde-3(gg66)* by *nrde-3(gg66)* negative control crosses, almost none of the mothers transmitted the phenotype (**Figure 4.1I**). However, in only one out of 10 crosses did *nrde-3(gg66)* mothers robustly (>80% penetrant) transmit the Dpy-11 RNAi phenotype to their wild-type cross progeny, while most *nrde-3(gg66)* mothers only partially transmitted the Dpy-11 RNAi phenotype (**Figure 4.1H; Table 4.5**). These results indicate that, although NRDE-3 activity in the mother is important for the production of a transmissible silencing signal or state, NRDE-3 function in the progeny is also important.

To directly determine whether nuclear processes, in the absence of maternal contributions, are important for silencing, we hatched L1 larvae in the presence of *dpy-11* or *qua-1* dsRNA expressing bacteria and scored the resulting adults for Dpy-11 or Qua-1 phenotypes. We found that *nrde-2(gg91)*, *nrde-3(gg66)*, and **NLS-nrde-3* rescued *nrde-3(gg66)* mutant strains all showed reduced silencing compared to wild type and *SV40NLS-nrde-3* rescued *nrde-3(gg66)* mutant strains (**Figure 4.1J; Tables 4.2, 4.3**). Together, these results suggest that the weak Rde effect observed in *nrde-3* mutants is due to both reduced transmission of a trans-generational silencing signal or state, likely silenced chromatin, and decreased *de novo* silencing within dsRNA exposed animals.

nrde-3 overexpression causes enhanced RNAi independent of *sago-1*

While analyzing the weak Rde phenotype of *nrde-3* mutants, we noticed that the transgenic rescue strains often exhibited a stronger RNAi response than the wild type animals (**Figure 4.2E,**

Table 4.5: Penetrance readings of Dpy animals in heterozygous *nrde-3* crosses shown in **Figure 4.1G-I**

Cross	Penetrance in response to OD_{600nm} 1.0 *dpy-11(RNAi)*										Average	SD	*p*-value
N2 *hermaphrodite* x ***sur-5::gfp*** *male*	60/64	29/47	49/53	29/32	26/40	42/46	42/48	49/54			0.84	0.13	
nrde-3(gg66) *hermaphrodite* x ***sur-5::gfp*** *male*	7/12	0/7	11/48	30/63	0/20	34/52	22/54	23/49	4/16	58/67	0.39	0.28	<0.001 to N2 <0.02 to *nrde-3(gg66)*
nrde-3(gg66) *hermaphrodite* x ***nrde-3(gg66); sur-5::gfp*** *male*	11/54	0/20	0/30	10/63	0/15	12/71	0/20	18/62			0.10	0.12	<0.001 to N2

G). Because *C. elegans* multi-copy transgenes are often over-expressed (PRAITIS *et al.* 2001), we hypothesized that NRDE-3 overexpression may enhance RNAi. We therefore crossed the transgene array into a wild-type background (so that there are at least two wild type copies of *nrde-3*) and compared the RNAi effectiveness of this strain to wild type. We found that this strain exhibited enhanced RNAi to *dpy-13(RNAi)* (**Figure 4.4A-C; Table 4.6**), as well as to *unc-15(RNAi)* and *unc-73(RNAi)* (**Figure 4.4C; Table 4.6**). As a control, we then crossed the **NLS-nrde-3-gfp* transgene array into a wild-type background, and found that this array did not robustly enhance RNAi compared to wild type (**Figure 4.4C; Table 4.6**), suggesting again that it is predominantly the nuclear functions of *nrde-3* that are contributing to exogenous RNAi.

A previous report had analogously overexpressed the cytoplasmic secondary Argonautes SAGO-1 and SAGO-2, necessary for endogenous secondary RNAi, and found that those particular strains enhanced RNAi (YIGIT *et al.* 2006). The SAGOs and NRDEs function in distinct cellular compartments and thus likely function in independent pathways. However, it is possible that *nrde-3* activity is required for the SAGO-overexpression associated Eri phenotype. Therefore, we crossed *nrde-3(gg66)* into a strain containing the *myo-3p::gfp-sago-1* construct used previously to demonstrate over-induced enhanced RNAi in muscle cells (**Figure 4.4D-G**). We observed that the *nrde-3(gg66); myo-3p::gfp-sago-1* strain remained Eri (**Figure 4.4H; Table 4.7**). Thus, SAGO-1 enhanced RNAi is independent of *nrde-3*. Furthermore, these results suggest that *sago-1* and *nrde-3* may define complementary silencing pathways.

nrde-3 is partially required for Eri mutants' enhanced RNAi

The availability of enzymes utilized by both endogenous and exogenous RNAi pathways, like SAGO-1 and SAGO-2 (YIGIT *et al.* 2006), plays a large role in determining the efficacy of

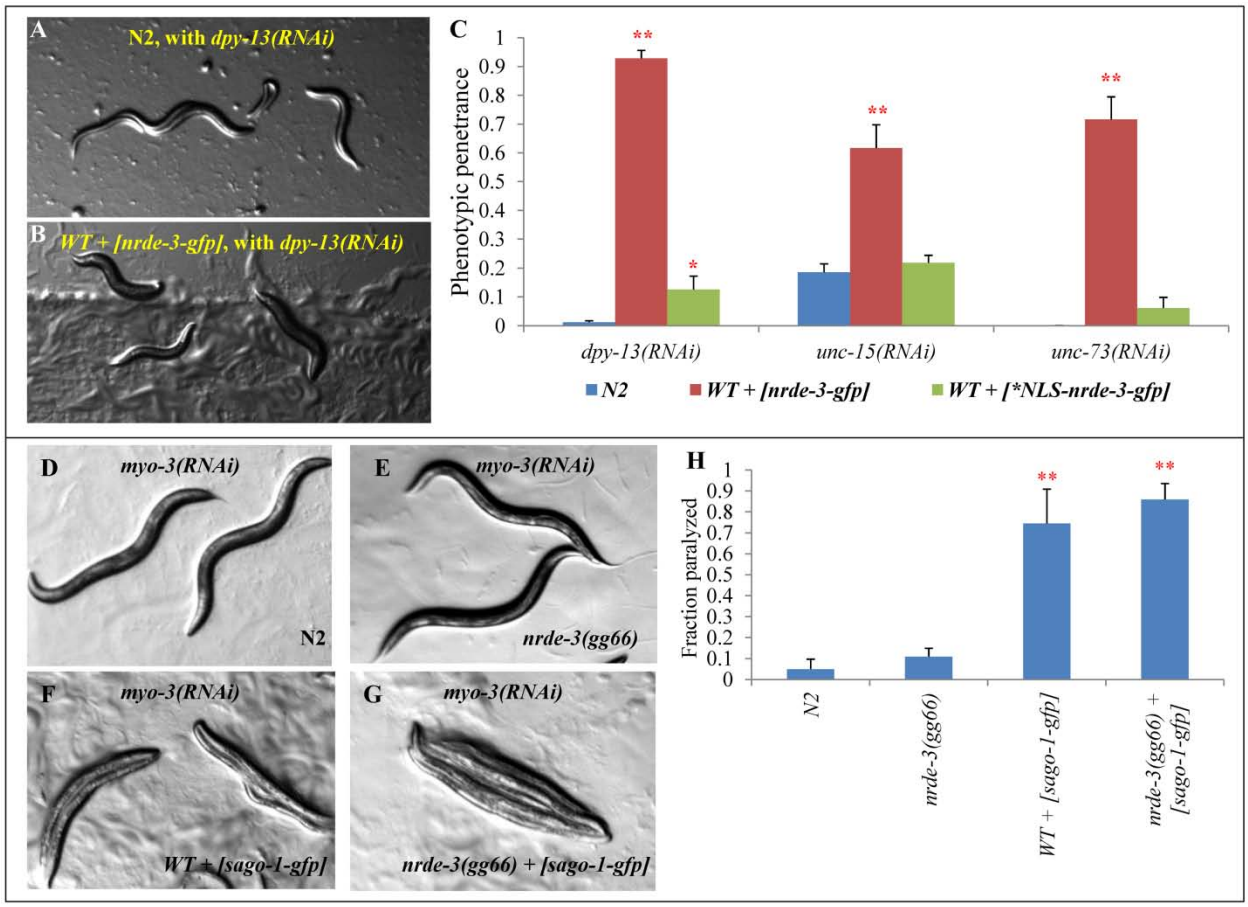

Figure 4.4: *nrde-3* overexpression causes enhanced RNAi independent of *sago-1*

(A-B) Representative images of progeny from L3 hermaphrodites of the indicated strains grown on *dpy-13(RNAi)* bacteria. **(C)** Penetrance of *dpy-13(RNAi)*, *unc-15(RNAi)*, and *unc-73(RNAi)* phenotypes for the indicated strains is shown. **(D-G)** Representative images of progeny from L3 hermaphrodites of the indicated strains grown on *myo-3(RNAi)* bacteria. **(H)** Penetrance of *myo-3(RNAi)*-induced paralysis for the indicated strains is shown. The *dpy-13(RNAi)* bacteria OD_{600nm}=1.5, *unc-15(RNAi)* bacteria OD_{600nm}=1.0, *unc-73(RNAi)* bacteria OD_{600nm}=4.0, and *myo-3(RNAi)* bacteria OD_{600nm}=3.0. The penetrances scored for **(C)** are listed in **Table 4.6** and for **(H)** in **Table 4.7**. *p*-values calculated by *t*-test; * indicates $p<0.05$ and ** indicates $p<0.01$.

Table 4.6: Penetrance readings of *nrde-3*-overexpression Eri phenotypes shown in **Figure 4.4C**

dpy-13(RNAi)				Average	SD
N2	1/92	1/119	1/58	0.012	0.005
WT + [*nrde-3-gfp*]	69/72	66/73	59/64	0.928	0.028
WT + [**NLS-nrde-3-gfp*]	7/79	14/79	11/99	0.126	0.046
unc-15(RNAi)					
N2	12/77	19/100	19/90	0.186	0.028
WT + [*nrde-3-gfp*]	29/44	23/44	46/69	0.616	0.081
WT + [**NLS-nrde-3-gfp*]	16/66	18/82	13/68	0.218	0.026
unc-73(RNAi)					
N2	0/30	0/30	0/30	0	0
WT + [*nrde-3-gfp*]	42/59	39/49	32/50	0.716	0.078
WT + [**NLS-nrde-3-gfp*]	4/39	3/61	3/94	0.061	0.037

Table 4.7: Penetrance readings of *sago-1*-overexpression Eri phenotypes shown in **Figure 4.4H**

Strain	Penetrance				Average	SD
N2	14/135	3/119	2/108		0.049	0.047
nrde-3(gg66)	12/81	7/100	15/137		0.109	0.039
WT+*[sago-1-gfp]*	98/112	91/114	32/57		0.745	0.163
nrde-3(gg66)+[sago-1-gfp]	108/118	146/173	88/116	23/25	0.859	0.076

exogenous RNAi. For example, mutations that reduce the abundance of endogenous siRNAs competing for SAGOs are thought to enhance exogenous RNAi silencing (**Figure 4.5**) (DUCHAINE *et al.* 2006). If this model is true, then mutations to these limiting RNAi resources should attenuate the Eri phenotype. Several observations indicate that *nrde-3* is a candidate for such a limiting RNAi resource. First, NRDE-3 nuclear localization is sensitive to endo- and exo-siRNA levels (GUANG *et al.* 2008). Second, like the SAGOs, *nrde-3* overexpression enhances RNAi (**Figure 4.4C**). Third, *nrde-3* was identified as a mutant that abolished the *eri-1*-dependent phenotype of pan-operon silencing (GUANG *et al.* 2008). Fourth, *nrde-3* is auxiliary to RNAi silencing: the Rde phenotype is only apparent when dsRNA trigger is limiting (**Figure 4.1A**).

To determine whether *nrde-3* is important for enhanced RNAi, we compared the penetrance and expressivity of RNAi silencing between *eri* single mutants and *eri;nrde-3(gg66)* double mutants. For these tests, we used each of the four widely conserved *C. elegans eri* genes (*eri-1*, *rrf-3*, *eri-6/7*, and *ergo-1/eri-8*). *nrde-3* is known to be important for RNAi targeting the *lir-1-lin-26* operon via *lir-1(RNAi)* (GUANG *et al.* 2008), and indeed in all four tested *eri; nrde-3* double mutants, silencing of *lin-26* by *lir-1(RNAi)* was eliminated (**Tables 4.8, 4.9, 4.10**). However, the *nrde-3*-dependence for enhanced RNAi is not limited to operons; all four *eri; nrde-3* double mutants also showed reduced RNAi efficacy targeting a variety of genes (**Tables 4.1, 4.8, 4.9, 4.10; Figure 4.6**). A second allele of *nrde-3*, *gg64*, in an *eri-1(mg366)* double mutant behaved similarly (**Table 4.11**). Furthermore, in an *eri-1(mg366);nrde-3(gg66)* background, the cytoplasmic-only **NLS-nrde-3* construct failed to rescue the enhanced RNAi, while the nuclear localized *SV40NLS-nrde-3* construct rescued the enhanced RNAi (**Table 4.8, 4.10**). Consistent with these results, *nrde-2(gg91)* mutants also disrupted enhanced silencing of non-operon genes (**Table 4.11**). These results suggest that *nrde-3* is a key factor whose accessibility is a rate

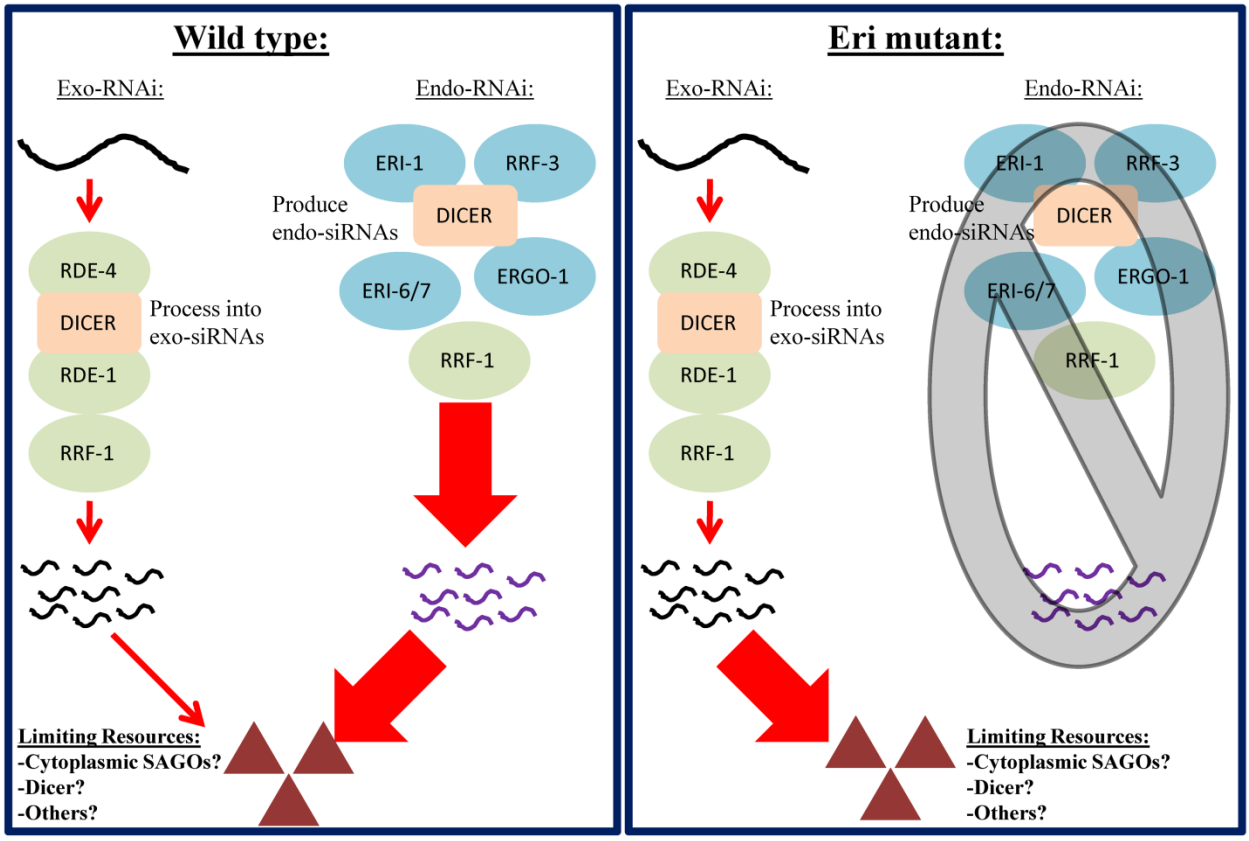

Figure 4.5: Model of competing small RNA pathways producing an Eri phenotype

Exogenous RNAi (exo-RNAi) and endogenous RNAi (endo-RNAi) pathways compete for limiting common resources, which limits the efficacy of the experimentally measurable, or exogenous, RNAi pathway. Mutations that disrupt the production or stability of endo-siRNAi (right) results in increased access to these limiting resources, thereby enhancing the exo-RNAi pathway. The identity of these limiting resources is largely speculative.

Table 4.8: *eri-1* mutant partially requires *nrde-3* for enhanced RNAi

RNAi Target	Operon or Homologous Sequences	N2	*nrde-3 (gg66)*	*eri-1 (mg366)*	*eri-1(mg366); nrde-3(gg66)*	*eri-1(mg366); nrde-3(gg66); [*NLS-nrde-3]*	*eri-1(mg366); nrde-3(gg66); [SV40-NLS-nrde-3]*
lir-1	Operon	+++	-	+++++	-	-	++++
dpy-13	91 Homologs	+	-	+++++	+	+	+++++
ifc-2	3 Homologs	+	-	+++++	+	++	+++++
unc-15	0 Homologs	-	-	+++++	+++	+++	+++++
hmr-1	1 homolog	+	-	+++++	+++	+++	+++++
dpy-28	0 homologs	-	-	+++++	++++	+++++	+++++
unc-73	0 homologs	-	-	+++++	++++	+++++	++++

The severity of RNAi phenotypes, from '-' to '+ + + + +', based on expressivity described in **Table 4.1** (illustrated for select mutants in **Figure 4.6**) and penetrances tabulated in **Table 4.10** of indicated strains for indicated RNAi gene targets are shown. All scores are normalized to the strongest Eri response for a particular RNAi assay as '+ + + + +' and no response as '-'. The enhanced RNAi response against genes in operons or with many homologs (highlighted in yellow) is most dependent on *nrde-3*. The number of homologous sequences was determined by the number unique genes with at least a 26mer match of perfect identity in mRNA. The bacteria OD_{600nm} concentrations used were *lir-1(RNAi)=3.0*, *dpy-13(RNAi)=1.5*, *ifc-2(RNAi)=3.5*, *unc-15(RNAi)=1.0*, *hmr-1(RNAi)=1.0*, *dpy-28(RNAi)=4.0*, and *unc-73(RNAi)=4.0*.

Figure 4.6: *nrde-3*-dependent enhanced *dpy-13(RNAi)* and *ifc-2(RNAi)* phenotypes

(A-D) Representative images of **(A)** N2, **(B)** *nrde-3*(*gg66),* **(C)** *eri-1(mg366),* and **(D)** *eri-1(mg366);nrde-3(gg66)* progeny from L3 hermaphrodites grown on *dpy-13(RNAi)* RNAi bacteria at OD_{600nm} 1.5. N2 animals exhibited very mild dumpiness, *nrde-3(gg66)* animals were unaffected, *eri-1(mg366)* animals exhibited grotesque dumpiness, and *eri-1(mg366);nrde-3(gg66)* animals exhibited very mild dumpiness. Scores from **Table 4.8** are indicated on the micrographs. Penetrances are shown in **Table 4.10**. **(E-H)** Representative images of **(E)** N2, **(F)** *nrde-3*(*gg66),* **(G)** *eri-1(mg366),* and **(H)** *eri-1(mg366);nrde-3(gg66)* progeny from L3 hermaphrodites grown on *ifc-2(RNAi)* RNAi bacteria at OD_{600nm} 3.5. N2 animals exhibited mild emaciation and posterior paralysis, *nrde-3(gg66)* animals were unaffected, *eri-1(mg366)* animals exhibited grotesque emaciation and paralysis, and *eri-1(mg366);nrde-3(gg66)* animals exhibited mild emaciation and posterior paralysis. Scores from **Table 4.8** are indicated on the micrographs. Penetrances are shown in **Table 4.10**.

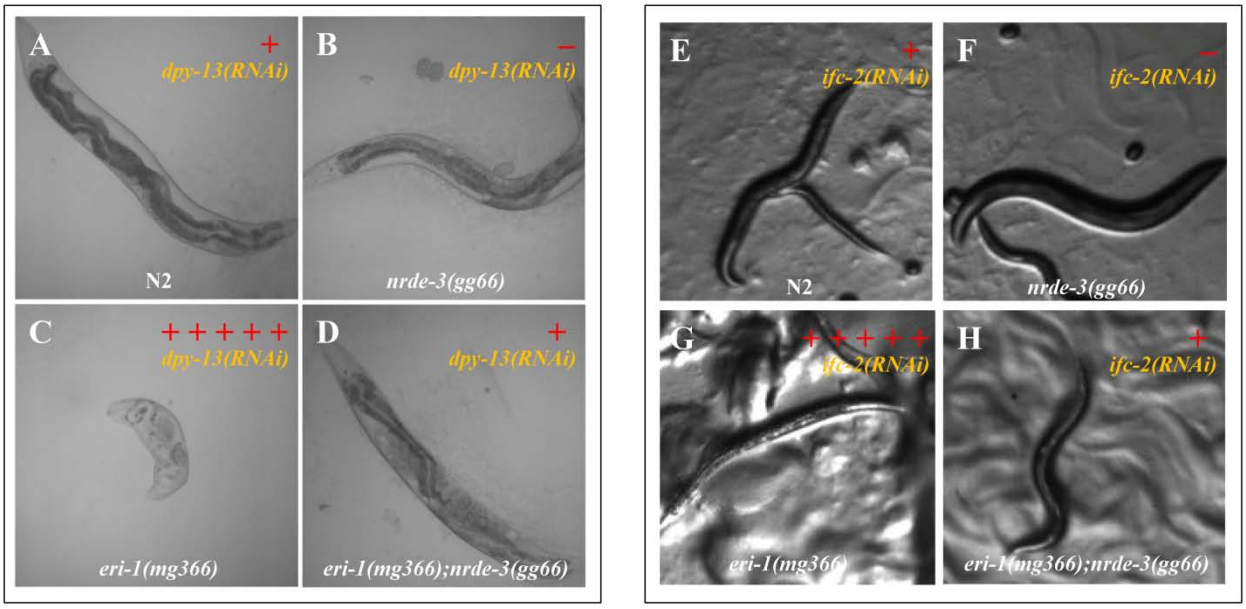

Figure 4.6 (Continued): *nrde-3*-dependent enhanced *dpy-13(RNAi)* and *ifc-2(RNAi)* phenotypes

Table 4.9: All Eri mutants partially require *nrde-3* for enhanced RNAi

RNAi Target	Operon or Homologous Sequences	N2	*nrde-3(gg66)*	*rrf-3(mg373)*	*rrf-3(mg373); nrde-3(gg66)*	*eri-6/7(tm1917)*	*eri-6/7(tm1917); nrde-3(gg66)*	*eri-8(gg100)*	*eri-8(gg100); nrde-3(gg66)*
lir-1	Operon	+++	-	+++++	-	+++++	-	+++++	-
dpy-13	91 Homologs	+	-	+++++	+	+++++	+	+++++	+
ifc-2	3 Homologs	+	-	+++++	++	+++++	+	+++++	+
hmr-1	1 Homolog	+	-	+++++	+++	+++++	+++	+++++	+++
unc-15	0 homologs	-	-	+++++	+++	+++++	+++	+++++	++
dpy-28	0 homologs	-	-	+++++	++++	+++++	++++	+++++	++++
unc-73	0 homologs	-	-	+++++	++++	+++++	++++	+++++	++++

The severity of RNAi phenotypes as described in **Table 4.8** is based on penetrances measurements presented in **Table 4.10.** The RNAi bacteria concentrations used were the same as **Table 4.8**. The enhanced RNAi response targeting genes most dependent on *nrde-3* (highlighted in yellow) holds the same pattern of RNAi responses as *eri-1(mg366)* and *eri-1(mg366);nrde-3(gg66)* mutants.

Table 4.10: Penetrance readings for Eri mutants' partial requirement of *nrde-3* for enhanced RNAi shown in **Table 4.8** and **4.9**

RNAi Target	N2	*nrde-3 (gg66)*	*eri-1 (mg366)*	*eri-1 (mg366); nrde-3(gg66)*	*eri-1(mg366); nrde-3(gg66); [*NLS-nrde-3]*	*eri-1(mg366); nrde-3(gg66); [SV40NLS-nrde-3]*	*rrf-3 (mg373)*	*rrf-3 (mg373); nrde-3(gg66)*	*eri-6/7 (tm1917)*	*eri-6/7 (tm1917); nrde-3(gg66)*	*eri-8 (gg100)*	*eri-8(gg100); nrde-3(gg66)*
lir-1	I: 0.00 II: 0.94 III: 0.06 n=179	I: 1.00 II: 0.00 III: 0.00 n=133	I:0.00 II: 0.00 III: 1.00 n=59	I: 0.89 II: 0.05 III: 0.06 n=136	I: 1.00 II: 0.00 III: 0.00 n>50	I: 0.01 II: 0.26 III: 0.73 n=305	I:0.00 II: 0.00 III: 1.00 n=100	I:1.00 II: 0.00 III: 0.00 n>50	I:0.00 II: 0.01 III: 0.99 n=75	I: 0.96 II: 0.02 III: 0.02 n=121	I:0.00 II: 0.00 III: 1.00 n>50	I:1.00 II: 0.00 III: 0.00 n>50
dpy-13	I: 0.00 II: 1.00 III: 0.00 n>30	I: 1.00 II: 0.00 III: 0.00 n>30	I: 0.00 II: 0.00 III: 1.00 n>30	I: 0.00 II: 1.00 III: 0.00 n>30	I: 0.19 II: 0.81 III: 0.00 n=176	I: 0.00 II: 0.03 III: 0.97 n=90	I: 0.00 II: 0.09 III: 0.91 n=110	I: 0.00 II: 1.00 III: 0.00 n>60	I: 0.00 II: 0.00 III: 1.00 n>30	I: 0.00 II: 1.00 III: 0.00 n>30	I: 0.00 II: 0.00 III: 1.00 n>30	I: 0.00 II: 1.00 III: 0.00 n>30
ifc-2	0.03 n=32	0.00 n=47	0.37 n=27	0.08 n=24	0.15 n=182	0.44 n=189	0.36 n=151	0.20 n=138	0.23 n=22	0.05 n=20	0.24 n=33	0.05 n=19
hmr-1	0.00 n=93	0.00 n=106	1.00 n=37	0.53 n=30	0.80 n=53	1.00 n=34	0.98 n=100	0.75 n=127	1.00 n=35	0.68 n=31	1.00 n=16	0.53 n=32
unc-15	I: 0.90 II: 0.10 III: 0.00 n=20	I: 1.00 II: 0.00 III: 0.00 n=21	I: 0.07 II: 0.43 III: 0.50 n=14	I: 0.13 II: 0.87 III: 0.00 n=31	I: 0.23 II: 0.76 III: 0.01 n=106	I: 0.00 II: 0.36 III: 0.64 n=264	I: 0.00 II: 0.08 III: 0.92 n=131	I: 0.21 II: 0.79 III: 0.00 n=90	I: 0.12 II: 0.44 III: 0.44 n=27	I: 0.31 II: 0.69 III: 0.00 n=39	I: 0.06 II: 0.12 III: 0.82 n=52	I: 0.67 II: 0.33 III: 0.00 n=15
dpy-28	0.03 n=31	0.02 n=47	0.56 n=25	0.48 n=25	0.58 n=50	0.73 n=59	0.62 n=74	0.47 n=72	0.58 n=31	0.47 n=15	0.54 n=70	0.41 n=22
unc-73	0.00 n=68	0.00 n=48	0.97 n=29	0.77 n=35	0.95 n=104	0.82 n=245	0.94 n=158	0.81 n=93	0.96 n=25	0.72 n=43	0.93 n=57	0.81 n=43

The RNAi phenotypes whose penetrances are tabulated and their corresponding descriptions for I, II, and III are listed in **Table 4.1**.

Table 4.11: *eri-1* mutants partially require *nrde-2* and *nrde-3* for enhanced RNAi

RNAi target	Notes	N2		*nrde-2(gg91)*		*nrde-3(gg64)*		*eri-1(mg366)*		*eri-1(mg366); nrde-2(gg91)*		*eri-1(mg366); nrde-3(gg64)*	
lir-1	Operon	I: 0.00 II: 1.00 III: 0.00 n>50	+++	I: 1.00 II: 0.00 III: 0.00 n=106	-	I: 1.00 II: 0.00 III: 0.00 n=108	-	I:0.00 II: 0.00 III: 1.00 n=60	+++++	I: 0.94 II: 0.00 III: 0.06 n=66	-	I: 0.94 II: 0.01 III: 0.05 n=136	-
dpy-13	91 Homologs	I: 0.00 II: 1.00 III: 0.00 n>30	+	I: 1.00 II: 0.00 III: 0.00 n=15	-	I: 1.00 II: 0.00 III: 0.00 n=13	-	I:0.00 II: 0.00 III: 1.00 n=13	+++++	I: 0.00 II: 1.00 III: 0.00 n=11	+	I: 0.00 II: 1.00 III: 0.00 n=21	+
ifc-2	3 Homologs	0.01 n=92	-	0.10 n=251	+	0.00 n=100	-	0.40 n=30	+++++	0.09 n=160	+	0.12 n=40	+
hmr-1	1 Homolog	0.00 n=40	-	0.04 n=90	-	0.00 n=100	-	1.00 n=94	+++++	0.27 n=96	+++	0.24 n=105	+++
unc-15	0 homologs	I: 0.95 II: 0.05 III: 0.00 n=20	-	I: 1.00 II: 0.00 III: 0.00 n=109	-	I: 1.00 II: 0.00 III: 0.00 n=95	-	I: 0.06 II: 0.41 III: 0.53 n=85	+++++	I: 0.28 II: 0.72 III: 0.00 n=134	+++	I: 0.34 II: 0.66 III: 0.00 n=68	+++
dpy-28	0 homologs	0.03 n=90	-	0.01 n=100	-	0.04 n=112	-	0.62 n=45	+++++	0.53 n=70	++++	0.50 n=56	++++
unc-73	0 homologs	0.00 n>100	-	0.00 n=137	-	0.00 n=17	-	0.96 n=27	+++++	0.82 n=17	++++	0.69 n=32	++++

The severity of RNAi phenotypes, from '-' to '+ + + + +', based on expressivity described in **Table 4.1** (with their corresponding descriptions for I, II, and III) and penetrances tabulated within of indicated strains for indicated RNAi gene targets are scored. All scores are normalized to the strongest Eri response for a particular RNAi assay as '+ + + + +' and no response as '-'. The RNAi bacteria OD_{600nm} concentrations used were the same as **Table 4.8**. The impact on the enhanced RNAi response for *nrde-2(gg91)* and *nrde-3(gg64)* strains holds the same pattern of RNAi responses as *eri-1(mg366)* and *eri-1(mg366);nrde-3(gg66)* mutants.

limiting factor for exogenous RNAi and that nuclear RNAi plays an important role in enhanced RNAi silencing phenomena.

Interestingly, the enhanced RNAi phenotype of some genes was completely dependent on *nrde-3*, while that of others was completely independent of *nrde-3* (**Table 4.8**). This suggests that expression of some genes may be more sensitive than others to nuclear RNAi silencing. In our limited analysis, *dpy-13* and *ifc-2* showed the most pronounced *nrde-3*-dependent enhanced RNAi phenotype (**Table 4.8; Figure 4.4**). These two genes are members of conserved and expansive gene families that share significant nucleotide identity (COX 1985; WOO *et al.* 2004). One possibility is that *nrde-3* dependent nuclear RNAi processes may preferentially silence multiple related genes.

***nrde-3* contributes to transitive RNAi**

Intriguingly, a mechanism that could explain the *nrde-3*-dependent enhanced RNAi targeting sequence-related multi-gene families is transitive RNAi. Transitive RNAi is the observation that RNAi silencing specificity can spread *in cis* along a target mRNA to target sequences not in the original trigger dsRNA. Mechanistically, this occurs during RNA directed RNA polymerase (RdRP) production of secondary siRNAs. Subsequently, and most importantly, these secondary siRNAs can then target other mRNA transcripts *in trans* (such as homologous transcripts), which is essential for the potency of RNAi in *C. elegans* (PAK *et al.* 2012). Transitive RNAi can be detected by sequencing small RNAs in response to exogenous RNAi (PAK and FIRE 2007), but it is more readily detected in *C. elegans* using transgenes that artificially fuse separate genes, resulting in secondary siRNAs that independently target both sequences (ALDER *et al.* 2003; HANNON 2002).

To determine whether *nrde-3* can contribute to transitive RNAi, we used a strain with an *elt-1-gfp* fusion transgene that when exposed to *gfp* dsRNA causes *elt-1*-related developmental defects (**Figure 4.7A**) (ALDER *et al.* 2003; SMITH *et al.* 2005). Specifically, we exposed wild-type, *nrde-3(gg66)*, and *eri-1(mg366)* strains that express the *elt-1-gfp* transgene to *gfp* dsRNA and scored the progeny for *elt-1*-related developmental defects. In a wild-type background, feeding *gfp* dsRNA to worms expressing the *elt-1-gfp* fusion causes mild levels of developmental deformities and embryonic lethality (**Figure 4.7B, E**), while in an *eri-1(mg366)* background, *gfp(RNAi)* causes near complete *elt-1*-related embryonic lethality (**Figure 4.7C, E**). In contrast, *gfp(RNAi)* in the *nrde-3(gg66)* single mutant and the *eri-1(mg366);nrde-3(gg66)* double mutant caused almost no *elt-1*-related phenotypes (**Figure 4.7D, E**). Furthermore, the **NLS-nrde-3* transgene failed to rescue transitive RNAi in an *nrde-3(gg66)* mutant, while the *SV40NLS-nrde-3* transgene-rescued *nrde-3(gg66)* strain behaved like wild type (**Figure 4.7E**), indicating that only nuclear localized NRDE-3 can contribute to transitive RNAi. Importantly, we also observed that *elt-1(RNAi)* was fully penetrant in all strains, thus *nrde-3* is not simply required for efficient silencing of the *elt-1* locus. Therefore, these results show that nuclear NRDE-3 contributes to transitive RNAi, which may in turn be the mechanism behind *nrde-3*'s contributions to exogenous RNAi silencing.

nrde-3 is required for endogenous gene regulation

Previous reports indicate that NRDE-3 nuclear localization is dependent on *eri* endo-siRNA levels and it co-immunoprecipitates with *eri* endo-siRNAs (GUANG *et al.* 2008). Furthermore, we observed that it is necessary and sufficient for enhanced RNAi (**Figure 4.4C, Table 4.8**). These observations suggest that *nrde-3* may function endogenously to regulate endo-siRNA targeted

Figure 4.7: *nrde-3* contributes to transitive RNAi

(A) Schematic for transitive RNAi showing the 5' spread of secondary siRNAs triggered by the introduced *gfp* dsRNA. The secondary siRNAs, which now include siRNAs complementary to *elt-1*, can act *in trans* to target the endogenous *elt-1* locus. **(B-D)** Representative phenotypes of **(B)** wild type (N2), **(C)** *eri-1(mg366)*, and **(D)** *nrde-3(gg66)* and *eri-1(mg366);nrde-3(gg66)* strains expressing an *elt-1-gfp* fusion transgene grown on *gfp* RNAi bacteria. Wild type animals had modest amounts of *elt-1* related developmental defects while *eri-1(mg366)* animals exhibited *elt-1* related embryonic lethality. In contrast, *nrde-3(gg66)* and *eri-1(mg366);nrde-3(gg66)* animals had very few, if any, *elt-1*-related developmental defects. **(E)** The penetrance of *elt-1*-like phenotypes for the indicated strains expressing an *elt-1-gfp* fusion transgene grown on *gfp(RNAi)* bacteria is shown. Images **(A-D)** courtesy of Dr. Stephen Banse. The wild type, *eri-1(mg366)*, and *eri-1(mg366);nrde-3(gg66)* strains with the *elt-1-gfp* transgene were constructed and initially characterized by Dr. Stephen Banse.

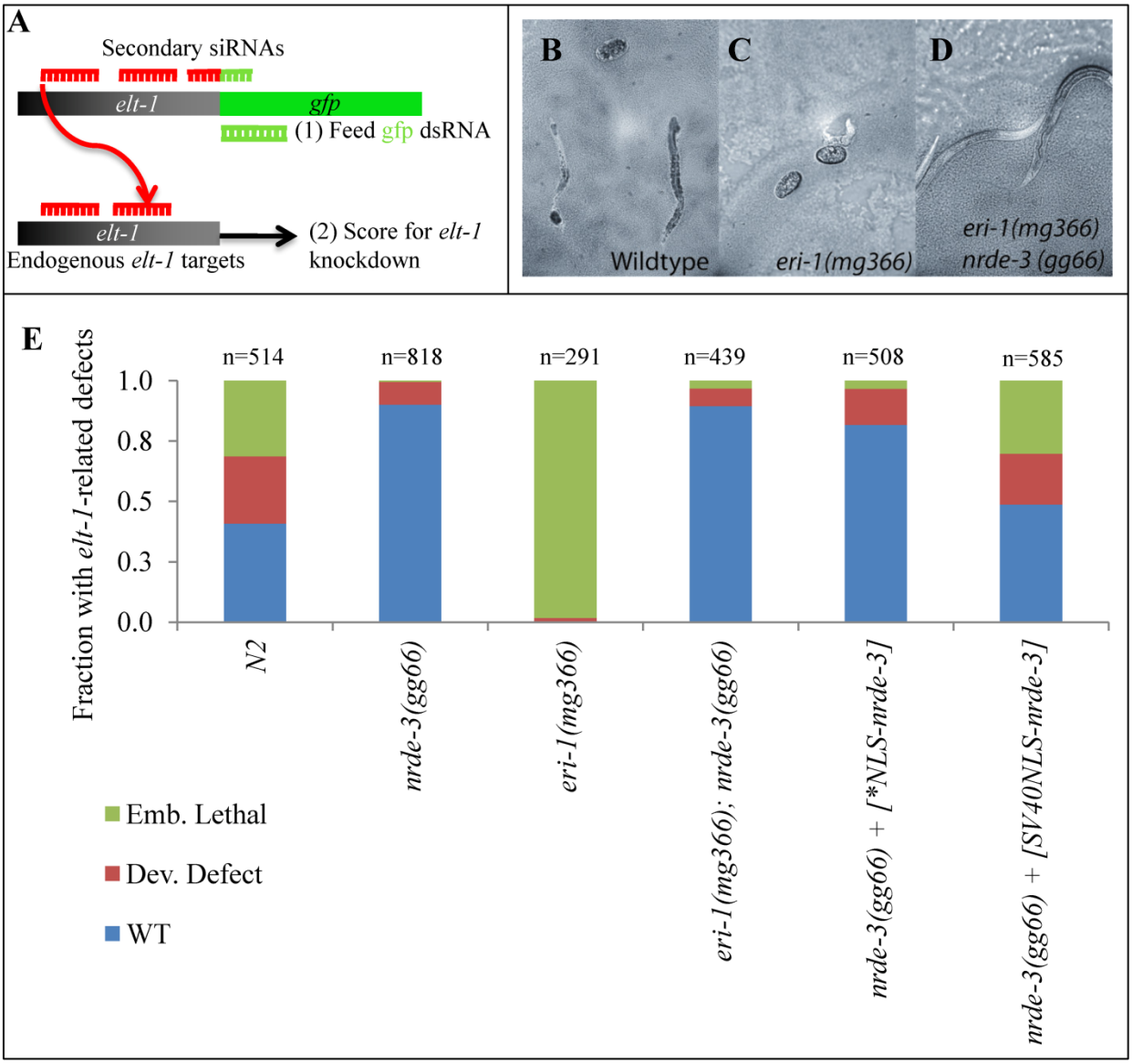

Figure 4.7 (Continued): *nrde-3* contributes to transitive RNAi

genes. To test this, we used qPCR to measure the expression level of five target genes of endo-siRNAs that are up-regulated in *rrf-3(pk1426)* mutants (GENT *et al.* 2010). If NRDE-3 uses *rrf-3*-dependent endo-siRNAs to repress gene expression, then the expression levels of these five genes should increase in *nrde-3* mutants. Specifically, we compared transcript abundances in wild type, *eri-1(mg366)*, *rrf-3(mg373)*, *rrf-3(pk1426)* and *nrde-3(gg66)* L4 larvae. We found that expressions of all five *rrf-3* siRNA target genes were increased in both *rrf-3* mutant alleles and the *nrde-3(gg66)* mutant (**Figure 4.8A**). To our knowledge, this is the first report of an endogenous function for *nrde-3*, as previous reports on *nrde* roles in germline maintenance implicated only *nrde-1*, *nrde-2*, and *nrde-4*. Consistent with previous reports, we observed that *eri-1* and *rrf-3* mutants had overlapping but incompletely shared effects on endogenous gene expression (**Figure 4.8A**) (ASIKAINEN *et al.* 2007; LEE *et al.* 2006).

***nrde-3* is required for transgene silencing**

Enhanced RNAi mutant backgrounds often enhance the frequency and penetrance of spontaneous silencing of multi-copy repetitive transgenes (KIM *et al.* 2005). To determine whether *nrde-2* and *nrde-3* are required for *eri*-enhanced silencing of repetitive transgene arrays, we compared the extent of silencing of the ubiquitously expressed *sur-5p::gfp* transgene in *eri-1(mg366)* single mutant to the silencing in the *eri-1(mg366);nrde-2(gg91)* and *eri-1(mg366);nrde-3(gg66)* double mutants. We found that both *nrde* genes are required for *eri-1*-induced silencing (**Figure 4.8E-H**). To determine whether this *nrde*-dependent transgene silencing activity represents an endogenous *nrde* function, or reflects only the unusual circumstances present in *eri*-mutant backgrounds, we examined *nrde*-dependent transgene expression in non-Eri backgrounds. Specifically, we compared the extent of silencing of

Figure 4.8: *nrde-3*-dependent silencing of endogenous RNAi targets and transgenes

(A) *eri-* and *nrde-3*-dependent changes in relative mRNA levels for select endo-siRNA target genes. Log2 ratio (relative to N2 = 0) of qPCR determined mRNA levels for the indicated genes from L4 larvae of the indicated genotypes. Expression of these five genes, which are targets of *rrf-3*-dependent endo-siRNAs, was previously reported to be up-regulated in *rrf-3* mutants (GENT *et al.* 2010). *p*-values calculated by *t*-test; *indicates p<0.05; ** indicates *p*<0.01. **(B-G)** Representative photomicrographs of *Psur-5::gfp* expression in **(B)** wild type **(C)** *nrde-2(gg91)* **(D)** *nrde-3(gg66)* **(E)** *eri-1(mg366)* **(F)** *eri-1(mg366);nrde-2(gg91)* and **(G)** *eri-1(mg366);nrde-3(gg66)* strains. The extensive transgene silencing that is readily apparent in intestinal cells (yellow arrows) in the *eri-1(mg366)* background is dependent on *nrde-2* and *nrde-3*. Compared to *nrde-2(gg91)* and *nrde-3(gg66)*, wild type animals show reduced *gfp* levels. **(H)** Average *gfp* fluorescence of hatch-synchronized 24 hour adult (20 ºC) worms. For each genotype the average whole body fluorescence (0.1 second exposure) of 10 worms is shown. Error bars represent standard deviation. *p*-values calculated by *t*-test; red asterisks are *p*<0.01 compared to wild type (N2) and blue asterisks are *p*<0.01 compared to *eri-1(mg366)*.

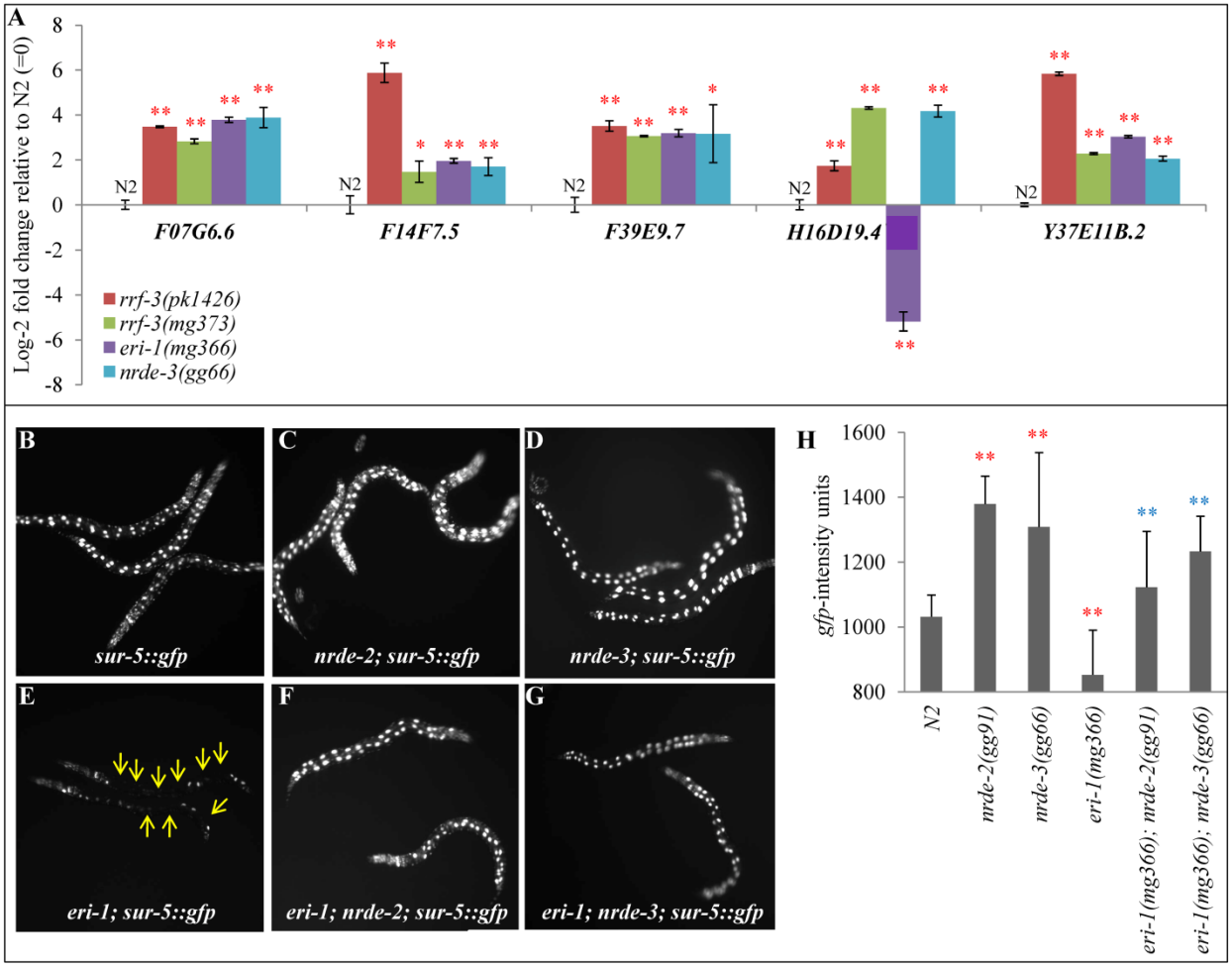

Figure 4.8 (Continued): *nrde-3*-dependent silencing of endogenous RNAi targets and transgenes

sur-5p::gfp in wild type versus *nrde-2(gg91)* and *nrde-3(gg66)* backgrounds. We found that the loss of *nrde-2* and *nrde-3* also increased transgene expression in non-Eri backgrounds (**Figure 4.8B, C, D, H**), indicating that silencing repetitive transgenes is likely another endogenous function of *nrde-3*.

***rrf-3(pk1426)* is likely associated with a non-allelic background mutation**

During this analysis, we noticed that the well-characterized deletion allele of *rrf-3*, *pk1426*, behaved differently in several assays from the missense *rrf-3(mg373)* allele, which is roughly indistinguishable from *eri-1(mg366).* First, the *rrf-3(pk1426);nrde-3(gg66)* double mutant was, like the *eri-1; nrde-3; pgl-1* triple mutant, non-Eri for all tested genes. This is at odds with all the other *eri; nrde-3(gg66)* double mutants, including the *rrf-3(mg373);nrde-3(gg66)* and *rrf-3(pk2042);nrde-3(gg66)* strains (**Table 4.12, 4.13**). Second, genes that were previously shown to be down-regulated in an *rrf-3(pk1426)* background (ASIKAINEN *et al.* 2007; LEE *et al.* 2006) showed a significantly different expression profile in an *rrf-3(mg373)* background (**Figure 4.9A**). Previous gene expression profile analyses also show little overlap between *rrf-3(pk1426)* and *eri-1(mg366)* (ASIKAINEN *et al.* 2007; LEE *et al.* 2006). This indicates either a different mechanism or set of targets for endogenous gene regulation. Third, qPCR designed to measure *dpy-13* mature and pre-mRNA transcript levels showed that *dpy-13(RNAi)* in *rrf-3(pk1426)* mutants more effectively reduced both mature and pre-mRNA levels than RNAi in *eri-1(mg366)* and *rrf-3(mg373)* mutants (**Figure 4.9B**). Given that two of the three *rrf-3* alleles are phenotypically similar to the other *eri* mutants, we hypothesize that these apparently allele-specific phenotypes are due to a *pk1426* allele-associated background effect.

Table 4.12: *rrf-3(pk1426)* has unique dependence on *nrde-3* for enhanced RNAi

RNAi Target	N2	*nrde-3 (gg66)*	*rrf-3 (mg373)*	*rrf-3 (mg373); nrde-3 (gg66)*	*rrf-3 (pk2042)*	*rrf-3 (pk2042); nrde-3 (gg66)*	*rrf-3 (pk1426)*	*rrf-3 (pk1426); nrde-3 (gg66)*	*rrf-3 (pk1426) + [WT rrf-3]*	*rrf-3 (mg373/pk1426)* het	*rrf-3 (mg373/pk1426); nrde-3 (gg66)* het
lir-1	+++	-	+++++	-	+++++	-	+++++	-	+++	+++++	-
dpy-13	+	-	+++++	+	+++++	+	+++++	-	+	+++++	+
ifc-2	+	-	+++++	++	+++++	++	+++++	+	-	+++++	+
hmr-1	+	-	+++++	+++	+++++	+++	+++++	-	+++	+++++	++
unc-15	-	-	+++++	+++	+++++	+++	+++++	-	++++	+++++	-
dpy-28	-	-	+++++	++++	+++++	+++++	+++++	-	++++	+++++	+
unc-73	-	-	+++++	++++	+++++	+++++	+++++	-	++++	++++	++

The severity of RNAi phenotypes as described in **Table 4.8** is based on penetrances measurements presented in **Table 4.13.** The RNAi bacteria concentrations used were the same as **Table 4.8**. The enhanced RNAi response targeting genes most dependent on *nrde-3* (highlighted in yellow) holds the same pattern of RNAi responses as the other Eri mutants, while the enhanced RNAi response targeting genes most dependent on *pgl-1* (highlighted in green) holds the same pattern of RNAi responses as the other Eri mutants for the *mg373* and *pk2042* alleles, but not the *pk1426* allele.

Table 4.13: Penetrance readings for *rrf-3(pk1426)*'s unique dependence on *nrde-3* for enhanced RNAi

The RNAi phenotypes whose penetrances are tabulated and their corresponding descriptions for I, II, and III are listed in **Table 4.1**. All *rrf-3* alleles are temperature sensitive sterile at 25°C, even in an *nrde-3(gg66)* background. The rescue construct restores viability at 25°C. A transgenic rescue using *rrf-3* with its native UTRs of the NL2099 strain containing the *pk1426* allele does not fully restore the wild type RNAi response against gene targets most dependent on *pgl-1*. The trans-heterozygous strains were mated using *rrf-3(pk1426)* or *rrf-3(pk1426);nrde-3(gg66)* hermaphrodites and *rrf-3(mg373);sur-5::gfp* or *rrf-3(mg373);nrde-3(gg66);sur-5::gfp* males for green cross progeny.

Table 4.13 (Continued): Penetrance readings for *rrf-3(pk1426)*'s unique dependence on *nrde-3* for enhanced RNAi

RNAi Target	N2	*nrde-3 (gg66)*	*rrf-3 (mg373)*	*rrf-3 (mg373); nrde-3 (gg66)*	*rrf-3 (pk2042)*	*rrf-3 (pk2042); nrde-3 (gg66)*	*rrf-3 (pk1426)*	*rrf-3 (pk1426); nrde-3 (gg66)*	*rrf-3 (mg373/pk1426)* het	*rrf-3 (mg373/pk1426); nrde-3 (gg66)* het	*NL2099: rrf-3 (pk1426) + [WT rrf-3]*
lir-1	I: 0.00 II: 0.94 III: 0.06 n=179	I: 1.00 II: 0.00 III: 0.00 n=133	I:0.00 II: 0.00 III: 1.00 n=100	I:1.00 II: 0.00 III: 0.00 n>50	I: 0.00 II: 0.00 III: 1.00 n=219	I: 1.00 II: 0.00 III: 0.00 n=131	I:0.00 II: 0.00 III: 1.00 n=16	I: 0.96 II: 0.04 III: 0.00 n=28	I:0.00 II: 0.00 III: 1.00 n=30	I:1.00 II: 0.00 III: 0.00 n=54	I:0.00 II: 1.00 III: 0.00 n=12
dpy-13	I: 0.00 II: 1.00 III: 0.00 n>30	I: 1.00 II: 0.00 III: 0.00 n>30	I: 0.00 II: 0.09 III: 0.91 n=110	I: 0.00 II: 1.00 III: 0.00 n>60	I: 0.00 II: 0.08 III: 0.92 n=331	I: 0.88 II: 0.12 III: 0.00 n=189	I: 0.00 II: 0.00 III: 1.00 n>30	I: 1.00 II: 0.00 III: 0.00 n>30	I: 0.00 II: 0.11 III: 0.89 n=19	I: 0.90 II: 0.10 III: 0.00 n=71	I: 0.00 II: 1.00 III: 0.00 n=14
ifc-2	0.03 n=32	0.00 n=47	0.36 n=151	0.20 n=138	0.41 n=336	0.17 n=210	0.38 n=38	0.08 n=25	0.33 n=12	0.06 n=54	0.00 n=17
hmr-1	0.00 n=93	0.00 n=106	0.98 n=100	0.75 n=127	1.00 n=221	0.71 n=77	1.00 n=22	0.00 n=23	1.00 n=14	0.13 n=48	0.80 n=15
unc-15	I: 0.90 II: 0.10 III: 0.00 n=20	I: 1.00 II: 0.00 III: 0.00 n=21	I: 0.00 II: 0.08 III: 0.92 n=131	I: 0.21 II: 0.79 III: 0.00 n=90	I: 0.00 II: 0.05 III: 0.95 n=192	I: 0.44 II: 0.56 III: 0.00 n=183	I: 0.00 II: 0.17 III: 0.83 n=36	I: 1.00 II: 0.00 III: 0.00 n=22	I: 0.00 II: 0.25 III: 0.75 n=12	I: 0.96 II: 0.04 III: 0.00 n=74	I: 0.35 II: 0.21 III: 0.44 n=29
dpy-28	0.03 n=31	0.02 n=47	0.62 n=74	0.47 n=72	0.73 n=123	0.53 n=107	0.65 n=48	0.00 n=54	0.62 n=13	0.07 n=104	0.42 n=24
unc-73	0.00 n=68	0.00 n=48	0.94 n=158	0.81 n=93	0.98 n=253	0.93 n=206	1.00 n=29	0.00 n=38	0.58 n=12	0.12 n=121	0.74 n=19
25°C sterile	No	No	Yes	Yes	Yes	Yes	Yes	Yes	Yes	Yes	No

To test this hypothesis, we determined whether a wild-type *rrf-3* genomic fragment could rescue each distinct *rrf-3(pk1426)* phenotype. We found that *rrf-3(pk1426); [rrf-3(wild type)]* transgenic animals were rescued for the temperature sensitive sterility associated with all *rrf-3* alleles (**Table 4.13**) (GENT *et al.* 2009; PAVELEC *et al.* 2009). In addition, these animals were rescued for the Eri phenotypes against the *nrde-3*-dependent target genes (e.g. *lir-1(RNAi), dpy-13(RNAi)*, *ifc-2(RNAi)*), but not against the *pgl-1*-dependent target genes (e.g. *dpy-28(RNAi), unc-73(RNAi)*) (**Table 4.12**). Thus, the wild-type *rrf-3* transgene specifically failed to rescue a phenotype that is unique to the *pk1426* allele, implicating a non-*rrf-3* lesion in the background of the *pk1426* strain. We also constructed and scored an *rrf-3(mg373/pk1426); nrde-3(gg66)* strain (**Table 4.12**). Consistent with a semi-dominant effect, the *rrf-3* trans-heterozygote strain was, at a very reduced level, Eri for some *pgl-1*-dependent targets. In summary, our results indicate that an *rrf-3(pk1426)* associated background effect, which may act via a *pgl-1*-dependent pathway, accounts for the unusual properties associated with the *rrf-3(pk1426)* strain.

DISCUSSION

We show that the nuclear RNAi Argonaute *nrde-3* contributes broadly and potently to RNAi triggered by exogenous dsRNA. Specifically, we found that nuclear RNAi contributes to silencing of genes that are members of multi-gene families and multi-copy transgenes, as well as the phenomena of transitive RNAi. Particularly intriguing was the finding that overexpression of NRDE-3 enhances RNAi, suggesting that, like the cytoplasmic secondary Argonautes, nuclear Argonautes may also be a limiting silencing resource. Furthermore, our analyses of *pgl-1* show that it is important for the enhanced RNAi phenotypes of a non-overlapping subset of target genes. These results thus define two separate and independent limiting RNAi resource pathways,

which establish *pgl-1* and *nrde-3* as two parallel activities that together are required for all detectable enhanced RNAi associated with *eri-1* and the other conserved *eri* mutants. Finally, our analysis of trans-generational silencing identified roles for nuclear RNAi in both the exposed parent and the unexposed progeny, which may indicate that a nuclear limited step mediates the transition from short-term RNAi processes that include PTGS of mature transcripts and longer-term RNAi processes, such as transgene silencing and trans-generational RNAi.

nrde-3 functions in exogenous RNAi are predominantly nuclear

NRDE-3 is a siRNA-binding protein that shuttles siRNAs between the cytoplasm and the nucleus, thus there is a possibility that NRDE-3 could function in either compartment. However, our analyses of nuclear restricted *nrde-2*, (BURTON *et al.* 2011; GUANG *et al.* 2010), as well as the **NLS-nrde-3* and *SV40NLS-nrde-3* constructs, provide strong evidence for the primary importance of nuclear limited RNAi steps. Nevertheless, this does not preclude prior or subsequent non-nuclear activities in these silencing processes. For example, transgene silencing, which is completely dependent on NRDE-3 in an Eri background, is partially dependent on SID-1, a dsRNA transporter that enables cell-to-cell spreading of RNAi silencing signals (JOSE *et al.* 2009). Therefore, NRDE-3 may either directly or indirectly use mobile silencing signals and/or NRDE-3-dependent processes may produce a silencing signal that can move between cells. Once the structure and origin of mobile silencing signals is known, it will be interesting to determine whether *nrde-3* is required for their biogenesis.

Interestingly, some of our analysis indicates that the **NLS-nrde-3-gfp* transgene sometimes do partially rescue the *nrde-3(gg66)* defects, especially in the contexts of weak exogenous Rde (**Figure 4.1A, J**) and overexpressor-induced Eri (**Figure 4.4C**) phenotypes. This

may be due to an incomplete removal of nuclear localization, although the lack of *gfp* nuclear localization suggests otherwise. This may also be due to the perhaps overexpressed transgene soaking up endogenous siRNAs – even if it's only present in the cytoplasm – so that the exogenous RNAi triggers have more access to competed-for cytoplasmic RNAi resources, hence creating an ever slight advantage in RNAi efficacy.

nrde-2 was initially characterized as a *nrde-3* effector (GUANG *et al.* 2010), thus it is interesting that many *nrde*-dependent functions, such as RNAi transmission and interaction with *hrde-1,* involve *nrde-2* but not *nrde-3* (BUCKLEY *et al.* 2012; BURKHART *et al.* 2011). Furthermore, *nrde-2* mutants have defects that *nrde-3* mutants do not, including germline mortality, suggesting that *nrde-2* responds to multiple inputs (GUANG *et al.* 2010). Additionally, at least four other loci were identified in the Nrde screen, suggesting that *nrde-3* may not function exclusively via *nrde-2*. Consequently, these observations may provide an explanation for why the *nrde-2* RNAi defects are less penetrant than *nrde-3* RNAi defects (**Figure 4.1A, J**). We therefore limit our interpretation of *nrde-2* results as an approximate confirmation of *nrde-3*'s RNAi functions within the nucleus.

nrde-3 is required for enhanced RNAi in *eri* mutants

Eri mutants are depleted for endogenous siRNAs, which are proposed to compete with exogenous siRNAs for silencing resources. It is this absence of competition for limiting RNAi resources that presumably accounts for enhanced exo-RNAi efficacy (**Figure 4.5**). *sago-1* has previously been proposed to be a downstream effector of the *eri* pathway, not because its absence attenuates the Eri phenotype, but because its over-expression relieves the competition for this limiting resource (YIGIT *et al.* 2006). Here we show that *nrde-3* is Rde (**Figure 4.1A**),

thus establishing a role for NRDE-3 in the exo-RNAi pathway. We also show that *nrde-3* mutations disrupt the expression of endogenous siRNA regulated genes (**Figure 4.8A**), confirming a role for NRDE-3 in the endogenous RNAi pathway(s). We then show that loss of *nrde-3* attenuates the Eri phenotype, at least for some genes (**Table 4.8**). Finally, we show that, like *sago-1*, over-expression enhances RNAi (**Figure 4.4A-C**). This preponderance of evidence supports a role for *nrde-3* as a downstream effector of the *eri* pathway.

Transitive RNAi and *nrde-3*'s contributions to RNAi

The result that transitive RNAi was not detectable in *nrde-3* mutants (**Figure 4.7**) may provide insight into the role of nuclear RNAi. The contribution of NRDE-3 to RNAi was most apparent when dsRNA is limiting (**Figure 4.1A**), thus it is reasonable to infer that trans-acting siRNAs are also limiting. This can be readily explained by the favorable stoichiometric ratio of siRNAs to expressed loci in the nucleus versus exported transcripts in the cytoplasm. While a relative few siRNAs may be sufficient to silence a gene in the nucleus, they would be insufficient to silence hundreds or thousands of cytoplasmic transcripts. This implies that, while at high dsRNA dose PTGS mechanisms are sufficient to enable *nrde-3*-independent silencing, at low dsRNA dose, the primary gene silencing response may be nuclear-based transcriptional gene silencing.

This model of complementary cytoplasmic and nuclear RNAi silencing processes also provides an attractive explanation for the enhanced silencing of both multi-gene families and multi-copy transgenes. In both cases, partial or incomplete gene silencing will not produce a phenotype, providing an explanation for why these target genes show exceptionally strong enhanced RNAi potential. For example, because *dpy-13(RNAi)* causes a much stronger Dpy phenotype than does a *dpy-13* null allele, it is likely that the RNAi targets other functionally

redundant collagen genes. In fact, the ingested *dpy-13* dsRNA trigger corresponds directly to a conserved collagen domain with near perfect identity with at least 30 other collagen members (COX 1985). Thus, a limited number of siRNAs targeting this conserved region could – if efficiently imported into the nucleus – effectively silence many genes in the nucleus, but would be ineffective targeting the very abundant cytoplasmic collagen transcripts. This model does not provide an explanation for *nrde-3*-dependent enhanced operon silencing; however, only two operons out of over 1300 *C. elegans* operons have been shown to be sensitive to *eri*-enhanced silencing.

Non-allelic background effects of *rrf-3(pk1426)*

Amongst the *eri* mutants, *rrf-3(pk1426)* has frequently been used as a reference allele for enhanced RNAi. In fact, it was the first Eri reported (SIMMER *et al.* 2002), first Eri implicated in endogenous gene regulation (GENT *et al.* 2009; PAVELEC *et al.* 2009), amongst the first Eri deep-sequenced for its endogenous small RNA profile (GENT *et al.* 2010), and is phenotypically the most robust (ZHUANG and HUNTER 2011). However, this allele has had two reported discrepancies. First, although it is phenotypically almost identical to *eri-1(mg366)*, two different groups reported that its gene expression profile is drastically different from e*ri-1(mg366)* (ASIKAINEN *et al.* 2007; LEE *et al.* 2006). Second, biochemical analysis indicates that the *rrf-3(pk1426)* mutant fails to form a RRF-3/ERI-5/DCR-1 endo-RNAi protein complex that is formed in the *rrf-3(mg373)* missense mutant (THIVIERGE *et al.* 2011).

Our results suggest that there's no simplistic model which could explain all the discrepancies in the *rrf-3(pk1426)* background. It is not a simple background Rde, because a rescued strain is still partially Eri (**Table 4.12**) and *rrf-3(pk1426)* exogenous RNAi seems more

robust (**Figure 4.9B**). It is not a simple background Eri, because a *rrf-3(pk1426);nrde-3(gg66)* double mutant is weaker in its RNAi responses than the *rrf-3(mg373);nrde-3(gg66)* and *rrf-3(pk2042);nrde-3(gg66)* double mutants (**Table 4.12**). Furthermore, our observations that *rrf-3(pk1426/mg373);nrde-3(gg66)* trans-heterozygotes behave mostly like *rrf-3(pk1426);nrde-3(gg66)* do not suggest simple recessive background effect(s) (**Table 4.12**).

Fortunately, it seems like most of the previously reported analysis of *rrf-3(pk1426)* is still valid. For instance, endo-siRNA targets found in the *rrf-3(pk1426)* background (GENT *et al.* 2010) seem to be confirmed in the *rrf-3(mg373)* background as well (**Figure 4.8A**), which makes us comfortable in using that reference dataset. With the three exceptions we described (**Table 4.12; Figure 4.9**), *rrf-3(pk1426)* seems to behave the same as all the other Eri mutants in all the rest of our analysis. Previously reported reference datasets of *rrf-3(pk1426)*, however, should still be used with caution without second-allele verification.

Endo-siRNA targeting and transgenes silencing are endogenous NRDE-3 functions

The depletion of endo-siRNAs that apparently underlies many *nrde-3*-dependent Eri phenotypes suggests that *nrde-3* might have a role in endo-siRNA target gene regulation. Indeed, similar to the *eri* mutants, we found that loss of *nrde-3* affects the gene expression of *eri* endo-siRNA targets (**Figure 4.8A**), supporting the hypothesis that endo-siRNAs mediate TGS in somatic cells. This is consistent with recent reports of *nrde-1,-2, and -4* functions in the germline, including transmission and maintenance of gene silencing (BUCKLEY *et al.* 2012).

Furthermore, it may be noteworthy that *eri-6/7* endo-siRNA targets show enrichment for duplicated genes (FISCHER *et al.* 2011), which suggests that RNAi targeting specific gene structures may indeed be a possible mechanism of action. An artificial analog to endogenous

repetitive arrays in the *C. elegans* genome is transgenes, because simple transgenic arrays are often incorporated as repetitive elements (PRAITIS *et al.* 2001). Our discovery of *nrde-3*'s contribution to transgene silencing in both Eri and non-Eri backgrounds further supports the broad endogenous roles *nrde-3* may play. These findings thus begin to form the funnel of broad upstream roles in endogenous and exogenous nuclear RNAi that ultimately channels into downstream effectors like the germline nuclear Ago *hrde-1* that impact fundamental biological processes such as germline maintenance.

MATERIALS AND METHODS

Strains: The following strains were used: (FX1917) *eri-6/7(tm1917)*, (GR1373) *eri-1(mg366)*, (HC195) *nrIs20 (sur-5::NLS-GFP)*, (HC745) *eri-1(mg366);nrIs20*, (HC758) *eri-1(mg366);nrde-3(gg66)*, (HC759) *eri-1(mg366);nrde-3(gg64)*, (HC760) *rrf-3(pk1426);nrde-3(gg66)*, (HC761) *eri-6/7(tm1917);nrde-3(gg66)*, (HC762) *eri-8(gg100);nrde-3(gg66)*, (HC763) *eri-1(mg366);vpIs9*, (HC764) *eri-1(mg366);nrde-3(gg66);vpIs9*, (HC765) *nrde-3(gg66);nrIs20*, (HC766) *eri-1(mg366);nrde-3(gg66);nrIs20*, (HC767) *rrf-3(pk1426);nrde-3(gg66);nrIs20*, (HC792) *eri-1(mg366);nrde-2(gg91)*, (HC794) *nrde-3(gg66);ggls01(nrde-3p::FLAG3x-gfp-nrde-3)*, (HC824) *nrde-2(gg91) nrIs20*, (HC831) *nrde-3(gg66); vpIs9*, (HC833) *eri-1(mg366) nrde-2(gg91) nrIs20*, (HC838) *eri-1(mg366); nrde-3(gg66); (nrde-3p::FLAG3x-gfp-nrde-3; *NLS)*, (HC839) *nrde-3(gg66);(nrde-3p::FLAG3x-gfp-nrde-3; *NLS);vpIs9*, (HC840) *rrf-3(mg373);nrde-3(gg66)*, (HC848) *nrde-3(gg66); (nrde-3p::FLAG3x-gfp-nrde-3; *NLS, SV40NLS); vpIs9*, (HC860) *nrde-3(gg66); neIs11*, (HC888) *rrf-3(pk2042)*, (HC889) *rrf-3(pk2042); nrde-3(gg66)*, (HC891) *(nrde-3p::FLAG3x-gfp-nrde-3; *NLS)*, (HC895) *rrf-3(mg373); nrIs20; nrde-3(gg66)*, (HC896) *rrf-3(pk1426); (rrf-3p::rrf-3; myo-3p::dsRed)*, (JG33)

vpIs9 (unc-119(+) + elt-1::GFP), (NL2099) *rrf-3(pk1426)*, (WM120) *Mago; neIs11(myo-3p::GFP::sago-1 + pRF4(rol-6(su1006)))*, (YY13) *rrf-3(mg373)*, (YY158) *nrde-3(gg66)*, (YY168) *eri-8(gg100)*, (YY174) *ggIs01(nrde-3p::FLAG3x-gfp-nrde-3)*, (YY186) *nrde-2(gg91)*, (YY238) *nrde-3(gg64),* (YY298) *nrde-3(gg66); (nrde-3p::FLAG3x-gfp-nrde-3;*NLS)*, and (YY362) *nrde-3(gg66); (nrde-3p::FLAG3x-gfp-nrde-3; *NLS,SV40NLS)*.

All strains tested wild type for the *mut-16(mg461)* background Rde allele. All strains and assays were maintained and performed at 20ºC as previously described (BRENNER 1974), except where indicated. The YY298 and YY362 strains that affect the nuclear localization signal of *nrde-3* were previously characterized (GUANG *et al.* 2008) and used in the same context as our experiments. The YY174 strain that rescues *nrde-3(gg66)* was previously characterized (GUANG *et al.* 2008) and used in the same context as our experiments. All three transgenes were documented to be expressed at comparable levels as wild type *nrde-3*. The WM120 strain that causes an Eri phenotype by *sago-1* overexpression was also previously characterized (YIGIT *et al.* 2006) and used in the same context as our experiments.

RNAi: RNAi assays were performed as previously described (TIMMONS and FIRE 1998). Bacteria engineered to express dsRNA against genes listed in **Table 4.1** were obtained from the Ahringer library (KAMATH and AHRINGER 2003) and verified by sequencing. Bacteria engineered to express dsRNA against *gfp* were prepared as previously described (WINSTON *et al.* 2002). All RNAi assays involving the dilution series were performed as previously described (ZHUANG and HUNTER 2011), unless explicitly stated otherwise. Briefly, individual L3 animals were placed on RNAi food at the indicated concentrations and their progeny were scored for previously published knockdown phenotypes. Feeding RNAi assays from the L1 were performed

by hypochlorite treating gravid adults on RNAi plates and scoring the surviving embryos in the same generation. All feeding RNAi assays were performed in triplicate and repeated three times. The penetrance shown is representative of all the assays performed.

The (JG33) *elt-1-gfp* strain was previously described (SMITH *et al.* 2005). In performing the transitive RNAi assay (**Figure 4.7**), knockdown of *gfp* levels was consistent across all strains tested, ensuring that the intake of dsRNA trigger was unaffected. In previously published transitive RNAi assays, the *elt-1-gfp* transgene was deemed the most efficacious in causing transitive RNAi (ALDER *et al.* 2003). The *vpIs9 (unc-119(+) + elt-1::GFP)* insertion is <2cM from *nrde-2*, and we were thus not able to make the *nrde-2(gg91);elt-1-gfp* double mutant.

Reverse transcription quantitative PCR: Hatch-synchronized (within 1 hour) mid-L4 worms from five NG large plates grown at 15ºC for 91 hours were pooled, washed extensively (M9) and allowed to swim for 20 minutes to clear gut content. RNA was isolated with Trizol (Invitrogen) followed by phenol:chloroform extraction (Amresco). The RNA pellets were subjected to DNase I (Roche) treatment, removed by RNeasy (Qiagen) per manufacturer's instruction. All RNA stock concentrations were adjusted to 150 ng/µL.

Reverse transcription was performed using 300 ng of input RNA by Thermoscript RT (Invitrogen), using gene specific RT primers (available upon request). cDNA quantification was performed using 2 µL of the 20 µL RT reaction in a 50 µL QuantiTect SYBR Green (Qiagen) reaction with nested PCR primers. The PCR reaction cycles were: 15 minutes 95 degrees, 15 seconds 94 degrees, 30 seconds 52 degrees, 1 minute 72 degrees, read, cycle to step 2 for 45 cycles, using an Eppendorf Mastercycler Realplex4 and Noiseband quantification. Subsequent analysis was performed using a ΔΔCT approach (LIVAK and SCHMITTGEN 2001), using *gpd-3*

RNA levels for normalization (WELKER *et al.* 2010), as previously described (ZHUANG and HUNTER 2012).

Cross Progeny Assays: Males were marked by the *sur-5::gfp* transgene while hermaphrodites were unmarked. Only green cross progeny were scored in all assays.

Transgene Silencing Assay: Hatch-synchronized (within 1 hour) young adult worms grown at 20ºC for 53 hours were imaged, at the same magnification and exposure for all strains indicated in **Fig. 4**. Outlined individual worms were analyzed using ImageJ (National Institutes of Health) by first "subtract background" and then "measure" functions for determining *gfp*-intensity units.

Penetrance calculations and statistical notes: All penetrance results were representative of at least three independent trials performed in triplicate. All assays with binary phenotypic penetrances (i.e. Dpy or WT) are represented by individual trials and their standard deviations or a representative trial set. All assays with trinomial phenotypic penetrances (i.e. emb. lethal, dev. arrest, or WT) are represented by sums of all trials; breakdown of individual trials are available upon request. All error bars indicate standard deviation. *p*-values calculated by *t*-test; * indicates $p<0.05$ and ** indicates $p<0.01$.

LITERATURE CITED

ALDER, M. N., S. DAMES, J. GAUDET and S. E. MANGO, 2003 Gene silencing in Caenorhabditis elegans by transitive RNA interference. RNA **9:** 25-32.

ASIKAINEN, S., M. STORVIK, M. LAKSO and G. WONG, 2007 Whole genome microarray analysis of C. elegans rrf-3 and eri-1 mutants. FEBS Lett **581:** 5050-5054.

BOSHER, J. M., P. DUFOURCQ, S. SOOKHAREEA and M. LABOUESSE, 1999 RNA interference can target pre-mRNA: consequences for gene expression in a Caenorhabditis elegans operon. Genetics **153:** 1245-1256.

BRENNER, S., 1974 The genetics of Caenorhabditis elegans. Genetics **77:** 71-94.

BUCKLEY, B. A., K. B. BURKHART, S. G. GU, G. SPRACKLIN, A. KERSHNER *et al.*, 2012 A nuclear Argonaute promotes multigenerational epigenetic inheritance and germline immortality. Nature.

BURKHART, K. B., S. GUANG, B. A. BUCKLEY, L. WONG, A. F. BOCHNER *et al.*, 2011 A pre-mRNA-associating factor links endogenous siRNAs to chromatin regulation. PLoS Genet **7:** e1002249.

BURTON, N. O., K. B. BURKHART and S. KENNEDY, 2011 Nuclear RNAi maintains heritable gene silencing in Caenorhabditis elegans. Proc Natl Acad Sci U S A **108:** 19683-19688.

COX, G. N., CARR, STEPHEN, KRAMER, JAMES M., AND HIRSH, DAVID, 1985 Genetic mapping of Caenorhabditis elegans collagen genes using dna polymorphisms as phenotypic markers. Genetics **109:** 513-528.

DUCHAINE, T. F., J. A. WOHLSCHLEGEL, S. KENNEDY, Y. BEI, D. CONTE, JR. *et al.*, 2006 Functional proteomics reveals the biochemical niche of C. elegans DCR-1 in multiple small-RNA-mediated pathways. Cell **124:** 343-354.

FIRE, A., S. XU, M. K. MONTGOMERY, S. A. KOSTAS, S. E. DRIVER *et al.*, 1998 Potent and specific genetic interference by double-stranded RNA in Caenorhabditis elegans. Nature **391:** 806-811.

FISCHER, S. E., M. D. BUTLER, Q. PAN and G. RUVKUN, 2008 Trans-splicing in C. elegans generates the negative RNAi regulator ERI-6/7. Nature **455:** 491-496.

FISCHER, S. E., T. A. MONTGOMERY, C. ZHANG, N. FAHLGREN, P. C. BREEN *et al.*, 2011 The ERI-6/7 helicase acts at the first stage of an siRNA amplification pathway that targets recent gene duplications. PLoS Genet **7:** e1002369.

GENT, J. I., A. T. LAMM, D. M. PAVELEC, J. M. MANIAR, P. PARAMESWARAN *et al.*, 2010 Distinct phases of siRNA synthesis in an endogenous RNAi pathway in C. elegans soma. Mol Cell **37:** 679-689.

GENT, J. I., M. SCHVARZSTEIN, A. M. VILLENEUVE, S. G. GU, V. JANTSCH *et al.*, 2009 A Caenorhabditis elegans RNA-directed RNA polymerase in sperm development and endogenous RNA interference. Genetics **183:** 1297-1314.

GRISHOK, A., H. TABARA and C. C. MELLO, 2000 Genetic requirements for inheritance of RNAi in C. elegans. Science **287:** 2494-2497.

GU, S. G., J. PAK, S. GUANG, J. M. MANIAR, S. KENNEDY *et al.*, 2012 Amplification of siRNA in Caenorhabditis elegans generates a transgenerational sequence-targeted histone H3 lysine 9 methylation footprint. Nat Genet **44:** 157-164.

GUANG, S., A. F. BOCHNER, K. B. BURKHART, N. BURTON, D. M. PAVELEC *et al.*, 2010 Small regulatory RNAs inhibit RNA polymerase II during the elongation phase of transcription. Nature **465:** 1097-1101.

GUANG, S., A. F. BOCHNER, D. M. PAVELEC, K. B. BURKHART, S. HARDING *et al.*, 2008 An Argonaute transports siRNAs from the cytoplasm to the nucleus. Science **321:** 537-541.

HANNON, G. J., 2002 RNA interference. Nature **418:** 244-251.

JOSE, A. M., J. J. SMITH and C. P. HUNTER, 2009 Export of RNA silencing from C. elegans tissues does not require the RNA channel SID-1. Proc Natl Acad Sci U S A **106:** 2283-2288.

KAMATH, R. S., and J. AHRINGER, 2003 Genome-wide RNAi screening in Caenorhabditis elegans. Methods **30:** 313-321.

KENNEDY, S., D. WANG and G. RUVKUN, 2004 A conserved siRNA-degrading RNase negatively regulates RNA interference in C. elegans. Nature **427:** 645-649.

KIM, J. K., H. W. GABEL, R. S. KAMATH, M. TEWARI, A. PASQUINELLI *et al.*, 2005 Functional genomic analysis of RNA interference in C. elegans. Science **308:** 1164-1167.

LEE, R. C., C. M. HAMMELL and V. AMBROS, 2006 Interacting endogenous and exogenous RNAi pathways in Caenorhabditis elegans. RNA **12:** 589-597.

LIVAK, K. J., and T. D. SCHMITTGEN, 2001 Analysis of relative gene expression data using real-time quantitative PCR and the 2(-Delta Delta C(T)) Method. Methods **25:** 402-408.

PAK, J., and A. FIRE, 2007 Distinct populations of primary and secondary effectors during RNAi in C. elegans. Science **315:** 241-244.

PAK, J., J. M. MANIAR, C. C. MELLO and A. FIRE, 2012 Protection from Feed-Forward Amplification in an Amplified RNAi Mechanism. Cell **151:** 885-899.

PAVELEC, D. M., J. LACHOWIEC, T. F. DUCHAINE, H. E. SMITH and S. KENNEDY, 2009 Requirement for the ERI/DICER complex in endogenous RNA interference and sperm development in Caenorhabditis elegans. Genetics **183:** 1283-1295.

PRAITIS, V., E. CASEY, D. COLLAR and J. AUSTIN, 2001 Creation of low-copy integrated transgenic lines in Caenorhabditis elegans. Genetics **157:** 1217-1226.

SIMMER, F., M. TIJSTERMAN, S. PARRISH, S. P. KOUSHIKA, M. L. NONET *et al.*, 2002 Loss of the putative RNA-directed RNA polymerase RRF-3 makes C. elegans hypersensitive to RNAi. Curr Biol **12:** 1317-1319.

SMITH, J. A., P. MCGARR and J. S. GILLEARD, 2005 The Caenorhabditis elegans GATA factor elt-1 is essential for differentiation and maintenance of hypodermal seam cells and for normal locomotion. J Cell Sci **118:** 5709-5719.

TABARA, H., M. SARKISSIAN, W. G. KELLY, J. FLEENOR, A. GRISHOK *et al.*, 1999 The rde-1 gene, RNA interference, and transposon silencing in C. elegans. Cell **99:** 123-132.

TABARA, H., E. YIGIT, H. SIOMI and C. C. MELLO, 2002 The dsRNA binding protein RDE-4 interacts with RDE-1, DCR-1, and a DExH-box helicase to direct RNAi in C. elegans. Cell **109:** 861-871.

THIVIERGE, C., N. MAKIL, M. FLAMAND, J. J. VASALE, C. C. MELLO *et al.*, 2011 Tudor domain ERI-5 tethers an RNA-dependent RNA polymerase to DCR-1 to potentiate endo-RNAi. Nat Struct Mol Biol **19:** 90-97.

TIMMONS, L., and A. FIRE, 1998 Specific interference by ingested dsRNA. Nature **395:** 854.

VASTENHOUW, N. L., K. BRUNSCHWIG, K. L. OKIHARA, F. MULLER, M. TIJSTERMAN *et al.*, 2006 Gene expression: long-term gene silencing by RNAi. Nature **442:** 882.

WELKER, N. C., D. M. PAVELEC, D. A. NIX, T. F. DUCHAINE, S. KENNEDY *et al.*, 2010 Dicer's helicase domain is required for accumulation of some, but not all, C. elegans endogenous siRNAs. RNA **16:** 893-903.

WINSTON, W. M., C. MOLODOWITCH and C. P. HUNTER, 2002 Systemic RNAi in C. elegans requires the putative transmembrane protein SID-1. Science **295:** 2456-2459.

WOO, W. M., A. GONCHAROV, Y. JIN and A. D. CHISHOLM, 2004 Intermediate filaments are required for C. elegans epidermal elongation. Dev Biol **267:** 216-229.

YIGIT, E., P. J. BATISTA, Y. BEI, K. M. PANG, C. C. CHEN *et al.*, 2006 Analysis of the C. elegans Argonaute family reveals that distinct Argonautes act sequentially during RNAi. Cell **127:** 747-757.

ZHANG, C., T. A. MONTGOMERY, H. W. GABEL, S. E. FISCHER, C. M. PHILLIPS *et al.*, 2011 mut-16 and other mutator class genes modulate 22G and 26G siRNA pathways in Caenorhabditis elegans. Proc Natl Acad Sci U S A **108:** 1201-1208.

ZHUANG, J. J., and C. P. HUNTER, 2011 Tissue Specificity of Caenorhabditis elegans Enhanced RNA Interference Mutants. Genetics **188:** 235-237.

ZHUANG, J. J., and C. P. HUNTER, 2012 The Influence of Competition Among C. elegans Small RNA Pathways on Development. Genes **3:** 671-685.

Chapter Five

Enhanced RNAi is dependent on *pgl-1*

The majority of the contents are a part of the in-press report ZHUANG, J. J., S.A. BANSE, and C. P. HUNTER, 2013. The Nuclear Argonaute NRDE-3 Contributes to Transitive RNAi in *Caenorhabditis elegans*. *Genetics* **doi: 10.1534/genetics. 113.149765**. Permission to reuse was granted by the Genetics Society of America.

ABSTRACT

We identified *pgl-1* as an additional limiting RNAi resource important for *eri*-dependent silencing of a non-overlapping subset of target genes to *nrde-3*, so that an *nrde-3; pgl-1; eri-1* triple mutant fails to show enhanced RNAi for any tested gene. These results suggest that *nrde-3* and *pgl-1* define separate and independent limiting RNAi resource pathways. We discovered that like NRDE-3, a PGL-1 functions to modulate endogenous siRNA gene regulation. However, we were unable to elucidate a mechanism of contribution for *pgl-1* after analyzing common RNAi mechanisms. Therefore, we prepared preliminary protocols for *C. elegans* small RNA sequencing in hopes of using the *pgl-1* mutant small RNA profile to better understand the mechanism of *pgl-1*'s roles in RNAi.

INTRODUCTION

Few concrete details are known about the function of PGL-1 and its interaction with RNAi. Some reports have suggested that it is as a component of germline perinuclear P-granule structures which are sites of mRNA export and possibly degradation (KAWASAKI *et al.* 1998; SHETH *et al.* 2010), and others have shown that these P-granules' structure or stability depends, at least indirectly, on RNAi components including CSR-1, EGO-1, DCR-1, DRH-3, PRG-1, and RDE-4 (BESHORE *et al.* 2011; CLAYCOMB *et al.* 2009; SPIKE *et al.* 2008; UPDIKE and STROME 2009). While PGL-1's link to RNAs is genetically and biochemically well-established (HANAZAWA *et al.* 2011; SCHISA *et al.* 2001), especially for those in the germline, there are conflicting reports on its role in RNAi. One report was unable to observe any effects on somatic RNAi via 3'UTR-targeted RNAi in a transgene (SHETH *et al.* 2010), while another report

suggested that germline RNAi silencing of a transgene was perturbed in a *pgl-1* mutant (ROBERT *et al.* 2005).

Perhaps the clearest link between RNAi and *pgl-1* was the observation that PGL-1 was overexpressed in the soma of an *rb* mutant, which is enhanced for RNAi (WANG *et al.* 2005). However, this enhanced RNAi was attributed more to the overall germline-to-soma transformation in an *rb* mutant, and *pgl-1* was simply used as a marker for demonstrating the presence of germline components. Indeed, a follow-up report showed that along with *pgl-1*, many germline components, including many involved in RNAi, were overexpressed an *rb* mutant's soma to induce enhanced RNAi (WU *et al.* 2012).

Here, we identify the peri-nuclear protein PGL-1 as important for the enhanced RNAi phenotypes of a non-overlapping subset of target genes to NRDE-3. These results thus define a unique and independent limiting RNAi resource pathway.

RESULTS

pgl-1 acts in parallel to *nrde-3*

Mutants that disrupt core RNAi functions, such as *rde-1* and *dcr-1*, have near 100 percent Rde penetrance (TABARA *et al.* 1999; TABARA *et al.* 2002), while the *nrde-3* Rde phenotype is only apparent at limiting dsRNA concentrations (**Figure 4.1A**). Furthermore, *nrde-3* is only essential for the enhanced RNAi phenotypes of a subset of target genes (**Table 4.8**). These observations indicate that *nrde-3* likely acts after the core RNAi components and that one or more additional post-core activities may act in parallel with *nrde-3* to mediate the full spectrum of enhanced RNAi phenotypes. The SAGOs are candidates for this parallel activity, as their overexpression enhances exo-RNAi independent of *nrde-3*. However, their functional redundancy (YIGIT *et al.*

2006) challenges analysis of *eri(-);sago(-)* double mutants. Therefore, to discover what other secondary RNAi pathways may act in parallel to *nrde-3*, we screened available mutants with functions associated with the nucleus for RNAi phenotypes analogous to *nrde-3(-)* mutants: weak Rde to exogenous RNAi and enhanced RNAi when overexpressed as a transgene (**Table 5.1**).

Among these mutants, the perinuclear P-granule component *pgl-1* emerged as a promising candidate. Like *nrde-3*, three different *pgl-1* mutant alleles were weakly Rde, while worms carrying a *pgl-1-gfp* transgene showed enhanced RNAi (**Figure 5.1A-C; Table 5.2**). To analyze the effects of *pgl-1* loss-of-function on the *eri-1* phenotype, we constructed and tested an *eri-1(mg366); pgl-1(bn101)* double mutant and an *eri-1(mg366); pgl-1(bn101); nrde-3(gg66)* triple mutant. Surprisingly, the *eri-1;pgl-1* double mutants maintained enhanced RNAi phenotypes for the target genes that require *nrde-3*, but failed to show enhanced RNAi phenotypes for the *nrde-3*-independent target genes (**Figure 5.1D, E**). The complementary nature of this pattern was confirmed by analyzing the *eri-1;pgl-1;nrde-3* triple mutant, which was non-Eri for all tested target genes (**Figure 5.1D, E**). A second allele, *pgl-1(bn102)*, behaved the same way (**Table 5.3**). The effect *pgl-1* loss had on enhanced RNAi was also observed for the other conserved Eri mutants: *rrf-3*, *eri-6/7*, and *ergo-1/eri-8* (**Table 5.3**). Finally, because PGL-1 is over-expressed in the *rb* mutants that enhance RNAi (WANG *et al.* 2005), we tested both *lin-15ab* and *lin-35* for *pgl-1* dependent Eri phenotypes. We found that *pgl-1(bn101);lin-15ab (n765)* and *pgl-1(bn101);lin-35(n745)* double mutants were non-Eri for the same subset of target genes as the *pgl-1(bn101); eri-1(mg366)* double mutants (**Table 5.3**). These results thus suggest *pgl-1* and *nrde-3* act as parallel activities that seemingly account for all *eri* mutant enhanced RNAi effects.

Table 5.1: Candidate screen of nuclear-associated factors with available mutants that may contribute to *nrde-3*-independent enhanced RNAi

Candidate	*dpy-11(RNAi)*	Annotation and Notes
N2 wild type	Dpy	**Almost completely penetrant**
ceh-30(n4289)	Dpy	Homeodomain protein
chd-3(ok1651)	**Mild Rde**	Chromodomain protein **Sensitive to *unc-22(RNAi)* and *bli-1(RNAi)* like WT**
daf-21(p673)	Dpy	Hsp90 chaperone
daf-3(ok3610)	Dpy	SMAD transcriptional regulator
daf-5(e1386)	Dpy	
daf-8(e1393)	Dpy	SMAD transcriptional regulator
efl-1(se1)	Dpy	E2F transcriptional repressor
egl-27(ok1670)	Dpy	MTA1 nucleosome remodeling deacetylase
gfl-1(gk321)	Dpy	ENL-class transcriptional factor
hpl-1(tm1624)	Dpy	Heterochromatin protein 1
let-418(n3536)	Dpy	CHD3 homolog nucleosome remodeling deacetylase
mab-10(e1248);him-5(e1490)	Dpy	
mes-1(ok2467)	Dpy	Receptor tyrosine kinase-like protein
mes-3(bn21)	Dpy	Polycomb chromatin repressive complex component
met-1(n4337)	Mild Eri	Histone methyltransferase **Mild Eri to *lir-1(RNAi)* as well**
mev-1(kn1)	Mild Eri	Cytochrome b integral membrane protein **Eri to *lir-1(RNAi)*, *dpy-13(RNAi)*, *unc-73(RNAi)*, and *hmr-1(RNAi)* as well**
pag-3(n3098)	Dpy	C2H2 zinc-finger protein
pgl-1(bn101)	**Rde**	RNA-binding protein with RGG box motifs **See data presented within text**
pop-1(hu9)	Mild Eri	TCF/LEF family transcription factor
prmt-5(gk357)	Dpy	Protein arginine Methyltransferase
sex-1(gk808)	Dpy	Nuclear hormone receptor family DNA-binding protein
sin-3(tm1276);him-5(e1490)	Dpy	Histone deacetylase subunit
sma-9(tm572)	Dpy	Zinc-finger domain protein
taf-11.1(gk648)	Dpy	TBP-associated transcription factor
taf-11.2(gk682)	Dpy	TBP-associated transcription factor
taf-4(ok1399)	**Rde**	TATA-binding protein associated factor **Rde to *unc-22*(RNAi), *bli-1*(RNAi), *lir-1*(RNAi), and *par-1*(RNAi) as well**
taf-7.1(gk696)	Dpy	TATA-binding protein associated factor
taf-9(ok2871)	Dpy	TBP-associated transcription factor
tag-235(ok1265)	Dpy	Histone Acetyltransferase
tbx-2(ut180)	Dpy	T-box transcription factor
unc-37(e262)	Dpy	Transducin-like WD-repeat protein
zag-1(zd86)	Dpy	ZFH class homeodomain protein
zfp-1(ok554)	Dpy	Leucin-zipper containing protein

The indicated strains were placed onto OD_{600nm} 1.0 *dpy-11(RNAi)* food as L3s and scored in the next generation. Any Rde phenotypes were followed up with additional RNAi tests as described.

Figure 5.1: Complementary contributions of *pgl-1* and *nrde-3* to *eri*-dependent enhanced RNAi phenotypes

(A) RNAi phenotypic penetrance for the indicated genes in N2 and three *pgl-1* alleles is shown. The progeny of L3 larvae placed on the RNAi food were scored as L4 larvae. The RNAi bacteria concentrations, phenotypes, and penetrances are listed in **Table 5.2**. *p*-values calculated by *t*-test; ** indicates $p<0.01$. **(B-C)** Representative images of progeny from L3 hermaphrodites of the indicated strains grown on *dpy-13(RNAi)* bacteria. **(D)** The severity of RNAi phenotypes, as described in **Table 4.8**, is based on expressivity measurements presented in **Table 4.1.** Representative examples are presented in **(E)**. Complete penetrances are tabulated in **Table 5.3**. The enhanced RNAi response targeting genes in operons or with many homologs (highlighted in yellow) is most dependent on *nrde-3*. The enhanced RNAi response targeting genes with few or no homologs (highlighted in green) is most dependent on *pgl-1*. The *eri-1*; *nrde-3*; *pgl-1* triple mutant (highlighted in salmon) is non-Eri. **(E)** Representative images of the expressivity of *dpy-13(RNAi)*, *unc-15(RNAi)*, and *unc-73(RNAi)* for the indicated strains is shown. The progeny of L3 larvae placed on the RNAi food were scored as L4 larvae. The stars correspond to RNAi responses as scored in **(D)**. The *eri-1(mg366);nrde-3(gg66)* double mutant is most like wild type in RNAi targeting genes with many homologs, like *dpy-13(RNAi)* (bracketed in yellow). The *eri-1(mg366);pgl-1(bn101)* double mutant is most like wild type in RNAi targeting unique genes, like *unc-73(RNAi)* (bracketed in green). The RNAi bacteria concentrations used in **(D)** and **(E)** were the same as **Table 4.8**.

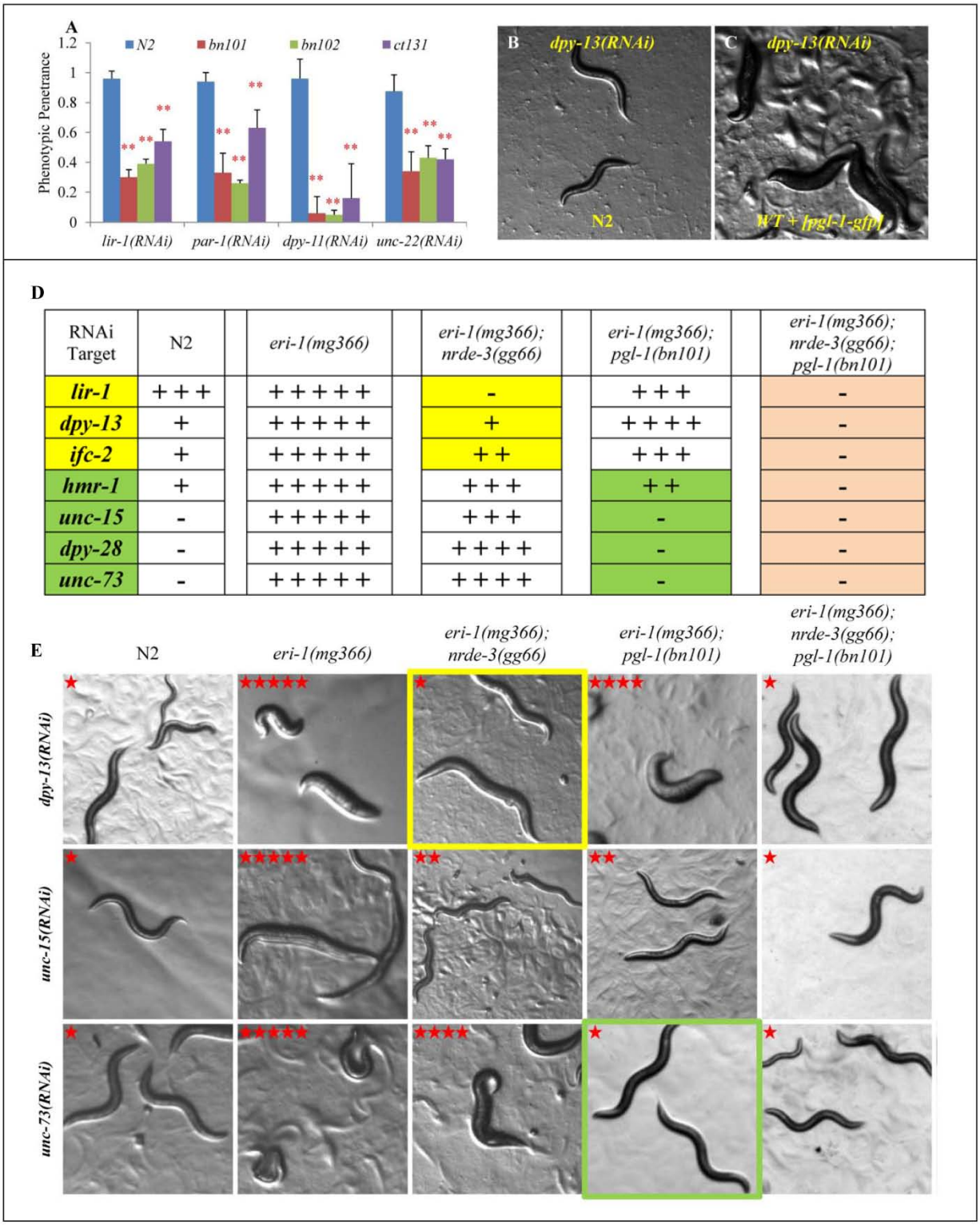

RNAi Target	N2	*eri-1(mg366)*	*eri-1(mg366); nrde-3(gg66)*	*eri-1(mg366); pgl-1(bn101)*	*eri-1(mg366); nrde-3(gg66); pgl-1(bn101)*
lir-1	+ + +	+ + + + +	-	+ + +	-
dpy-13	+	+ + + + +	+	+ + + +	-
ifc-2	+	+ + + + +	+ +	+ + +	-
hmr-1	+	+ + + + +	+ + +	+ +	-
unc-15	-	+ + + + +	+ + +	-	-
dpy-28	-	+ + + + +	+ + + +	-	-
unc-73	-	+ + + + +	+ + + +	-	-

Figure 5.1 (Continued): Complementary contributions of *pgl-1* and *nrde-3* to *eri*-dependent enhanced RNAi phenotypes

Table 5.2: Penetrance of Rde phenotypes of *pgl-1(bn101)*, *pgl-1(bn102)*, and *pgl-1(ct131)* mutants shown in **Figure 5.1A**

Strain	RNAi Food	Phenotype	Penetrance									Avg	SD
N2	*lir-1* OD_{600nm} 3.5	L1/L2 arrest	146/151	154/166	85/91	126/130	100/103	71/72				**0.96**	**0.02**
pgl-1(bn101)			37/126	39/124	18/94	52/169	27/74	19/61				**0.30**	**0.06**
pgl-1(bn102)			37/109	21/98	31/104	83/171	39/73	55/116				**0.39**	**0.13**
pgl-1(ct131)			19/49	9/21	64/90	56/126	44/76	37/62	63/94	55/117	53/93	**0.54**	**0.11**
N2	*par-1* OD_{600nm} 2.0	Embryonic lethality	167/180	170/192	157/158	162/167	133/144	138/157				**0.93**	**0.05**
pgl-1(bn101)			31/129	62/122	31/170	71/141	70/237	79/195	34/95	8/47		**0.33**	**0.13**
pgl-1(bn102)			22/110	14/102	34/139	58/175	85/207					**0.26**	**0.11**
pgl-1(ct131)			16/31	66/118	99/128	54/115	115/165	77/100	120/155	86/135	23/50	**0.63**	**0.13**
N2	*dpy-11* OD_{600nm} 4.0	Very dumpy worms	73/80	89/91	114/119	87/88	80/83	92/94				**0.96**	**0.03**
pgl-1(bn101)			2/48	8/92	2/84	7/112	3/38	3/55				**0.06**	**0.02**
pgl-1(bn102)			3/59	4/40	2/52	5/79	1/47	3/64				**0.05**	**0.03**
pgl-1(ct131)			5/33	6/42	3/13	5/47	3/26	11/32	5/41	4/38		**0.16**	**0.08**
N2	*unc-22* OD_{600nm} 3.0	Paralyzed sticks	88/92	51/59	50/62	55/62	56/69					**0.87**	**0.06**
pgl-1(bn101)			11/47	9/46	6/35	11/29	10/28	10/24	9/17	9/22		**0.34**	**0.12**
pgl-1(bn102)			4/13	12/25	19/28	30/38	5/26	16/51	9/35			**0.43**	**0.23**
pgl-1(ct131)			2/7	10/21	21/40	5/13	5/13	14/32	5/12	5/11		**0.42**	**0.07**

Table 5.3: Penetrance readings for Eri mutants' partial requirement of *pgl-1* for enhanced RNAi

The RNAi phenotypes whose penetrances are tabulated and their corresponding descriptions for I, II, and III are listed in **Table 4.1**. The RNAi bacteria OD_{600nm} concentrations used were the same as **Table 4.8**. The *eri*-class enhanced RNAi response against gene targets most dependent on *pgl-1* holds the same pattern of RNAi responses as *eri-1(mg366)* and *eri-1(mg366);pgl-1(bn101)* for *rrf-3(pk1426)*, *eri-6/7(tm1917)*, *eri-8(tm1860)*, and their doubles with *pgl-1(bn101)*. The impact on the enhanced RNAi response for *pgl-1(bn102)* holds the same pattern of RNAi responses as *pgl-1(bn101)* mutants. The *eri-1(mg366);nrde-3(gg66);pgl-1(bn101)* strain is completely wild type in its response to all tested RNAi targets. The *rb*-class (*lin-15ab(n765)* and *lin-35(n745)*) enhanced RNAi response against gene targets do not depend on *nrde-3(gg66)*, but against gene targets most dependent on *pgl-1* in the *eri*-class, the *lin-15ab(n765);pgl-1(bn101)* and *lin-35(n745);pgl-1(bn101)* mutants hold the same pattern of RNAi responses as *eri-1(mg366);pgl-1(bn101)*.

Table 5.3 (Continued): Penetrance readings for Eri mutants' partial requirement of *pgl-1* for enhanced RNAi

RNAi Target	N2	*pgl-1 (bn101)*	*eri-1 (mg366)*	*eri-1 (mg366); pgl-1 (bn101)*	*eri-1 (mg366); pgl-1 (bn102)*	*eri-1 (mg366); pgl-1 (bn101); nrde-3 (gg66)*	*rrf-3 (pk1426)*	*rrf-3 (pk1426); pgl-1 (bn101)*	*eri-6/7 (tm1917)*	*eri-6/7 (tm1917); pgl-1 (bn101)*	*eri-8 (tm1860)*	*eri-8 (tm1860); pgl-1 (bn101)*	*lin-15ab (n765)*	*lin-15ab (n765); nrde-3 (gg66)*	*lin-15ab (n765); pgl-1 (bn101)*	*lin-35 (n745)*	*lin-35 (n745); nrde-3 (gg66)*	*lin-35 (n745); pgl-1 (bn101)*
lir-1	I: 0.02 II: 0.98 III: 0.00 n=83	I: 0.67 II: 0.22 III: 0.11 n=164	I: 0.00 II: 0.00 III: 1.00 n=89	I: 0.15 II: 0.69 III: 0.16 n=355	I: 0.05 II: 0.50 III: 0.45 n=312	I: 1.00 II: 0.00 III: 0.00 n=90	I: 0.00 II: 0.00 III: 1.00 n=84	I: 0.22 II: 0.70 III: 0.08 n=80	I: 0.00 II: 0.00 III: 1.00 n=75	I: 0.04 II: 0.61 III: 0.35 n=23	I: 0.00 II: 0.00 III: 1.00 n=97	I: 0.08 II: 0.92 III: 0.00 n=153	I: 0.00 II: 0.00 III: 1.00 n=106	I: 0.13 II: 0.87 III: 0.00 n=55	I: 0.09 II: 0.91 III: 0.00 n=138	I: 0.00 II: 0.00 III: 1.00 n=57	I: 0.08 II: 0.78 III: 0.14 n=88	I: 0.25 II: 0.56 III: 0.19 n=109
dpy-13	I: 0.93 II: 0.07 III: 0.00 n=121	I: 1.00 II: 0.00 III: 0.00 n=141	I: 0.00 II: 0.01 III: 0.99 n=70	I: 0.15 II: 0.15 III: 0.70 n=88	I: 0.00 II: 0.19 III: 0.81 n=63	I: 1.00 II: 0.00 III: 0.00 n=40	I: 0.00 II: 0.00 III: 1.00 n=156	I: 0.07 II: 0.05 III: 0.88 n=57	I: 0.00 II: 0.00 III: 1.00 n=64	I: 0.16 II: 0.27 III: 0.57 n=37	I: 0.00 II: 0.00 III: 1.00 n=170	I: 0.21 II: 0.05 III: 0.74 n=58	I: 0.00 II: 0.23 III: 0.67 n=97	I: 0.00 II: 0.20 III: 0.80 n=99	I: 0.08 II: 0.22 III: 0.70 n=53	I: 0.00 II: 0.30 III: 0.70 n=101	I: 0.00 II: 0.21 III: 0.79 n=63	I: 0.00 II: 0.36 III: 0.64 n=33
ifc-2	0.09 n=137	0.06 n=188	0.51 n=81	0.23 n=228	0.32 n=82	0.05 n=153	0.76 n=134	0.43 n=60	0.50 n=56	0.33 n=27	0.51 n=71	0.43 n=60	0.40 n=45	0.40 n=182	0.28 n=64	0.33 n=153	0.21 n=124	0.32 n=76
unc-15	I: 0.94 II: 0.06 III: 0.00 n=106	I: 0.99 II: 0.01 III: 0.00 n=146	I: 0.00 II: 0.12 III: 0.88 n=67	I: 0.67 II: 0.23 III: 0.00 n=270	I: 0.41 II: 0.59 III: 0.00 n=95	I: 0.94 II: 0.06 III: 0.00 n=103	I: 0.00 II: 0.03 III: 0.94 n=80	I: 0.69 II: 0.31 III: 0.00 n=51	I: 0.00 II: 0.04 III: 0.96 n=114	I: 0.72 II: 0.28 III: 0.00 n=18	I: 0.00 II: 0.17 III: 0.83 n=70	I: 0.28 II: 0.72 III: 0.00 n=46	I: 0.30 II: 0.70 III: 0.00 n=63	I: 0.30 II: 0.70 III: 0.00 n=40	I: 0.35 II: 0.65 III: 0.00 n=88	I: 0.33 II: 0.67 III: 0.00 n=110	I: 0.50 II: 0.50 III: 0.00 n=52	I: 0.73 II: 0.27 III: 0.00 n=44
hmr-1	I: 0.94 II: 0.06 III: 0.00 n=72	I: 0.89 II: 0.05 III: 0.06 n=125	I: 0.00 II: 0.00 III: 1.00 n=34	I: 1.00 II: 0.00 III: 0.00 n=100	I: 0.73 II: 0.03 III: 0.24 n=186	I: 1.00 II: 0.00 III: 0.00 n=116	I: 0.00 II: 0.00 III: 1.00 n=61	I: 1.00 II: 0.00 III: 0.00 n=158	I: 0.00 II: 0.00 III: 1.00 n=121	I: 0.89 II: 0.11 III: 0.00 n=54	I: 0.00 II: 0.00 III: 1.00 n=136	I: 1.00 II: 0.00 III: 0.00 n=76	I: 0.11 II: 0.23 III: 0.66 n=184	I: 0.62 II: 0.32 III: 0.06 n=117	I: 1.00 II: 0.00 III: 0.00 n=116	I: 0.23 II: 0.11 III: 0.66 n=62	I: 0.66 II: 0.22 III: 0.12 n=94	I: 0.66 II: 0.32 III: 0.02 n=91
dpy-28	0.00 n=14	0.00 n=60	0.79 n=43	0.00 n=140	0.02 n=123	0.00 n=100	0.67 n=21	0.00 n=58	0.70 n=67	0.00 n=17	0.69 n=36	0.00 n=68	0.65 n=34	0.74 n=74	0.00 n=65	0.68 n=31	0.64 n=64	0.22 n=68
unc-73	0.00 n=38	0.01 n=205	0.96 n=45	0.00 n=100	0.01 n=142	0.00 n=40	1.00 n=122	0.00 n=59	1.00 n=96	0.00 n=40	0.94 n=136	0.07 n=121	0.77 n=61	0.69 n=152	0.00 n=96	0.36 n=142	0.34 n=74	0.05 n=81

pgl-1 acts to regulate endo-RNAi target gene expression

NRDE-3 interacts with endo-siRNAs and is required to regulate *rrf-3* endo-siRNA target genes (**Figure 4.8A**) (GUANG *et al.* 2008). To determine whether *pgl-1* is also required for endo-siRNA target gene regulation, we used qPCR to measure the RNA levels for seven endo-siRNA regulated genes in embryos, L4 larvae, and mixed stage worms, comparing wild-type, *rrf-3*, and *pgl-1* mutants. In all three conditions, a subset of these genes showed significant changes in the *pgl-1* mutant compared to wild type (**Figure 5.2A-C**), although we failed to discern a definitive pattern among these changes. However, despite our lack of mechanistic insight, our results suggest that *pgl-1* is important for endo-siRNA regulated gene expression via a process that may compete with exogenous RNAi.

Possible mechanisms of *pgl-1*'s contribution to enhanced RNAi

Our observations that a *pgl-1* mutant is weakly defective for RNAi against both germline and somatic targets in both Eri and non-Eri backgrounds (**Figure 5.1A, D**) leads us to believe that *pgl-1* is indeed involved in RNAi. These RNAi assays were performed via standard feeding of L3 mothers and scoring in the next generation; we were unable to observe a difference between N2 wild type and *pgl-1* mutants' *dpy-11(RNAi)* responses in same-generation RNAi assays via feeding from a bleached embryo (25±2% versus 21±4% penetrance, n>50 in each of the triplicates). Therefore, *pgl-1*'s contribution to exogenous RNAi is likely through the germline. Because of the overwhelming number of germline components associated with P-granules (UPDIKE and STROME 2010), it is challenging to find a mechanism of how *pgl-1* contributes to general exogenous RNAi.

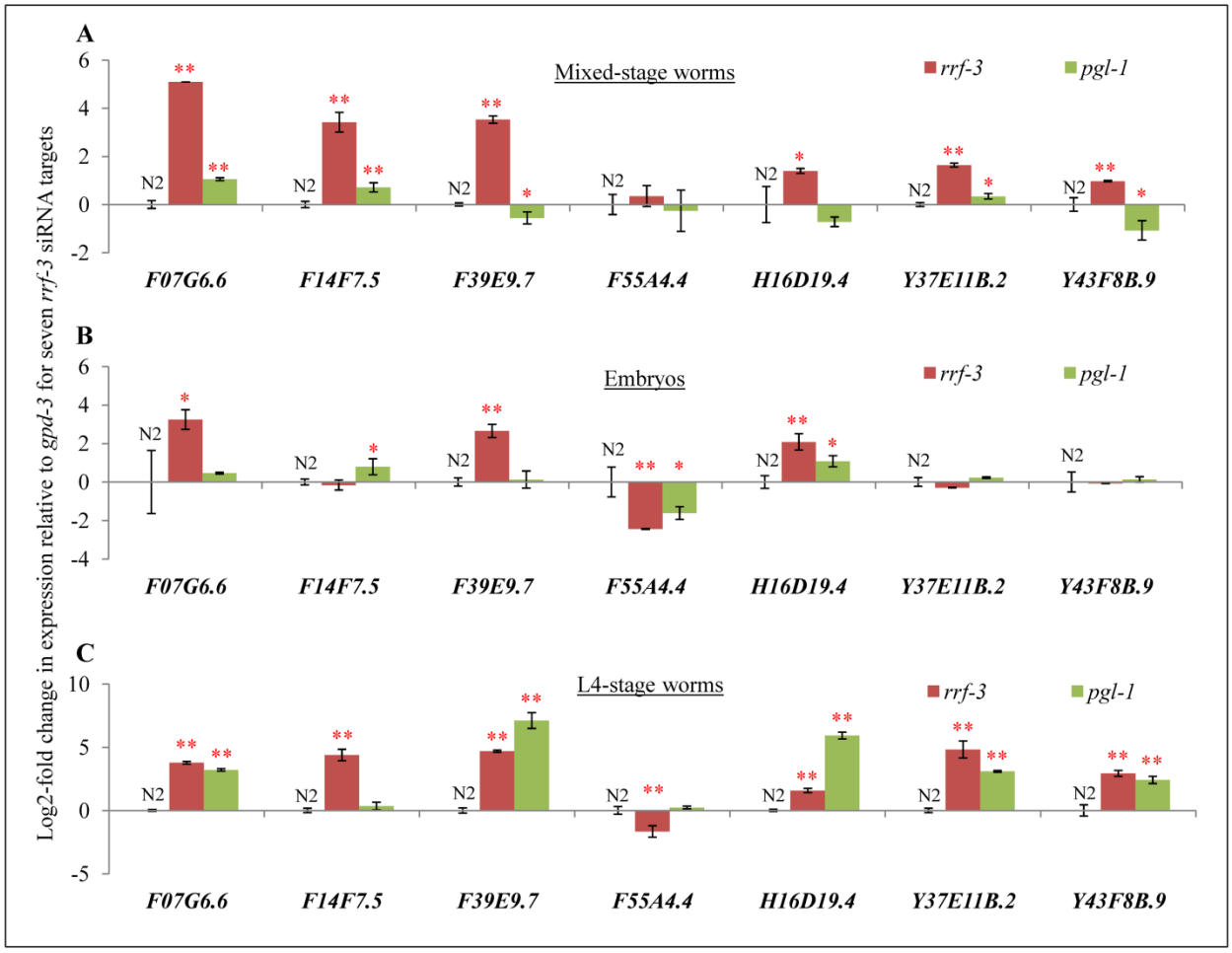

Figure 5.2: *pgl-1* mutant misexpression of *rrf-3* siRNA targets

rrf-3(pk1426) and *pgl-1(bn101)* dependent changes in relative mRNA levels for select endo-siRNA target genes. Log2 ratio (relative to N2 = 0) of qPCR determined mRNA levels for the indicated genes from **(A)** mixed-stage worms, **(B)** embryos, and **(C)** L4 worms of the indicated genotypes. These seven genes were previously reported to be targets of *rrf-3*-dependent endo-siRNAs (GENT *et al.* 2010). *p*-values calculated by *t*-test; * indicates $p<0.05$ and ** indicates $p<0.01$.

However, our findings that *pgl-1* contributes to *eri* mutants' enhanced RNAi in a complementary fashion to *nrde-3* and that *pgl-1* impacts some of *rb* mutant's enhanced RNAi responses (**Table 5.3**) allowed us a significantly narrower guided search for possible mechanisms. We therefore examined roles analogous to *nrde-3*'s contribution to the *eri* pathway and developmentally-related roles that *rb* genes control (which have RNAi implications) as the bases of a candidate search for a possible *pgl-1* RNAi mechanism(s).

pgl-1 does not contribute to transgene silencing

Enhanced RNAi mutants show increased spontaneous transgene silencing (**Figure 4.8E, H**). Since we observed that *nrde-3* loss alleviates some of this spontaneous transgene silencing (**Figure 4.8G, H**), we wondered if *pgl-1* loss does the same. We compared the extent of silencing of the ubiquitously expressed *sur-5p::gfp* transgene in *eri-1(mg366)* single mutant to the silencing in the *eri-1(mg366);nrde-3(gg66)* and *eri-1(mg366);pgl-1(bn101)* double mutants. We found that *pgl-1* was not required for *eri-1*-induced silencing (**Figure 5.3A-C**). Therefore, it seems that *pgl-1* does not contribute to enhanced RNAi via facilitating the silencing of repetitive transgene arrays.

pgl-1 does not contribute to *NRDE-3* nuclear localization

Although *nrde-3* and *pgl-1* seem to act in parallel pathways due to their contribution to the Eri response against non-overlapping sets of gene targets (**Figure 5.1D-E**), we nevertheless wondered if *pgl-1* loss had any impact on *nrde-3* nuclear localization due to PGL-1's perinuclear location. In wild type backgrounds, *nrde-3-gfp* localizes to the nucleus, most prominently observed in the seam cells (**Figure 5.3D**). In a *pgl-1(bn101)* background, this localization still

Figure 5.3: *pgl-1* does not contribute to common RNAi-related processes

(A-C) Representative micrographs of **(A)** *eri-1(mg366)*, **(B)** *eri-1(mg366);nrde-3(gg66)*, and **(C)** *eri-1(mg366);pgl-1(bn101)* strains expressing a *Psur-5::gfp* transgene. In the *eri-1(mg366)* background, there is extensive silencing of *gfp* (red arrows) in the intestinal cells; in the *eri-1(mg366);nrde-3(gg66)* strains, there is no such extensive transgene silencing. The *eri-1(mg366);pgl-1(bn101)* strain still exhibits extensive silencing of *gfp* (red arrows) in the intestinal cells, suggesting no alleviation of spontaneous transgene silencing like *nrde-3* loss exhibits. **(D-E)** Representative micrographs of **(D)** *nrde-3(gg66)* and **(E)** *pgl-1(bn101)* strains expressing an *nrde-3-gfp* transgene. In both backgrounds, there is nuclear localization of the *gfp* in the seam cells (red arrows), suggesting *pgl-1* loss does not affect *nrde-3* nuclear localization. **(F)** The severity of RNAi phenotypes, from '-' to '+ + + + +', based on expressivity described in **Table S1** of indicated strains for *dpy-13(RNAi)* and *unc-73(RNAi)*, with the same OD_{600nm} concentrations as **Table 1**, are scored. All scores are normalized to the strongest Eri response for a particular RNAi assay as '+ + + + +' and no response as '-'. DCAP-1 and SMG-7 are P-granule components proposed to interact with PGL-1; *dcap-1*, *smg-7*, and *mes-4* have also all been previously implicated in RNAi-processes, especially in the germline, where *pgl-1* is expressed. The *eri-1(mg366)* enhanced RNAi response does not hold the same pattern upon *pgl-1* loss as *dcap-1*, *mes-4*, or *smg-7* loss. **(G-I)** Representative micrographs of **(G)** *lin-15ab(n765)*, **(H)** *lin-15ab(n765);pgl-1(bn101)*, **(I)** *let-23(sa62)*, and **(J)** *let-23(sa62);pgl-1(bn101)* strains' multi-vulva (Muv) phenotype. Inappropriate induction of growth in the *rb* mutants (*lin-15ab*) can cause germline-to-soma transformations which lead to enhanced RNAi. *pgl-1* loss however only suppresses the Muv phenotype of the *rb* mutant, but not a general growth induction pathway like the EGF receptor mutant *let-23(sa62)*. **(K-L)** *rb* mutants are perturbed in their starvation

Figure 5.3 (Continued): *pgl-1* does not contribute to common RNAi-related processes

response and starved worms are more RNAi-sensitive than well-fed ones. During starvation, *daf-16::gfp* localizes to the nucleus; in a *rb* mutant, this nuclear localization is increased with or without food. The knockdown of *pgl-1* had no effect on *daf-16::gfp* nuclear localization as indicated by the penetrance of the indicated strains who were placed onto *pgl-1(RNAi)* food as L3s and scored in the next generation **(K)**, even though *pgl-1(RNAi)* increased the penetrance of temperature-sterility at 25°C like *pgl-1* loss does **(L)**, suggesting a functional knockdown. *pgl-1* loss thus does not seem to impact the *daf-16* starvation response. **(M)** *rb* mutants misexpress germline genes in the soma, including *pgl-1*. qPCR of 15ºC hour 122 adult worms for their expression levels of the indicated genes in the various mutant strains are shown, with expression of N2 wild type set to 1.0 for each gene. Compared to the "amount" of germline, approximated by *mex-3* expression, *lin-35(n745)* mutants have overexpression of *pgl-1*, consistent with previous reports. *eri-1* or *rrf-3* loss does not seem to perturb *pgl-1* expression, suggesting *pgl-1* overexpression is unlikely to be a mechanism of *eri*-class enhanced RNAi. *p*-values calculated by *t*-test; ** indicates $p<0.01$.

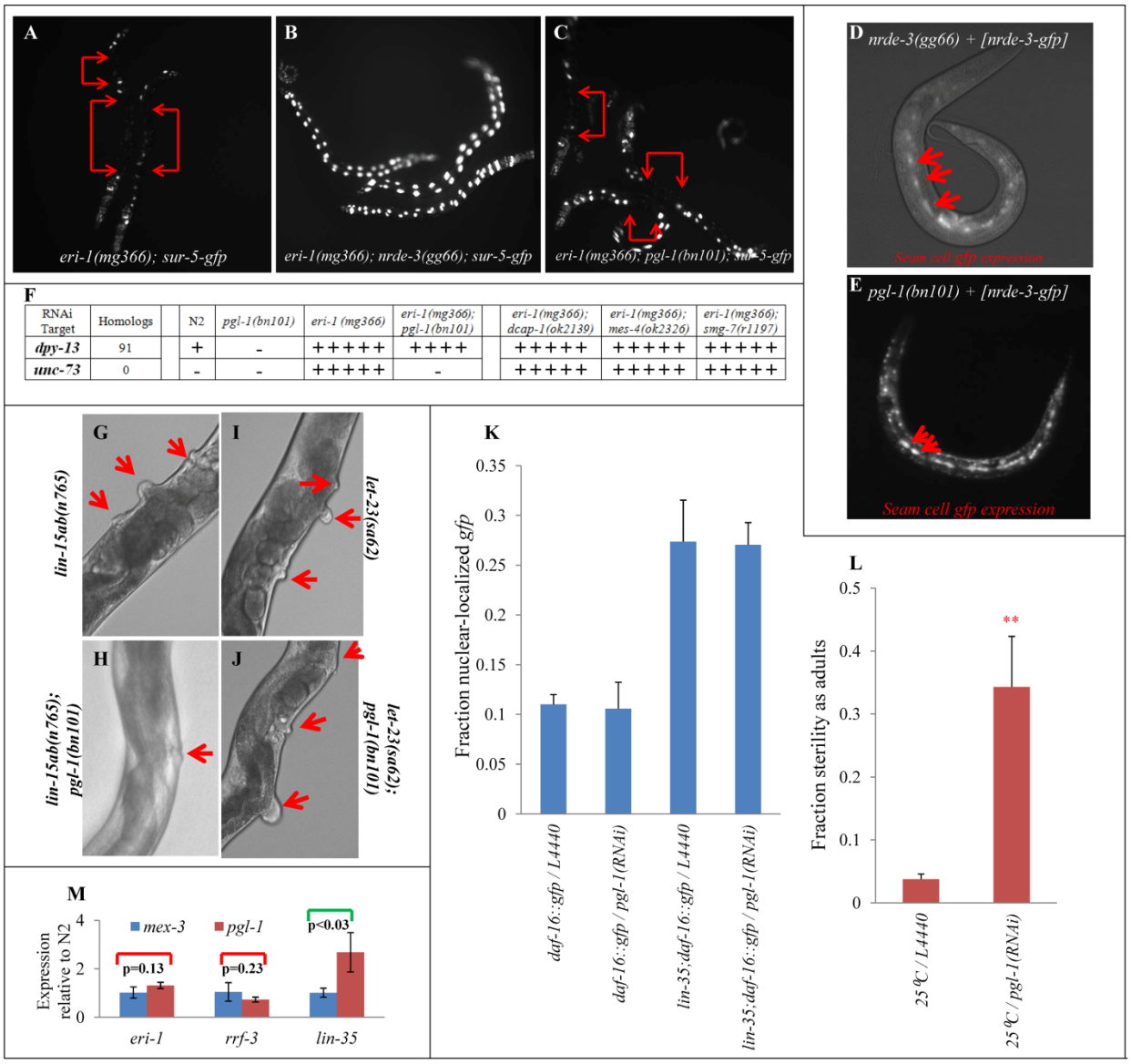

Figure 5.3 (Continued): *pgl-1* does not contribute to common RNAi-related processes

occurs (**Figure 5.3E**). Therefore, it seems that *pgl-1* loss does not impact enhanced RNAi via perturbing *nrde-3* nuclear localization.

dcap-1, *mes-4*, and *smg-7* loss do not affect enhanced RNAi the way *pgl-1* loss does

Due to the motifs present in PGL-1, one mechanistic possibility is that it plays a structural role in maintaining P-granules (KAWASAKI *et al.* 1998), whose components include the RNAi effector(s) responsible for contributing to enhanced RNAi. We therefore selected three candidates, *dcap-1*, *mes-4*, and *smg-7*, who interacts with PGL-1 within P-granules (UPDIKE and STROME 2010) and have previous been known to have RNAi-associated phenotypes (DOMEIER *et al.* 2000; DUDLEY *et al.* 2002; SQUIRRELL *et al.* 2006), to examine their loss' effects on enhanced RNAi. Because DCAP-1 is part of the mRNA decapping complex, MES-4 is important for germline maintenance and RNA metabolism, and SMG-7 is part of the nonsense mediated decay complex, they all have mechanistic potential for eliminating mRNAs. The *eri-1(mg366);dcap-1(ok2139)*, *eri-1(mg366);mes-4(ok2326)*, and the *eri-1(mg366);smg-7(r1197)* double mutants all did not behave like the *eri-1(mg366);pgl-1(bn101)* mutant on *unc-73(RNAi)* (**Figure 5.3F**); loss of *dcap-1*, *mes-4*, and *smg-7* essentially had no effect on the *eri-1* enhanced RNAi response. Therefore, it seems that PGL-1 does not contribute to enhanced RNAi via facilitating DCAP-1, MES-4, or SMG-7 mechanisms.

pgl-1 loss does not impact *lin-3* growth pathway

The *rb* gene family normally represses gene expression; their mutants are enhanced for RNAi because there is an induction of germline expressed genes in the soma (WANG *et al.* 2005; WU *et al.* 2012). One result of this unrepressed expression is inappropriate induction of growth; in the

Rb mutants, there's a multi-vulva (Muv) phenotype because of unrepressed epidermal growth induction (**Figure 5.3G**) (SAFFER *et al.* 2011). To determine whether *pgl-1* functions in the growth pathway, we looked for the repression of the Muv phenotype in *lin-15ab(n765)* and EGF growth factor (*lin-3*) receptor constitutive mutant *let-23(sa62)* backgrounds (**Figure 5.3I**). While the *lin-15ab(n765);pgl-1(bn101)* double mutant was no longer Muv (**Figure 5.3H**), the *let-23(sa62);pgl-1(bn101)* double mutant still was (**Figure 5.3J**). Therefore, it seems that *pgl-1* functions to repress in the *rb* pathway rather than in a general growth response pathway.

pgl-1 knockdown does not affect *daf-16::gfp* nuclear localization

Starved worms are more responsive to RNAi (ZHUANG and HUNTER 2012) and *rb* mutants have a perturbed *daf-16* starvation response (KIRIENKO *et al.* 2008). To test if *pgl-1* acts to enhance RNAi via the starvation response, we tested for *daf-16::gfp* nuclear localization which occurs in the absence of food and is abnormally high in *lin-35(n745)* mutants regardless of food status (KIRIENKO *et al.* 2008). We found that knocking down *pgl-1*, which induced a temperature-sensitive sterility phenotype much like *pgl-1* loss does (**Figure 5.3L**), had no effect on the *daf-16::gfp* nuclear localization in either wild type or *lin-35(n745)* backgrounds (**Figure 5.3K**). Therefore, it seems that *pgl-1* loss does not perturb the *daf-16* starvation response pathway as a mechanism of enhancing RNAi.

pgl-1 is not overexpressed in *eri-1* and *rrf-3* mutants

Although not previously reported, it could be possible that the *eri* mutants, like the *rb* mutants, misexpress some components of the germline, including *pgl-1*, to cause their enhanced RNAi phenotype. qPCR of 15ºC hour 122 adult *eri-1(mg366)*, *rrf-3(pk1426)*, and *lin-35(n745)* worms

for their expression levels of *pgl-1* and *mex-3* were normalized to N2 wild type expression (**Figure 5.3M**). Compared to the "amount" of germline approximated by *mex-3* expression, *lin-35(n745)* mutants have overexpression of *pgl-1*, consistent with previous reports (WANG *et al.* 2005). *eri-1* or *rrf-3* loss does not seem to perturb *pgl-1* expression. Therefore, it seems *pgl-1* overexpression is unlikely to be a mechanism of *eri*-class enhanced RNAi.

Two classes of systemically mobile transgene silencing

During our analysis of *pgl-1*'s role in transgene silencing (**Figure 5.3A-C**), we analyzed the relationship between *pgl-1* loss and enhanced transgene silencing induced by *rb* mutations. We discovered that the *rb* mutant's enhanced transgene silencing (**Figure 5.4G**) is not affected by either *nrde-3* loss or *pgl-1* loss (**Figure 5.4H, I**), unlike the *eri* mutant's (**Figure 5.4D, E**). While our hypothesis that the *rb* mutant's transgene silencing depended on *pgl-1* was incorrect, our data do suggest two distinct classes or mechanisms of enhanced transgene silencing (**Figure 5.4**).

Previous work has shown that part of the *eri* class mutants' enhanced transgene silencing depended on the systemic double stranded RNA channel SID-1 (JOSE *et al.* 2009), suggesting that these silencing signals are likely mobile. We observed that in an *eri-1(mg366);lin-15ab(n765);sur-5::gfp* background (**Figure 5.5D, F**), the transgene silencing is significantly more prominent than in either *eri-1(mg366);sur-5::gfp* (**Figure 5.5B, F**) or *lin-15ab(n765);sur-5::gfp* (**Figure 5.5C, F**) backgrounds. This suggested that the two distinct classes of transgene silencing are additive in effect. We therefore examined a *lin-15(n765);sid-1(qt9)* mutant and observed that its transgene silencing was significantly reduced (**Figure 5.5E, F**). This observation suggests that, like the *eri* class enhanced transgene silencing, the *rb* mutants' enhanced transgene silencing is likely also mobile and systemic.

Figure 5.4: *eri-1* and *lin-15ab* depend on different mechanisms for transgene silencing

Representative micrographs of **(A)** wild type, **(B)** *nrde-3(gg66)*, **(C)** *pgl-1(bn101),* **(D)** *eri-1(mg366)*, **(E)** *eri-1(mg366);nrde-3(gg66)*, **(F)** *eri-1(mg366);pgl-1(bn101)*, **(G)** *lin-15ab(n765)*, **(H)** *lin-15ab(n765);nrde-3(gg66)*, and **(I)** *lin-15ab(n765);pgl-1(bn101)* strains expressing a *Psur-5::gfp* transgene. In the *eri-1(mg366)* background, there is extensive silencing of *gfp* (red arrows) in the intestinal cells; in the *eri-1(mg366);nrde-3(gg66)* strains, there is no such extensive transgene silencing. The *eri-1(mg366);pgl-1(bn101)* strain still exhibits extensive silencing of *gfp* (red arrows) in the intestinal cells, suggesting no alleviation of spontaneous transgene silencing. In the *lin-15ab(n765)* background, there is extensive silencing of *gfp* (red arrows) in the intestinal cells. The *lin-15ab(n765);nrde-3(gg66)* and *lin-15ab(n765);pgl-1(bn101)* strains still exhibits extensive silencing of *gfp* (red arrows) in the intestinal cells, suggesting no alleviation of spontaneous transgene silencing.

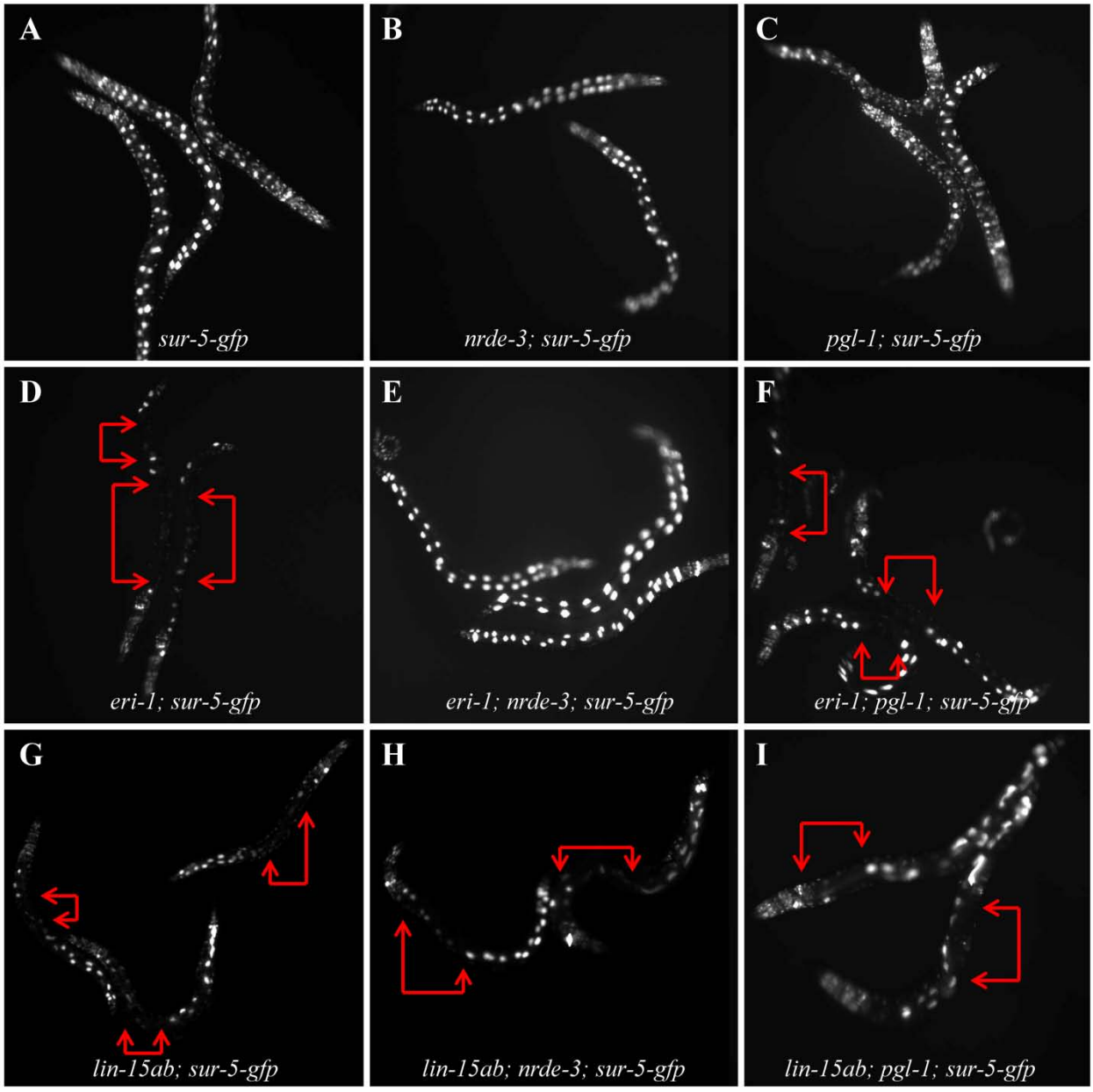

Figure 5.4 (Continued): *eri-1* and *lin-15ab* depend on different mechanisms for transgene silencing

Figure 5.5: *lin-15ab* transgene silencing partially depends on *sid-1*

(A-E) Representative micrographs of **(A)** wild type, **(B)** *eri-1(mg366)*, **(C)** *lin-15ab(n765)*, **(D)** *eri-1(mg366);lin-15ab(n765)*, and **(E)** *sid-1(qt9);lin-15ab(n765)* strains expressing a *Psur-5::gfp* transgene. In the *eri-1(mg366)* and *lin-15ab(n765)* backgrounds, there is extensive silencing of *gfp* (red arrows) in the intestinal cells. In the *eri-1(mg366);lin-15ab(n765)* strains, there is even greater transgene silencing (red arrows). The *sid-1(qt9);lin-15ab(n765)* strain exhibits significantly reduced levels of *gfp* silencing. **(F)** The enhanced transgene silencing (TGS) is quantified by counting the *gfp*-positive intestinal nuclei in worms from each strain background, with each worm quantified represented by a black dot and with the median denoted in red. The mean and standard deviations are indicated below each strain. *p*-values are determined by *t*-test. There is a significant difference in potency between *eri-1*- and *lin-15ab*-induced enhanced TGS, with the two mutations' effects additive in the double mutant. The *lin-15ab* enhanced TGS is also significantly reduced in a *sid-1(-)* mutant background.

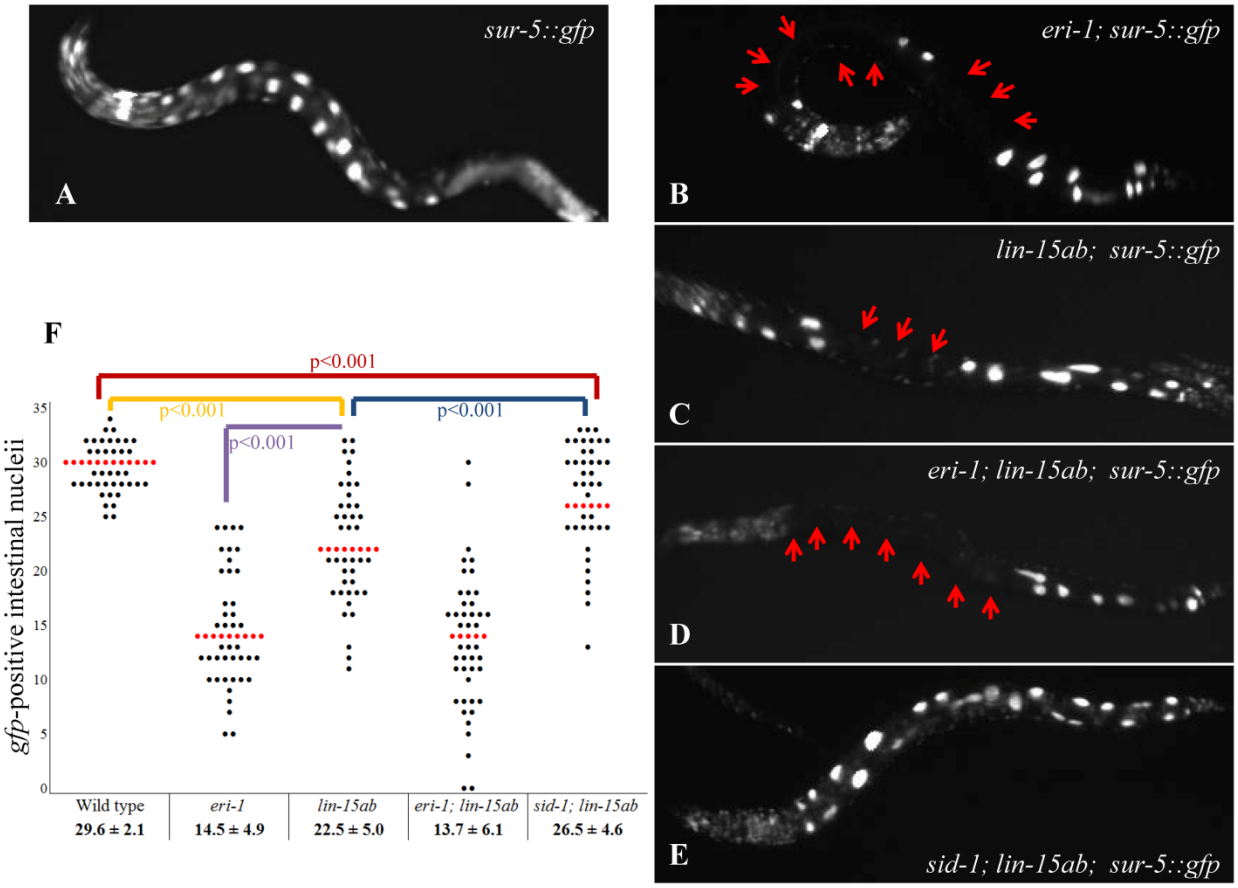

Figure 5.5 (Continued): *lin-15ab* transgene silencing partially depends on *sid-1*

DISCUSSION

nrde-3 and *pgl-1* are required for enhanced RNAi in *eri* mutants

Our analysis shows that *pgl-1* is a likely *eri*-effector. Similar to *nrde-3, pgl-1* mutants are weakly Rde (**Figure 5.1**), *pgl-1* overexpression enhances RNAi (**Figure 5.1B-C**), *pgl-1* mutants disrupt the expression of endo-siRNA regulated genes (**Figure 5.2**), and loss of *pgl-1* attenuates the Eri phenotypes, at least for some genes (**Figure 5.1D-E**). Remarkably, the simultaneous loss of both *pgl-1* and *nrde-3* broadly depletes enhanced RNAi in the *eri-1* mutant background (**Figure 5.1D-E**). This result suggests that these two genes define the totality of *eri-1* and likely endo-siRNA competitive effector pathways.

PGL-1 expression and/or localization is expanded in the Rb pathway mutants, including *lin-15* and *lin-35*, that enhance RNAi and lead to efficient transgene silencing (WANG *et al.* 2005; WU *et al.* 2012). However, *pgl-1* mutants abrogated *lin-15* and *lin-35* enhancement for the same genes *pgl-1* is important for in *eri-1* enhancement (**Table 5.3**). Furthermore, *lin-15; pgl-1* and *lin-35; pgl-1* double mutants continued to show RNAi enhancement for *nrde-3*-dependent gene targets. Thus, the importance of *pgl-1* for enhanced RNAi is not likely via the Rb pathway. Attempts to correlate *pgl-1* phenotypes to previously defined RNAi mechanisms were not informative, thus failing to reveal how *pgl-1* activity contributes to gene silencing (**Figure 5.2, 5.3**). However, our analysis clearly establishes that *pgl-1* contributes to both exogenous and endogenous RNAi (**Figure 5.1, 5.2**).

pgl-1 mutant small RNA deep sequencing likely to yield broader perspectives on its roles

While we were unable to attribute any of the aforementioned common and/or *rb*-associated RNAi mechanisms to *pgl-1*, our results do show an effect on endo-RNAi in *pgl-1* mutants

(**Figure 5.2**). A recent report has suggested that perinuclear structures similar to P-granules are important for siRNA amplification due to RRF-1 recruitment in both exogenous and endogenous contexts (PHILLIPS *et al.* 2012). Therefore, future small RNA deep sequencing should yield rich results for the many roles that *pgl-1* likely plays. Like the *eri* mutants, sequencing and analysis of its small RNA profile will likely shed light on its endogenous roles and contributions to RNAi silencing.

MATERIALS AND METHODS FOR SMALL RNA SEQUENCING

The following preliminary protocols were developed for extracting total small RNAs from wild type, *eri-1(mg366)*, and *pgl-1(bn101) C. elegans* worms. It requires further optimization for preparing Illumina sequencing-quality samples, and is thus currently undergoing troubleshooting. However, the framework is thoroughly developed for a full preparation of small RNA sequencing, and it is based off of protocols provided courtesy of Dr. Weifeng Gu and Dr. Darryl Conte of University of Massachusetts Worcester.

General Notes:

*-Steps in **red** can and should be continued into the next phase without a -80°C freeze down or overnight delay.*

-Whenever possible, add as much isopropanol as the tube volume will take when precipitating RNA; with glycogen, greater volume of isopropanol means better pelleting.

-To keep reagents as RNase-free as possible, all stocks should only be opened in a tissue-culture hood and mixtures should be prepared there; for reagents coming in large bottles, take into the TC hood, open up, wipe mouth with RNase-out wipe, pour out an aliquot into a RNase-free epitube, wipe mouth again with RNase-out wipe, close, and take back to bench.

STEP ZERO

(1) I will start with ~200-350 µL[1] of L4 worms frozen at -80°C in **ddH2O**.

(2) Rinse glass-metal douncer by **ddH2O**, **RNase-Out**, and then **DEPC-treated ddH2O**. *Repeat this step in between different samples.*

(3) Prepare 1 phase lock gel column per sample by spinning at ***13,000 rpm*** for *1 minute* in Biofuge spinner at RT.

(4) Add 400 µL **Trizol** to iced-worm sample tube.

(5) Vortex **Trizol**-worm mixture vigorously at RT as it thaws until it's a slurry.

(6) Take up solution in RNase-free glass Pasteur pipette and transfer into glass douncer placed on ice. Make sure to pipette into the douncer's vertical chamber, and avoid liquid touching the upper pouring chamber.

(7) Dounce the slurry in a twisting motion 20 times on ice.

(8) Transfer worm lysis to the phase-lock gel tube by glass pipette. Do not exceed 750 µL total volume.[2]

(9) Add 80 µL of **chloroform** into each tube.[3]

(10) Turn up and down the tube for mixing for *1 minute*.

(11) Let the tubes rest at RT for *5 minutes*.

(12) Centrifuge at ***12,000 rpm*** for *15 minutes* at 4°C in Eppendorf spinner.[4]

(13) Transfer the top aqueous layer into a new RNase-free siliconized epitube. There may be some phase-lock gel at the top of the aqueous layer after the spin. Poke a hole through it using a pipette tip, and then using a fresh tip, go in and pipette. In eluting to a

[1] 10 HG large plates grown full, bleach synchronized for one hour, and then grown to L4s on 5 NG larges at 15°C
[2] According to Eppendorf manufacturer's protocols, the phase-lock heavy columns can ONLY be used with Trizol. NEITHER RiboZol/RNAzol NOR saturated Phenol alone will work.
[3] Trizol to chloroform ratio should always be 5:1.
[4] ~15K x g; there should be no "worm pellet" at the bottom after this spin if Trizol vortexing/douncing had worked

new tube, leave the tip in the air and pipette out to the new tube to make sure the residual gel at the tip do not enter. The gel plug should be at an angle after the spin, so take up fluid from the tube **vertically** to ensure that **ALL** the aqueous layer gets taken.[5]

(14) Add *(in this order)* 50 µL of **5M NaCl**, 2.5 µL of **20 mg/mL glycogen**[6] and 650-900 µL[7] **isopropanol** into these tubes.

(15) Mix by inverting for 1 minute.

(16) Leave in -80°C for an hour to precipitate RNA.

(17) Spin at ***10,000 rpm*** for *15 minutes* at 4°C Eppendorf spinner.[8]

(18) Pipette out the supernatant while avoiding the pellet.

(19) Wash with 500µL of **ice-cold EtOH**.[9]

(20) Spin at ***13,000 rpm*** for *1 minute* at 4°C in Biofuge spinner.[10]

(21) Remove the supernatant while avoiding the pellet. Do not let the pellet dry completely.

(22) Immediately dissolve in 83µL of **DEPC-treated ddH_2O**.[11]

(23) *(If necessary)* Let re-suspension occur at RT[12] while repeatedly pipetting up and down at regular intervals.

(24) Quantitate what the concentration is with a 1/10X solution using 1 µL of this RNA. If it is ≥12,000 ng/µL, split into two and dilute to 80 µL each.[13]

(25) These epitubes can be stored -80ºC after this step.

---

[5] Will be about 400 to 500 µL.
[6] for a 0.05 µg/µl concentration in ~1mL solution
[7] or whatever makes adds up to at least 1mL, but no less than 1X volume of extraction
[8] ~11K x g; spin as a frozen ice block
[9] This is to remove leftover salt, so no need to dislodge the pellet.
[10] ~11K x g
[11] Can do two aliquots of 42 µL if the pellets are thin and there are two samples to combine
[12] With glycogen, if this tube is on ice, it'll solidify easily
[13] Want <1mg of RNA in 80 µL

STEP 1A

1) Prepare in 1 siliconized epitube added in the following order: 80 µL **total RNA**[14], 400 µL **MirVana lysis/binding buffer**, and 48 µL **MirVana homogenate buffer**.
2) Mix up and down by pipetting, and keep at RT for *5 minutes*.
3) Add 176 µL **EtOH**, mix by pipetting.
4) Spin at ***6.4K rpm*** for *4 minutes* at RT in Biofuge spinner.[15]
5) Transfer supernatant to new siliconized epitube.
6) Add in 800 µL **isopropanol**.
7) Mix by inverting for 1 minute.
8) Leave in -80°C for *an hour* to precipitate RNA.
9) Spin at ***13.8K rpm*** for *15 minutes* in the 4°C Eppendorf spinner.[16]
10) Pipette out the supernatant while avoiding the pellet.
11) Wash with 500 µL of **ice-cold 70% EtOH**.
12) Spin at ***13,000 rpm*** for *1 minute* at 4°C in Biofuge spinner.
13) Remove the supernatant while avoiding the pellet.[17]
14) Dissolve in 22 µL of **TE**.
15) *(If necessary)* Let re-suspension occur at RT while repeatedly pipetting up and down at regular intervals.
16) Quantitate what the concentration is with a 1/5X solution using 2 µL of this RNA. Depending on the enrichment efficiency, there can be up to 10% of previous amount recovered from Step I #24.

[14] <12K ng/µl
[15] ~2500 x g; this is to pellet the large RNA. There should be a small but visible pellet.
[16] Pellets small RNAs. 20,000 x g for 15 minutes at 4°C. Eppendorf rotor FA-45-30-11 has a 9.5cm radius. Fischer siliconized epitubes can take up to 30,000 x g. Smaller pellet than previous spin.
[17] Pellet at this step becomes dislodged easily, so be careful when removing the supernatant.

17) Ideally, half of this can be stored at -80°C for backup while the other half is used directly for the next step.

STEP 1B – PART I

1) Wash the two gel plates[18], 2 spatulas, 2 razors, 1 stirrer, 2 pairs of tweezers, 1 pair of scissors, 1 glass pasteur pipette, and 3 beakers (2x 100mL & 1L) in RNase Out, wrap individually in aluminum foil, and bake at 250°C **overnight** in high-temp oven.[19]
2) For things that are not glass or metal, like the combs for the wells, spacer, 1 blue plastic pestle per sample, and glass plate with spacer, soak in RNase Out (preferably overnight), then rinse off in RNase-free water.
3) Make 10 mL of **10% APS** by adding 1 g of APS and filling volume up to 10 mL with **ddH2O** in a 15 mL falcon. Aliquot (~500 µL) and keep in -20°C.
4) Set up the gel plates:

   a. Line up the bottom spacer as close to the edge of the bottom plate as possible, and then seal the bottom and the sides of the spacer with a steady stream injection (18 gauge syringe) of Vaseline.

   b. Align the top plate and press them together.

   c. Using electrical tape, seal the bottom edge of the plates. Add extra flaps to the sides of the bottom because those spots are most likely to leak.

   d. Using three metal clips on each side, clamp the two plates together. The bottom corners are most susceptible to leaking, so clamp that area especially tightly.

   e. Make sure the bottom clips are even and symmetrical, flip the clasps onto the glass, and the clips themselves serve as a base stand.

[18] Plate with rubber spacer glued in should NOT be baked
[19] Mark aluminum foil with a sharpie; the ink should become stale if it was heated; autoclave tape should be browned out, but keep it on the foil (and not the glassware) as it will stick.

f. Pour freshly opened **molecular grade ddH2O** into the gel rig and let it sit for 10 minutes. See if there are any egregious leaks; if so, start over from *part (c)*. If not, pour out water, and wick off the last bits with a paper towel, let it stand while proceeding to the next step.

5) Plug in a balance in the hood.
6) To make a *15cm x 14cm x 1mm* (30 mL) of **15% PAGE (19:1) / 7M Urea**, add the following to a beaker:
   a. 12.6 g **Urea**
   b. 11.26 ml **40% acrylamide/bis-acrylamide (19:1)** solution
   c. 3 mL **10X TBE** buffer
   d. 6.5 mL **ddH2O**.
7) Plug in a hot plate stirrer and heat to 40°C in the hood.
8) Warm the beaker and stir to mix the solution and dissolve the urea.
9) In the 1L beaker, add in 100mL **10X TBE** and 900mL molecular **grade ddH2O**. Mix by stirring with an RNase-free spatula.
10) Add in 150 µl **10% ammonium persulfate** (APS) and 15 µl **TEMED** to the gel beaker, swirl the beaker, and then immediately pour the gel by tilting the plates back and pouring into the crevice in a FAST steady stream to avoid air bubbles. Pour all the way to the top because otherwise combs will cause air bubbles at the bottom of the wells.
11) Add in large wide combs to 1/3 inch depth if possible. If there are any air bubbles at the bottom of the wells, even if tiny, pull out and try again, because the wells needs to be perfectly horizontal at the bottom.

12) There will be some well wall height loss due to evaporation or slow leakage, so don't wick off any overflow as they'll serve as a buffer. Try to keep the lanes in the middle of the gel as good as possible – no air bubbles, no well wall loss due to leak, perfectly horizontal bottoms – because that's where to preferentially load.
13) Takes about 45 minutes for the gel to fully solidify. Leak check: corners near the side well will most likely to drop in level immediately if there is a leak. Stay watching the gel for the first 10-15 minutes to check for leaks.
14) Unless a leak is egregious, there are two ways to fix a slow leak:

    a. pour the leftover gel solution from beaker onto the combs while tilting the plates back, that should add more volume to the leaking parts

    b. push the combs a little deeper into the gel and that'll raise the height of the well walls (try using *part (a)* first!)
15) Remove bottom clips and the tape. To remove the bottom spacer, poke one corner slightly into the gel with a spatula to get the other corner to pop out beyond the glass plates, and then use tweezers to pull the entire spacer out using that dislodged corner.
16) Fill bottom reservoir with **1X TBE**, clamp plates onto the rig, including a dummy plate on the other side. Make sure the clamps to the rig reach the very top of the plates because that causes the least obvious leaks.
17) Using a bent 18 gauge syringe, inject 1X TBE into the space at the bottom of the gel where the spacer was to get rid of that air bubble. Inject and push sideways eliminates the air bubble most effectively.
18) Fill out the top reservoir with **1X TBE** as well.

19) Pull out the comb and rinse the wells of the gel with **1X TBE** using an RNase-free Pasteur pipette. There should be some acrylamide being forced up from the wells as it is rinsed hard several times.

20) Pre-run the gel in **1x TBE** buffer for *30 min* at **200 V**.

21) Mix samples and small RNA ladder (Zymo ssRNA: 29, 25, 21, 17 is pretty good) with loading dye provided with the MirVana kit. Try to limit loading to 10 µL of sample/ladder mixed with 10 µL of loading buffer per lane.

22) Heat samples to 70°C for *2 min*, then immediately chill by transferring samples onto ice.

23) Check upper reservoir buffer levels before loading. If they have dropped up, top it off again. Otherwise, what's loaded will float out into the buffer if the buffer level is at the level of the mouth of the plates.

24) Load the samples into the lanes using a newly opened box of needle-point tips. Pick the best lanes for loading.

25) Run gel at **200 V** until the Bromophenol blue (bottom band in MirVana loading buffer, which is purplish blue) migrates **4-4.5 inches**.[20]

26) Prepare for SybrGold staining as follows:

a. Warm vial to RT, and spin briefly.

b. Rinse a polypropenlene container thoroughly with RNase-Out.

c. Add 10 µL of **SybrGold** to 50 mL of **1X TBE** in an RNase-free 50mL tube and mix by vortexing.

d. immediately wrap this mixture in aluminum foil

27) When the gel is finished running, remove the clamps and using a spatula, pop open the glass plates by snapping at the top corner right above a vertical spacer.

[20] Takes about 1 hour per inch of migration in this type of gel

28) Using a razor, remove extraneous portions of the gel before staining. Keep the entire *length* of a lane intact! Leave the wells on, and cut a mark somehow to indicate gel up-down orientation.[21]

29) Place resized gel and staining solution in container, then swirl on shaker for *one hour* at **25 RPM**, while covering it with aluminum foil.[22]

30) After staining, place the gel into Saran wrap that's been washed with RNase-Out, wrap it up, and place on top of a glass plate, before placing in UV box.

31) Place two UV rulers above and to the left of the gel. Using a UV imager, use between 8/30 to 16/30 second exposure to get the gel, and then bright light to image the rulers.

32) Cut between the 15 and 30 mer regions in the hood, using the imaged rulers as a reference for x,y axis position.

33) Place gel fragments into 1.5 mL siliconized tubes and grind them using blue plastic pestles. Grind until the gel is in tiny bits.

34) For every 2 reactions, prepare a mixture by adding 60 µL **5M NaCl** to 940 µL **TE pH 7.5**.

35) Add 500 µL of above mixture into gel fragment tube.

36) Briefly vortex. The mixture should already be a slurry. Grind it some more with the blue plastic pestles.

37) Parafilm the opening of the tube. Vortex overnight in 4°C by double-back rubber banding tubes to vortex: two across horizontal axis and one straight across the length of the tube.

STEP 1B – PART II

[21] Because the dyes' colors get removed during the wash
[22] Look at the swirling pattern before covering to make sure the liquid is getting all of the gel.

1) Cut off the tip of a filtered P1000 tip[23] using baked scissors, and filter the slurry mixture through TWO **0.45 um Nanosept filters** by splitting into two aliquots of <500 µL and spinning them at ***11.5K rpm***[24] in Eppendorf spinner for *10 minutes* at 4°C.
2) Transfer the filtrate[25] into a new siliconized tube.[26]
3) Add *(in this order)* 75 µL of **5M NH4Ac**[27], 3.75 µL of **20 mg/mL glycogen**[28] and 900 µL **isopropanol** to ~1.5 mL total volume into these tubes.
4) Mix by inverting for *1 minute*.
5) Leave in -80°C for *an hour* to precipitate RNA.
6) Spin at ***13.8K rpm***[29] for *15 minutes* at 4°C Eppendorf spinner.
7) Pipette out the supernatant while avoiding the pellet.
8) Wash with 500 µL of **ice-cold 70% EtOH**.
9) Spin at ***13,000 rpm*** for *1 minute* at 4°C in Biofuge spinner.
10) Remove the supernatant while avoiding the pellet.
11) Dissolve in 10 µL of **next step's treatment/ligation mixture**.
12) *(If necessary)* Let re-suspension occur at RT while repeatedly pipetting up and down at regular intervals.

STEP 2 and STEP 3 – PART I:

1) On ice, prepare a 1/10X dilution of **10 mg/mL BSA**, and dissolve **1 nm of modban**[30] in 20 µL of **DEPC-treated ddH2O** for making **50 µM modban**.

[23] Using baked scissors
[24] 14K x g
[25] Which contains the small RNAs
[26] There should be gel-like substance on the filter, and almost the entire volume in liquid form as the filtrate.
[27] For destaining the SybrGold
[28] for a 0.05 µg/ul concentration in ~1.5 mL solution
[29] ~20K x g

2) In an RNase-free PCR tube, add in the following order (multiplied by the number of samples):

   a. 1 µL of **10X TAP buffer**

   b. 0.5 µL of **20U/µL Superasin**

   c. 0.5 µL of **TAP**

   d. 8 µL of **ddH_2O**

3) Dissolve the collected enriched small RNA pellet from previous step in this mixture.

4) Incubate the reaction in PCR machine at 37°C for *1 hour*.

5) Prepare 3 phase-lock gel columns per sample by *1 minute* **13K rpm** spins.

6) Add 190 µL **ddH2O** to these TAP-tubes and mix.

7) Transfer RNA incubation to a phase-lock gel column, and then add in 200 µL **Acid Phenol:Chloroform:IAA (125:24:1) pH 4.5**.

8) Mix by gently inverting the tubes.

9) Centrifuge at ***12,000 rpm*** for *5 minutes* at 4°C in Eppendorf spinner.

10) Transfer the top aqueous layer[31] into a new phase-lock gel column, and then add in 200 µL **Acid Phenol:Chloroform:IAA (125:24:1) pH 4.5**.

11) Mix by gently inverting the tubes.

12) Centrifuge at ***12,000 rpm*** for *5 minutes* at 4°C in Eppendorf spinner.

13) Transfer the top aqueous layer into a new phase-lock gel column, and then add in 40 µL **Chloroform:IAA (24:1)**.

14) Mix by gently inverting the tubes.

---

[30] 3' adapter

[31] There may be some phase-lock gel at the top of the aqueous layer after the spin. Poke a hole through it using a pipette tip, and then using a fresh tip, go in and pipette up. In eluting to a new tube, leave the tip in the air and pipette out to the new tube to make sure the residual gel at the tip do not enter. The gel plug should be at an angle after the spin, so just pipette up the fluid from the tube vertically so that ALL the aqueous layer gets taken up.

15) Centrifuge at ***12,000 rpm*** for *5 minutes* at 4°C in Eppendorf spinner.

16) Transfer the top aqueous layer into an RNase-free siliconized epitube.

17) Add *(in this order)* 20 µL of **3M NaAc pH 5.2** and 800 µL[32] **ethanol** into these tubes.

18) Mix by inverting for *1 minute*.

19) Leave in -80°C for *an hour* to precipitate RNA.

20) On ice, prepare the following in a RNase-free PCR tube (multiply for each additional sample + 1 no RNA control):

a. 1 µL **10X T4 ligase buffer**

b. 0.5 µL **20U/µL Superasin**

c. 1 µL **1 mg/mL BSA**

d. 2 µL **10U/µL T4 RNA Ligase 1**

e. 1 µL **50 µM modban**

f. 1 µL **DMSO**

g. 3.5 µL **ddH2O**

21) Spin frozen RNA cube at ***13.8K rpm*** for *15 minutes* at 4°C Eppendorf spinner.[33]

22) Pipette out the supernatant while avoiding the pellet.

23) Wash with 500µL of **ice-cold 70% EtOH**.[34]

24) Spin at ***13,000 rpm*** for *1 minute* at 4°C in Biofuge spinner.

25) Remove the supernatant while avoiding the pellet. Do not let the pellet dry completely.

26) Immediately dissolve in 10µL of ligation reaction prepared above. Pipette up and down and rinse the walls of the tube until it is thoroughly mixed.

[32] 4X+ volume of extraction
[33] ~20K x g; spin as a frozen ice block
[34] This is to remove leftover salt, so no need to dislodge the pellet.

27) Transfer to a new RNase-free PCR tube, and incubate in a PCR machine at 15°C for *2 hours* and then 4°C *overnight*.

STEP 3 – PART II:

1) FOLLOW **STEP 1B PART I** protocols for running the reaction out in a PAGE gel (blue 4+ inches from well)[35], with the following modifications:
2) Use DNA ladder instead. The 3' adapter is 19 bp in length. Modban-modban self-ligation, if they happen, will be 38 bp in length. Be sure to run that no-RNA control! CMO16385 and CMO16386 should demarcate the correct range (***33*** and ***48***). Bands should be in 22+19=41 and 26+19=45 range. Mix and load 2µL of each of the **50 ng/µL** DNA size ladders.

STEP 3 – PART III and STEP 5:

1) FOLLOW **STEP 1B PART II** protocols for filtering gel slice's RNA, with the following notes:
2) Keep cutting out and using the -RNA for subsequent measurements as well!
3) As the RNA is being frozen at -80°C, prepare a 100µM stock of the **5' RNA adapter**, by adding 10x nm amount in µL **DEPC-treated ddH20**. ***Each stock corresponds to one barcode.***
4) As the RNA is being frozen at -80°C, prepare the following ligation mixes (1 unique mix per barcode + the -RNA control):

   a. 1 µL **10X T4 ligase buffer**

   b. 1 µL **10mM ATP**

   c. 0.5 µL **20U/µL Superasin**

   d. 1 µL **1 mg/mL BSA**

[35] For resolving adapter-dimers from true RNA-adapter complexes

e. 2 µL **10U/µL T4 RNA Ligase 1**

f. 1 µL **100 µM 5' adapter barcode**

g. 1 µL **DMSO**

h. 2.5 µL **ddH2O**.

5) Dissolve pellets from gel-extracted TAP-3'-ligated RNAs in ligation buffer above.
6) Pipette up and down and rinse the walls of the tube until it is thoroughly mixed.
7) Transfer to a new RNase-free PCR tube, and incubate in a PCR machine at 15°C for *6 hours* and then 4°C *overnight*.

STEP 5 – PART II:

1) FOLLOW **STEP 1B PART I** protocols for running the reaction out in a PAGE gel (blue 4+ inches from well), with the following modifications:
2) Use DNA ladder instead. The 5' adapter is 21 bp in length. CMO16387 and CMO16388 should demarcate the correct range (***54***, ***69*** respectively). Bands should be in 19+21+22=62 and 19+21+26=66 range. Mix and load 2µL of each of the **50 ng/µL** DNA size ladders.

STEP 5 – PART III and STEP 6:

1) FOLLOW **STEP 1B PART II** protocols for filtering gel slice's RNA.
2) While ligated RNAs are in -80°C precipitating, On ice, prepare the following in a RNase-free PCR tube (multiply for each additional sample): *a.* 0.5 µL **100 µM RT DNA oligo**

   b. 1 µL **10 mM dNTP mix**

   c. 8.5 µL **ddH2O**
3) Immediately dissolve doubly-ligated RNA pellet in 10µL of cocktail reaction prepared above. Pipette up and down and rinse the walls of the tube until it is thoroughly mixed.

4) Transfer to a new RNase-free PCR tube, and incubate in a PCR machine at 65°C for *5 minutes* and then ice for *2 minutes*.

5) Add into the tubes on ice the following:

   a. 4 µL **5X SSIII buffer**

   b. 2 µL **100 mM DTT**

   c. 0.5 µL **20U/µL Superasin**

   d. 0.5 µL **SSIII enzyme**

6) Incubate in a PCR machine 50°C for *1 hour*, and then 85°C for *5 minutes*.

7) Add in 1 µL **RNase H** to each tube, and incubate at 37°C for *20 minutes*.

8) Can freeze at -20 or -80°C.

STEP 7:

1) Prepare a PCR mixture (and multiply by the number of samples – be sure to include a -cDNA sample):

   a. 5 µL **10X Taq Buffer**

   b. 0.5 µL **short F primer**

   c. 0.5 µL **short R primer**

   d. 5 µL **2.5mM dNTPs**

   e. 0.5 µL **ExTaq**

   f. 36.5 µL **ddH2O**

2) Add 48 µL of above mixture to 2 µL of each sample's cDNA and mix by pipetting.

3) Run the following PCR program: (i) 94°C for 30 seconds, (ii) 94°C for 20 seconds, (iii) 55°C for 20 seconds, (iv) 72°C for 20 seconds, (v) back to *(ii)* for 20 to 35 cycles, (vi) 72°C for 30 seconds, (vii) 4°C hold in the Eppendorf PCR machine.[36]
4) Prepare a PCR mixture (and multiply by the number of samples – be sure to include a -cDNA sample):
   a. 5 µL **10X Taq Buffer**
   b. 1 µL **long F primer**
   c. 1 µL **long R primer**
   d. 5 µL **2.5mM dNTPs**
   e. 0.5 µL **ExTaq**
   f. 12.5 µL **ddH2O**
5) Add 25 µL of above mixture to 25 µL of a sample from PCR in Step 3 (split into two).
6) Run the same PCR program in Step 3 with two different cycle numbers. For low abundance preps, use 35 and 45 cycles.
7) Make a 150mL **3% agarose gel with ethidium bromide**, run out PCR samples with a **1KB+ ladder**, at **85V** for *2.5 hours*.
8) Check to see if there are any bands ~110bp range. If too much other bands:
   a. if too much ABOVE the 110, decrease the second PCR cycle number
   b. if too much BELOW the 110, decrease the first PCR cycle number
9) If there are ~110 bp bands, perform PCR with rest of cDNA accordingly, run out on **non-denaturing 8% PAGE gel** and excise to extract the DNA for cloning QC and Solexa sequencing.

[36] Because of the short incubation periods, the shift between temperatures is sometimes longer than the cycle itself in older PCR machines.

The materials and reagents used in this protocol are listed in **Table 5.4**. The primers used in this protocol were designed specifically for the sequencing preparation guidelines; these proprietary barcodes are available upon request through major sequencing facilities and Illumina sequencing kits.

Table 5.4: Reagents used in preliminary small RNA sequencing protocol

Reagent	Vendor
RNase-free 40% acrylamide/bis-acrylamide (19:1) solution, 100mL	EMD Millipore
RNase-free TEMED, 25mL	EMD Millipore
Siliconized Microcentrifuge Tubes, 1.5mL	Fischer Scientific
Phase Lock Gel, 2mL, Heavy	Fischer Scientific
TE, pH 7.5, RNase-free, 1L	IDT
DEPC-treated water, 1L	Life Technologies
Trizol, 100 mL	Life Technologies
mirVana™ miRNA Isolation Kit	Life Technologies
5M NH4Acetate, RNase-free, 100mL	Life Technologies
RNase-free 5M NaCl, 100mL	Life Technologies
RNase-free 10X TBE, 4x1L	Life Technologies
RNase-free urea, 1 kg	Life Technologies
SYBR Gold Nucleic Acid Gel Stain	Life Technologies
RNase-free Ammonium Persulfate, 25g	Promega
Anhydrous chloroform, 100mL	Sigma-Aldrich
Ethanol, molecular grade, 200 proof, 500mL	Sigma-Aldrich
Glycogen, RNA-grade, 0.2mL of 20mg/mL	Thermo Scientific
Nanosep MF, 0.45 µm, 24x	VWR
RNase-out refills, 1L	VWR
PTFE-coated spatula	VWR
PTFE Tissue Grinder, Serrated Plunger, 2mL	VWR
Polystyrene Weigh Boats, 20mL	VWR
2-Propanol, ACS Grade, 1L	VWR
PTFE Tissue Grinder, Glass Vessel, 2mL	VWR
ZR small-RNA Ladder, 10 ug	Zymo Research
RNase-free 40% acrylamide/bis-acrylamide (19:1) solution, 100mL	EMD Millipore
Nanosep MF, 0.45 µm, 24x	VWR
NaAc, 3M, pH 5.2, RNase-free	EMD Millipore
Tobacco Acid Pyrophosphatase (TAP), 10U/uL, 100 units	Epicentre
SUPERase•In (20 U/µL)	Life Technologies
T4 RNA Ligase 1 (ssRNA Ligase)	NEB
RNase-free BSA	NEB
RNase-free DMSO-50mL	Sigma-Aldrich
RNase-free dNTP mix, 10 mM, 0.2mL	Sigma-Aldrich
SuperScript III RT, 200U/uL, 10,00 Units	Life Technologies
RNase H, 10U/uL, 200 units	Life Technologies

LITERATURE CITED

BESHORE, E. L., T. J. MCEWEN, M. C. JUD, J. K. MARSHALL, J. A. SCHISA *et al.*, 2011 C. elegans Dicer interacts with the P-granule component GLH-1 and both regulate germline RNPs. Dev Biol **350:** 370-381.

CLAYCOMB, J. M., P. J. BATISTA, K. M. PANG, W. GU, J. J. VASALE *et al.*, 2009 The Argonaute CSR-1 and its 22G-RNA cofactors are required for holocentric chromosome segregation. Cell **139:** 123-134.

DOMEIER, M. E., D. P. MORSE, S. W. KNIGHT, M. PORTEREIKO, B. L. BASS *et al.*, 2000 A link between RNA interference and nonsense-mediated decay in Caenorhabditis elegans. Science **289:** 1928-1931.

DUDLEY, N. R., J. C. LABBE and B. GOLDSTEIN, 2002 Using RNA interference to identify genes required for RNA interference. Proc Natl Acad Sci U S A **99:** 4191-4196.

GUANG, S., A. F. BOCHNER, D. M. PAVELEC, K. B. BURKHART, S. HARDING *et al.*, 2008 An Argonaute transports siRNAs from the cytoplasm to the nucleus. Science **321:** 537-541.

HANAZAWA, M., M. YONETANI and A. SUGIMOTO, 2011 PGL proteins self associate and bind RNPs to mediate germ granule assembly in C. elegans. J Cell Biol **192:** 929-937.

JOSE, A. M., J. J. SMITH and C. P. HUNTER, 2009 Export of RNA silencing from C. elegans tissues does not require the RNA channel SID-1. Proc Natl Acad Sci U S A **106:** 2283-2288.

KAWASAKI, I., Y. H. SHIM, J. KIRCHNER, J. KAMINKER, W. B. WOOD *et al.*, 1998 PGL-1, a predicted RNA-binding component of germ granules, is essential for fertility in C. elegans. Cell **94:** 635-645.

KIRIENKO, N. V., J. D. MCENERNEY and D. S. FAY, 2008 Coordinated regulation of intestinal functions in C. elegans by LIN-35/Rb and SLR-2. PLoS Genet **4:** e1000059.

PHILLIPS, C. M., T. A. MONTGOMERY, P. C. BREEN and G. RUVKUN, 2012 MUT-16 promotes formation of perinuclear mutator foci required for RNA silencing in the C. elegans germline. Genes Dev **26:** 1433-1444.

ROBERT, V. J., T. SIJEN, J. VAN WOLFSWINKEL and R. H. PLASTERK, 2005 Chromatin and RNAi factors protect the C. elegans germline against repetitive sequences. Genes Dev **19:** 782-787.

SAFFER, A. M., D. H. KIM, A. VAN OUDENAARDEN and H. R. HORVITZ, 2011 The Caenorhabditis elegans synthetic multivulva genes prevent ras pathway activation by tightly repressing global ectopic expression of lin-3 EGF. PLoS Genet **7:** e1002418.

SCHISA, J. A., J. N. PITT and J. R. PRIESS, 2001 Analysis of RNA associated with P granules in germ cells of C. elegans adults. Development **128:** 1287-1298.

SHETH, U., J. PITT, S. DENNIS and J. R. PRIESS, 2010 Perinuclear P granules are the principal sites of mRNA export in adult C. elegans germ cells. Development **137:** 1305-1314.

SPIKE, C. A., J. BADER, V. REINKE and S. STROME, 2008 DEPS-1 promotes P-granule assembly and RNA interference in C. elegans germ cells. Development **135:** 983-993.

SQUIRRELL, J. M., Z. T. EGGERS, N. LUEDKE, B. SAARI, A. GRIMSON *et al.*, 2006 CAR-1, a protein that localizes with the mRNA decapping component DCAP-1, is required for cytokinesis and ER organization in Caenorhabditis elegans embryos. Mol Biol Cell **17:** 336-344.

TABARA, H., M. SARKISSIAN, W. G. KELLY, J. FLEENOR, A. GRISHOK *et al.*, 1999 The rde-1 gene, RNA interference, and transposon silencing in C. elegans. Cell **99:** 123-132.

TABARA, H., E. YIGIT, H. SIOMI and C. C. MELLO, 2002 The dsRNA binding protein RDE-4 interacts with RDE-1, DCR-1, and a DExH-box helicase to direct RNAi in C. elegans. Cell **109:** 861-871.

UPDIKE, D., and S. STROME, 2010 P granule assembly and function in Caenorhabditis elegans germ cells. J Androl **31:** 53-60.

UPDIKE, D. L., and S. STROME, 2009 A genomewide RNAi screen for genes that affect the stability, distribution and function of P granules in Caenorhabditis elegans. Genetics **183:** 1397-1419.

WANG, D., S. KENNEDY, D. CONTE, JR., J. K. KIM, H. W. GABEL *et al.*, 2005 Somatic misexpression of germline P granules and enhanced RNA interference in retinoblastoma pathway mutants. Nature **436:** 593-597.

WU, X., Z. SHI, M. CUI, M. HAN and G. RUVKUN, 2012 Repression of germline RNAi pathways in somatic cells by retinoblastoma pathway chromatin complexes. PLoS Genet **8:** e1002542.

YIGIT, E., P. J. BATISTA, Y. BEI, K. M. PANG, C. C. CHEN *et al.*, 2006 Analysis of the C. elegans Argonaute family reveals that distinct Argonautes act sequentially during RNAi. Cell **127:** 747-757.

ZHUANG, J. J., and C. P. HUNTER, 2012 RNA interference in Caenorhabditis elegans: uptake, mechanism, and regulation. Parasitology **139:** 560-573.

Chapter Six

The influence of competition among *C. elegans* small RNA pathways on development

The contents were previously published in ZHUANG, J. J., and C. P. HUNTER, 2012. The Influence of Competition Among *C. elegans* Small RNA Pathways on Development. *Genes* **3:** 671-685.

ABSTRACT

Small RNAs play a variety of regulatory roles, including highly conserved developmental functions. *Caenorhabditis elegans* not only possesses most known small RNA pathways, it is also an easy system to study their roles and interactions during development. It has been proposed that in *C. elegans*, some small RNA pathways compete for access to common limiting resources. The strongest evidence supporting this model is that disrupting the production or stability of endogenous short interfering RNAs (endo-siRNAs) enhances sensitivity to experimentally induced exogenous RNA interference (exo-RNAi). Here, we examine the relationship between the endo-siRNA and microRNA (miRNA) pathways, and find that, consistent with competition among these endogenous small RNA pathways, endo-siRNA pathway mutants may enhance miRNA efficacy. Furthermore, we show that exo-RNAi may also compete with both endo-siRNAs and miRNAs. Our data thus provide support that all known Dicer-dependent small RNA pathways may compete for limiting common resources. Finally, we observed that both endo-siRNA mutants and animals experiencing exo-RNAi have increased expression of miRNA-regulated stage-specific developmental genes. These observations suggest that perturbing the small RNA flux and/or the induction of exo-RNAi, even in wild-type animals, may impact development via effects on the endo-RNAi and microRNA pathways.

INTRODUCTION

Non-coding RNAs regulate a myriad of biological processes (FISCHER 2010; KAIKKONEN *et al.* 2011). Two broad classes of highly conserved non-coding regulatory RNA pathways were discovered in the nematode *Caenorhabditis elegans*. First, microRNAs (miRNAs) were identified as transcribed RNAs corresponding to mutant loci that disrupted stage-specific

developmental processes (LEE *et al.* 1993; REINHART *et al.* 2000). These small RNAs are complementary to nucleotide sequences in the 3'UTR of inferred target mRNAs and act to inhibit translation and/or mRNA target stability (LEE *et al.* 1993; PASQUINELLI *et al.* 2000; REINHART *et al.* 2000). Subsequent genomic analysis identified scores of 22 nucleotide miRNAs, many broadly conserved in plants and animals (KAWAJI and HAYASHIZAKI 2008; PASQUINELLI *et al.* 2000). Second, mechanistic investigation of the widely used technique of RNA interference (RNAi) revealed the existence of regulatory pathways that produce and use short interfering RNAs (siRNAs), whether derived from exogenous dsRNA (exo-siRNAs) or endogenous loci (endo-siRNAs) (FIRE *et al.* 1998; GENT *et al.* 2010; GRISHOK 2005; LEE *et al.* 2006; TABARA *et al.* 1999). Investigations in other systems, including *Drosophila*, *Arabidopsis*, and mammalian cultures, have identified additional non-coding RNA pathways, including piwi-interacting RNA (piRNAs) and long non-coding RNA (lncRNAs), both of which have also been found in *C. elegans* (DAS *et al.* 2008; SIFUENTES-ROMERO *et al.* 2011; WILUSZ *et al.* 2009). The biological processes regulated by these small RNAs are quite extensive, including germline maintenance (DAS *et al.* 2008), chromosomal segregation (CLAYCOMB *et al.* 2009), protection against transgenic parasites (OHTA *et al.* 2008), multi-generational inheritance of RNAi signals (GU *et al.* 2012), and developmental regulation (AZIMZADEH JAMALKANDI and MASOUDI-NEJAD 2011).

Genetic screens have identified mutants in *C. elegans* with enhanced exo-RNAi responses (Eri mutants) (DUCHAINE *et al.* 2006; FISCHER *et al.* 2008; KENNEDY *et al.* 2004; PAVELEC *et al.* 2009; SIMMER *et al.* 2002). Confoundingly, these mutants which enhance exo-RNAi disrupt endo-RNAi (DUCHAINE *et al.* 2006; FISCHER *et al.* 2008; GENT *et al.* 2009; PAVELEC *et al.* 2009). One proposed explanation is that endo-RNAi and exo-RNAi pathways compete for one or more limited common enzymatic resources, so that reduced endo-RNAi

activity (FISCHER *et al.* 2011; GENT *et al.* 2010) results in greater flux of small RNAs through the exo-RNAi pathway (DUCHAINE *et al.* 2006; LEE *et al.* 2006). Additional support for this competition model is provided by the identification of limiting RNAi components that are both necessary for the enhanced RNAi response and, when over-expressed, confer enhanced RNAi (DUCHAINE *et al.* 2006; YIGIT *et al.* 2006).

Although competition has only been inferred between endo- and exo-RNAi pathways, because *C. elegans* has only one *dicer* homolog – *dcr-1* – this competition model has been hypothesized to include other small RNA pathways, particularly the microRNA pathway (DUCHAINE *et al.* 2006; YIGIT *et al.* 2006). This model proposes that various *dcr-1*-dependent non-coding RNAs compete for limited common enzymatic resources, including RNA-dependent RNA polymerases (RdRPs) that produce abundant secondary siRNAs and secondary siRNA binding Argonouates (SAGOs) (DUCHAINE *et al.* 2006) (**Figure 6.1A**). Consistent with this model, over-expression of some of these resources, specifically the secondary Agos SAGO-1 and SAGO-2, can enhance exo-RNAi (DUCHAINE *et al.* 2006; YIGIT *et al.* 2006). However, direct evidence to support this broader competition model is lacking, especially with respect to small RNA pathways other than exo- and endo-RNAi. Moreover, many of these non-coding small RNAs, particularly miRNAs like *lin-4* and *let-7*, are developmentally regulated (LEE *et al.* 1993; REINHART *et al.* 2000), which challenges simple interpretations of the extent of competition. For instance, the loss of one RNAi pathway may impact development, which in turn affects the production or stability of another pathway's small RNAs. Such competition would not be for common RNAi resources, but rather reflect an indirect result of the physiological changes. The fact that weak alleles or maternal rescue of *dicer* causes sickly phenotypes in animals (KNIGHT and BASS 2001; PAVELEC *et al.* 2009) may suggest that this is a realistic concern.

Here, we examine the relationship between endo-RNAi and miRNAi pathways and show that, although the *eri-1* mutant partially rescues the *let-7* mutant's physiological defects, thus apparently enhancing residual *let-7* activity, Eri mutants also show increased expression of *let-7* targets *lin-14*, *lin-41*, and *daf-12,* thus appearing to simultaneously decrease *let-7* activity. Similarly, we show that engaging the exo-RNAi pathway, by exposing animals to *gfp* dsRNA, also appears to reduce the efficacy of both endoRNAi and miRNAi pathways. Finally, we observed that the relative expression of stage-specific developmental genes differs amongst small RNA pathway mutants, suggesting that in addition to competition for common limiting RNAi resources, perturbing small RNA flux also impacts developmental regulation. This may have large and indirect effects on the activity of endogenous small RNA pathways.

RESULTS AND DISCUSSION

Rescue of let-7 phenotypes by the eri-1 mutant

To determine whether the *eri* pathway competes with the miRNA pathway (**Figure 6.1A**), we sought to determine whether, like the genetic interaction between the exo-RNAi and endo-RNAi pathways, similarly disrupting the endo-RNAi pathway could abrogate miRNA developmental defects. To detect changes in miRNA pathway efficacy, we scored fertility and vulva integrity (KETTING *et al.* 2001) of *let-7(n2853)* single and *let-7(n2853);eri-1(mg366)* double mutant animals. The *n2853* allele is a partial loss-function mutation that remains viable at 15ºC (REINHART *et al.* 2000). We found that the *eri-1;let-7* double mutant exhibited a significant reduction in the burst vulva phenotype (**Figure 6.1B**), and an increase in brood size compared to the *let-7(n2853)* single mutant (**Figure 6.1C**). Although the rescue was incomplete, these results indicate a genetic interaction between these two small RNA pathways. Because the disruption of

Figure 6.1: *eri-1* dependent *let-7* reduction-of-function phenotypes

(A) Schematic of proposed competing small RNA pathways. MicroRNAs, experimentally introduced double stranded RNAs (dsRNA), and endogenous short interfering RNAs (endo-siRNAs) were proposed (YIGIT *et al.* 2006) to compete for limiting shared resources, including the single *C. elegans* DICER homolog, *dcr-1*, the RNA-directed RNA polymerase RRF-1, and the secondary Argonautes (SAGOs), including the *C. elegans* specific worm Argonautes (WAGOs) that mediated siRNA-dependent silencing. The competition for limiting shared resources implies that reduced flux through one pathway allows for increased access to limiting resources for the other pathways. **(B)** Spontaneous vulva bursting rate of *let-7(n2853)* single (n=9) and *eri-1(mg366);let-7(n2853)* double (n=10) mutants at 15ºC. The average of n complete broods is shown. The *eri-1(mg366)* single mutant does not exhibit any burst vulva phenotype. **(C)** Average brood size of *let-7(n2853)* and *eri-1(mg366)* single mutants (n=5) and *eri-1(mg366);let-7(n2853)* double mutants (n=8) at 15ºC. Standard deviations are shown. *p*-values are calculated by *t*-test.

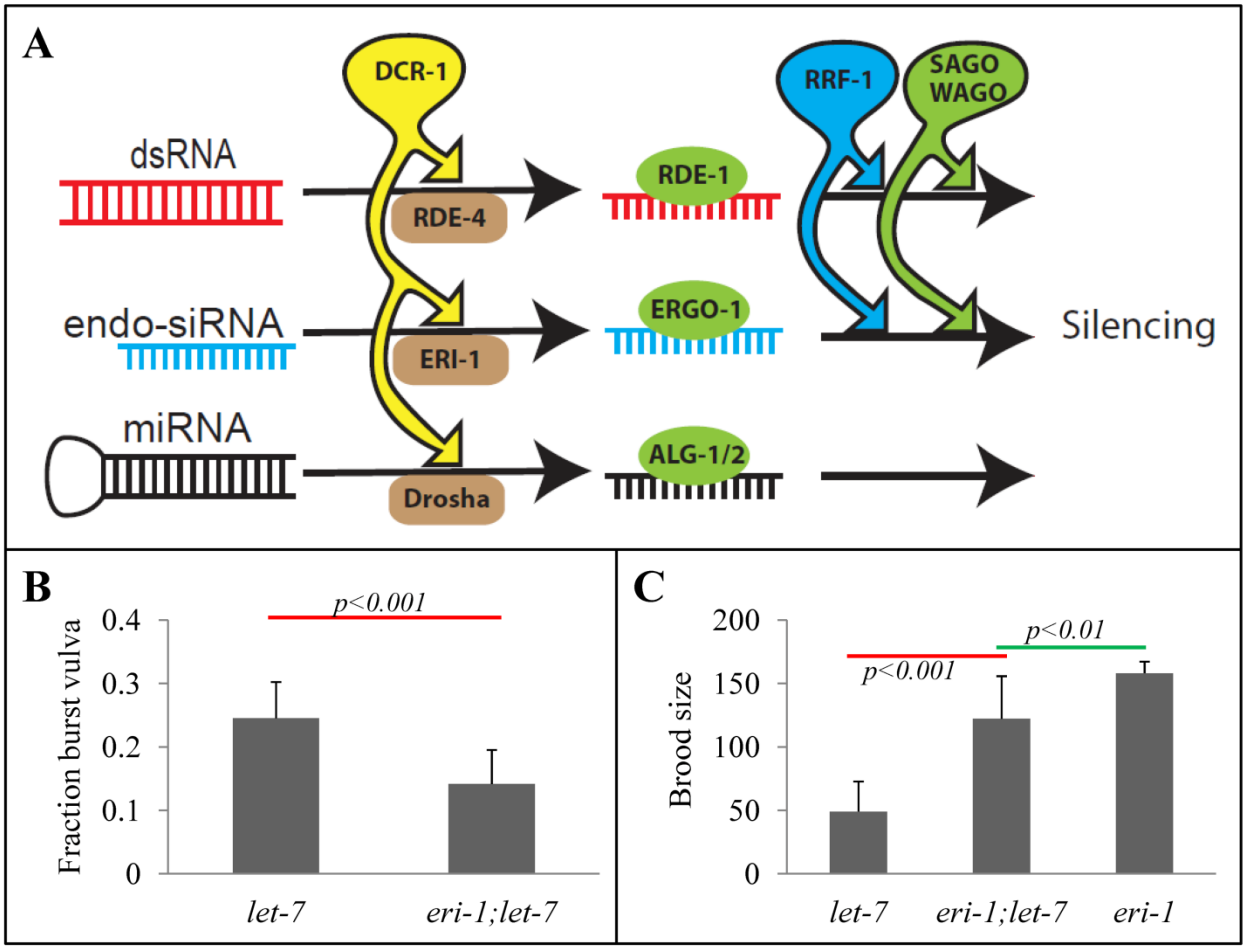

Figure 6.1 (Continued): *eri-1* dependent *let-7* reduction-of-function phenotypes

endogenous siRNAs seems to suppress the *let-7* phenotypes, the implication is that the endo-siRNA pathway may compete with the miRNA pathway. To our knowledge, this is the first reported genetic interaction between these two pathways.

eri-1 mutant worms have higher expression of let-7 regulated genes at mid-L4

To determine whether the observed genetic interaction reflects enhanced miRNA efficacy (rather than indirect effects, for example loss of a specific siRNA), we measured the abundance of *let-7* regulatory targets, which increase in abundance in *let-7* mutants (REINHART *et al.* 2000). If *eri-1*-mediated repression of *let-7* is via reduced competition and consequently the production of higher *let-7* levels or more effective use of *let-7* miRNA, then the target genes should decrease in abundance in the *eri-1* mutant relative to wild type. However, if the phenotypic suppression of *let-7(2853)* in an *eri-1* mutant background is indirect, then no effect on *let-7* target mRNA levels is expected. An advantage of assaying target mRNA levels is that the competition model does not make any predictions about which stage of small RNA processing or activity the competition occurs. This means the production, stability, or even efficacy of small RNAs could be rate-limiting. A complication is that *let-7* regulates temporally expressed genes, thus it is critical to measure RNA levels from precisely staged animals. Therefore, RNA was extracted from mid-fourth larval stage (L4) worms hatch-synchronized to within 1 hour and then raised at 15ºC for an additional 69 hours. As an additional level of control, we normalized gene expression to *bli-1*, an L4-specific collagen gene that is not known to be regulated by endogenous small RNAs (PAGE 1997). Thus, in essence, developmental time is redundantly staged, by both "human time" – 69 hours post-hatching – as well as "worm time" – *bli-1* mRNA expression. Surprisingly, we observed that the *let-7*-regulated genes *lin-14*, *lin-41*, and *daf-12*

(PASQUINELLI *et al.* 2000) all showed increased expression in an *eri-1* mutant background (**Figure 6.2A**). To ensure that this is not unique to *bli-1* normalization, we assayed for expression levels of *lin-41* normalized to the glyceraldehyde 3-phosphate dehydrogenase *gpd-3*, a stably expressed housekeeping gene that is commonly used for *C. elegans* mRNA normalization (WELKER *et al.* 2010). Again, *lin-41* showed increased expression in an *eri-1* mutant background (**Figure 6.2A**), suggesting that this observation is not a normalization artifact. Thus, *let-7*-regulated genes are affected by endo-siRNA depletion, but rather than an increase in *let-7* activity, we observed an increase in target mRNA levels, which suggests an apparent decrease in *let-7* efficacy.

All Eri mutants have higher expression of let-7-regulated genes at mid-L4

Biochemically, the endo-siRNA pathway is diverse and includes RdRPs (RRF-3), siRNases (ERI-1), RNA binding Tudor domain proteins (ERI-5), helicases (ERI-4, ERI-6/7), and Agos (ERI-8). To determine whether the observed increase in *let-7* target mRNA levels is specific to *eri-1(mg366)*, or represents a more general effect of reduced function in the endo-siRNA pathway, we determined the expression levels of *lin-14* and *lin-41* in *rrf-3(pk1426)*, *dcr-1/eri-4(mg375)*, *eri-6/7(tm1917)*, and *ergo-1/eri-8(gg100)* mutant backgrounds. Consistent with our *eri-1* observations, these mutants also showed increased expression of the two *let-7* targets (**Figure 6.2B**), suggesting that a functional endo-siRNA pathway is important for *let-7* efficacy.

Included in these experiments were three independent controls. First, as expected, *lin-14* and *lin-41* expression increased between 20 to 60 fold in *let-7(n2853)* mutants compared to N2 wild type. Similarly, the viable *dcr-1(mg375)* allele showed a very strong upward effect on the *let-7* target mRNA levels, as would be expected for a mutation that directly affects miRNA

Figure 6.2: Expression of *let-7*-regulated transcripts in endo-RNAi mutant backgrounds

(A) *bli-1* normalized abundance of the *let-7*-repressed *lin-14*, *lin-41*, and *daf-12* transcripts in *eri-1(mg366)* mid-L4 animals (69 hours post hatching at 15°C) relative to N2 wild type. *gpd-3* normalized *lin-41* transcripts in *eri-1(mg366)* mid-L4 animals relative to N2 is indicated by "*lin-41*/[*gpd-3*]c". **(B)** *bli-1* normalized abundance of the *lin-14* and *lin-41* transcripts in the indicated endo-RNAi and control (N2 and *sid-1(qt9)*) mid-L4 animals. **(C)** Developmental analysis of *lin-41* transcripts during the L4-stage in *eri-1(mg366)* and N2 strains, normalized to *gpd-3*. Although *lin-41* transcripts become rare, Ct values remained reliable through 69 hours post hatching (≤30); but by 73 hours post hatching, Ct values were greater than 34 and therefore considered undetectable and unreliable(KARLEN *et al.* 2007; SHEN *et al.* 2010). Error bars indicate standard deviation in **(A)** and **(B)**, and 95% confidence interval in **(C)**. * indicates $p<0.05$; ** indicates $p<0.01$; no asterisks indicate statistical insignificance. *p*-values are calculated by *t*-test.

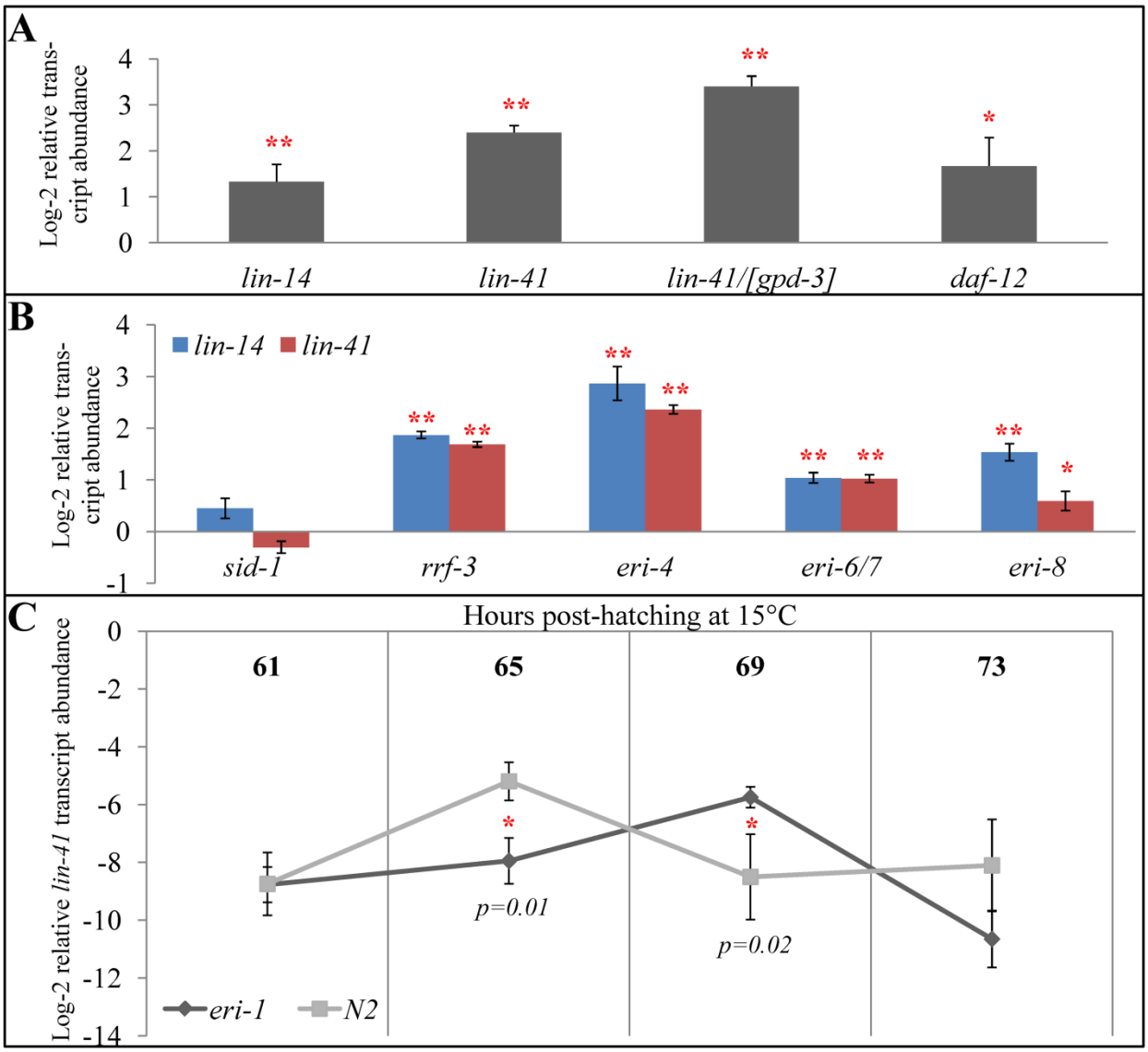

Figure 6.2 (Continued): Expression of *let*-7-regulated transcripts in endo-RNAi mutant backgrounds

biogenesis(PAVELEC *et al.* 2009). Finally, as a negative control, we assayed *lin-14* and *lin-41* expression levels in a *sid-1(qt9)* background. Because *C. elegans* miRNAs seem to act cell autonomously (ZHANG and FIRE 2010), their activity should not require the systemic double-stranded RNA channel SID-1. As expected, *lin-14* and *lin-41* expression levels were indistinguishable between *sid-1(qt9)* and N2 animals (**Figure 6.2B**).

eri-1 mutants may have delayed down-regulation of lin-41

Our findings thus far indicate that mutations in the endo-siRNA pathway phenotypically suppress *let-7*, consistent with the proposed competition model, whereas the effect on the *let-7* target mRNAs was opposite to expectations, showing an increase instead of a decrease (**Figure 6.2A, B**). While there are many possible explanations, including post-transcriptional silencing versus translational repression, one possibility that should be considered and that can be directly tested is that developmental time is affected in the endo-RNAi mutants. *let-7* acts as a temporal developmental switch, down-regulating target genes to control stage-specific differentiation. Therefore, minor effects on *let-7* temporal activity would be amplified. Although we attempted to control for this possibility by normalizing mRNA levels to the L4-specific collagen *bli-1*, the apparent increase in the abundance of *let-7* target transcripts in endo-RNAi mutants may reflect a developmental time point before *let-7* accumulates to effective levels. That is, the endo-RNAi mutants may slow worm developmental time relative to human time, delaying both accumulation of *let-7* and the predicted transition to L4 gene expression patterns. To test this hypothesis, we collected RNA from hatch-synchronized worms raised at 15ºC for 61, 63, 69 and 73 hours to measure *lin-41* levels prior, during, and after *let-7* regulation.

Consistent with previous observations, in a wild type background, *lin-41* levels were high at the beginning of the L4 stage (hours 61 to 65), but dropped to undetectable levels at later L4 stages (hours 69 to 73) (REINHART *et al.* 2000) (**Figure 6.2C**). Interestingly, in an *eri-1(-)* background, *lin-41* transcript levels remained at the higher level for at least an additional four hours. In wild type, the decrease in *lin-41* levels was detectable at 65 hours, whereas in *eri-1* mutants, the decrease was first detectable at 69 hours. This seems to suggest that there was a temporal delay in the decrease of *lin-41* expression (**Figure 6.2C**). Although the number of time points is limited, these observations are consistent with a hypothesis that developmental time runs slower in endo-RNAi mutants. Consequently, miRNAs would not be as effective at a particular human time point (i.e. hour 69) because the *eri-1(-)* worms haven't reached the equivalent worm time (mid-L4) for a maximum *let-7* efficacy.

However, other trivial explanations may also fit the data, including a very likely possibility that data points at hours 65 and 69 were noise fluctuations in two genes' expression between the two strains (**Figure 6.2C**). Unfortunately, we were unable to distinctly quantify differences in *let-7* transcripts itself because of its relative rarity and the relatively subtle differences in expression between mutants, which prevented us from drawing additional support for this delayed development hypothesis.

Perturbations to small RNA pathways affect developmental timing

Therefore, to test, confirm, and generally expand the hypothesis that development is slowed in endo-RNAi mutants, we performed real-time PCR to measure the relative expression levels of a variety of stage-specific mRNAs relative to stable housekeeping genes. The collagen *bli-1* is transcribed specifically during the L4 stage(PAGE 1997). Consistent with our hypothesis,

bli-1 transcript levels relative to *gpd-3* transcript levels – which are transcribed stably throughout development (WELKER *et al.* 2010; ZHANG *et al.* 2012) – were reduced in all the endo-RNAi mutants compared to N2 wild type (**Figure 6.3A**). As with *let-7* target genes, the systemic RNAi mutant *sid-1(qt9)* had no detectable effect. Furthermore, both *let-7(n2853)* and *dcr-1/eri-4(mg375)* mutants, which are known to have significant sickness (PASQUINELLI *et al.* 2000; PAVELEC *et al.* 2009; REINHART *et al.* 2000; ZHUANG and HUNTER 2011), showed much larger *bli-1* versus *gpd-3* differences than the other endo-RNAi mutants (**Figure 6.3A**). Finally, the *ergo-1/eri-8(gg100)* allele, which causes the least sterility and brood size reduction (ZHUANG and HUNTER 2011) of the tested endo-RNAi mutants, showed only a small and not statistically significant reduction in relative *bli-1* transcript levels (**Figure 6.3A**).

These findings suggests that either endo-RNAi mutants slow development leading to lower *bli-1* levels 69 hours post hatching, or that these mutants affect metabolism leading to an increase in *gpd-3* levels. To control for this second possibility, we used two additional stably expressed housekeeping genes: *ama-1* (a measure of RNAPII levels) and *pmp-3* (a measure of peroxisome activity) (ZHANG *et al.* 2012), in addition to *gpd-3*, to normalize *bli-1* transcript levels (**Figure 6.3B**). We found that *eri-1* mutants have lower expression of *bli-1* relative to all three stable housekeeping markers compared to N2 and *sid-1(qt9)* mutants. This analysis confirms that at 69 hours post hatching, *eri-1(mg375)* worms compared to N2 and *sid-1(qt9)* worms likely exhibit slowed development. Therefore, these results further suggest that the endo-RNAi mutants reduce the accumulation of L4 specific *bli-1* transcript due to a delay in development.

Combined with the measurements of *lin-41* transcripts (**Figure 6.2C**), these results seem to suggest that endo-RNAi mutants delay development to the mid-L4 stage. To determine

Figure 6.3: Abundance of developmentally regulated transcripts in endo-RNAi mutants

(A) *gpd-3* normalized *bli-1* transcript abundance at mid-L4 (69 hours post hatching at 15°C) in the indicated mutants. **(B)** Relative *bli-1* transcript levels in *eri-1(mg366)* compared to N2 and *sid-1(qt9)* at mid-L4, normalized to the three indicated housekeeping genes. **(C)** Relative expression of the indicated developmental stage-specific genes at the denoted stages in *eri-1(mg366)* and *rrf-3(pk1426)* mutants compared to N2. At 15°C, L1 worms had their RNA extracted 22 hours post-hatching, L4 worms had their RNA extracted 69 hours post-hatching, young adult ("YA") worms had their RNA extracted 80 hours post-hatching, and mature adults ("MA") worms had their RNA extracted 100 hours post-hatching. Error bars indicate standard deviation. * indicates $p<0.05$; ** indicates $p<0.01$; no asterisks indicate statistical insignificance. *p*-values are calculated by *t*-test.

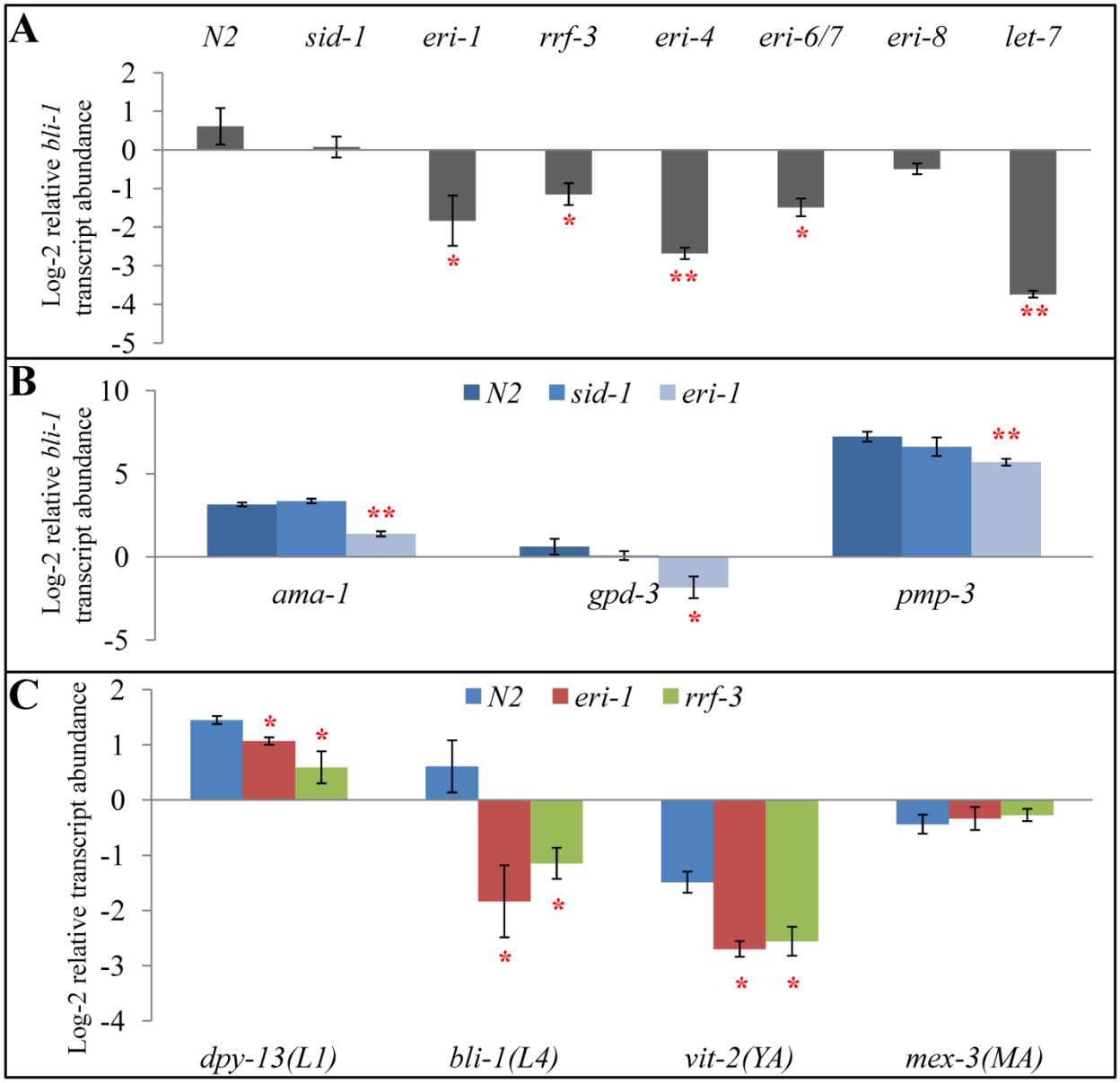

Figure 6.3 (Continued): Abundance of developmentally regulated transcripts in endo-RNAi mutants

whether other developmental transitions are delayed in endo-RNAi mutants, we measured in both *eri-1* and *rrf-3* mutants the relative transcript levels of the L1 specific collagen *dpy-13* (JOHNSTONE and BARRY 1996) 22 hours after hatching, the yolk protein gene *vit-2* (SCHEDIN *et al.* 1991) in young adult 80 hours after hatching, and the germline specific RNA binding protein *mex-3* (YANAI *et al.* 2008) in mature adults 100 hours after hatching. We found that when compared to N2, the *eri-1* and *rrf-3* mutants showed significantly lower *dpy-13*, *bli-1*, and *vit-2* relative expression levels (**Figure 6.3C**). However, the expression levels of the germline specific *mex-3* were not affected in either mutant (**Figure 6.3C**). These results confirm that endo-RNAi mutants display mild developmental delays throughout development, but that by the mature adult stage 24 hours past the last molt, the effect is either no longer distinguishable or that *mex-3* is not a sufficiently sensitive temporal marker.

Impact of developmental timing disturbances on expression studies

The developmental delay associated with endo-RNAi mutants may introduce a confounding factor for gene expression and RNAi phenotypic studies. Specifically, we detected two to four fold differences in measured developmental transcript levels in endo-RNAi mutants relative to wild type (**Figure 6.3A**). Because these differences are likely associated with developmental delays (**Figure 6.2C**), small changes in gene expression may not reflect a causal relationship between small RNA regulation and transcript abundance. Thus, careful calibration for developmental markers may be required before assigning significance to gene expression changes less than 4-fold among the many current *C. elegans* gene-expression datasets performed in endo-RNAi mutants (GENT *et al.* 2010). In addition, many exoRNAi studies use endo-RNAi

mutant backgrounds for their enhanced exo-RNAi phenotype, possibly further subtly confounding the findings.

Exogenous RNAi causes higher expression of some let-7- and rrf-3- regulated genes

The competition model for interactions among the small RNA pathways further predicts that engaging the exo-RNAi pathway will reduce available resources for microRNA-regulated gene expression, resulting in increased target gene expression. To test this prediction, we compared the expression of *lin-14* and *lin-41* between control animals and the same strain exposed to dsRNA. Specifically, a strain expressing the ubiquitous *sur-5::gfp* transgene was grown on either empty vector L4440 bacteria (control) or *gfp*-dsRNA expressing bacteria (exo-RNAi(+)) (**Figure 6.4A**). RNA was then extracted from mid-L4 (69 hour hatch-synchronized) worms raised at 15ºC on each of the bacteria. Quantitative PCR analysis showed that the *lin-14* and *lin-41* transcripts, normalized to *bli-1*, were both elevated when this strain was grown on *gfp*-RNAi food (**Figure 6.4B**). Similar results are obtained when transcripts levels were normalized to *gpd-3* (**Figure 6.4B**).

To similarly test for competition between the exo-RNAi pathway and the endo-RNAi pathway, we measured the transcript levels of the recently identified *rrf-3*-siRNA targets *F14F7.5* and *Y43F8B.9* (GENT *et al.* 2010). As a control, we found these transcripts to be nearly sixty-fold and nearly eight-fold, respectively, more abundant in *rrf-3(pk1426)* mutant than in wild type mid-L4 worms, similar to previously published findings (GENT *et al.* 2010). Consistent with the competition model, *gfp(RNAi)*-treated animals exhibited higher expression levels of the *Y43F8B.9* gene (**Figure 6.4B**). However, we found that *gfp(RNAi)*-treated animals

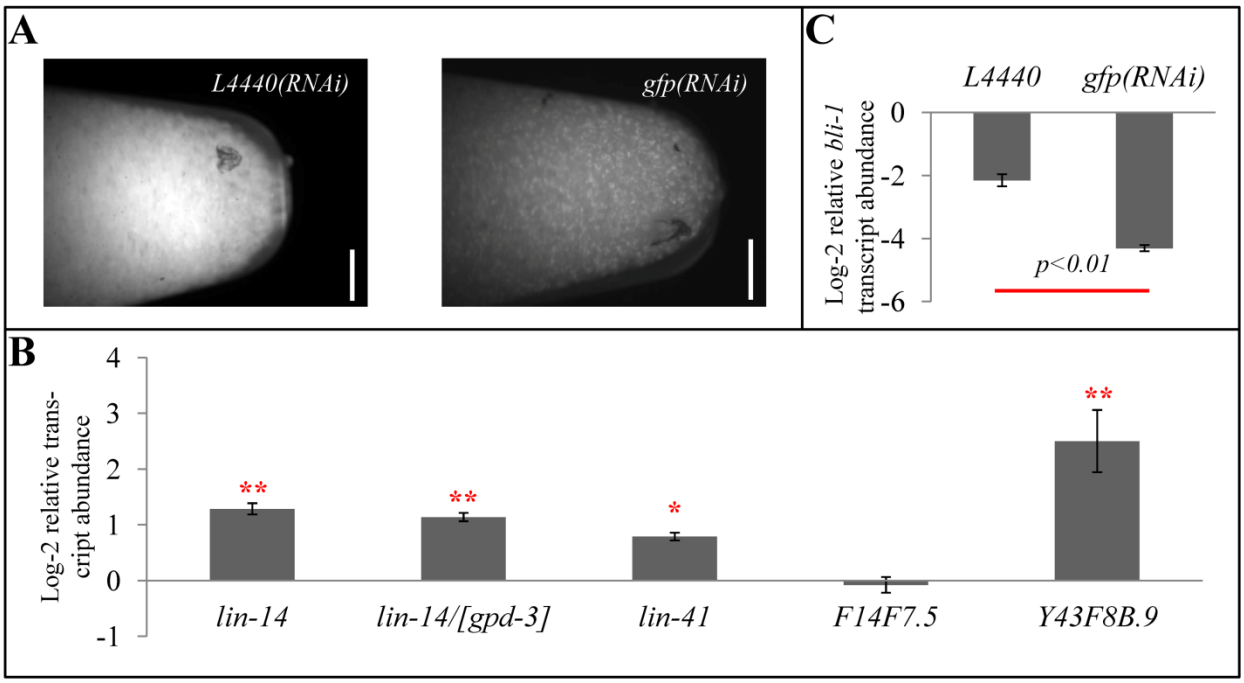

Figure 6.4: The effect of exogenous RNAi on transcript abundance of miRNA- and endo-RNAi-regulated genes

(A) Photomicrograph of ~200µL of *sur-5::gfp* animals grown on control (empty L4440 vector) or *gfp(RNAi)* bacteria prior to RNA extraction. Scale bar indicates 1 mm. **(B)** *bli-1* normalized relative *lin-14, lin-41, F14F7.5,* and *Y43F8B.9* transcript levels in mid-L4 (69 hours post hatching at 15°C) *gfp(RNAi)*-treated *sur-5::gfp* animals compared to L4440 vector-fed *sur-5::gfp* animals. *gpd-3* normalized *lin-14* transcripts in mid-L4 *gfp(RNAi)*-treated *sur-5::gfp* animals compared to L4440 vector-fed *sur-5::gfp* animals is indicated by "*lin-14*/[*gpd-3*]". **(C)** *gpd-3* normalized relative *bli-1* transcript levels in mid-L4 *gfp(RNAi)*-treated *sur-5::gfp* animals compared to L4440 vector-fed *sur-5::gfp* animals. * indicates $p<0.05$; ** indicates $p<0.01$; no asterisks indicate statistical insignificance. *p*-values are calculated by *t*-test.

did not exhibit significant differences in expression levels of *F14F7.5* compared to vector L4440-treated animals (**Figure 6.4B**).

Our results support expanding the competition model to include the microRNA pathway. We hypothesize that mounting an exo-RNAi response reallocates common resources necessary for miRNA and endo-RNAi pathways towards the exo-RNAi pathway, resulting in less effective repression of *let-7* and *rrf-3* target genes. To our knowledge, this is the first reported investigation of the interaction between exoRNAi and miRNA functions. Furthermore, while prior studies of the competition between endoRNAi and exoRNAi focused on the enhanced exoRNAi phenotype of endo-RNAi mutants, we presented data showing that engaging the exo-RNAi pathway compromises the silencing of at least one endoRNAi target.

Interestingly, engaging the exo-RNAi pathway also reduced a worm's relative *bli-1* expression at mid-L4 (**Figure 6.4C**). This result is consistent with delayed development associated with reduced endo-RNAi activity (**Figure 6.2C**). We therefore propose that reduced small RNA flux through endo-RNAi pathways enhances miRNA and exo-RNAi pathways by enabling greater access to limiting resources as well as independently delaying development.

Chicken and egg: Development and small RNAs?

Our findings show that perturbed small RNA flux delays development. This may be caused by interference with miRNA-mediated regulation of the heterochronic genes that control temporal transitions, or the delayed expression of the heterochronic genes may simply reflect non-specific developmental delays. In either case the effects are likely to recursive, such that small initial differences are amplified as development progresses. As more small RNA deep sequencing data and analysis becomes available, it will be intriguing to analyze development

from the perspective of small RNAs as master regulators. From an experimental standpoint, it is already important to consider such assumptions. Our data strongly suggest that endo-RNAi pathways are important for development, and although subtle, the effects may confound gene expression studies.

Conclusions and Future Scope

Recent publications report on competitive regulation schemes akin to the *C. elegans* small RNA competition model (LEE *et al.* 2006) for RNAs in mammalian systems (CESANA *et al.* 2011; KARRETH *et al.* 2011; KHVOROVA and WOLFSON 2012; SUMAZIN *et al.* 2011; TAY *et al.* 2011). These reports identify competitive endogenous RNAs (ceRNAs) that soak up miRNAs involved in tumorigenicity (KHVOROVA and WOLFSON 2012). The use of miRNA profiling to diagnose cancer is becoming common, thus our findings in *C. elegans*, which suggest that developmental timing is intricately tied to small RNA expression, provides a cautionary caveat to these approaches. That is, while the functions of these ceRNAs are robustly demonstrated *in vitro*, when and how they are expressed *in vivo* for their putative regulation of miRNAs is not fully known. It is reasonable to assume that these ceRNAs are spatially and temporally regulated. Defects in tumors growth can impact small RNA expression, thus attributing causal relationships when developmental factors may indirectly affect both miRNAs and ceRNAs should be done with caution.

Therapeutic delivery of small RNAs has been a commercial goal of RNAi for many years (LEUSCHNER *et al.* 2011). Because the mammalian RNAi response apparently lacks an amplified secondary response (STEIN *et al.* 2003), and the *C. elegans* limiting RNAi resources are largely involved in the biogenesis or execution of the secondary response, analogies to the *C. elegans*

competition model were deemed inapplicable. However, our observation that engaging the exoRNAi pathway via experimental dsRNA can cause developmental delays suggests that the indirect aspect of the *C. elegans* small RNA competition can still serve as a model. Off-target effects have long been assumed to result from promiscuous siRNA binding, but our results suggest that perturbed small-RNA flux may also indirectly misregulate biological processes, including development.

MATERIALS AND METHODS

Strains

The following strains were used: (FX1917) *eri-6/7(tm1917)*, (GR1373) *eri-1(mg366)*, (HC195) *nrIs20 (sur-5::NLS-GFP)*, (HC196) *sid-1(qt9)*, (HC793) *eri-1(mg366);let-7(n2853)*, (MT7626) *let-7(n2853)*, (NL2099) *rrf-3(pk1426)*, (YY168) *ergo-1/eri-8(gg100)*, and (YY470) *dcr-1/eri-4(mg375)*. All strains and assays were maintained and performed at 15ºC as previously described (BRENNER 1974).

gfp(RNAi)

gfp(RNAi) assays were performed as previously described (TIMMONS and FIRE 1998). Bacteria engineered to express dsRNA against *gfp* were prepared as previously described (WINSTON *et al.* 2002).

Reverse transcription real-time PCR

Hatch-synchronized to within 1 hour, worms from NG large plates, *gfp(RNAi)* plates, or L4440 vector plates grown at 15ºC for needed number of hours were pooled, washed extensively

(M9) and then allowed to swim for 20 minutes to clear gut content. RNA was isolated with proteinase K (Omega) followed by phenol:chloroform extraction (Amresco). The RNA pellets were subjected to DNase I (Roche) treatment, and cleaned by RNeasy (Qiagen) per manufacturer's instructions. All initial RNA input concentrations were normalized to ~30-200ng/μL.

Reverse transcription was performed using 20μL reactions of ~150-600ng of input RNA by Thermoscript RT (Invitrogen), using gene specific RT primers (available upon request). cDNA quantification was performed using 2μL of the RT reaction in a 50μL QuantiTect SYBR Green (Qiagen) reaction with nested PCR primers. The PCR reaction cycles were: 15 minutes 95 degrees, 15 seconds 94 degrees, 30 seconds 52 degrees, 1 minute 72 degrees, read, cycle to step 2 for 45 cycles, using an Eppendorf Mastercycler Realplex4 and Noiseband quantification. Subsequent analysis was performed using the ΔCT approach for expression normalized to another gene, or the ΔΔCT approach for expression normalized to another gene and then relative to wild type's expression (LIVAK and SCHMITTGEN 2001).

Three to five biological replicates of worms were combined for an RNA prep. This RNA was then quantified in triplicates (error bar generation), and repeated two to four times (representative shown), to determine the precision of relative RNA abundance, similar to prior small RNA qPCR experiments (FISCHER *et al.* 2011).

LITERATURE CITED

AZIMZADEH JAMALKANDI, S., and A. MASOUDI-NEJAD, 2011 RNAi pathway integration in Caenorhabditis elegans development. Funct Integr Genomics **11:** 389-405.

BRENNER, S., 1974 The genetics of Caenorhabditis elegans. Genetics **77:** 71-94.

CESANA, M., D. CACCHIARELLI, I. LEGNINI, T. SANTINI, O. STHANDIER *et al.*, 2011 A long noncoding RNA controls muscle differentiation by functioning as a competing endogenous RNA. Cell **147:** 358-369.

CLAYCOMB, J. M., P. J. BATISTA, K. M. PANG, W. GU, J. J. VASALE *et al.*, 2009 The Argonaute CSR-1 and its 22G-RNA cofactors are required for holocentric chromosome segregation. Cell **139:** 123-134.

DAS, P. P., M. P. BAGIJN, L. D. GOLDSTEIN, J. R. WOOLFORD, N. J. LEHRBACH *et al.*, 2008 Piwi and piRNAs act upstream of an endogenous siRNA pathway to suppress Tc3 transposon mobility in the Caenorhabditis elegans germline. Mol Cell **31:** 79-90.

DUCHAINE, T. F., J. A. WOHLSCHLEGEL, S. KENNEDY, Y. BEI, D. CONTE, JR. *et al.*, 2006 Functional proteomics reveals the biochemical niche of C. elegans DCR-1 in multiple small-RNA-mediated pathways. Cell **124:** 343-354.

FIRE, A., S. XU, M. K. MONTGOMERY, S. A. KOSTAS, S. E. DRIVER *et al.*, 1998 Potent and specific genetic interference by double-stranded RNA in Caenorhabditis elegans. Nature **391:** 806-811.

FISCHER, S. E., 2010 Small RNA-mediated gene silencing pathways in C. elegans. Int J Biochem Cell Biol **42:** 1306-1315.

FISCHER, S. E., M. D. BUTLER, Q. PAN and G. RUVKUN, 2008 Trans-splicing in C. elegans generates the negative RNAi regulator ERI-6/7. Nature **455:** 491-496.

FISCHER, S. E., T. A. MONTGOMERY, C. ZHANG, N. FAHLGREN, P. C. BREEN *et al.*, 2011 The ERI-6/7 Helicase Acts at the First Stage of an siRNA Amplification Pathway That Targets Recent Gene Duplications. PLoS Genet **7:** e1002369.

GENT, J. I., A. T. LAMM, D. M. PAVELEC, J. M. MANIAR, P. PARAMESWARAN *et al.*, 2010 Distinct phases of siRNA synthesis in an endogenous RNAi pathway in C. elegans soma. Mol Cell **37:** 679-689.

GENT, J. I., M. SCHVARZSTEIN, A. M. VILLENEUVE, S. G. GU, V. JANTSCH *et al.*, 2009 A Caenorhabditis elegans RNA-directed RNA polymerase in sperm development and endogenous RNA interference. Genetics **183:** 1297-1314.

GRISHOK, A., 2005 RNAi mechanisms in Caenorhabditis elegans. FEBS Lett **579:** 5932-5939.

GU, S. G., J. PAK, S. GUANG, J. M. MANIAR, S. KENNEDY *et al.*, 2012 Amplification of siRNA in Caenorhabditis elegans generates a transgenerational sequence-targeted histone H3 lysine 9 methylation footprint. Nat Genet **44:** 157-164.

JOHNSTONE, I. L., and J. D. BARRY, 1996 Temporal reiteration of a precise gene expression pattern during nematode development. EMBO J **15:** 3633-3639.

KAIKKONEN, M. U., M. T. LAM and C. K. GLASS, 2011 Non-coding RNAs as regulators of gene expression and epigenetics. Cardiovasc Res **90:** 430-440.

KARLEN, Y., A. MCNAIR, S. PERSEGUERS, C. MAZZA and N. MERMOD, 2007 Statistical significance of quantitative PCR. BMC Bioinformatics **8:** 131.

KARRETH, F. A., Y. TAY, D. PERNA, U. ALA, S. M. TAN *et al.*, 2011 In vivo identification of tumor- suppressive PTEN ceRNAs in an oncogenic BRAF-induced mouse model of melanoma. Cell **147:** 382-395.

KAWAJI, H., and Y. HAYASHIZAKI, 2008 Exploration of small RNAs. PLoS Genet **4:** e22.

KENNEDY, S., D. WANG and G. RUVKUN, 2004 A conserved siRNA-degrading RNase negatively regulates RNA interference in C. elegans. Nature **427:** 645-649.

KETTING, R. F., S. E. J. FISCHER, E. BERNSTEIN, T. SIJEN, G. J. HANNON *et al.*, 2001 Dicer functions in RNA interference and in synthesis of small RNA involved in developmental timing in C-elegans. Genes & Development **15:** 2654-2659.

KHVOROVA, A., and A. WOLFSON, 2012 New competition in RNA regulation. Nat Biotechnol **30:** 58-59.

KNIGHT, S. W., and B. L. BASS, 2001 A role for the RNase III enzyme DCR-1 in RNA interference and germ line development in Caenorhabditis elegans. Science **293:** 2269-2271.

LEE, R. C., R. L. FEINBAUM and V. AMBROS, 1993 The C. elegans heterochronic gene lin-4 encodes small RNAs with antisense complementarity to lin-14. Cell **75:** 843-854.

LEE, R. C., C. M. HAMMELL and V. AMBROS, 2006 Interacting endogenous and exogenous RNAi pathways in Caenorhabditis elegans. RNA **12:** 589-597.

LEUSCHNER, F., P. DUTTA, R. GORBATOV, T. I. NOVOBRANTSEVA, J. S. DONAHOE *et al.*, 2011 Therapeutic siRNA silencing in inflammatory monocytes in mice. Nat Biotechnol **29:** 1005-1010.

LIVAK, K. J., and T. D. SCHMITTGEN, 2001 Analysis of relative gene expression data using real-time quantitative PCR and the 2(-Delta Delta C(T)) Method. Methods **25:** 402-408.

OHTA, H., M. FUJIWARA, Y. OHSHIMA and T. ISHIHARA, 2008 ADBP-1 regulates an ADAR RNA-editing enzyme to antagonize RNA-interference-mediated gene silencing in Caenorhabditis elegans. Genetics **180:** 785-796.

PAGE, A. P., JOHNSTONE, I.L., 1997 The cuticle (March 19, 2007), pp. WormBook, ed. The C. elegans Research Community, WormBook, doi/10.1895/wormbook.1.138.1, http://www.wormbook.org.

PASQUINELLI, A. E., B. J. REINHART, F. SLACK, M. Q. MARTINDALE, M. I. KURODA *et al.*, 2000 Conservation of the sequence and temporal expression of let-7 heterochronic regulatory RNA. Nature **408:** 86-89.

PAVELEC, D. M., J. LACHOWIEC, T. F. DUCHAINE, H. E. SMITH and S. KENNEDY, 2009 Requirement for the ERI/DICER complex in endogenous RNA interference and sperm development in Caenorhabditis elegans. Genetics **183:** 1283-1295.

REINHART, B. J., F. J. SLACK, M. BASSON, A. E. PASQUINELLI, J. C. BETTINGER *et al.*, 2000 The 21-nucleotide let-7 RNA regulates developmental timing in Caenorhabditis elegans. Nature **403:** 901-906.

SCHEDIN, P., C. P. HUNTER and W. B. WOOD, 1991 Autonomy and nonautonomy of sex determination in triploid intersex mosaics of C. elegans. Development **112:** 863-879.

SHEN, J., K. XIE and L. XIONG, 2010 Global expression profiling of rice microRNAs by one-tube stem-loop reverse transcription quantitative PCR revealed important roles of microRNAs in abiotic stress responses. Mol Genet Genomics **284:** 477-488.

SIFUENTES-ROMERO, I., S. L. MILTON and A. GARCIA-GASCA, 2011 Post-transcriptional gene silencing by RNA interference in non-mammalian vertebrate systems: where do we stand? Mutat Res **728:** 158-171.

SIMMER, F., M. TIJSTERMAN, S. PARRISH, S. P. KOUSHIKA, M. L. NONET *et al.*, 2002 Loss of the putative RNA-directed RNA polymerase RRF-3 makes C. elegans hypersensitive to RNAi. Curr Biol **12:** 1317-1319.

STEIN, P., P. SVOBODA, M. ANGER and R. M. SCHULTZ, 2003 RNAi: mammalian oocytes do it without RNA-dependent RNA polymerase. RNA **9:** 187-192.

SUMAZIN, P., X. YANG, H. S. CHIU, W. J. CHUNG, A. IYER *et al.*, 2011 An extensive microRNA-mediated network of RNA-RNA interactions regulates established oncogenic pathways in glioblastoma. Cell **147:** 370-381.

TABARA, H., M. SARKISSIAN, W. G. KELLY, J. FLEENOR, A. GRISHOK *et al.*, 1999 The rde-1 gene, RNA interference, and transposon silencing in C. elegans. Cell **99:** 123-132.

TAY, Y., L. KATS, L. SALMENA, D. WEISS, S. M. TAN *et al.*, 2011 Coding-independent regulation of the tumor suppressor PTEN by competing endogenous mRNAs. Cell **147:** 344-357.

TIMMONS, L., and A. FIRE, 1998 Specific interference by ingested dsRNA. Nature **395:** 854.

WELKER, N. C., D. M. PAVELEC, D. A. NIX, T. F. DUCHAINE, S. KENNEDY *et al.*, 2010 Dicer's helicase domain is required for accumulation of some, but not all, C. elegans endogenous siRNAs. RNA **16:** 893-903.

WILUSZ, J. E., H. SUNWOO and D. L. SPECTOR, 2009 Long noncoding RNAs: functional surprises from the RNA world. Genes Dev **23:** 1494-1504.

WINSTON, W. M., C. MOLODOWITCH and C. P. HUNTER, 2002 Systemic RNAi in C. elegans requires the putative transmembrane protein SID-1. Science **295:** 2456-2459.

YANAI, I., L. R. BAUGH, J. J. SMITH, C. ROEHRIG, S. S. SHEN-ORR *et al.*, 2008 Pairing of competitive and topologically distinct regulatory modules enhances patterned gene expression. Mol Syst Biol **4:** 163.

YIGIT, E., P. J. BATISTA, Y. BEI, K. M. PANG, C. C. CHEN *et al.*, 2006 Analysis of the C. elegans Argonaute family reveals that distinct Argonautes act sequentially during RNAi. Cell **127:** 747-757.

ZHANG, H., and A. Z. FIRE, 2010 Cell autonomous specification of temporal identity by Caenorhabditis elegans microRNA lin-4. Dev Biol **344:** 603-610.

ZHANG, Y., D. CHEN, M. A. SMITH, B. ZHANG and X. PAN, 2012 Selection of reliable reference genes in Caenorhabditis elegans for analysis of nanotoxicity. PLoS One **7:** e31849.

ZHUANG, J. J., and C. P. HUNTER, 2011 Tissue Specificity of Caenorhabditis elegans Enhanced RNA Interference Mutants. Genetics **188:** 235-237.

Chapter Seven

Discussion

HISTORICAL CONTEXTS

The history of the endo-siRNA field is intricately tied with the history of RNAi and general small RNA biology. Advances from within the endo-siRNA field and from studies of other small RNAs have pushed along our understanding of the cellular roles of endogenous small RNAs, as well as their relationship to experimental RNAi and its efficacy. More specifically, the advances made in the *eri* field can be categorized as arising from genetic and genomic approaches. Tracing the history of these advances (**Figure 7.1**) sheds light on where the field is headed, as well as broadens the context of how these findings may advance the RNAi field in general.

Genomic Approach

The first perspective from which to examine the *eri* field is through looking at large-scale genomic analyses from the last twelve years. Advances in DNA sequencing technology have made tremendous progress during this time period (BENTLEY *et al.* 2008). The *eri* field has taken full advantage of those advances, as well as spearheading its own advances for sequencing (AMBROS *et al.* 2003; LAU *et al.* 2001; RUBY *et al.* 2006). Specifically, the newly available next-generation sequencing technologies offer the ability to sequence directly on a flow cell channel, thus spatially separating while simultaneously capturing millions of individual sequencing reads (HOLT and JONES 2008). The level of density offered by such technologies is precisely what's needed to examine the tremendously plentiful, though subtly different, small RNA populations.

After the discovery of the first microRNAs *lin-4* and *let-7*, the Bartel and Ambros groups set out to sequence endogenous small RNAs in *C. elegans* in hopes of finding new microRNAs. While doing so, they inadvertently discovered new classes of endo-siRNAs (AMBROS *et al.*

2003; RUBY *et al.* 2006), thus starting a field that will eventually cross paths with the *eri*s. Because microRNAs undergo many processing steps before maturity (SOKOL 2012), the two groups prepared their RNA libraries differently in hopes of capturing different microRNA species (or at different points of abundances). The Bartel group used direct ligation of size-selected RNAs onto the 5' adapter, thus selecting for small RNA populations with a 5' monophosphate (RUBY *et al.* 2006). The Ambros group phosphatase-treated size-selected RNAs, then kinase-treated the RNAs prior to 5' adapter ligation (AMBROS *et al.* 2003); as it turns out, this capture method selected for RNA populations with a 5' triphosphate (PAK and FIRE 2007). While both groups discovered a 22mer species that predominately begin with a G (thus named 22Gs), the 5' monophosphate bias also discovered a rarer 26mer species that also predominately beings with a G (thus named 26Gs) (AMBROS *et al.* 2003; RUBY *et al.* 2006). Interestingly enough, ppp22Gs have two free hydroxyl groups in their 3' terminus, but p26Gs seem to have at least its 3' OH group modified (RUBY *et al.* 2006; VASALE *et al.* 2010).

Around the time these first deep-sequencing experiments were being performed, genetic analysis from the Bass, Zamore, and Plasterk groups discovered that the enzyme Dicer was essential to all small RNAi pathways (HUTVAGNER *et al.* 2001; KETTING *et al.* 2001; KNIGHT and BASS 2001). This led to a study in which Duchaine and Mello used proteomics to analyze all the cellular gene products that interact with DICER (DUCHAINE *et al.* 2006). They discovered, as expected, genes whose mutation causes an RNAi-defective phenotype. Surprisingly, they also discovered genes whose mutation causes an enhanced RNAi phenotype. This finding, along with Lee and Ambros' discovery that Eri mutants are missing many endo-siRNAs, led to the now generally accepted model of enhanced RNAi (LEE *et al.* 2006).

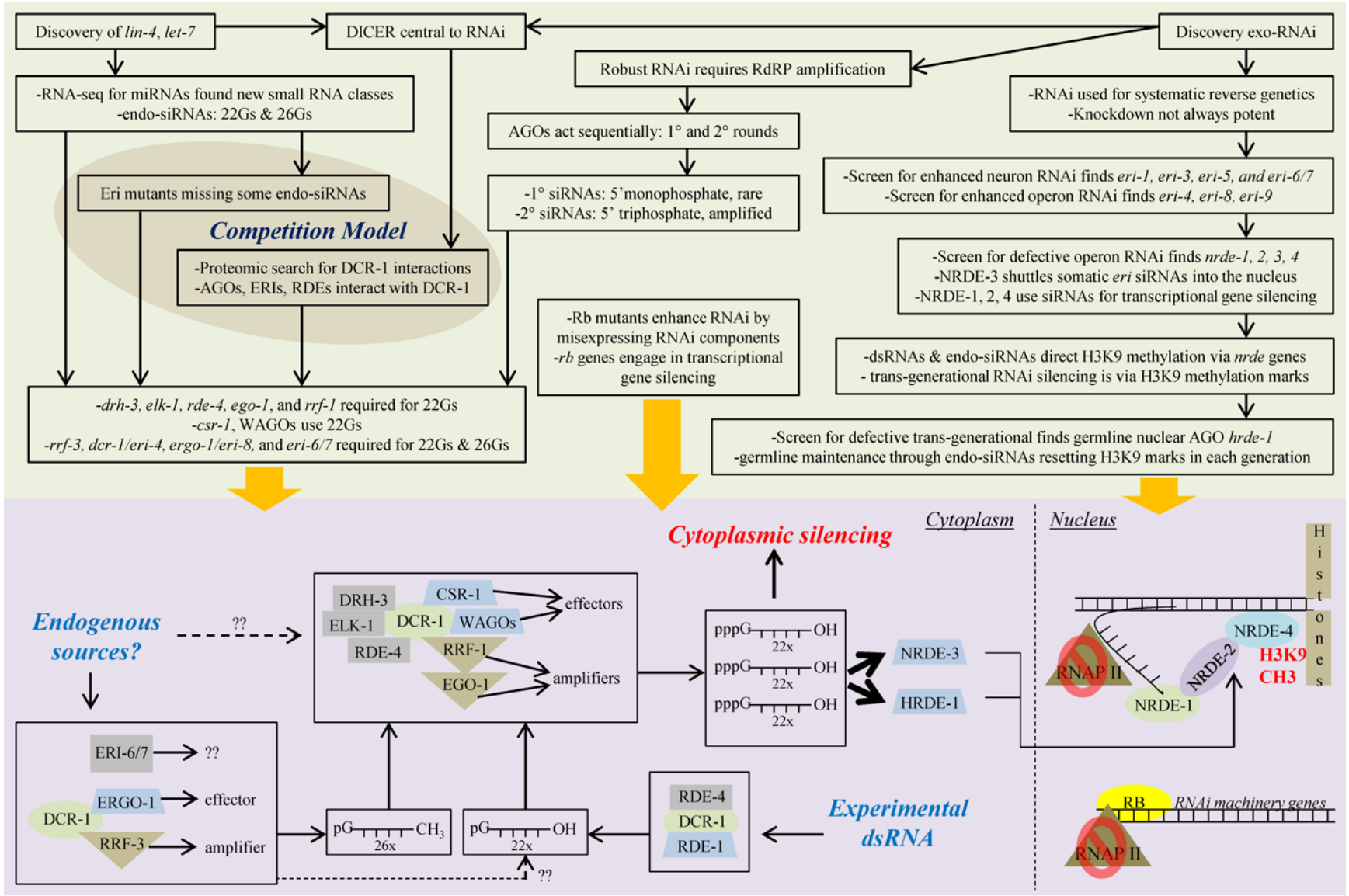

Figure 7.1: Seminal discoveries in the history of the endo-siRNA field (green) that led to the current mechanistic model (magenta)

It was proposed then in 2006 that ERI genes produce endo-siRNAs, and these endo-siRNAs compete with experimentally introduced RNAi triggers for a common, limiting pool of resources. Therefore, eliminating an *eri* gene reduces this competition, hence making experimental RNAi more effective (DUCHAINE *et al.* 2006; LEE *et al.* 2006).

Subsequently, Yigit and Mello discovered that the *C. elegans* Argonautes acted in phases, with distinct primary and secondary rounds (YIGIT *et al.* 2006). Almost simultaneously, Pak and Fire discovered that *C. elegans* siRNA species, both endogenous and experimental, come in two populations: one rare and 5' monophosphated, and one abundant and 5' triphosphated (PAK and FIRE 2007). These two discoveries thus suggested that RNAi occurs in two rounds. The distinctions between endogenous and exogenous RNAi and between primary and secondary RNAi therefore shaped the *eri* field to build the model that stands today.

Recently, Gent and Fire discovered that the endo-RNAi RdRP mutant *rrf-3* lacks 26Gs and 22Gs (GENT *et al.* 2010); Welker and Bass discovered that the Dicer helicase mutant *eri-4* also lacks 26Gs and 22Gs (WELKER *et al.* 2010); Vasale and Mello discovered that the endo-RNAi Ago mutant *ergo-1*/*eri-8* lacks 26Gs and 22Gs (VASALE *et al.* 2010); and finally, Fischer and Ruvkun discovered that the Eri mutant *eri-6/7* also lacks 26Gs and 22Gs (FISCHER *et al.* 2011). Based on the molecular nature of these genes and small RNAs, a model hypothesizes that endo-siRNAs are made *de novo* by the RdRP RRF-3, with assistance by ERI-4 and ERI-6/7, and the Ago ERI-8 acts as the initial effector. However, the relationship between the rarer 26Gs and more abundant 22Gs remains unclear from these findings alone.

Simultaneous to these discoveries, Gu and Mello discovered that the exo-RNAi genes *drh-3*, *elk-1*, and *rrf-1* are required only for making 22Gs (GU *et al.* 2009), while Maniar and Fire similarly discovered that the exo-RNAi genes *rde-4* and *ego-1* are also required only for

making 22Gs (MANIAR and FIRE 2011). Claycomb and Mello also discovered that the secondary Agos CSR-1 and WAGOs use 22Gs (CLAYCOMB *et al.* 2009). Combined with the model above, these findings suggest that the ERI genes act more upstream and make the rarer 26Gs, which get amplified by the RdRPs RRF-1 or EGO-1, with help from DRH-3, ELK-1, and RDE-4, into the abundant 22Gs which interacts with downstream Agos (CONINE *et al.* 2010; VASALE *et al.* 2010).

Genetic Approach

The second perspective from which to examine the *eri* field is through looking at classical genetic analyses from the last nine years. After the discovery of the first controlled case of experimental RNAi (FIRE *et al.* 1998), the Fire and Ahringer groups set out to utilize RNAi as a convenient and systematic method for reverse genetics in *C. elegans* (KAMATH and AHRINGER 2003; KAMATH *et al.* 2003; TIMMONS and FIRE 1998). Though RNAi was potent and specific under most contexts, there were limits to this potency. Certain tissues or gene targets are not very tractable to RNAi (ZHUANG and HUNTER 2012), a fact highlighted by the fortuitous discovery of the enhanced RNAi mutant *rrf-3* (SIMMER *et al.* 2003).

To examine the precise nature of the negative regulation of RNAi, Kennedy and Rukvun began a systematic screen for enhancers of RNAi by looking for silencing of a neuronal *gfp* that is normally intractable to *gfp(RNAi)* (KENNEDY *et al.* 2004). Using this screen, *eri-1*, *rrf-3*, *eri-3*, *eri-5*, and *eri-6/7* were discovered (DUCHAINE *et al.* 2006; FISCHER *et al.* 2008; KENNEDY *et al.* 2004). In order to find more Eri mutants, Pavelec and Kennedy screened for enhanced pan-operon silencing (PAVELEC *et al.* 2009), and discovered *dcr-1/eri-4*, *ergo-1/eri-8*, and *eri-9*. During this second screen, it was observed that some Eri mutants were temperature sensitive sterile at 25°C while others were not. This led to the finding that the *eri* genes produce endo-

siRNAs important for proper spermatogenesis (GENT *et al.* 2009; PAVELEC *et al.* 2009), which spurred the deep-sequencing of these mutants for their small RNA profiles as previously described.

Meanwhile, Guang and Kennedy performed a screen opposite of the second Eri screen: for defective pan-operon silencing; they discovered the nuclear Ago NRDE-3 and the nuclear factors NRDE-1,2,4 (BURKHART *et al.* 2011; GUANG *et al.* 2010; GUANG *et al.* 2008). It was found that NRDE-3 shuttles endo-siRNAs made by the ERIs into the nucleus, interacts with NRDE-1,2,4, and uses the siRNA guide to match a cognate nascent pre-mRNA to block RNA polymerase II transcription and induce H3K9 methylation for epigenetic transcriptional silencing (BURKHART *et al.* 2011; GUANG *et al.* 2010).

These seminal findings linked endo-siRNAs to functions inside the nucleus, specifically transcriptional gene silencing and epigenetics. The patent implication of this is that it is likely the mechanism behind trans-generational RNAi that's been previously observed in worms (VASTENHOUW *et al.* 2006) and previously carefully characterized in plants (DJUPEDAL and EKWALL 2009). Indeed, Burton and Kennedy along with Gu and Fire found that both exo- and endo-siRNAs can indeed drive H3K9 methylation through NRDE-1,2,4 to induce trans-generational RNAi silencing (BURTON *et al.* 2011; GU *et al.* 2012a). This finding that an experience in the somatic cells – externally encountered dsRNAs inducing gene silencing – during the lifetime of an animal can be passed onto the next generation is quite revolutionary because of its Lamarckian implications.

To fully realize this implication, Buckley and Kennedy specifically screened for a trans-generational RNAi defective mutant, and discovered the germline nuclear Ago HRDE-1 (BUCKLEY *et al.* 2012). *hrde-1* is thought to be responsible for resetting the H3K9 methylation

marks in the germline in each generation in response to encountered endo-siRNA, and is thus vital for maintaining germline immortality (BUCKLEY *et al.* 2012).

In parallel to the discovery of the *eri* class of enhanced RNAi mutants, Wang and Ruvkun discovered that mutations to the *rb* tumor suppressor transcription factor family also enhanced RNAi (WANG *et al.* 2005). It was initially hypothesized that because germline cells in *C. elegans* are more sensitive to RNAi (SMARDON *et al.* 2000), the *rb* mutants were turning somatic cells into germline-like, thus enhancing RNAi (WANG *et al.* 2005). This hypothesis has been recently partially confirmed, as sequencing of *rb* mutants revealed that many RNAi factors which are predominantly expressed in the germline are indeed overexpressed in the *rb* mutant worms (WU *et al.* 2012).

FUTURE DIRECTIONS

Next experiments

Since the most recent findings in the *eri* field have implicated exo-siRNAs and endo-siRNAs in inheritance (BUCKLEY *et al.* 2012), the previously discussed Lamarckian implications are very significant. The findings by Buckley and Kennedy robustly demonstrate a mechanism in place to respond to and transmit small RNA messages through the generations. However, to truly demonstrate a Lamarckian method of inheritance, there needs to be one additional step of experimentally demonstrating how signals experienced by the somatic cells are translated into small RNAs for passage to the germline and subsequent generations. For example, after subjecting *C. elegans* to a stress like heat or osmotic shock, it'd be very interesting to determine a precise gene circuit in the soma that responds to this stress, encodes small RNAs in response to this stress, and modifies the germline accordingly to pass this "stressed" gene expression profile

onto the next generations. If such a mechanism can be demonstrated, then the next generation(s) should accordingly respond to the same stress in a much more efficient manner. Such a discovery would then truly provide the endogenous relevance of the siRNA-mediated inheritance mechanism currently elucidated as the endpoint of the *eri* pathway.

Stylistic shift

Currently, the awe of using deep-sequencing technology for small RNA profiling is allowing more and more building blocks of the RNAi pathway to have their impacts on small RNA production analyzed. Combined with the genetic studies discussed above, soon there will be enough small RNA profiles of RNAi mutants to begin drawing comparisons and even predictions from analogous contexts once the overarching model is confirmed. I predict that future studies after that point, then, will refocus on the genetic interactions, rather than genomic analysis, and use the available small RNA profiles as a confirmatory tool.

This trend is already beginning to appear in recent literature of the *eri* field. For instance, in Buckley *et al.*, the seminal finding that *hrde-1* drives trans-generational memory of H3K9 methylation is mostly observed through easier-to-manipulate experimental siRNAs; the known endo-siRNA loci were analyzed to confirm the endogenous relevance of this finding (BUCKLEY *et al.* 2012). Similarly, my findings of the roles of NRDE-3 was performed mostly through experimentally introduced RNAi triggers, such as feeding RNAi and transitive RNAi; the subsequently deduced relationships such as the *eri-nrde-3* interactions were confirmed via profiling expression levels of known endo-siRNA targets.

The benefits of this stylistic shift are twofold. First, for those outside of the *eri* field hoping to utilize RNAi merely as a technology, which was the first purpose of screening for

enhanced RNAi mutants anyways, there is better contextualization of small RNA data. The refocus onto the genetics will help a broader audience understand which components of the RNAi pathway are limiting and essential, and can thus perhaps be over-expressed for facilitating RNAi sensitivity in other systems. For most audiences, knowing that thousands of endo-siRNA reads ultimately converge onto NRDE-3 or HRDE-1 for transcriptional gene silencing and germline maintenance is more meaningful than knowing what the nature of those reads were. Second, for those in the *eri* field, the refocus on genetics can crystallize findings into "choke-points." Had it not been the genetic analysis of the Eri and Nrde mutants, merely having the sequencing data of *rrf-3*, *ergo-1*, and *eri-6/7* would not have easily led to the mechanistic model of shuttling siRNAs from the cytoplasm to the nucleus for germline maintenance, especially given the immense number of endo-siRNAs missing and the germline-soma role separation of EGO-1 and RRF-1 mutants (MANIAR and FIRE 2011; VASALE *et al.* 2010). In other words, having the enormous amount of sequencing data available for all endogenous RNAi pathway genes will ultimately have to lead back to crystallizing how those endo-siRNAs' expressions are controlled at a higher level, and genetic pathway analysis will shed much light on that question.

Content shift

In terms of the contents of future studies then, I predict the field will circle back to more fully characterize each individual gene of the endogenous RNAi pathway once the overall framework – through sequencing – has been confirmed and fully explored, especially because many important lingering questions remain. For instance, why do helicases (DRH-3, ERI-4) play such prominent roles in endo-siRNA stability? How are mRNAs targeted by endo-siRNAs ultimately eliminated? And what are the roles of the ERI genes other than RRF-3 and ERGO-1?

Fully characterizing the individual genes in question, beyond what endo-siRNAs they produce, would go a long way in answering these questions.

One method of answering these questions is through biochemistry. For instance, Gabel and Ruvkun resolved the longstanding question of if ERI-1's 3'-to-5' exonuclease activity is directly used as a negative regulator of siRNAs (KENNEDY *et al.* 2004). They showed that this activity is irrelevant to maintaining endo-siRNAs and is used for a different purpose of trimming 5.8S rRNAs (GABEL and RUVKUN 2008). In another example, Thivierge and Duchaine showed that the subtle differences in Eri responses amongst the *eri* mutants (ZHUANG and HUNTER 2011) is because they form differential complexes with DICER; ERI-1/ERI-3/DCR-1 forms a distinct complex from RRF-3/ERI-5/DCR-1 (THIVIERGE *et al.* 2011). A second method of answering these questions is through genetics. As more and more Rde and Eri mutants are discovered, their reported phenotypes are understandably more and more subtle (ZHANG *et al.* 2012) because the earlier mutants were likely easier to screen for. These weak RNAi phenotypes only exhibit themselves prominently under certain genetic contexts. For instance, my work has shown that *nrde-3* mutants only have a weak RNAi defect on their own, but they're completely defective for transitive RNAi, and in a *pgl-1* mutant background, they completely abolish the Eri response. In another example, the *C. elegans* RdRP RRF-2 was thought to have no known function (SIJEN *et al.* 2001), until sequencing showed that it is over-expressed in *rb* mutants, spurring Wu and Ruvkun to discover that it is involved in germline RNAi (WU *et al.* 2012).

Future in-depth studies of individual components of the RNAi machinery will therefore shed much new light through this blend of genetics and biochemistry. In many regards, the current efforts of small RNA profiling is very much akin to previous microarray studies, which

usually gave an informative survey of trends, but ultimately still required individual gene-by-gene analysis to fully comprehend a genetic pathway in-depth.

However, one area of research which I believe remains extremely exciting regardless of a genomics versus genetics prioritization is the chemical nature of the small RNAs themselves. A prominent question arising from the nature of the small RNAs concerns their ends. Until Pak and Fire used a 5'-unbiased cloning approach, most endo-siRNAs were missing from sequencing (PAK and FIRE 2007). Then analogously, it could be argued that perhaps 26Gs are not as rare as their sequencing profiles indicate, but are instead inefficiently cloned because of their 3'-OH modification (RUBY *et al.* 2006). Kamminga and Ketting recently reported that a lack of HENN-1 methylation in *C. elegans* piRNAs does not completely disrupt their stability, but does thoroughly impact the stability of some 26G endo-siRNAs (KAMMINGA *et al.* 2012), suggesting inherent differences in the chemical nature of small RNAs classes, which deserves future investigation. In fact, the same report suggests that the requirement of 26Gs for 3' methylation is also correlated with the Ago they associate with. An even broader question would be to understand why there is a preponderance of G at the beginning of endo-siRNAs. If it's meant to act as a cap like in mRNAs, why are ~40% of endo-siRNAs without the G also the same length as the ones with G? And if it's meant to act as a conserved "starting sequence" like piRNAs, why are most endo-siRNAs very different beyond the first nucleotide? The genetic tools available in *C. elegans* and the push in RNAi biotechnology for chemical modifications to increase delivery stability (BRAMSEN and KJEMS 2013) lead me to believe this area of research, with its many unanswered questions, will be highly topical in the future.

Context shift

The third and most important realm of future studies, I believe, will try to reconcile the different forms of transcriptional regulation via RNAi mechanisms. Wu and Ruvkun have recently showed that the expression of RNAi genes themselves is regulated at the transcriptional level by the RB tumor suppressor family (WU *et al.* 2012). It'd be interesting to examine what the relationship between this "higher" level of transcriptional gene silencing driven by protein transcription factors versus those driven by endo-siRNAs is. One way to look at such a relationship is to deep-sequence individual *rb* mutant (or at least representatives of their classes) and analyze its small RNA expression profile versus that of a RNAi mutant whose regulation depends on that particular RB.

An even broader contextual perspective is to examine the relationship between different small RNA driven silencing processes, especially now that RNAi in the nucleus and RNAi transcriptional gene silencing has been well-established (**Table 7.1**). Currently, one area of intense interest in small RNA biology is the study of piRNAs (ISHIZU *et al.* 2012), in part due to its high conservation across species (KUMAR and CHEN 2012). The precise mechanism of piRNA origin and generation is currently not completely clear (BATISTA *et al.* 2008; GU *et al.* 2012b), but its ultimate "conversion" to 22G endo-siRNAs for its germline silencing activities, at least in *C. elegans* (LEE *et al.* 2012), seems to suggest that it is likely related to other endo-siRNA processes. Another highly topical area of research is the study of long noncoding RNAs (LEE 2012). A recent report suggested that perhaps some lncRNAs serve as templates for primary endo-siRNA production in *C. elegans* (NAM and BARTEL 2012). Understanding these relationships will be a seminal breakthrough because it'd broaden the horizons of analyzing all small RNAs, rather than the currently somewhat myopic approaches of examining individual pathways and outputs.

Table 7.1: Classes of endo-siRNAs, their effectors, and functions

Primary Round				Secondary Round				Function(s)
RdRP	**Ago**	**siRNA**		**RdRP**	**Ago**	**siRNA**		
??	PRG-1/2	21U	→	EGO-1*	WAGO	22G	→	Germline gene silencing High temp. fertility Transposon silencing Trans-generational silencing
RRF-3	ALG-3/4	26G		EGO-1*	WAGO	22G		High temp. sperm viability
RRF-3	ERGO-1	26G		RRF-1	WAGO	22G		Gene duplication silencing
??				EGO-1	CSR-1	22G		Proper chromosomal segregation

The RNA-dependent RNA polymerase (RdRP), the Argonaute effector (Ago), and the nature of the short-interfering RNA (siRNA) involved in each of the four currently known distinct endo-siRNA pathways. A secondary round is categorized as the round which produces siRNAs that perform the listed gene regulatory functions. Asterisks indicate inferences drawn based on tissue of action and known expression patterns of EGO-1 versus RRF-1; all other entries have direct experimental evidence.

Therefore, I believe the *eri* field will ultimately converge and emerge with the rest of small RNA biology research to shed light on the importance of a fundamental and ancient biomolecule. The RNA world may have never left.

LITERATURE CITED

AMBROS, V., R. C. LEE, A. LAVANWAY, P. T. WILLIAMS and D. JEWELL, 2003 MicroRNAs and other tiny endogenous RNAs in C. elegans. Curr Biol **13:** 807-818.

BATISTA, P. J., J. G. RUBY, J. M. CLAYCOMB, R. CHIANG, N. FAHLGREN *et al.*, 2008 PRG-1 and 21U-RNAs interact to form the piRNA complex required for fertility in C. elegans. Mol Cell **31:** 67-78.

BENTLEY, D. R., S. BALASUBRAMANIAN, H. P. SWERDLOW, G. P. SMITH, J. MILTON *et al.*, 2008 Accurate whole human genome sequencing using reversible terminator chemistry. Nature **456:** 53-59.

BRAMSEN, J. B., and J. KJEMS, 2013 Engineering small interfering RNAs by strategic chemical modification. Methods Mol Biol **942:** 87-109.

BUCKLEY, B. A., K. B. BURKHART, S. G. GU, G. SPRACKLIN, A. KERSHNER *et al.*, 2012 A nuclear Argonaute promotes multigenerational epigenetic inheritance and germline immortality. Nature.

BURKHART, K. B., S. GUANG, B. A. BUCKLEY, L. WONG, A. F. BOCHNER *et al.*, 2011 A pre-mRNA-associating factor links endogenous siRNAs to chromatin regulation. PLoS Genet **7:** e1002249.

BURTON, N. O., K. B. BURKHART and S. KENNEDY, 2011 Nuclear RNAi maintains heritable gene silencing in Caenorhabditis elegans. Proc Natl Acad Sci U S A.

CLAYCOMB, J. M., P. J. BATISTA, K. M. PANG, W. GU, J. J. VASALE *et al.*, 2009 The Argonaute CSR-1 and its 22G-RNA cofactors are required for holocentric chromosome segregation. Cell **139:** 123-134.

CONINE, C. C., P. J. BATISTA, W. GU, J. M. CLAYCOMB, D. A. CHAVES *et al.*, 2010 Argonautes ALG-3 and ALG-4 are required for spermatogenesis-specific 26G-RNAs and thermotolerant sperm in Caenorhabditis elegans. Proc Natl Acad Sci U S A **107:** 3588-3593.

DJUPEDAL, I., and K. EKWALL, 2009 Epigenetics: heterochromatin meets RNAi. Cell Res **19:** 282-295.

DUCHAINE, T. F., J. A. WOHLSCHLEGEL, S. KENNEDY, Y. BEI, D. CONTE, JR. *et al.*, 2006 Functional proteomics reveals the biochemical niche of C. elegans DCR-1 in multiple small-RNA-mediated pathways. Cell **124:** 343-354.

FIRE, A., S. XU, M. K. MONTGOMERY, S. A. KOSTAS, S. E. DRIVER *et al.*, 1998 Potent and specific genetic interference by double-stranded RNA in Caenorhabditis elegans. Nature **391:** 806-811.

FISCHER, S. E., M. D. BUTLER, Q. PAN and G. RUVKUN, 2008 Trans-splicing in C. elegans generates the negative RNAi regulator ERI-6/7. Nature **455:** 491-496.

FISCHER, S. E., T. A. MONTGOMERY, C. ZHANG, N. FAHLGREN, P. C. BREEN *et al.*, 2011 The ERI-6/7 Helicase Acts at the First Stage of an siRNA Amplification Pathway That Targets Recent Gene Duplications. PLoS Genet **7:** e1002369.

GABEL, H. W., and G. RUVKUN, 2008 The exonuclease ERI-1 has a conserved dual role in 5.8S rRNA processing and RNAi. Nat Struct Mol Biol **15:** 531-533.

GENT, J. I., A. T. LAMM, D. M. PAVELEC, J. M. MANIAR, P. PARAMESWARAN *et al.*, 2010 Distinct phases of siRNA synthesis in an endogenous RNAi pathway in C. elegans soma. Mol Cell **37:** 679-689.

GENT, J. I., M. SCHVARZSTEIN, A. M. VILLENEUVE, S. G. GU, V. JANTSCH *et al.*, 2009 A Caenorhabditis elegans RNA-directed RNA polymerase in sperm development and endogenous RNA interference. Genetics **183:** 1297-1314.

GU, S. G., J. PAK, S. GUANG, J. M. MANIAR, S. KENNEDY *et al.*, 2012a Amplification of siRNA in Caenorhabditis elegans generates a transgenerational sequence-targeted histone H3 lysine 9 methylation footprint. Nat Genet **44:** 157-164.

GU, W., H. C. LEE, D. CHAVES, E. M. YOUNGMAN, G. J. PAZOUR *et al.*, 2012b CapSeq and CIP-TAP Identify Pol II Start Sites and Reveal Capped Small RNAs as C. elegans piRNA Precursors. Cell **151:** 1488-1500.

GU, W., M. SHIRAYAMA, D. CONTE, JR., J. VASALE, P. J. BATISTA *et al.*, 2009 Distinct argonaute-mediated 22G-RNA pathways direct genome surveillance in the C. elegans germline. Mol Cell **36:** 231-244.

GUANG, S., A. F. BOCHNER, K. B. BURKHART, N. BURTON, D. M. PAVELEC *et al.*, 2010 Small regulatory RNAs inhibit RNA polymerase II during the elongation phase of transcription. Nature **465:** 1097-1101.

GUANG, S., A. F. BOCHNER, D. M. PAVELEC, K. B. BURKHART, S. HARDING *et al.*, 2008 An Argonaute transports siRNAs from the cytoplasm to the nucleus. Science **321:** 537-541.

HOLT, R. A., and S. J. JONES, 2008 The new paradigm of flow cell sequencing. Genome Res **18:** 839-846.

HUTVAGNER, G., J. MCLACHLAN, A. E. PASQUINELLI, E. BALINT, T. TUSCHL *et al.*, 2001 A cellular function for the RNA-interference enzyme Dicer in the maturation of the let-7 small temporal RNA. Science **293:** 834-838.

ISHIZU, H., H. SIOMI and M. C. SIOMI, 2012 Biology of PIWI-interacting RNAs: new insights into biogenesis and function inside and outside of germlines. Genes Dev **26:** 2361-2373.

KAMATH, R. S., and J. AHRINGER, 2003 Genome-wide RNAi screening in Caenorhabditis elegans. Methods **30:** 313-321.

KAMATH, R. S., A. G. FRASER, Y. DONG, G. POULIN, R. DURBIN *et al.*, 2003 Systematic functional analysis of the Caenorhabditis elegans genome using RNAi. Nature **421:** 231-237.

KAMMINGA, L. M., J. C. VAN WOLFSWINKEL, M. J. LUTEIJN, L. J. KAAIJ, M. P. BAGIJN *et al.*, 2012 Differential impact of the HEN1 homolog HENN-1 on 21U and 26G RNAs in the germline of Caenorhabditis elegans. PLoS Genet **8:** e1002702.

KENNEDY, S., D. WANG and G. RUVKUN, 2004 A conserved siRNA-degrading RNase negatively regulates RNA interference in C. elegans. Nature **427:** 645-649.

KETTING, R. F., S. E. J. FISCHER, E. BERNSTEIN, T. SIJEN, G. J. HANNON *et al.*, 2001 Dicer functions in RNA interference and in synthesis of small RNA involved in developmental timing in C-elegans. Genes & Development **15:** 2654-2659.

KNIGHT, S. W., and B. L. BASS, 2001 A role for the RNase III enzyme DCR-1 in RNA interference and germ line development in Caenorhabditis elegans. Science **293:** 2269-2271.

KUMAR, M. S., and K. C. CHEN, 2012 Evolution of animal Piwi-interacting RNAs and prokaryotic CRISPRs. Brief Funct Genomics **11:** 277-288.

LAU, N. C., L. P. LIM, E. G. WEINSTEIN and D. P. BARTEL, 2001 An abundant class of tiny RNAs with probable regulatory roles in Caenorhabditis elegans. Science **294:** 858-862.

LEE, H. C., W. GU, M. SHIRAYAMA, E. YOUNGMAN, D. CONTE, JR. *et al.*, 2012 C. elegans piRNAs mediate the genome-wide surveillance of germline transcripts. Cell **150:** 78-87.

LEE, J. T., 2012 Epigenetic regulation by long noncoding RNAs. Science **338:** 1435-1439.

LEE, R. C., C. M. HAMMELL and V. AMBROS, 2006 Interacting endogenous and exogenous RNAi pathways in Caenorhabditis elegans. RNA **12:** 589-597.

MANIAR, J. M., and A. Z. FIRE, 2011 EGO-1, a C. elegans RdRP, modulates gene expression via production of mRNA-templated short antisense RNAs. Curr Biol **21:** 449-459.

NAM, J. W., and D. P. BARTEL, 2012 Long noncoding RNAs in C. elegans. Genome Res **22:** 2529-2540.

PAK, J., and A. FIRE, 2007 Distinct populations of primary and secondary effectors during RNAi in C. elegans. Science **315:** 241-244.

PAVELEC, D. M., J. LACHOWIEC, T. F. DUCHAINE, H. E. SMITH and S. KENNEDY, 2009 Requirement for the ERI/DICER complex in endogenous RNA interference and sperm development in Caenorhabditis elegans. Genetics **183:** 1283-1295.

RUBY, J. G., C. JAN, C. PLAYER, M. J. AXTELL, W. LEE *et al.*, 2006 Large-scale sequencing reveals 21U-RNAs and additional microRNAs and endogenous siRNAs in C. elegans. Cell **127:** 1193-1207.

SIJEN, T., J. FLEENOR, F. SIMMER, K. L. THIJSSEN, S. PARRISH *et al.*, 2001 On the role of RNA amplification in dsRNA-triggered gene silencing. Cell **107:** 465-476.

SIMMER, F., C. MOORMAN, A. M. VAN DER LINDEN, E. KUIJK, P. V. VAN DEN BERGHE *et al.*, 2003 Genome-wide RNAi of C. elegans using the hypersensitive rrf-3 strain reveals novel gene functions. PLoS Biol **1:** E12.

SMARDON, A., J. M. SPOERKE, S. C. STACEY, M. E. KLEIN, N. MACKIN *et al.*, 2000 EGO-1 is related to RNA-directed RNA polymerase and functions in germ-line development and RNA interference in C. elegans. Curr Biol **10:** 169-178.

SOKOL, N. S., 2012 Small temporal RNAs in animal development. Curr Opin Genet Dev **22:** 368-373.

THIVIERGE, C., N. MAKIL, M. FLAMAND, J. J. VASALE, C. C. MELLO *et al.*, 2011 Tudor domain ERI-5 tethers an RNA-dependent RNA polymerase to DCR-1 to potentiate endo-RNAi. Nat Struct Mol Biol **19:** 90-97.

TIMMONS, L., and A. FIRE, 1998 Specific interference by ingested dsRNA. Nature **395:** 854.

VASALE, J. J., W. GU, C. THIVIERGE, P. J. BATISTA, J. M. CLAYCOMB *et al.*, 2010 Sequential rounds of RNA-dependent RNA transcription drive endogenous small-RNA biogenesis in the ERGO-1/Argonaute pathway. Proc Natl Acad Sci U S A **107:** 3582-3587.

VASTENHOUW, N. L., K. BRUNSCHWIG, K. L. OKIHARA, F. MULLER, M. TIJSTERMAN *et al.*, 2006 Gene expression: long-term gene silencing by RNAi. Nature **442:** 882.

WANG, D., S. KENNEDY, D. CONTE, JR., J. K. KIM, H. W. GABEL *et al.*, 2005 Somatic misexpression of germline P granules and enhanced RNA interference in retinoblastoma pathway mutants. Nature **436:** 593-597.

WELKER, N. C., D. M. PAVELEC, D. A. NIX, T. F. DUCHAINE, S. KENNEDY *et al.*, 2010 Dicer's helicase domain is required for accumulation of some, but not all, C. elegans endogenous siRNAs. RNA **16:** 893-903.

WU, X., Z. SHI, M. CUI, M. HAN and G. RUVKUN, 2012 Repression of germline RNAi pathways in somatic cells by retinoblastoma pathway chromatin complexes. PLoS Genet **8:** e1002542.

YIGIT, E., P. J. BATISTA, Y. BEI, K. M. PANG, C. C. CHEN *et al.*, 2006 Analysis of the C. elegans Argonaute family reveals that distinct Argonautes act sequentially during RNAi. Cell **127:** 747-757.

ZHANG, C., T. A. MONTGOMERY, S. E. FISCHER, S. M. GARCIA, C. G. RIEDEL *et al.*, 2012 The Caenorhabditis elegans RDE-10/RDE-11 complex regulates RNAi by promoting secondary siRNA amplification. Curr Biol **22:** 881-890.

ZHUANG, J. J., and C. P. HUNTER, 2011 Tissue-specificity of Caenorhabditis elegans Enhanced RNAi Mutants. Genetics.

ZHUANG, J. J., and C. P. HUNTER, 2012 RNA interference in Caenorhabditis elegans: uptake, mechanism, and regulation. Parasitology **139:** 560-573.

Addendum

Analyses of *sid-1* homologs

Experiments performed with assistance from Elizabeth Y. Wang

INTRODUCTION

The presence of systemic RNAi in *C. elegans* is one of the reasons why RNAi is so potent in these nematodes (JOSE and HUNTER 2007). The dsRNA channel SID-1 is a major mechanism of systemic RNAi in *C. elegans* (JOSE *et al.* 2009; SHIH *et al.* 2009; WINSTON *et al.* 2002) and is extremely well-conserved across evolution (ZHUANG and HUNTER 2012). While there has been some reports of *sid-1* homologs in other systems inducing systemic RNAi (DONG and FRIEDRICH 2005; DUXBURY *et al.* 2005), the exact endogenous function(s) of any *sid-1*-related genes has not been well reported, not even for *C. elegans*.

Interestingly enough, SID-1 homologs are present in organisms ranging from single-cell amoebas to mammals (DIEZ-ROUX *et al.* 2011; XU and HAN 2008), sometimes in contexts that make systemic RNAi unlikely. Furthermore, the *C. elegans sid-1* gene is not the closest relative to the mouse *Sidt2* gene; rather, it is one of the other five *C. elegans sid-1* homologs *chup-1* that's more closely related (ZHUANG and HUNTER 2012).

Like I demonstrated for NRDE-3 in Chapter 4 and PGL-1 in Chapter 5, overexpressing SID-1 has also been previously shown to cause an enhanced RNAi phenotype (CALIXTO *et al.* 2010). Therefore, investigating the nature of *sid-1*'s contribution to the mechanism of RNAi is extremely relevant in understanding the regulation of small RNAs. While there has been tremendous progress in understanding the characteristics of SID-1, its homologs in *C. elegans* have not been nearly as well-characterized, despite their aforementioned pertinence.

Here, I list and annotate the five *C. elegans sid-1* homologs with respect to homology to the mouse *Sidt2* gene. I then describe the mutant alleles available for these genes and their limitations. Finally, I demonstrate using a unique RNAi knockdown method that some of these homologs do cause an Rde phenotype when targeted via RNAi.

RESULTS AND DISCUSSION

Using a BLAST search using mouse Sidt2 amino acid sequence against the *C. elegans* genome, I discovered five *sid-1* homologs. I named these genes *sid-1-like* (*sidl*).

sidl-1, also known as *C08A9.3*, has 739 amino acids. It has two alleles: (1) *tm760*, which deletes the tiny first exon that one splice form doesn't use, and (2) *gk235*, which also deletes the tiny first exon that one splice form doesn't use and inserts 6 bases. Its prominent homology is that it contains an N-terminal region similar to mouse *Sidt2* N-terminal region, and it contains a C-terminal region similar to latter three-quarters of the C-terminal region of the *C. elegans sid-1*.

sidl-2, also known as *ZK721.1*, *tag-130*, or *chup-1*, has 756 amino acids. It has one allele: *gk245*, which deletes the 5'UTR and the first two exons. Its prominent homology is that it contains an N-terminal region similar to mouse *Sidt2* N-terminal region, and it contains a C-terminal region similar to first one-quarter of the N-terminal region of the *C. elegans sid-1*.

sidl-3, also known as *C30E1.6*, has 247 amino acids. There are no alleles available for this gene. Its prominent homology is that it is similar to the C-terminal latter one-fifth of the *C. elegans sid-1*.

sidl-4, also known as *C30E1.4*, has 239 amino acids. There are no alleles available for this gene. Its prominent homology is that it is similar to the mouse *Sidt2* N-terminal region. Its genomic proximity to *sidl-3* (within 10KB) and their relatively small sizes may suggest that *sidl-3* and *sidl-4* are two "half" gene products.

sidl-5, also known as *Y37H2C.1*, has 718 amino acids. It has one allele: *tm5525*, which deletes the first four exons. Its prominent homology is that it is similar to the mouse *Sidt2* N-terminal region.

Previous analysis of *sidl-2(gk245)* has shown that it is not Rde to feeding RNAi (Jennifer Whangbo, unpublished). I attempted to analyze *sidl-1(gk235)* on *bli-1(RNAi)* and discovered that it responded quite similarly to N2 wild type: 51/118 versus 68/103 with blisters, respectively. The limitation with the *gk235* allele is that it only eliminates one exon that is part of another gene (*sod-3*) and which one predicted isoform does not even use. Combined with the fact that no *C08A9.3* mRNA transcript has ever been detected, the penetrance of the *gk235* allele in knocking out *sidl-1* is in doubt. I also attempted to analyze *sidl-5(tm5525)* on *dpy-11(RNAi)* and *unc-22(RNAi)*, and discovered that it also responded exactly the same as the N2 wild type. The limitation with the other *sidl* genes is that there are no mutant alleles available.

Therefore, to analyze if their loss of function affected RNAi, I along with Elizabeth Wang performed RNAi knockdown of the *sidl* genes to analyze their effects on RNAi sensitivity. To ensure efficacy of this RNAi-of-RNAi setup, we fed the worms dsRNA against *sidl* in one generation and dsRNA against *dpy-11* in the second generation, because simultaneous double RNAi has been shown to be ineffective (MIN *et al.* 2010). To ensure maximum knockdown of the *sidl* genes, we took advantage of the fact that the Eri phenotype is maternally rescued. Therefore, we allowed an *eri-1* hermaphrodite and several *gfp*-marked wild type N2 males to mate on a *sidl(RNAi)* or control *gfp(RNAi)* plate. We then placed the cross progeny (F1) on a *dpy-11(RNAi)* plate and scored their progeny (F2) for Dpy (**Figure 8.1**). The rationale for the setup is to have the *sidl* knockdown occur in an Eri background, while the *eri-1*/+ hets are the worms exposed to the *dpy-11* knockdown. And because of maternal rescue, the wild type *eri* copy in the cross progeny hets ensured that their progeny (the scored F2s) are all phenotypically wild type as well. Since we're examining for possible Rde phenotypes, even if maternal rescue goes awry, the bias is towards an enhanced RNAi response, thus negating any false positives.

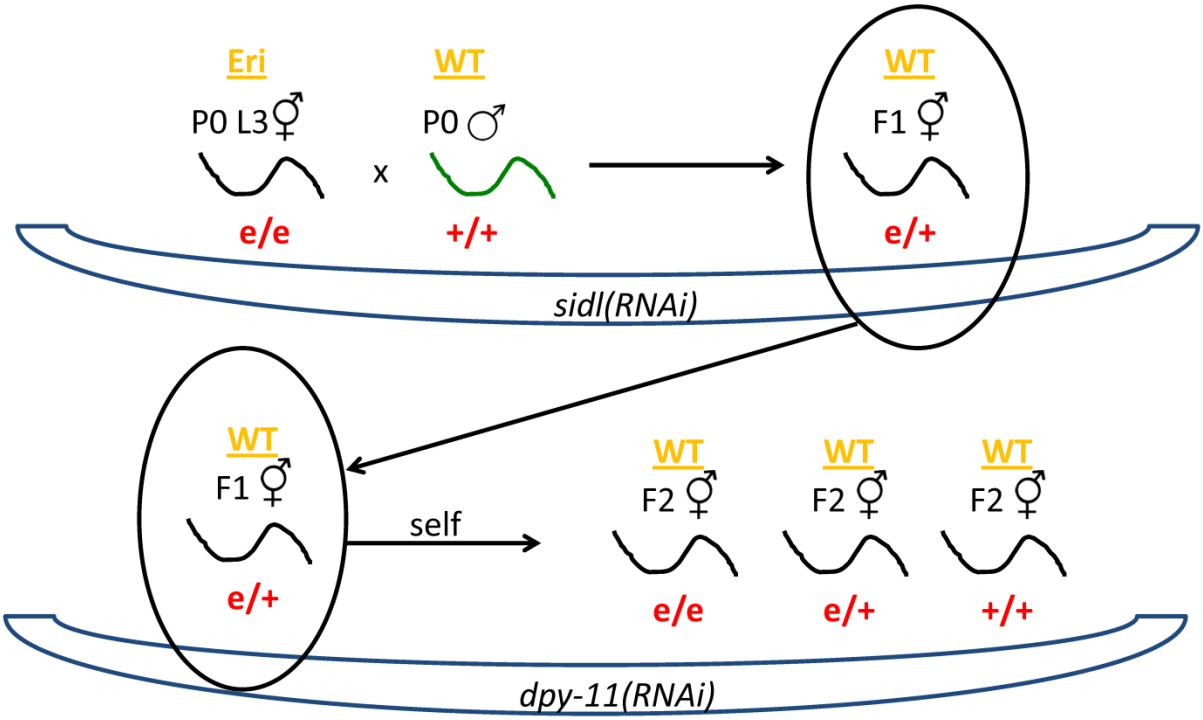

Figure 8.1: Cross to test the effects of RNAi of *sidl* genes

eri-1 hermaphrodites at L3 were placed in the presence of marked wild type males on a plate with bacteria engineered to express dsRNA against the *sidl* genes. The F1 cross progeny were then transferred to the assay readout plate with bacteria engineered to express dsRNA against *dpy-11*. The F2 progeny, which are all phenotypically non-Eri because of the maternal rescue by the heterozygous F1 mother, are scored for the penetrance of the Dpy-11 phenotype.

As a control and proof-of-principle that this Eri RNAi-of-RNAi knockdown is more efficacious than merely performing the same experiment on N2 wild type worms, we tested the effects of *sid-1(RNAi)* using this cross. RNAi knockdown of *sid-1* has previously been shown to be ineffective, presumably because functional SID-1 is necessary to uptake additional *sid-1* dsRNA (Jennifer Whangbo, unpublished). However, using this new RNAi knockdown method, I observed that *sid-1(RNAi)* treated worms were nearly completely insensitive to *dpy-11(RNAi)*, whereas the *gfp(RNAi)* treated worms were still fully sensitive to *dpy-11(RNAi)* (**Figure 8.2**).

We subsequently assayed *sidl-1(RNAi)*, *sidl-2(RNAi)*, *sidl-3(RNAi)*, and *sidl-4(RNAi)* treated worms for sensitivity to *dpy-11(RNAi)*, and discovered that *sidl-1* and *sidl-3* knockdown caused a large drop in sensitivity to *dpy-11(RNAi)* (**Figures 8.3, 8.4**). In all cases, the *gfp(RNAi)* treated worms were still fully sensitive to *dpy-11(RNAi)*. This suggests that perhaps *sidl-1* and *sidl-3* also contribute to systemic RNAi, although perhaps at a subtler level than *sid-1*.

Because of their homology, there is always concern that the RNAi knockdowns caused an off-target effect to induce *sid-1* knockdown instead. However, the homology between the *sidl* genes and *sid-1* is largely at the amino acid level. *sidl-1*'s feeding RNAi clone used (KAMATH and AHRINGER 2003) covers nucleotides 1456 until stop. This stretch, when subjected to pairwise BLASTn against entire *sid-1* sequence, comes up with only one region of an 11mer matching; no other matches are reported for even the remainder of the transcript. *sidl-4*'s feeding RNAi clone used (KAMATH and AHRINGER 2003) covers ATG until nucleotide 828. This stretch, when subjected to pairwise BLASTn against entire *sid-1* sequence, also comes up with only one region of an 16mer matching; no other matches are reported for even the remainder of the transcript. *sidl-2* and *sidl-3* transcripts have no matches at all when subjected to pairwise BLASTn against entire *sid-1* sequence. RNAi off-target effects causing the reported results thus seem unlikely.

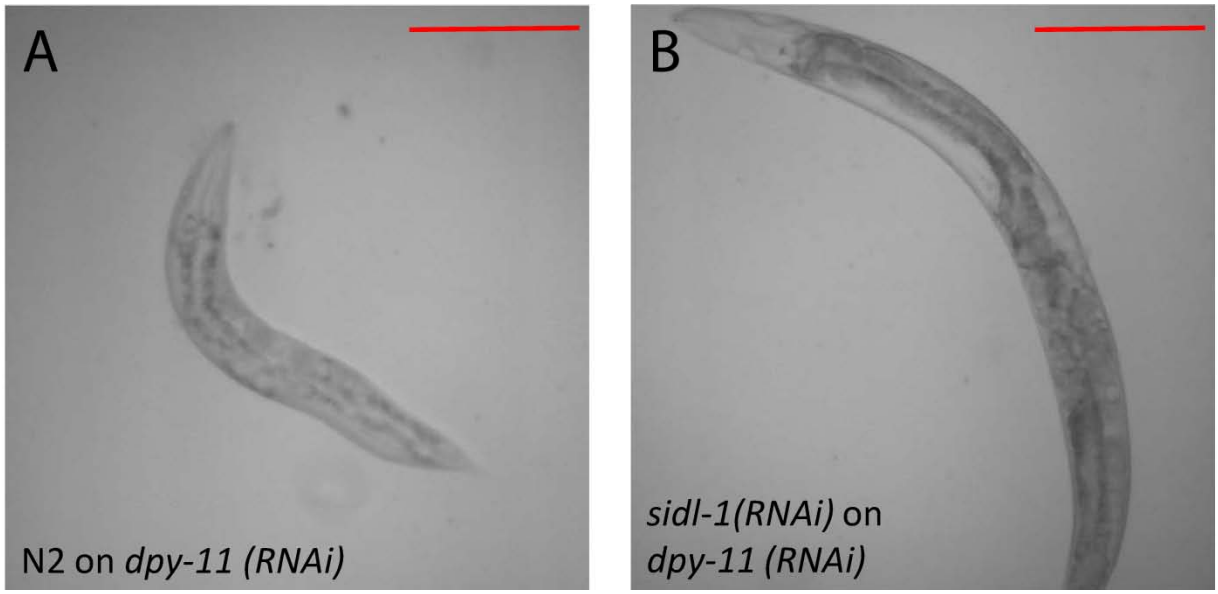

Figure 8.2: Expressivity of Rde phenotype caused by *sidl-1(RNAi)* knockdown

N2 worms fed OD_{600nm} 2.0 *dpy-11(RNAi)* starting from L3 and imaged in the next generation looks very Dpy (A). Conversely, *sidl-1(RNAi)*-treated animals also fed OD_{600nm} 2.0 *dpy-11(RNAi)* starting from L3 and imaged in the next generation does not look Dpy (B). Both images are magnified and scaled the same. Red bar indicates 0.1mm.

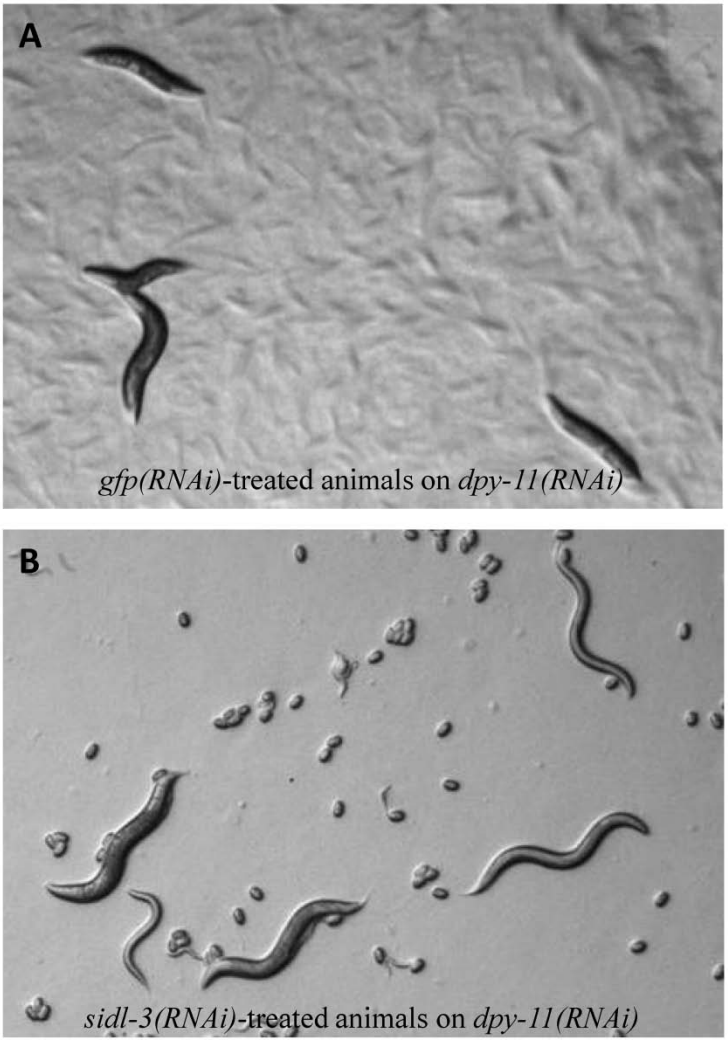

Figure 8.3: Expressivity of Rde phenotype caused by *sidl-3(RNAi)* knockdown

gfp(RNAi)-treated worms fed OD_{600nm} 2.0 *dpy-11(RNAi)* starting from L3 and imaged in the next generation looks very Dpy (A). Conversely, *sidl-3(RNAi)*-treated animals also fed OD_{600nm} 2.0 *dpy-11(RNAi)* starting from L3 and imaged in the next generation does not look very Dpy (B). Both images are magnified and scaled the same.

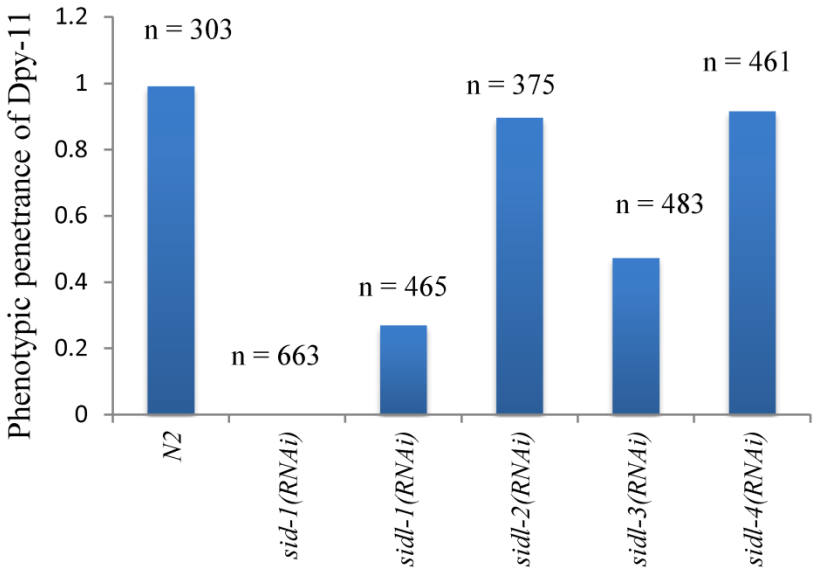

Figure 8.4: Penetrance of Rde phenotype caused by *sidl(RNAi)* knockdowns

Various indicated RNAi-treated worms were fed OD_{600nm} 2.0 *dpy-11(RNAi)* starting from L3 and imaged in the next generation for the Dpy-11 phenotype. The observed pattern was representative of the experiment repeated three times.

Two areas of subsequent analysis could further elucidate the exact nature of the *sidl* genes' possible contributions to systemic RNAi or other *sid-1*-related endogenous functions. First, because there are no (robust) mutant alleles available for *sidl-1* and *sidl-3*, genetic analysis needs to be performed via overexpression. Driving these genes via the *sid-1* promoter in a *C. elegans* transgene could help understand the nature of possible redundancy amongst these homologs for contributing to RNAi. Furthermore, expressing *sidl-1* or *sidl-3* cDNA in *Drosophila S2* cells can help shed light on these gene products' molecular interactions with RNAs (MCEWAN *et al.* 2012; SHIH and HUNTER 2011). Second, recent observations that *C. elegans sid-1* may have stress and/or starvation phenotypes (Jacqueline Brooks, Kenneth Pang, Stephen Banse, and Eric Wu, unpublished) may help create a suite of new assays for testing the *sidl* genes' possible endogenous roles. For example, *sidl-2* and *sidl-5* have robust mutant alleles available but do not seem to cause an Rde phenotype when knocked down/out, suggesting perhaps their role is more related to *sid-1*'s contributions to the stress response than systemic RNAi. Our findings that some, but not all, *sidl* genes have an Rde phenotype upon knockdown are the first characterizations of an important gene family. These findings lay the foundation for future in-depth analysis.

LITERATURE CITED

CALIXTO, A., D. CHELUR, I. TOPALIDOU, X. CHEN and M. CHALFIE, 2010 Enhanced neuronal RNAi in C. elegans using SID-1. Nat Methods **7:** 554-559.

DIEZ-ROUX, G., S. BANFI, M. SULTAN, L. GEFFERS, S. ANAND *et al.*, 2011 A high-resolution anatomical atlas of the transcriptome in the mouse embryo. PLoS Biol **9:** e1000582.

DONG, Y., and M. FRIEDRICH, 2005 Nymphal RNAi: systemic RNAi mediated gene knockdown in juvenile grasshopper. BMC Biotechnol **5:** 25.

DUXBURY, M. S., S. W. ASHLEY and E. E. WHANG, 2005 RNA interference: a mammalian SID-1 homologue enhances siRNA uptake and gene silencing efficacy in human cells. Biochem Biophys Res Commun **331:** 459-463.

JOSE, A. M., and C. P. HUNTER, 2007 Transport of sequence-specific RNA interference information between cells. Annu Rev Genet **41:** 305-330.

JOSE, A. M., J. J. SMITH and C. P. HUNTER, 2009 Export of RNA silencing from C. elegans tissues does not require the RNA channel SID-1. Proc Natl Acad Sci U S A **106:** 2283-2288.

KAMATH, R. S., and J. AHRINGER, 2003 Genome-wide RNAi screening in Caenorhabditis elegans. Methods **30:** 313-321.

MCEWAN, D. L., A. S. WEISMAN and C. P. HUNTER, 2012 Uptake of extracellular double-stranded RNA by SID-2. Mol Cell **47:** 746-754.

MIN, K., J. KANG and J. LEE, 2010 A modified feeding RNAi method for simultaneous knock-down of more than one gene in Caenorhabditis elegans. Biotechniques **48:** 229-232.

SHIH, J. D., M. C. FITZGERALD, M. SUTHERLIN and C. P. HUNTER, 2009 The SID-1 double-stranded RNA transporter is not selective for dsRNA length. RNA **15:** 384-390.

SHIH, J. D., and C. P. HUNTER, 2011 SID-1 is a dsRNA-selective dsRNA-gated channel. RNA.

WINSTON, W. M., C. MOLODOWITCH and C. P. HUNTER, 2002 Systemic RNAi in C. elegans requires the putative transmembrane protein SID-1. Science **295:** 2456-2459.

XU, W., and Z. HAN, 2008 Cloning and phylogenetic analysis of sid-1-like genes from aphids. J Insect Sci **8:** 1-6.

ZHUANG, J. J., and C. P. HUNTER, 2012 RNA interference in Caenorhabditis elegans: uptake, mechanism, and regulation. Parasitology **139:** 560-573.